

Copper-catalyzed transformations of carboradicals
generated by electrochemical and photochemical
methods: oxidative amination and polyfluoroarylation

Présentée le 6 septembre 2021

Faculté des sciences de base
Laboratoire de synthèse et de catalyse inorganique
Programme doctoral en chimie et génie chimique

pour l'obtention du grade de Docteur ès Sciences

par

Xiangli YI

Acceptée sur proposition du jury

Prof. J. Zhu, président du jury
Prof. X. Hu, directeur de thèse
Prof. M. Rueping, rapporteur
Prof. D. Leonori, rapporteur
Prof. J. Waser, rapporteur

Acknowledgements

Finally, the journey of four years is close to an end. This journey of doctorate has completely changed my life, making me a different person from what I was four years ago. I have to express my deep gratitude to my supervisor, Prof. Xile Hu. He was so kind to have accepted me into the group and provided me an excellent environment for doing research. He is very knowledgeable and has a superb understanding of the chemical science. He has not only taught me methods of vigorous research, but has also helped me develop a taste of good science. I had many dark times, hit by all kinds of difficulties. He was always there, encouraging me, discussing with me, enlightening me. Without these, I would not have been able to accomplish the research work for this thesis.

I would like to thank Prof. Jieping zhu, Prof. Jérôme Waser, Prof. Magnus Rueping, and Prof. Daniele Leonori for being the jury members of my defense. The discussion with them enabled me to have a deeper inspection of my research work. Thank Zhikun Zhang for proofread the thesis for me. Thank Albert Daubry for polishing the French abstract for me.

I have so many excellent colleagues, who have helped and inspired me a lot. I would like to thank Dr. Lei Zhang, Dr. Zhikun Zhang, Dr. Srikrishna Bera and Dr. Runze Mao for the frequent scientific discussions and for giving me many useful advices. I would like to thank Dr. Chi Wai Cheung, Dr Fang Song, Dr. Huijie Pan, Dr. Renyi Shi, Dr. Deyun Qian, Dr. Jun Gu, Dr. Pengzuo Chen, Dr. Lichen Bai, Dr. Laurent Liardet, Dr. Marten Ploeger, Dr. Aliko Moysiadou, Dr. Seunghua Lee, Dr. Murat Alkan-Zambada, Dr. Guido Barzanò, Weiyan Ni, Albert Daubry, Xingyu Wu, Céline Prange and many others, from the same group but working on various research topics. Working together with them really broadened my horizon on science and offered me all kinds of technical helps that I needed. I also need to thank all the group members for passing these four years together with me. They made my doctoral career an experience full of joy!

The Institute of Chemical Sciences and Engineering has very supportive teams for administration and technology. I would like to thank Christina Zamanos-Epremian, our dear secretary, for all the assistances and advice on living in Switzerland. Thank Anne-Lene Odegaard and Roque Séverine for their generous help in terms of courses and teaching. Thank the team of chemical shop,

especially Maio Maurizio Carmelo, who was always so responsible and willing for solving our problems on the chemical inventory. Thank MS team, NMR team, IT team, and many others for their tremendous support.

Lastly, I have to thank my parents and my grandparents. I come from a small village. I have been away from home since I was 18, and now I am 29 already. No matter what decisions I make, they are always there supporting me. We do not talk that much, but I know that they love me. And I always love them too.

Abstract

Organic radicals are highly active species that can undergo various transformations. Electrochemistry and photochemistry are efficient methods for the generation of these species of high energy, through single electron transfer processes under mild conditions. These methods have been frequently used to form various carboradical intermediates, for example, via the addition of N-centered radicals to alkenes (Section 1.4). Copper is a versatile transition metal that can transform carboradicals for the formation of various chemical bonds (Section 1.6). Combining electrochemistry or photochemistry for the generation of carboradicals with the copper-catalyzed carboradical functionalization will potentially lead to a large chemical space of useful organic reactions. So far, this intersection of electrochemistry or photochemistry with copper chemistry is still highly underdeveloped. In this thesis, we have developed three useful reactions, testifying the practicability of this concept.

In Chapter 2, we describe an intramolecular oxidative amination reaction (or a formal aza-Wacker cyclization) by integrating electrochemical oxidation with Cu catalysis. Electrochemical oxidation readily generates N-radical from N-H for the intramolecular cyclization to double bonds, and then the resultant carboradicals are transformed into a new double bond via copper-catalyzed oxidative elimination (Section 1.6.1). A wide range of 5-membered N-containing heterocycles (e.g. oxazolidinone, imidazolidinone, thiazolidinone, pyrrolidinone and isoindolinone) bearing a pendant, functionalizable alkene moiety can be synthesized under mild conditions. Mechanistic studies revealed that direct oxidation on the electrode couldn't efficiently convert primary and secondary alkyl radical intermediates into alkenes, and that the assistance of copper was indispensable.

In Chapter 3, an intermolecular oxidative amination reaction of unactivated alkenes by integrating photoredox with Cu catalysis is described. This method relied on photochemical reduction of a hydroxylamine derivative to generate amidyl radical which then adds to unactivated alkenes. The obtained carboradicals are trapped by the copper catalyst for the formation of allylic amines. The reaction exhibited a broad scope and excellent tolerance for functional groups including highly

polar groups. The mechanistic studies provided evidence for a Cu^{III}-alkyl intermediate in the copper mediated oxidative elimination process.

In Chapter 4, we report a decarboxylative coupling reaction of aliphatic acids with polyfluoroaryl nucleophiles by integrating photoredox with copper catalysis. A set of diaryl zinc reagents with different F-content and F-substitution patterns on the aryl group were prepared and applied to the coupling. The aliphatic esters of N-hydroxyphthalimide (NHPI esters) were transformed into alkyl radicals by photoreduction. Then, the trapping of the radical by the copper catalyst and subsequent reductive elimination render the alkyl polyfluoroarenes as products. This method allows the installation of polyfluoroaryls with variable F-content (2F -5F) and F-substitution patterns on primary or secondary alkyl groups, with good compatibility of functional groups. Mechanistic studies revealed that an anionic [Cu-(Ar_F)₂] species could be responsible for the transfer of polyfluoroaryl groups to the alkyl radicals.

In summary, this thesis demonstrates the combination of electrochemistry and photochemistry with copper catalysis to construct useful synthetic methods. Considering the diversity of radicals that could be generated by electrochemical and photochemical methods, and the versatility of copper catalyzed functionalization of carboradicals, we believe that this combination has far more potential beyond these three reactions.

Keywords

Electrocatalysis, copper catalysis, amidyl radicals, aza-Wacker cyclization, photocatalysis, unactivated alkenes, oxidative amination, coupling reaction, polyfluoroaryl zinc reagents, alkyl carboxylic acids, NHPI esters.

Résumé

Les radicaux organiques sont des espèces hautement réactives qui peuvent subir diverses transformations. L'électrochimie et la photochimie sont des méthodes efficaces pour la génération de ces espèces de haute énergie, par des processus de transfert unitaires d'électrons dans des conditions modérées. Ces méthodes ont été fréquemment utilisées pour former divers intermédiaires radicalaires de carbone, par exemple via l'ajout de radicaux N-centrés aux alcènes (section 1.4). Le cuivre, qui est un métal de transition, permet de transformer des radicaux C-centrés pour la formation de diverses liaisons chimiques (section 1.6). La génération de radicaux C-centrés par voie l'électrochimie ou photochimie, catalysée par le cuivre, ouvre la possibilité pour un grand nombre de réactions organiques désirées. Jusqu'à présent, cette intersection entre l'électrochimie, la photochimie et la chimie du cuivre est encore très sous-développée. Dans cette thèse, nous avons développé trois réactions utiles, témoignant de la praticabilité de ce concept.

Dans le chapitre 2, nous décrivons une réaction d'amination oxydative intramoléculaire (ou une cyclisation aza-Wacker formelle) en intégrant l'oxydation électrochimique à la catalyse de cuivre. L'oxydation électrochimique génère facilement des radicaux N-centrés à partir de liaisons N-H pour la cyclisation en doubles liaisons intramoléculaires, puis les radicaux C-centrés résultants sont transformés en une nouvelle double liaison via une élimination oxydative catalysée par le cuivre (section 1.6.1). Une large gamme d'hétérocycles à 5 chaînons contenant de l'azote (par exemple, oxazolidinone, imidazolidinone, thiazolidinone, pyrrolidinone et isoindolinone) portant un fragment alcène fonctionnalisable, peut être synthétisée dans des conditions modérées. Des études mécanistiques ont révélé que l'oxydation directe sur l'électrode ne pouvait pas convertir efficacement les intermédiaires alkylcarboradicaux primaires et secondaires en alcènes, et que l'aide du cuivre était indispensable.

Dans le chapitre 3, une réaction d'amination oxydative intermoléculaire d'alcènes non-activés par photocatalyse intégrée avec catalyse Cu est décrite. Cette méthode dépendait de la réduction photochimique d'un dérivé d'hydroxylamine pour générer un radical amidyle, qui s'ajoutait ensuite aux alcènes non-activés. Les radicaux C-centrés obtenus sont piégés par le catalyseur de cuivre

pour la formation d'amines allyliques. La réaction a présenté une versatilité et une excellente tolérance pour les différents groupes fonctionnels, y compris les groupes hautement polaires. Les études mécanistiques ont fourni des preuves d'un intermédiaire Cu^{III} -alkyle dans le processus d'élimination oxydative médiée par le cuivre.

Dans le chapitre 4, nous rapportons une réaction de couplage décarboxylatif d'acides aliphatiques avec des nucléophiles polyfluoroaryles en intégrant la photocatalyse à la catalyse du cuivre. Une gamme de réactifs diaryl zinc avec différents teneurs en fluorine et différents arrangements de substitution de fluorine sur le groupe aryle a été préparée et appliquée aux réactions de couplage. Les esters aliphatiques de N-hydroxyphtalimide (esters de NHPI) ont été transformés en radicaux alkyle par photoréduction. Ensuite, le piégeage du radical par le catalyseur de cuivre et l'élimination réductrice subséquente produisent les alkyl polyfluoroarènes. Cette méthode permet l'installation de polyfluoroaryles avec une teneur variable en fluorine (2F -5F) sur des groupes alkyles primaires ou secondaires, avec une bonne compatibilité avec une multitude de groupes fonctionnels. Des études mécanistiques ont révélé qu'une espèce anionique $[\text{Cu}-(\text{Ar}_\text{F})_2]$ pourrait être responsable du transfert de groupes polyfluoroaryle aux radicaux alkyles.

En résumé, cette thèse démontre que la combinaison de l'électrochimie et de la photochimie avec la catalyse du cuivre permet de construire des méthodes synthétiques utiles. Compte-tenu de la diversité des radicaux qui peuvent être générés par des méthodes électrochimiques et photochimiques, et de la polyvalence de la fonctionnalisation catalysée par le cuivre des carboradicaux, nous pensons que cette combinaison a un potentiel beaucoup plus vaste que ces trois réactions.

Mots-clés

Electrocatalyse, catalyse au cuivre, radicaux amidyle, cyclisation aza-Wacker, photocatalyse, alcènes non-activés, amination oxydative, réaction de couplage, réactifs polyfluoroaryl zinc, acides alkylcarboxyliques, esters de NHPI.

Abbreviations

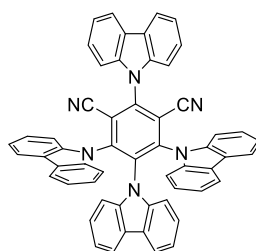
1,10-phen

1,10-phenanthroline

1,4-CHD

1,4-cyclohexanediene

4CzIPN



ATRA

Atom transfer radical addition

ATRP

Atom transfer radical polymerization

BDE

Bond dissociation energy

Boc

tert-Butyloxycarbonyl

bpy

Bipyridine

Bz

Benzoyl

Cl4NHPI

N-hydroxyl- tetrachlorophthalimide

CV

Cyclic voltammetry

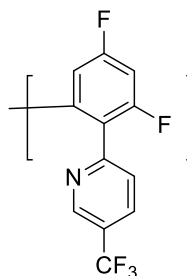
DCE

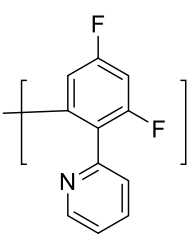
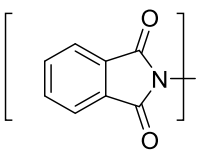
1,2-dichloroethane

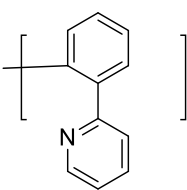
DCM

dichloromethane

dFCF₃ppy



dFppy	
DMA	N,N-dimethylacetamide
DMAP	4-Dimethylaminopyridine
DME	1,2-dimethoxyethane
DMP oxidant	Dess–Martin periodinane
DMPU	1,3-Dimethyl-3,4,5,6-tetrahydro-2(1H)-pyrimidinone
DMSO	dimethylsulfoxide
dOMebpy	4,4'-dimethoxybipyridine
dtbbpy	4,4'-di- <i>tert</i> -butylbipyridine
DTBP	di- <i>tert</i> -butyl peroxide
EWG	Electron withdrawing group
Fc	Ferrocene
HAT	Hydrogen atom transfer
HOMO	Highest occupied orbital
LUMO	Lowest unoccupied orbital
NBS	N-Bromosuccinimide
NCR	Nitrogen centred radical
NCS	N-Chlorosuccinimide
NFSI	N-Fluorobenzenesulfonimide
NHC	N-heterocyclic carbene
NHP	
NHPI	N-hydroxyphthalimide
OPC	Organic photocatalyst
PCET	Proton coupled electron transfer
Piv	Pivaloyl

ppy	
RAE	Redox active ester
RVC	Reticulated Vitreous Carbon
SCE	Saturated calomel electrode
SOMO	Singly occupied molecular orbital
TEMPO	(2,2,6,6-Tetramethylpiperidin-1-yl)oxyl
TMS	trimethylsilyl
Troc	2,2,2-Trichloroethoxycarbonyl
Ts	p-Toluenesulfonyl
EDC	1-ethyl-3-(3-dimethylaminopropyl)carbodiimide

Contents

Acknowledgements.....	i
Abstract	iii
Keywords.....	iv
Résumé.....	v
Mots-clés	vi
Abreviations	vii
Chapter 1 Introduction.....	13
1.1 General.....	13
1.2 Photochemistry for the generation of radicals	15
1.3 Electrochemistry for the generation of radicals.....	18
1.4 Addition of N-centered radicals to alkenes.....	21
1.4.1 A brief introduction to N-centered radicals	21
1.4.2 Intramolecular cyclization	23
1.4.3 Addition to activated alkenes.....	28
1.4.4 Addition to unactivated alkenes.....	30
1.5 N-hydroxyphthalimide esters as a source of alkyl radicals	34
1.5.1 Direct reduction	34
1.5.2 Photoreduction.....	36
1.6 Copper-catalyzed functionalization of alkyl radicals.....	39
1.6.1 Oxidative elimination.....	40
1.6.2 Oxidative substitution.....	42
1.6.3 Atom transfer	43
1.6.4 C(sp ³)-O bond formation	44
1.6.5 C(sp ³)-S bond formation	46
1.6.6 C(sp ³)-N bond formation	47
1.6.7 C(sp ³)-C(sp) bond formation, cyanation and alkynylation	50
1.6.8 C(sp ³)-C(sp ²) bond formation, arylation and polyfluoroarylation.....	53
1.6.9 C(sp ³)-C(sp ³) bond formation, polyfluoroalkylation.....	54
1.7 The goal of the thesis	58
References:.....	60
Chapter 2 Formal aza-Wacker cyclization by dual electrooxidation and copper catalysis	71

2.1	Background	71
2.2	Reaction optimizations.....	73
2.3	Reaction scope studies.....	75
2.4	Mechanistic investigations.....	78
2.5	The proposed reaction mechanism.....	81
2.6	Conclusion	82
2.7	Experiments	83
2.7.1	General consideration	83
2.7.2	Procedures for substrate synthesis	84
2.7.3	Procedures for electrochemical reaction setup	85
2.7.4	Procedures for cyclic voltametry.....	86
2.7.5	Characterization data for the products	86
2.7.6	NMR spectra of 2-2 (an example of the products).....	98
References :		99
Chapter 3 Intermolecular oxidative amination of unactivated alkenes by dual photoredox and copper catalysis 101		
3.1	Background	101
3.2	Reaction optimizations.....	104
3.3	Scope investigations.....	109
3.4	Mechanistic studies.....	111
3.4.1	Photochemical studies.....	111
3.4.2	Radical process	113
3.4.3	The role of copper	113
3.5	The proposed reaction Mechanism	116
3.6	Conclusion	117
3.7	Experiments	118
3.7.1	General consideration	118
3.7.2	Procedures for synthesis of substrates, catalysts and additives.....	118
3.7.3	Procedures for the photochemical reaction	120
3.7.4	Exprimental details for mechanistic studies.....	122
3.7.5	Characterization data for the products	124
3.7.6	NMR spectra of 3-13 (an example of the products).....	140
References		141
Chapter 4 Decarboxylative coupling of aliphatic acids with polyfluoroaryl nucleophiles by dual photoredox and copper catalysis..... 143		
4.1	Background	143
4.2	Reaction optimizations.....	146
4.3	Scope investigations.....	151
4.4	Mechanistic investigations.....	154
4.5	The proposed reaction mechanism.....	159
4.6	Conclusion	160
4.7	Experiments	161
4.7.1	General consideration	161
4.7.2	Synthesis of NHPI esters and zinc reagents.....	161

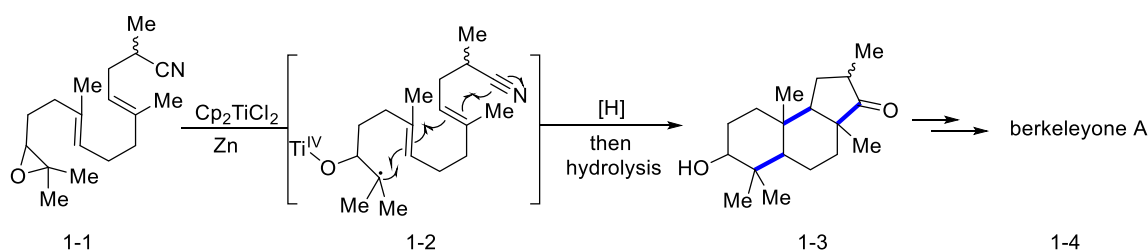
4.7.3 Procedures for the decarboxylative coupling reaction	170
4.7.4 Mechanistic investigations	171
4.7.5 Characterization data of the products	172
4.7.6 NMR spectra of 4-3 (an example of the products).....	189
References :	191
Chapter 5 Conclusion	195
5.1 Achieved results	195
5.2 Future development.....	196
Curriculum Vitae	197

Chapter 1 Introduction

1.1 General

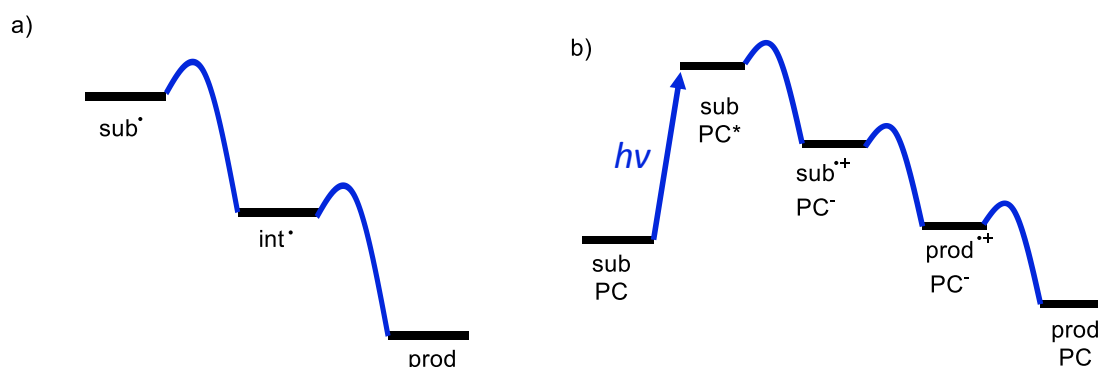
Organic radicals are highly reactive species with an unpaired electron. In the past, they used to be considered as unpredictable and prone to form complex mixture as products. Beginning in the 1980s, substantial contributions have been made by Barton, Curran, Beckwith and others on the methods for radical generation, the kinetic understanding of radical reactions and the applications of radicals for C-C bond formation.^[1] Today, the reactivity of radicals has been much better understood and the radical reaction becomes a routine tool to develop new organic reactions and to design synthetic routes to complex organic compounds.^[2-4]

In most cases, organic radicals have a solution lifetime of less than 1 microsecond. They are so reactive that they react with most types of organic molecules.^[1,5] The organic radicals can add to unsaturated bonds such as C=C bonds, C≡C bonds and arenes. They can abstract atoms and groups including hydrogen and halogen. They can couple with another radical. They can be oxidized or reduced. Last but not least, they can react with metal complexes leading to various outcomes. Compared to organic cation and anion intermediates, radicals are not sensitive to polar functional groups, which renders them advantageous in the construction of pharmaceuticals and natural products. An elegant example is displayed in the synthetic route to berkeleyone A (Scheme 1.1), showcasing the application of radical reaction in building up molecular complexity.^[6] This reaction utilized Ti^{III} to induce the epoxyl to form a carboradical, which then consecutively cyclized to form 3 new rings before the final quench via hydrogen transfer. This cascade process would otherwise be complicated without the radical approach.



Scheme 1.1 Application of radical reaction for the construction of berkeleyone A.

From the point of view of energy, a typical radical reaction is thermodynamically downhill along the reaction path with low barriers (Scheme 1.2a).^[7] This means that the initial radicals are usually high energy species which could not be easily generated from stable functional groups. However, the developments of photochemistry and electrochemistry have greatly facilitated radical generation, because they can input photoenergy or electric energy into the system, so that radical formation becomes thermodynamically favorable. Take photocatalysis as an example (Scheme 1.2b): The absorption of light by the photocatalyst (PC) raises the energy level of the system, which enables the electron transfer between substrate and PC to give the radical species. Electrochemistry, on the other hand, enables radical generation by applying certain electric potentials. Substrates go through single-electron oxidation or reduction when a sufficiently positive or negative potential is applied. These methods are able to transform ubiquitous stable functional groups into active radical species and thus have tremendously enriched the existing radical chemistry.

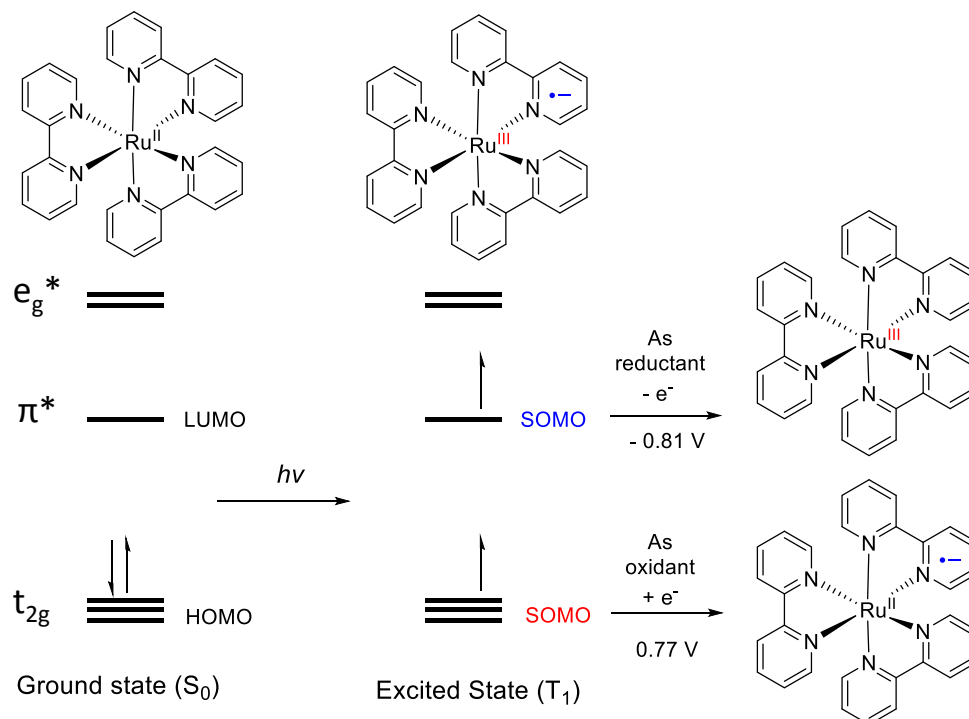


Scheme 1.2 a) An efficient radical reaction requires an initial radical of high energy level. b) The energy of photon facilitates the generation of reactive radical species.

1.2 Photochemistry for the generation of radicals

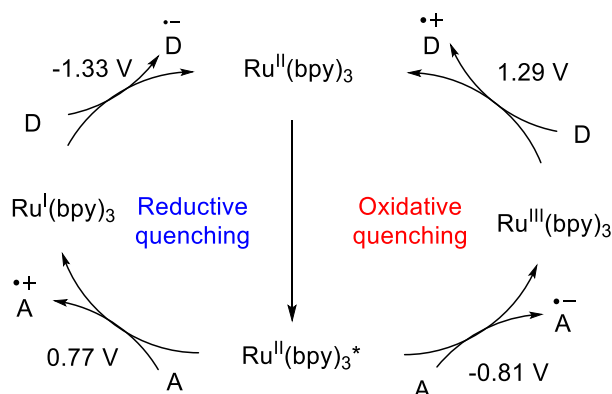
Photoredox catalysis has become a vibrant field of research in synthetic organic chemistry since the pioneering work of McMillan and co-workers.^[8] As mentioned in Section 1.1, this method incorporates photoenergy into the reaction system to facilitate the generation of reactive radicals. Understanding how photocatalysis occurs on a mechanistic level would greatly help the design and implementation of photocatalytic reactions.^[9-11]

$\text{Ru}(\text{bpy})_3^{2+}$ is one of the most prevalent photocatalyst, the working mechanism of which has now been well investigated (Scheme 1.3).^[9, 10] By the absorption of visible light, one electron in a metal-centered t_{2g} orbital can transfer to a ligand-centred π^* orbital. Then, vibrational relaxation and intersystem crossing lead to a triplet state (T_1), which has a relatively long lifetime. The photocatalyst in T_1 has a SOMO of high energy and a SOMO of low energy. When interacting with substrates, the excited Ru complex can transfer one electron from the high-energy π^* orbital to substrates, which makes it a good reductant with $E[\text{Ru}^{\text{III}}(\text{bpy})_3 / \text{Ru}^{\text{II}}(\text{bpy})_3^*] = -0.81 \text{ V}$ (vs SCE, saturated calomel electrode). Besides, it can also obtain one electron from substrates into the low-energy t_{2g} orbital, which makes it, in the meantime, a good oxidant with $E[\text{Ru}^{\text{II}}(\text{bpy})_3^* / \text{Ru}^{\text{I}}(\text{bpy})_3] = 0.77 \text{ V}$.



Scheme 1.3 Orbital description of $\text{Ru}^{\text{II}}(\text{bpy})_3$ photochemistry.

In order to make the reaction catalytic, the Ru complex needs to return to the original form of $\text{Ru}^{\text{II}}(\text{bpy})_3$ to keep circulating during the reaction (Scheme 1.4). For example, if the excited $\text{Ru}^{\text{II}}(\text{bpy})_3$ begins the reaction by oxidizing a substrate (referred to as reductive quenching of the photocatalyst), $\text{Ru}^{\text{I}}(\text{bpy})_3$ would be generated. Then, $\text{Ru}^{\text{I}}(\text{bpy})_3$ will need to be somehow oxidized back to $\text{Ru}^{\text{II}}(\text{bpy})_3$. Therefore, the potentials of $E[\text{Ru}^{\text{II}}(\text{bpy})_3^* / \text{Ru}^{\text{I}}(\text{bpy})_3]$ and $E[\text{Ru}^{\text{II}}(\text{bpy})_3 / \text{Ru}^{\text{I}}(\text{bpy})_3]$ are an important pair of parameters that we need to consider for the design of a photocatalytic reaction. In a plausible catalytic cycle, there should be suitable reductive species that matches the potential of reductive quenching and there should also be oxidative species that matches the potential of catalyst regeneration. Alternatively, if the excited $\text{Ru}^{\text{II}}(\text{bpy})_3$ begins the reaction by reducing a substrate, the process would be an oxidative quenching. In this case, the potentials of $E[\text{Ru}^{\text{II}}(\text{bpy})_3^* / \text{Ru}^{\text{III}}(\text{bpy})_3]$ and $E[\text{Ru}^{\text{III}}(\text{bpy})_3 / \text{Ru}^{\text{II}}(\text{bpy})_3]$ would be important values of reference so as to fit the photocatalyst into a catalytic reaction.

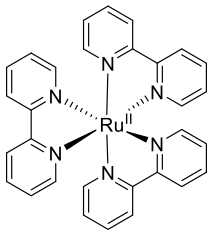
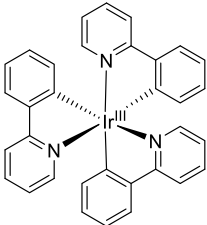
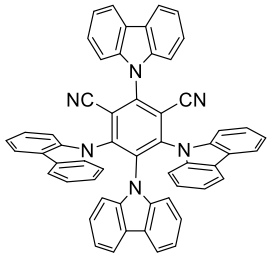
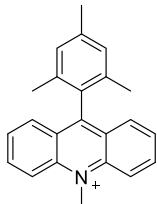


Scheme 1.4 Reductive quenching and oxidative quenching of the excited $\text{Ru}^{\text{II}}(\text{bpy})_3$.

Besides Ruthenium complexes, there are many other compounds that can serve as photocatalysts including Iridium complexes, organic compounds such as 4CzIPN^[12] and Acridinium.^[13] These photocatalysts feature different potential values, and thus they can be used for different types of reaction system (Table 1.1). $\text{Ir}(\text{ppy})_3$, for example, have a very negative value of $E[\text{Ir}^{\text{III}}(\text{ppy})_3^* / \text{Ir}^{\text{II}}(\text{ppy})_3]$ (-1.73 V), while $E[\text{Ir}^{\text{IV}}(\text{ppy})_3 / \text{Ir}^{\text{III}}(\text{ppy})_3^*]$ is only 0.31 V. This means that $\text{Ir}(\text{ppy})_3$ is more likely to activate a substrate in a reductive manner and less likely in an oxidative manner.^[14] For example, they are usually used to reduce N-N or N-O containing reagents to give N-centered radicals.^[15] The excited 4CzIPN has both impressive oxidation potential (1.04 V) and reductive potential (-1.35 V) of the excited state, making it competent for both oxidative and reductive activation of

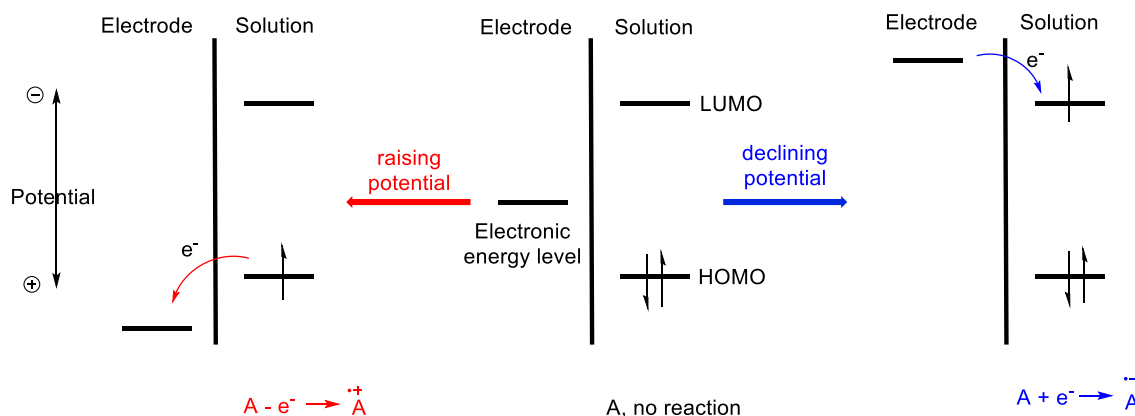
substrates.^[12] In contrast, the excited 9-mesityl-10-methylacridin-10-ium is better in the photooxidation of substrates with an oxidation potential of 2.18 V. It is even eligible to oxidize unactivated alkenes into radical cations when can then be subjected to the reaction with various nucleophiles.^[16,17]

Table 1.1 Redox potentials of selected photocatalysts.

				
	Ru(bpy) ₃ ²⁺	Ir(ppy) ₃	4CzIPN	Mes-Acr-Me ⁺
E(PC [*] /PC [•])=	0.77 V	0.31 V	1.04 V	2.18 V
E(PC ⁺ /PC [*])=	-0.81 V	-1.73 V	-1.35 V	
E(PC/PC [•])=	-1.33 V	-2.19 V	-1.21 V	-0.49 V
E(PC ⁺ /PC)=	1.29 V	0.77 V	1.52 V	

1.3 Electrochemistry for the generation of radicals

Since 2000, electrochemistry has witnessed a renaissance for its application in organic synthesis.^[18-20] Compared to photochemistry, electrochemistry activates substrates in a different manner. It uses an applied potential to control the oxidation or reduction of the substrates for the generation of radicals. In Bard's book, the potential of electrode is referred to as a descriptor of the energy level of electrons on the electrode.^[21] Higher potential of the electrode means a lower energy level of electrons on the electrode, and thus it has a strong tendency to obtain electrons from the substrates in solution. The energy diagram in Scheme 1.5 could describe how oxidation and reduction happen on the electrode. When the electronic energy level lies between the HOMO and LUMO of the substrate (A) in solution (Scheme 1.5 middle), the system is stable and no electron transfer occurs. When potential rising drives the electronic energy level to go below the HOMO of A (Scheme 1.5 left), the electron of A would be able to transfer to the electrode. Thus, an oxidation current could be observed. On the other hand, when potential declining drives the electronic energy level to go above the LUMO of A (Scheme 1.5 right), the electron transfer from electrode to A would be thermodynamically favorable. Thus, a reductive current could be observed.

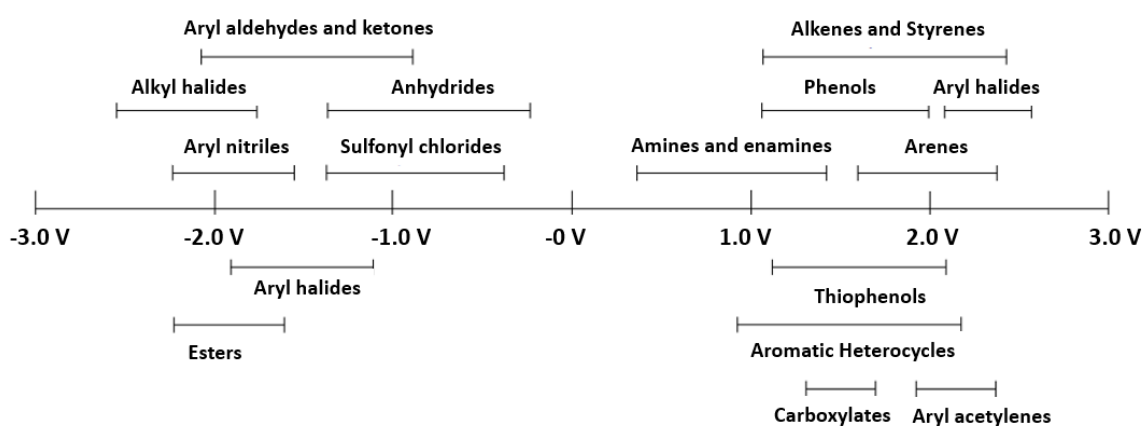


Scheme 1.5 Energy diagram of oxidation and reduction process on electrode.

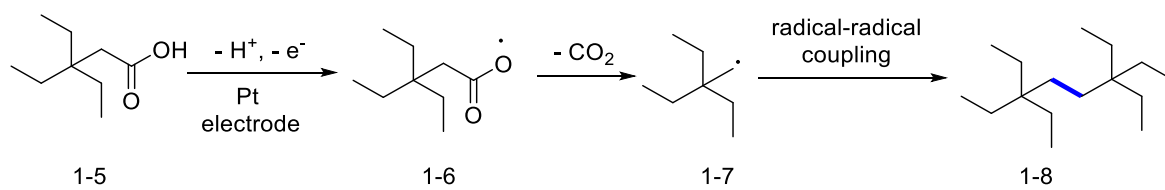
All the organic compounds have their feature potential values, which means that at a certain potential they will have electron transfer with the electrode to give radicals (scheme 1.6).^[22] Substrates including sulfonyl chlorides, aryl aldehydes and ketones, alkyl and aryl halides, etc. could be reduced on electrode for the generation of radicals or radical anions. Amines, styrenes, carboxylates, etc. could be oxidized on electrode for the generation of radicals and radical cations. Even

for saturated hydrocarbons which has an ultra high oxidation potential, people have devised the strategy of mediators to enable their conversion to radicals. ^[23-25]

There are several advantages of using electrochemistry for organic reactions. ^[26] First, chemoselectivity could be well controlled by the adjustable potential. In photochemistry or conventional redox chemistry, however, the redox potential for excited photocatalyst or redox reagents can not be adjusted in an easy and consecutive manner. Second, the rate of electrochemical reactions can be determined by the reaction current, providing another handle to control the reaction. Besides, electrochemistry not only provides an alternative for conventional oxidants and reductants, it also enables new reactivity that can hardly be achieved so far by directly using oxidants and reductants. For example, the electrochemical oxidation on Platinum electrode enables decarboxylative coupling of two alkyl carboxylic acids (Kolbe reaction, Scheme 1.7). ^[27] The reaction occurs via the coupling of two alkyl radicals, which is extremely challenging in bulk solution because the probability of two short-life radicals colliding each other is very low. However, electrochemical reactions are not homogenous reactions. The reactions take place mostly on the surface of the electrode and in the double electrical double layer. ^[28] The limited space increases the chance of transient radicals to meet each other, and this could be the reason for the successful radical-radical coupling in Kolbe reaction. This feature of electrochemistry should be borne in mind when we develop an electroorganic reaction: despite the advantage, it could also impede the active radicals to react with reactants in the bulk solution.



Scheme 1.6 Oxidation and reduction potentials for different categories of organic compounds.

**Scheme 1.7** Kolbe oxidation of carboxylic acid.

1.4 Addition of N-centered radicals to alkenes.

The construction of C-N bond has always been a fundamental area for organic synthesis because of the ubiquity of nitrogen-containing compounds in natural products, pharmaceuticals and many other fields.^[29,30] To form a C-N bond from easily available alkenes, most methods so far employ the nucleophilicity of the N atom.^[29-31] One of the important reactions for this purpose is aza-Wacker reaction, in which palladium is used to activate alkenes and facilitate the attack of N-nucleophiles to the alkenes.^[32-33] Addition of N-centered radicals to alkenes is an alternative approach.^[31,34] These highly reactive species provide great opportunities in the assembly of C-N bonds with different retrosynthetic disconnections, distinctive reaction selectivity and good tolerance of functional groups. The lack of convenient routes to generating N-centered radicals used to be a major barricade hindering this field.^[35] Recently, the rapid development in photochemistry and electrochemistry have created many convenient and efficient approaches for the generation of N-centered radicals.^[31,36] With these methods, numerous amination reactions for alkenes have been discovered based on the addition of N-centered radicals.

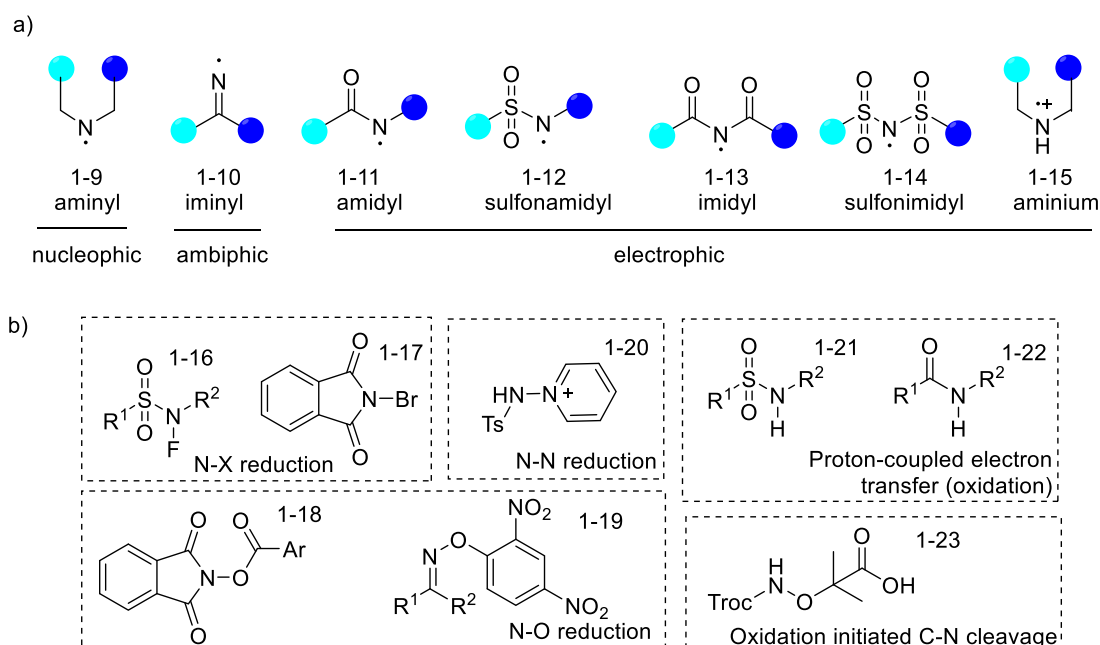
1.4.1 A brief introduction to N-centered radicals

N-centered radicals could be divided into different categories based on the hybridization of nitrogen and the substitutions on the nitrogen (Scheme 1.8a) and they could have different reactivities.^[31] Aminyl radicals are nucleophilic radicals. They have weak capability for hydrogen abstraction and are usually not reactive for addition to alkenes or arenes.^[35,37] However, they are reported to add to transition metal catalyst for C-N formation in some cases.^[38,39] Iminyl radicals are ambiphilic radicals. They readily undergo intramolecular addition to alkenes and intramolecular hydrogen abstraction.^[31] In contrast, amidyl, imidyl, sulfonamidyl and sulfonimidyl radicals are all electrophilic radicals, and they are highly reactive for hydrogen abstraction and addition to alkenes as well as arenes, enabling not only intramolecular reactions but also intermolecular reactions.^[31,35] Recently, aminium radicals have attracted considerable attention.^[40] By simply protonating the aminyl radical, the philicity could be totally reversed. Aminium radicals are highly electrophilic, and has reactivities more similar to those of amidyl radicals.^[41]

In order to generate N-centered radicals, both single electron oxidation and reduction could be applied, depending on the type of precursors that are used (Scheme 1.8b). N-X reagents, e.g. 1-16 and 1-17, are the most traditional and prevalent precursors for N-centered radicals.^[42, 43] Upon

reduction, the more electronegative halogen would leave as an anion and thus a N radical could be obtained. This process occurs quite readily even with Cu^{I} , which is a weak reductant.^[44, 45] Photo-reduction is not required in most cases. The N-O reagents (e.g. 1-18 and 1-19)^[31] and N-N reagents (e.g. 1-20)^[46] have been widely used for photochemical generation of N-centered radicals, since the seminal work of Sanford with the N-acyloxypthalimides 1-18.^[47] One thing that needs special attention is that the leaving part needs to be enough electron-deficient. In the case of 1-18, for example, if the Ar- is replaced by alkyl, the nitrogen part would become phthalimide anion instead of corresponding N radical upon photoreduction.

Oxidation for N-centered radical generation is relatively more challenging because the oxidation potential for the N-H precursors of electrophilic N radicals are usually very high.^[48] To solve this problem, Knowles and co-workers combined a strongly oxidizing photocatalyst and a proper base to effect a proton-coupled electron transfer (PCET) process for the generation of amidyl or sulfonamidyl radicals. The Studer group and the Leonori group successfully circumvented this problem by using α -amino-oxy acids, which provides a more facile and general way to afford amidyl or iminyl radicals.^[31] Oxidation of the acid leads to a carboxylic radical, which subsequently extrudes a carbondioxide and an acetone to get the N-centered radical.



Scheme 1.8 a) different N-centered radicals and their philicity. b) Various precursors leading to N-centered radicals via either oxidation or reduction.

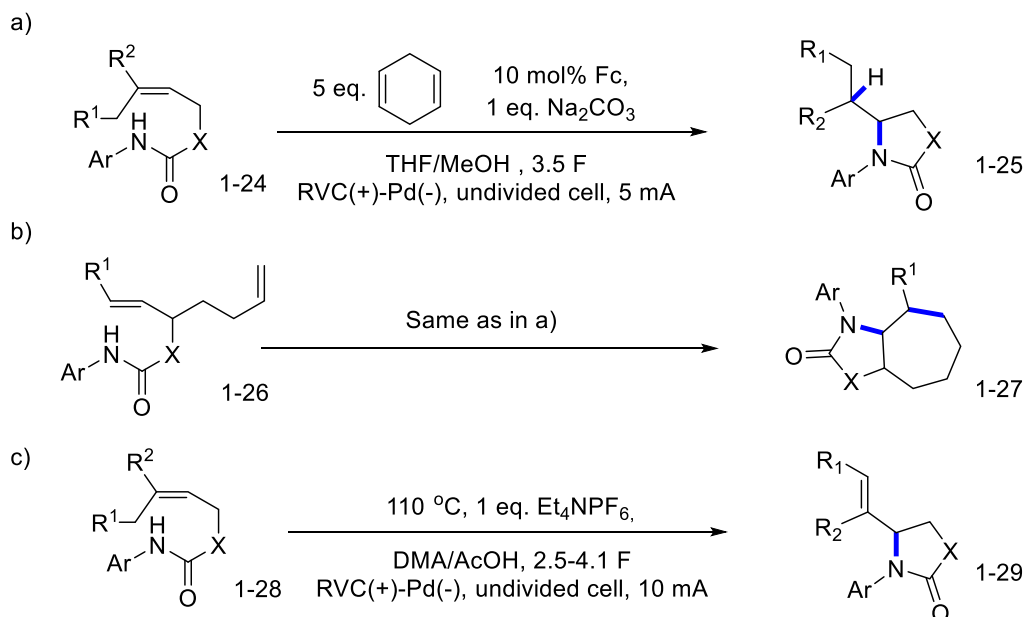
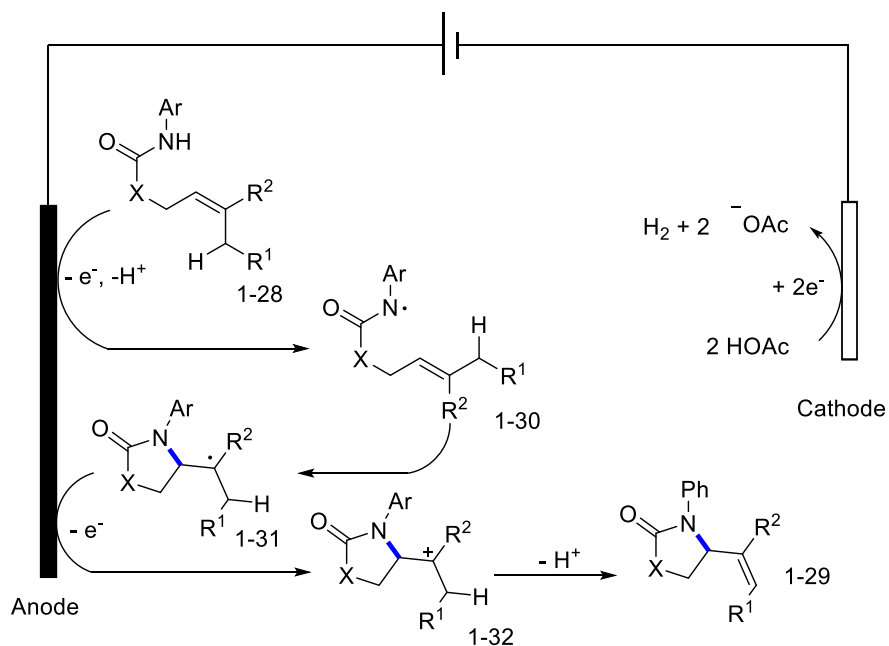
1.4.2 Intramolecular cyclization

Cyclization of N-centered radicals to alkenes provides an efficient approach to constructing N-containing rings.^[35,49,50] Compared to analogous cyclization of carboradicals, the 5-exo-trig cyclization of N radicals, such as iminyl radicals and amidyl radicals, is much faster kinetically, and readily forms 5-member rings.^[51] After the cyclization, a new carboradical would be obtained, which can react with hydrogen donors, SOMOphiles or transition metals to give the final products.

1.4.2.1 Electrochemical oxidation of N-H for cyclization

With N-arylamide 1-24 as substrate, Xu and co-workers realized an elegant intramolecular hydroamidation reaction via electrochemical oxidation (Scheme 1.9a).^[52] The aryl substituent was necessary in order to have a relatively low oxidation potential of the amide. The addition of base could further facilitate the oxidation of N-H by assisting deprotonation. After a 5-exo-trig cyclization of amidyl radical to alkene, a carboradical would be formed which could abstract a hydrogen to form the final product 1-25. The addition of 5 eq. of 1,4-CHD (cylcohexadiene) could substantially improve the reaction yield, which also verified the importance of hydrogen atom transfer (HAT) for the product formation. In a following work, the substrate with an additional pendant double bond 1-26 was tested (Scheme 1.9b).^[53] Rather than a HAT of the carboradical, the 7-endo-trig cyclization to the second double bond was preferred. Then, a final HAT led to the bicyclic product 1-27.

Besides HAT process, it is possible for the carboradical from 1-28 to be further oxidized.^[54, 55] The loss of proton in the following step could forge a new double bond (Scheme 1.9c).^[55] This strategy enabled the formation of diverse trisubstituted and tetrasubstituted double bonds linking to N-containing 5-member rings, which is difficult to achieve with the Pd-mediated aza-Wacker process. The mechanism of this electrooxidation process is shown in Scheme 1.10. Initially, 1-28 undergoes single electron oxidation and deprotonation to give an amidyl radical 1-30, which cyclizes to afford the carboradical 1-31. Then, the second oxidation step takes place leading to the carbocation 1-32. By deprotonation, the final product 1-29 could be obtained. There are two key points for the success of this reaction. First, the oxidation of 1-31 required the carboradical to be tertiary radical, which would lead to a much more stable tertiary carbocation (compared to secondary carbocation). Second, a careful selection of solvents and elevated temperature were necessary to guarantee the selectivity for the final elimination step. Otherwise, the addition of nucleophiles to the carbocation 1-32 could lower the reaction efficiency.

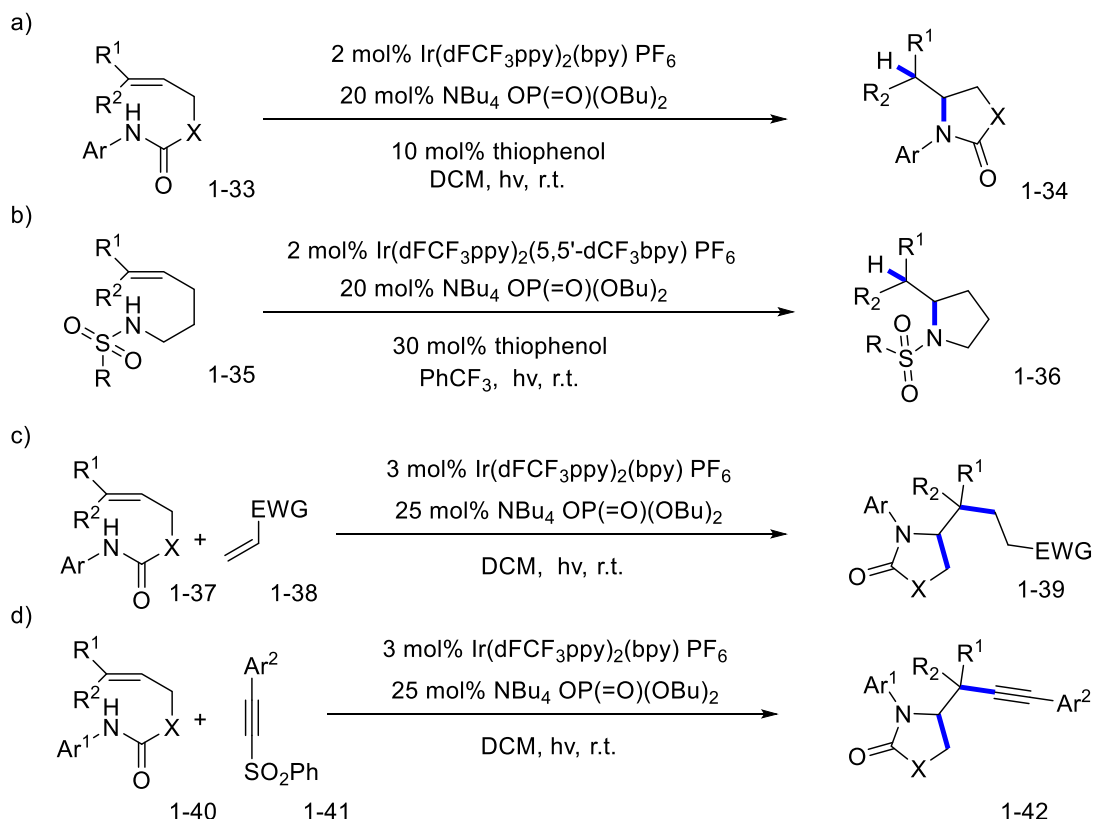
**Scheme 1.9** Electrochemical oxidation of N-H for N radical cyclization.**Scheme 1.10** The proposed mechanism for the electrochemical oxidative amination.

1.4.2.2 Photochemical oxidation of N-H

The same base-assisted N-H oxidation could also be realized with photochemical oxidation. Using $\text{Ir}(\text{dFCF}_3\text{ppy})_2(\text{bpy}) \text{PF}_6$ as photocatalyst and $\text{NBu}_4\text{OP}(\text{O})(\text{OBu})_2$ as base, Knowles and co-workers generated N-radicals from the oxidation of N-H bonds in amides, ureas, carbamates, and thio-carbamates 1-33 (Scheme 1.11a).^[56, 57] Thiophenol was used as a co-catalyst which can transfer a hydrogen to the carboradical formed from amidyl radical cyclization, and thus the hydroamidation product 1-34 could be obtained.^[56] The generated phenylthiyl radical will be reduced by Ir^{II} to recycle the thiophenol and Ir^{III} photocatalyst at the same time. In a sulfonamide without N-aryl substitution, the N-H bond has a higher oxidation potential and thus it is more challenging as a source for N-radicals.^[58] By using a more oxidizing photocatalyst $\text{Ir}(\text{dFCF}_3\text{ppy})_2(5,5'\text{-dCF}_3\text{bpy}) \text{PF}_6$, the sulphonamide substrate 1-35 could be successfully converted to N-radicals for the formation of the hydrosulfonamidation product 1-36 (Scheme 1.11b). Notably, when a photocatalyst with a lower oxidation potential was used, an obvious decline in reaction yield would be observed.

To increase the complexity of the product, some SOMOphiles were utilized for the capture of the carboradical intermediate after cyclization. The Knowles group used electron-deficient alkenes, such as acrylates, acrylonitriles and alkenyl ketones, to form diverse heterocyclic products 1-39 (Scheme 1.11c).^[57] The Rueping group used alkynyl sulfone 1-41 as SOMOphile, which can be added by the carboradicals.^[59] Then, the extrusion of a sulfonyl radical would lead to the alkynylation product 1-42 (Scheme 1.11d). The installation of a triple bond provide a handle for subsequent potential derivatizations.

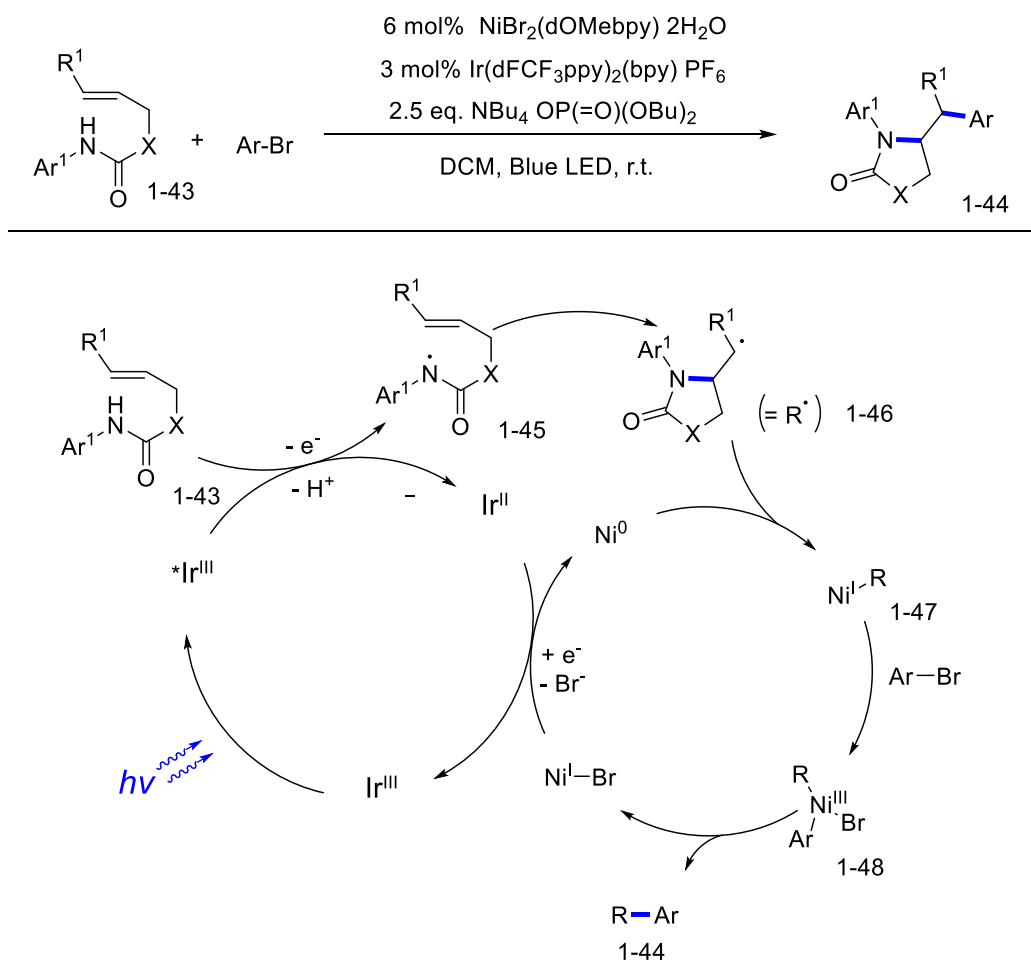
In 2019, the Molander group disclosed a novel photoredox PCET/Ni dual catalytic strategy to functionalize the carboradical from amidyl radical cyclization (Scheme 1.12).^[60] Instead of directly quenching the active amidyl radical, the Ni species preferred a combination with carboradical to effect the arylation reaction with aryl bromide. In the proposed mechanism (Scheme 1.12 bottom), the reaction starts with a photochemical oxidation followed by cyclization to give carboradical 1-46. Ni^0 was proposed to be the intermediate that captures 1-46 to form Ni^{I} species 1-47, which can be oxidatively added by aryl bromide. Then, the obtained Ni^{III} species 1-48 readily undergoes reductive elimination to give the amidoarylation product 1-44. Finally, the $\text{Ni}^{\text{I}}\text{-Br}$ acts as an oxidant for Ir^{II} to enable the regeneration of the photocatalyst.



Scheme 1.11 Photochemical oxidation of N-H for N-radical cyclization.

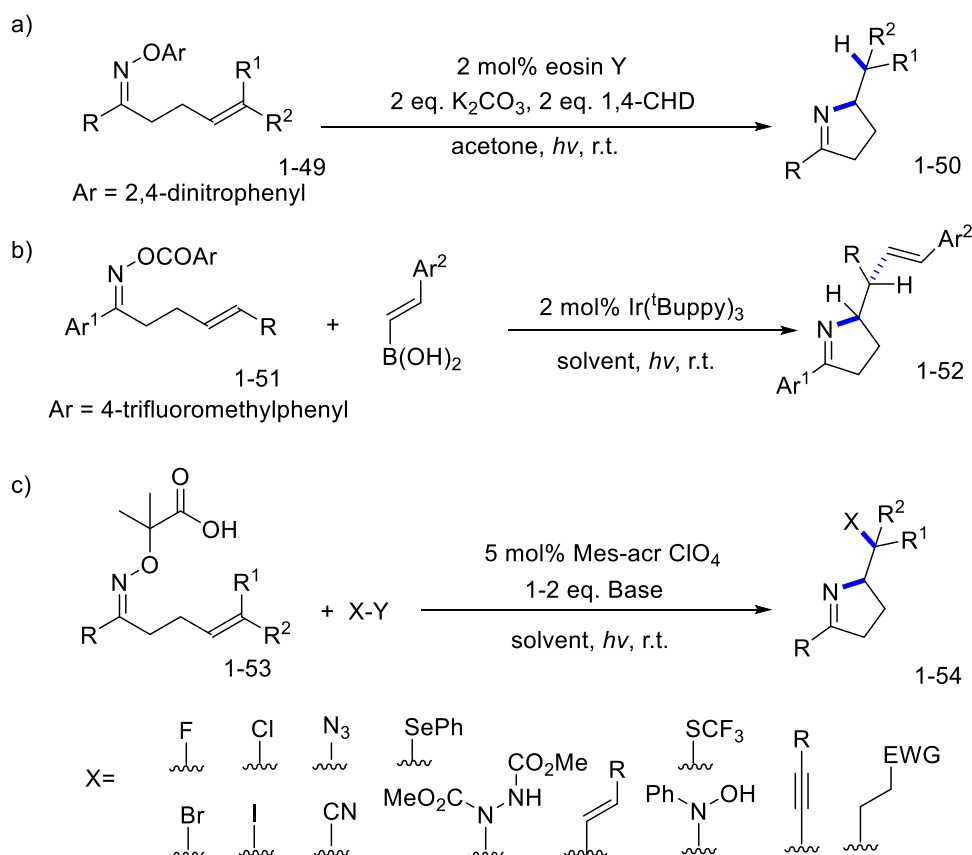
1.4.2.3 Photochemical induced cleavage of N-O bond.

Because of the low bond energy of N-O bond (BDE ca. 50 kcal/mol), the use of precursors containing N-O bond for the generation of N-centered radicals, although less step- and atom-economic, is an easier and more general approach compared to direct oxidation of N-H (BDE ca. 100 kcal/mol).^[31] Leonori and co-workers developed intramolecular hydroamination reactions using the O-2,4-dinitrophenyl precursors.^[61, 62] Under radiation, the excited eosin Y can reduce the N-O bond in 1-49 for the generation of an iminyl radical, which can then undergo cyclization and HAT to give 1-50 (Scheme 1.13a).^[61] Notably, stoichiometric amount of 1,4-CHD was required as hydrogen donor to ensure the redox neutrality, in contrast to catalytic amount of thiophenol as hydrogen donor in the reaction of Scheme 1.11a. Yu and co-workers used an O-4-trifluoromethylbenzoyl precursor 1-51, which also successfully led to iminyl radical upon photoreduction by excited Ir catalyst (Scheme 1.13b).^[63] Alkenyl boronic acids were utilized to capture the carboradicals for the alkenylation reaction. The interaction between the boronic acid with the nitrogen atom was disclosed to contribute to an excellent diastereoselectivity for this reaction.



Scheme 1.12 Photoredox PCET/Ni dual catalysis for intramolecular amidoarylation of alkenes.

α -Imino-oxy acids 1-53 were applied, independently by the Studer group and the Leonori group, for the oxidative generation of iminyl radicals.^[64, 65] Though more complicated in terms of preparation compared to 1-49 or 1-51, α -Imino-oxy acids enable the use of oxidative SOMOphiles which are more diverse (e.g. electron-deficient $\text{C}=\text{C}$, $\text{N}=\text{N}$, $\text{N}=\text{O}$ and hypervalent iodine). 1-49 and 1-51, however, require the use of reductive SOMOphiles which are scarce (e.g. alkenyl boronic acid in Scheme 1.13b). This is well demonstrated by Leonori and co-workers in the reaction in 1.13c. By using various oxidative SOMOphiles, they realized diversified functionalization of the carboradical intermediates to form C-C, C-X, C-N, C-S and C-Se bonds.^[65]



Scheme 1.13 Photochemical induced cleavage of N-O bond for N-radical cyclization.

1.4.3 Addition to activated alkenes

In addition to intramolecular reactions, the electrophilic N-radicals have shown their capability for intermolecular addition to activated alkenes.^[34,66,67] After the N-radical addition, a relatively stable carboradical could be obtained, which is stabilized by the conjugation with arenes, unsaturated bonds or heteroatoms. The carboradical could then be subjected to many subsequent process, such as single electron oxidation and addition to metal complex, to realize amino difunctionalization of alkenes.

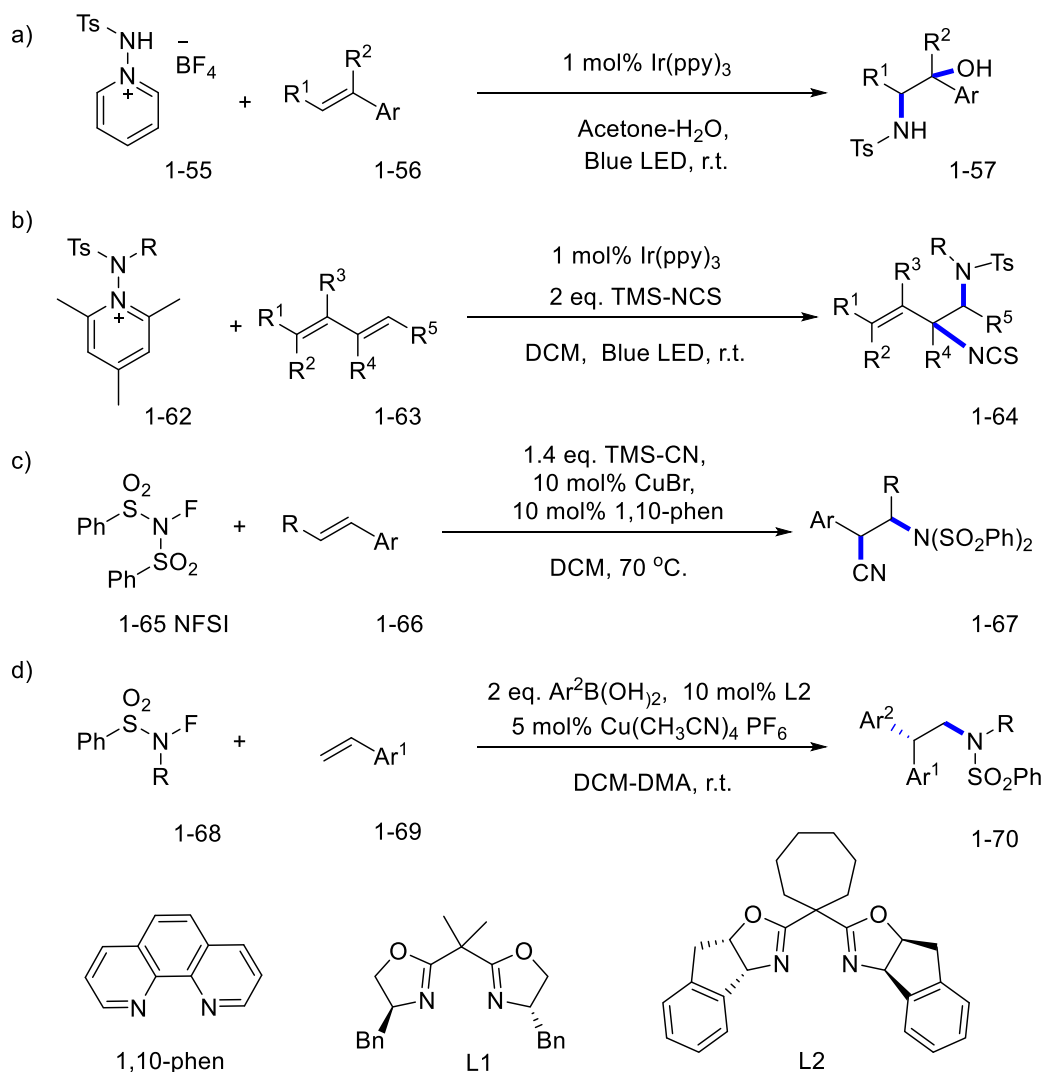
In 2015, Akita and co-workers applied N-protected 1-aminopyridium salts for the generation of sulfonamidyl radicals with Ir(ppy)₃ as photocatalyst (Scheme 1.14a).^[68] A set of α -amino-alcohol derivatives 1-57 were synthesized from styrenes. This reaction took advantage of the addition of sulfonamidyl radicals to styrenes (Scheme 1.15), and then the formed benzyl radical 1-60 could be oxidized by Ir^{IV} to give a benzyl carbocation 1-61. Notably, an aryl substitution is indispensable for this step, because it facilitates the oxidation of the radical by stabilizing the positive charge in the

product. Later, water acted as a quencher for the cation 1-61 to realize the aminohydroxylation process. Following this work, many difunctionalizations were realized by quenching the carbocation with other nucleophiles, such as chloride, fluoride,^[69] acetone and acetonitrile.^[70] With DCM as solvent, the carbocations could also be trapped intramolecularly by the sulfonamide group for the formation of arziridines.^[71]

Recently, this strategy was successfully applied to dienes by the Zhu Group (Scheme 1.14b).^[72] The allyl carboradical intermediates could also be oxidized by $\text{Ir}(\text{ppy})_3^+$ to an allylic carbocation, which was then trapped by TMS-NCS. A selective 1,2-diamination of 1,3-dienes was realized with the introduction of two orthogonally protected amino groups.

Apart from direct oxidation, copper catalyst was also used to mediate the transformation of the carboradical (Scheme 1.14c).^[73] Zhang and co-workers used NFSI as a precursor which, upon reduction by Cu^{I} , generates a highly active imidyl radical that readily adds to styrenes. A cyano group could then transfer to the obtained carboradical with the assistance of copper catalyst. With this reaction, styrenes can be converted to synthetically useful N-protected β -amino nitriles 1-67. One advantage of using metal catalysis is the possibility to control the stereochemistry. The Liu group later developed an enantioselective version of this reaction with a bisoxazoline ligand L1 instead of 1,10-phenanthroline.^[74]

The enantioselective copper catalysis could be extended for the arylation of the carboradicals to effect aminoarylation of styrenes (Scheme 1.14d).^[75] The reaction process is displayed in Scheme 1.16. The sulfonamidyl radical 1-71 was generated by the reduction of 1-68 with Cu^{I} . Then, addition to styrenes led to benzyl radicals 1-72. Aryl group was transferred from the chiral Cu^{II} catalyst to 1-72 to form the aminoarylation product 1-70. NFSI was not a good precursor of N-radicals in this reaction because of the mismatch of reaction rates of the different steps. A computational study showed that the imidyl radical from NFSI could add to styrene barely with energy barrier, while amidyl radical 1-71 from precursor 1-68 adds to styrenes with a barrier of around 15 kcal/mol. The transmetalation process of arylboronic acids is also relatively slow, which matches better with a slower N-radical addition process of 1-71.

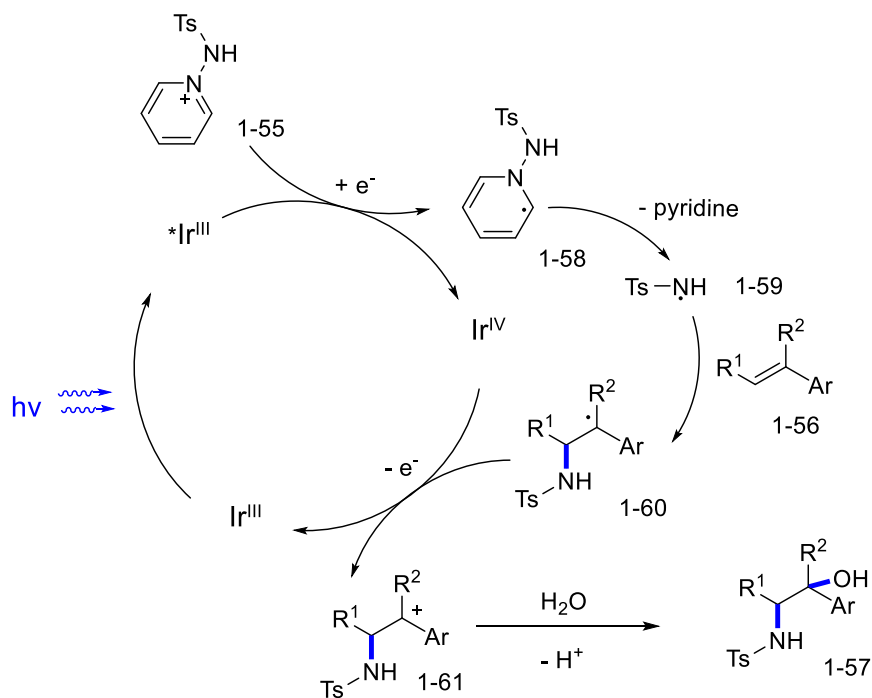


Scheme 1.14 N-radical addition to activated alkenes for aminodifunctionalization reactions.

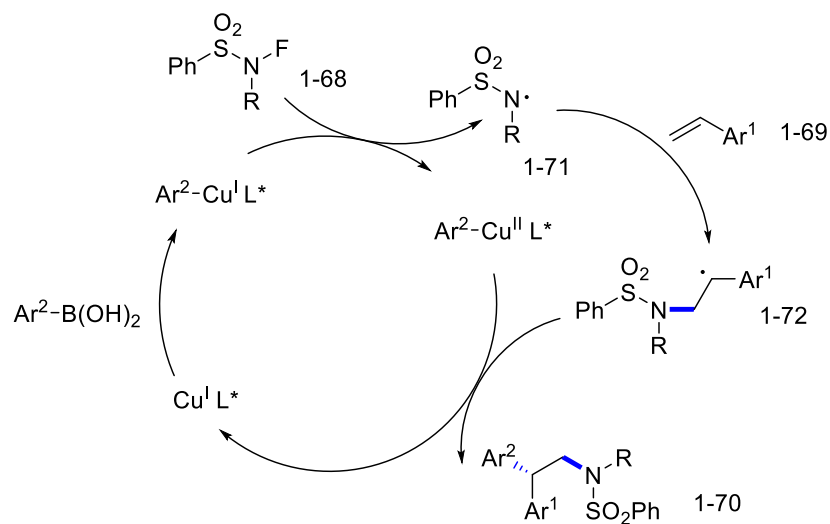
1.4.4 Addition to unactivated alkenes

Compared to the addition to activated alkenes, the addition of N-radicals to unactivated alkenes leads to more active carboradicals with shorter lifetime. As a result, the selective trapping of the carboradicals is more difficult, and the functionalization of unactivated alkenes via N-radical addition remains largely underdeveloped. As early as in 1978, it was discovered that N-halogen imides 1-73 (e.g. NBS, NCS) could react with alkenes using photoinitiation (Scheme 1.17a).^[76] The radical chain process led to the aminohalogenation product 1-75 in moderate yields. The key of success for this reaction is the weak N-X bond which allows easy homolysis for imidyl radical formation, and

the facility of halogen transfer from N-X bond to carboradical. This strategy has barely been successful for other reagents containing N-H, N-C, N-O, N-N or N-F bond, because these bonds are either too strong for homolysis, or they can't act as an efficient group transfer reagent to the carboradicals.



Scheme 1.15 The proposed mechanism of photochemical aminohydroxylation of styrenes.



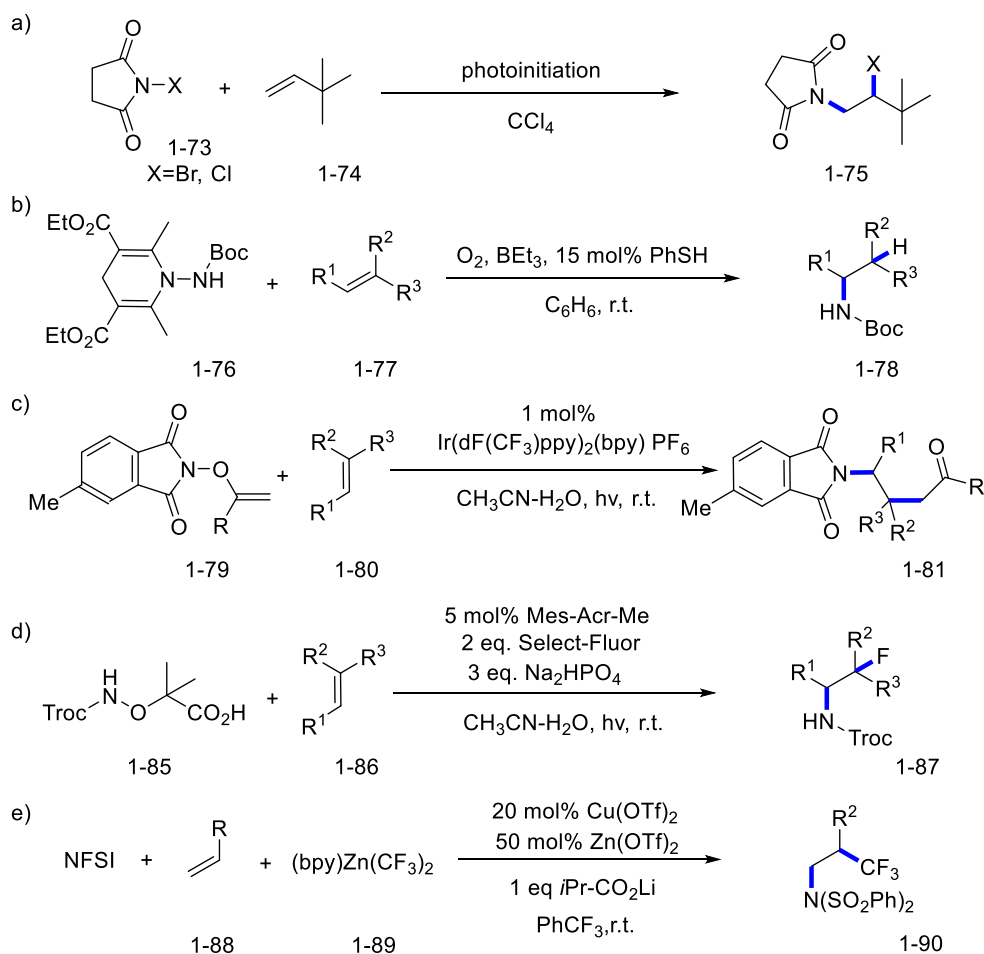
Scheme 1.16 The proposed mechanism of Cu-catalyzed enantioselective aminoarylation of styrenes.

To realize aminohydrogenation via radical chain pathway, Studer and coworkers devised N-aminated dihydropyridines 1-76 (Scheme 1.17b).^[77] By hydrogen abstraction on the methylene in 1-76, a carbon radical is generated and then aromatization occurs to form a pyridine and releases a Boc-protected N radical, which readily adds to alkenes. The thiophenol acts as a hydrogen transfer catalyst, which gives the hydrogen to the carboradical from the previous step and then is regenerated by abstracting a hydrogen from 1-76. Knowles and co-workers adopted photochemical PCET strategy to realize the intermolecular aminohydrogenation with sulfonamides.^[58] In their reaction thiophenol was also used as a hydrogen donor to quench the carboradicals. Recently, another effective radical chain was reported using a combination of N-hydroxyphthalimide with P(OEt)₃. N-hydroxyphthalimide acted as the hydrogen transfer reagent.^[78]

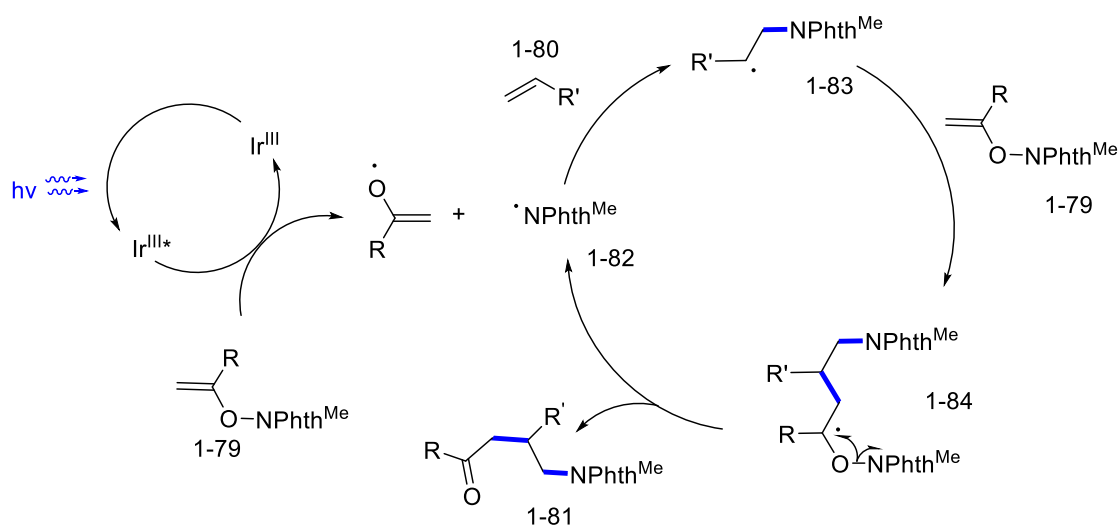
In 2019, Feng and co-workers achieved a radical aminocarbonation of unactivated alkenes with N-alkenoxypthalimide 1-79 (Scheme 1.17c).^[79] Although with Iridium photocatalyst, this reaction is likely to be a photoinitiated radical chain process instead of a photocatalytic process (Scheme 1.18). Energy transfer from the excited photocatalyst can activate 1-79 for the generation of imidyl radical 1-82. The imidyl radical adds to unactivated alkene 1-80, and then reacts with another molecule of 1-79. The obtained intermediate 1-84 undergoes fragmentation forms the product 1-81. An imidyl radical was released in the meantime to continue the radical chain.

A few other SOMOphiles were successfully applied to intercept the carboradical intermediates from unactivated alkenes. The Studer group used α -amino-oxy acids 1-85 for the photooxidative generation of Troc-protect N-radical (Scheme. 17d).^[80] The carboradicals from N-radical addition to alkenes was successfully trapped by Select-Fluor for the aminofluorination reaction. Trapping with electron-deficient alkenes^[81] and hypervalent iodine reagents^[82] were also reported based on the same system to realize the alkylation, alkynylation, alkenylation and cyanation.

The strategy of trapping the carboradical with a metal catalyst is highly underdeveloped so far. Li and co-workers reported the only reaction that combines transition metal catalysis with N-radical addition to unactivated alkenes.^[83] NFSI was used together with the bis(trifluoromethyl)zinc reagent 1-89 to effect an aminotrifluoromethylation reaction (Scheme 1.17e). The reaction mechanism is analogous to that in Scheme 1.16. Interestingly, the copper-catalysed cylation and arylation, which were achieved with activated alkenes (Scheme 1.14d&e), have not been realized so far with unactivated alkenes.



Scheme. 1.17 N-radical addition to unactivated alkenes for aminodifunctionalization reactions.



Scheme. 1.18 Proposed mechanism for the aminocarbonation of unactivated alkenes with N-alkenoxypthalimide.

1.5 N-hydroxyphthalimide esters as a source of alkyl radicals

Alkyl carboxylic acids are stable, highly naturally occurring organic compounds. They are usually less expensive and toxic compared with the alkyl halide analogues, and have attracted numerous interests in using them in coupling reactions.^[84] However, because of their stability, the decarboxylative activation of the acids is not easy. Oxidation of the carboxylates offers one attractive solution, which converts carboxylates into alkyl radicals via decarboxylation of carboxylic radicals.^[85, 86] Strong oxidants or oxidizing excited state of photocatalysts^[87, 88] can be used to enable this conversion. Preformation of redox active esters (RAE) plus single-electron reduction represents another solution which generates alkyl radicals in a milder and more controllable manner. In 1988, Oda and co-workers first demonstrated that the bench-stable N-hydroxyphthalimide (NHPI) esters could readily generate alkyl radicals via photoreduction and then decarboxylation.^[89] In the 2010s, due to the contribution of many research groups including Fu and Baran, the NHPI esters have become more and more prevalent in the development of coupling reactions.

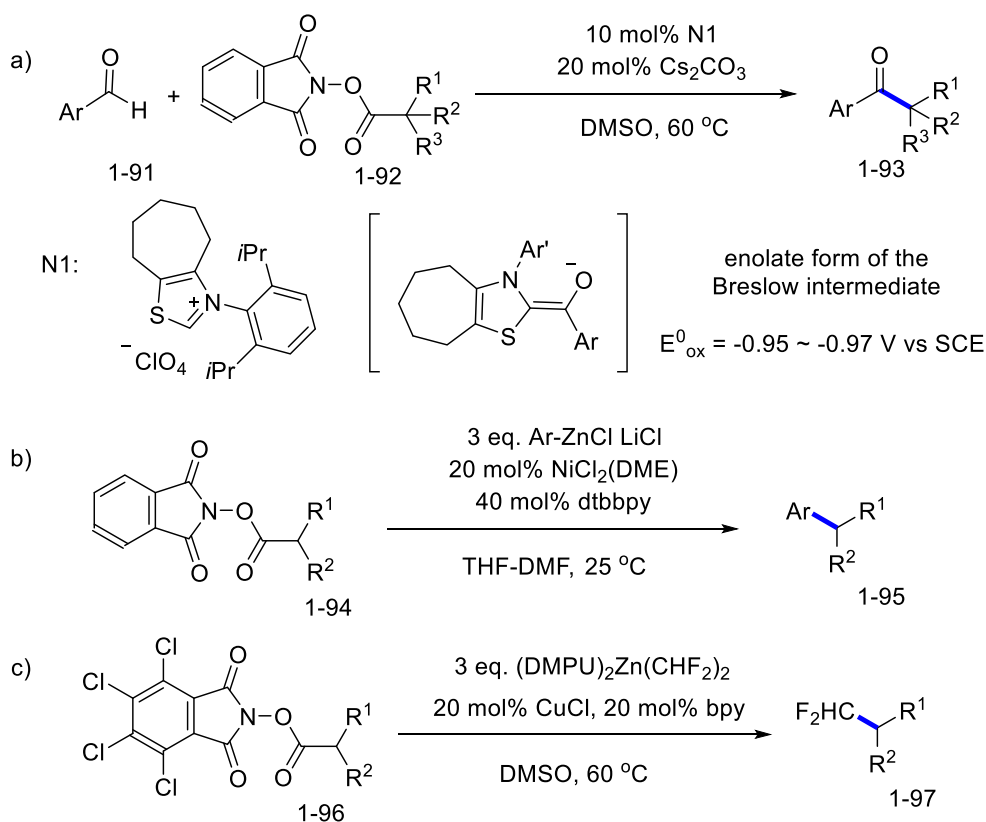
1.5.1 Direct reduction

The NHPI esters could be reduced directly by reductive intermediates to effect coupling reactions. In 2019, Ohmiya and co-workers reported an elegant procedure for coupling NHPI esters with aryl aldehydes (Scheme 1.19a).^[90] NHC carbene N1 was used as a catalyst which can form Breslow intermediate with aldehydes 1-91. After deprotonation, the Breslow intermediate becomes very reducing ($-0.95 \sim -0.97$ V vs SCE), and can reduce the NHPI ester 1-92 to give an alkyl radical. Based on a radical-radical coupling, a set of hindered arylalkylketones 1-93 could be obtained as products.

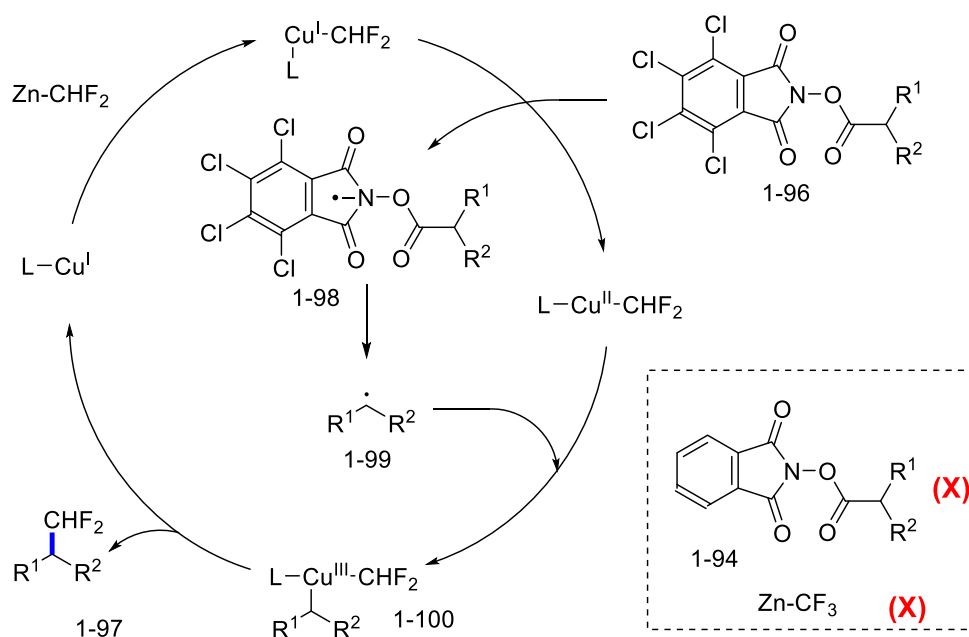
Compared to pure organic reductants, low-valent transition metal intermediates are more widely applied for the reduction of NHPI esters. The Baran group has developed a series of Ni-catalyzed coupling reactions based on NHPI esters, including sp^3 - sp , sp^3 - sp^2 , sp^3 - sp^3 C-C coupling and also C-B coupling.^[91-94] In these reactions low-valent Nickel reduces NHPI ester for the formation of alkyl radicals. For example, in the alkyl-aryl coupling in Scheme 1.19b, the Ni^I -Ar was considered to act as the reductant.^[92]

In a rare case, the low-valent Cu was reported to reduce the NHPI esters to achieve the difluoromethylation of alkyls (Scheme 1.19c).^[95] After ligand transfer from the zinc reagent, Cu^I - CHF_2 is formed which is reductive enough to transfer an electron to Cl_4 NHPI ester 1-96 (Scheme

1.20). The generated alkyl radical 1-99 will combine with the $\text{Cu}^{\text{II}}\text{-CHF}_2$ species to form a Cu^{III} intermediate. Reductive elimination from Cu^{III} delivers the difluoromethylated products 1-97. Notably, this reaction clearly showed a boundary for the reduction of NHPI esters (Scheme 1.20 right bottom). Using a less electron-rich trifluoromethyl zinc reagent would disable the reaction to happen. On the other hand, using a less electron-deficient NHPI ester 1-94 would also disable the reduction by $\text{Cu}^{\text{I}}\text{-CHF}_2$. This indispensable match between the redox potentials of substrates brings an obvious restriction for developing the coupling reactions of NHPI esters.



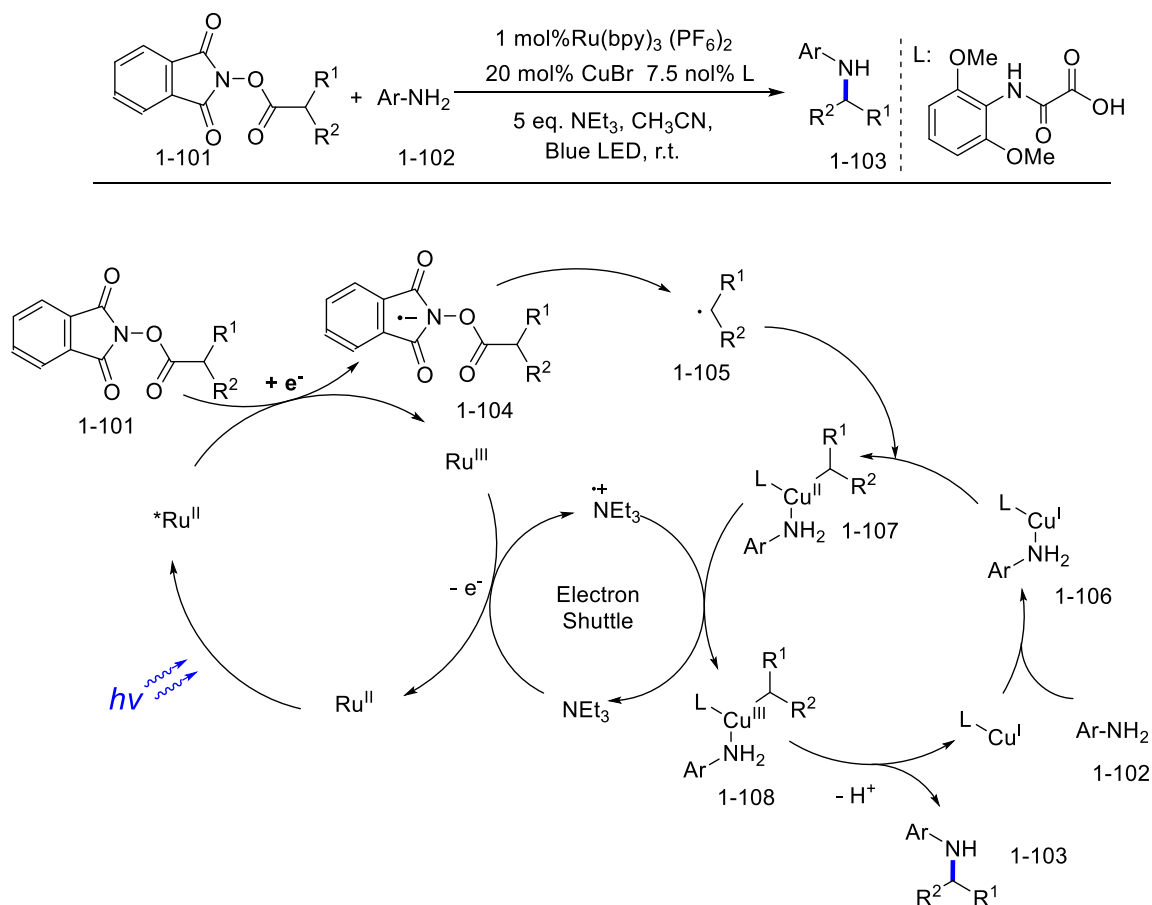
Scheme 1.19 Direct reduction of NHPI ester for coupling reactions.



Scheme 1.20 The proposed mechanism of Cu-catalyzed difluoromethylation of NHPI esters.

1.5.2 Photoreduction

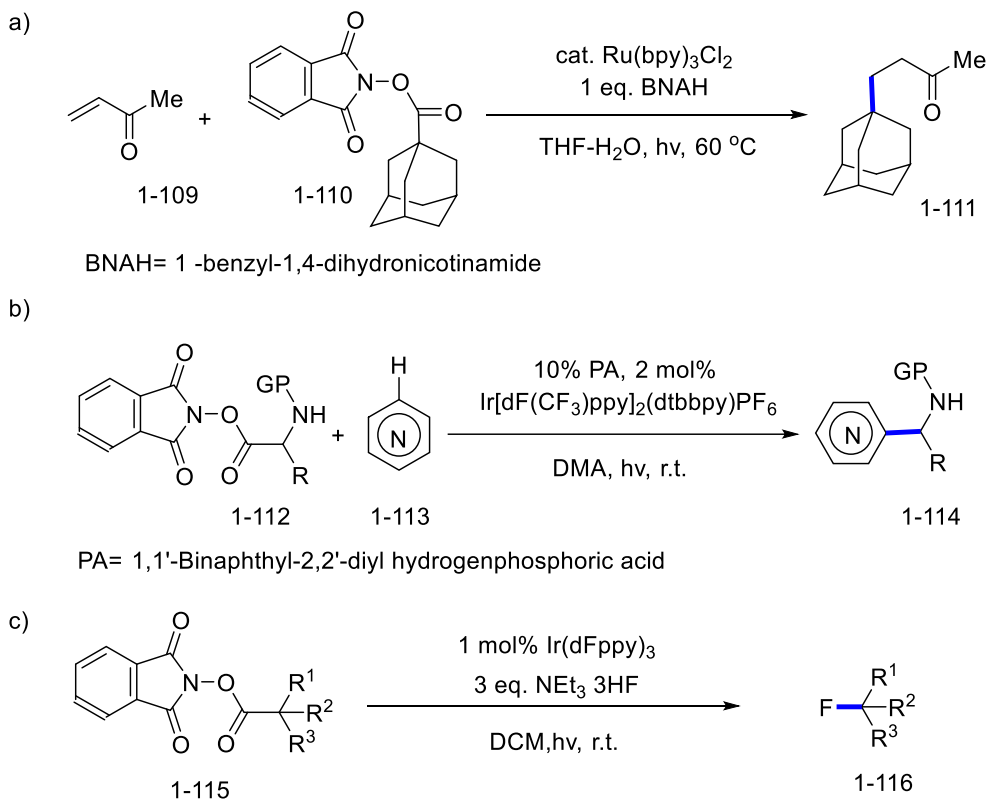
The introduction of photo catalysis to the reaction system can well resolve the problem above. The use of excited photocatalyst for the reduction of NHPI esters could relieve other reagents from the role of reductant, and thus enables more diverse reagents to couple with NHPI esters. In 2017, our group reported a decarboxylative C(sp³)-N cross coupling via dual photoredox and copper catalysis (Scheme 1.21).^[96] Various primary anilines 1-102 were coupled to NHPI esters 1-101 under mild conditions with good tolerance for functional groups. Based on mechanistic experiments and DFT calculations, a plausible mechanism was proposed as shown in Scheme 1.21 (bottom). The reaction starts by reducing 1-101 with the excited Ruthenium catalyst for the formation of alkyl radical 1-105. Then, the radical can be trapped by the Cu^I-NH₂-Ar complex 1-106 to give Cu^{II} intermediate 1-107, which was further oxidized to Cu^{III} by Ru^{III} yet via the mediation of triethylamine. The electron shuttle role of triethylamine is based on DFT calculation which showed a lower energy barrier of the electron shuttle process compared to the direct oxidation. Finally, reductive elimination for Cu^{III} intermediate forges the C-N bond. Without photocatalysis, this reaction could not be possible because the Cu^I-NH₂-Ar complex 1-106 does not possess the ability to reduce 1-101. Based on the same strategy, our group also realized the coupling of NHPI esters to imines and phenols.^[97,98]



Scheme 1.21 Proposed mechanism for dual photo- and copper-catalyzed coupling of NHPI esters with anilines.

With the easier access to alkyl radicals by photoreduction, many reactivities of NHPI esters are unlocked. Many reactions have been disclosed based on the trapping of the alkyl radicals by a SOMOphile. For example, the seminal work of Oda and co-workers demonstrated the addition of the alkyl radical to electron-deficient alkenes (Scheme 1.22a).^[99] This reaction is a good method to construct a new quaternary carbon center (in 1-111), which already found applications in total synthesis.^[100] The trapping by heterocycle is also possible.^[101] By oxidative rearomatization following the radical addition, this reaction provides efficient methods for alkylation of heterocycles (Scheme 1.22b). Recently, Doyle and co-workers showed another possibility with this radical intermediate. Through a direct oxidation by the oxidized photocatalyst, a carbocation was formed which is subsequently trapped by nucleophilic fluoride (Scheme 1.22c).^[102] Tertiary carboradicals and other carboradicals with a stabilizing group (aryl or heteroatoms) could be well converted to alkyl fluorides

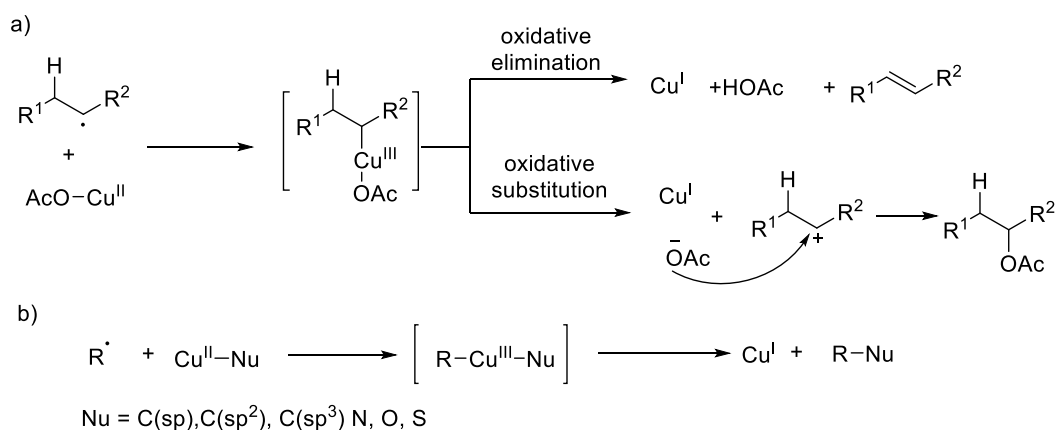
1-116. The efficiency of this reaction was also demonstrated by the installation of radioactive ^{18}F on the NHPI esters.



Scheme 1.22 Various reactions via alkyl radicals from the photoreduction of NHPI esters.

1.6 Copper-catalyzed functionalization of alkyl radicals

Transition-metal catalysis creates numerous possibilities for the functionalization of alkyl radicals.^[5,103,104] Over the years, many first-row transition metals have been applied for transformation of alkyl radicals into various products. Among these metals, copper has stood out as the most versatile catalyst, enabling the C(sp³) atom of the alkyl radical to connect to C(sp), C(sp²), C(sp³), N, O, S and halogen atoms.^[105] As early as in 1960s, Prof. J. Kochi and co-workers input tremendous efforts for the study of oxidation of alkyl radicals by Cu^{II} metal salts.^[106,107] This oxidation process in the presence of acetic acid generally led to two kinds of products: alkene and alkyl acetate. By detailed kinetic analysis, they established a reaction model for the reaction (Scheme 1.23a).^[106] First, alkyl radical adds to Cu^{II} to form Cu^{III}-alkyl species, which is the rate determining step. Then, the acetate can assist the elimination of a β-hydrogen to give the alkene product, acid and Cu^I (oxidative elimination). In a competing process, heterolysis gives Cu^I and a carbocation, which can be captured by the acetate or acetic acid to form the alkyl acetate (oxidative substitution). Polar solvent and substituents that stabilize the positive charge would favor the oxidative substitution process. Otherwise, oxidative elimination would predominate. Based on this chemistry, a lot of useful reactions were developed later on. In recent years, however, more and more reactions have been developed following the reaction mode in Scheme 1.23b.^[105] By radical addition to Cu^{II} and then reductive elimination from Cu^{III}, chemical bonds including C-C, C-N, C-O and C-S bonds were successfully constructed from alkyl radicals. These reactions have generally shown very good tolerance for functional groups. Compared to other transition metals like Ni and Pd, Cu catalysts hardly suffer from the side reaction of β-hydrogen elimination, unless certain ligands are intentionally used (e.g. carboxylate in the oxidative elimination process).



Scheme 1.23 General mechanism for copper-mediated functionalization of alkyl radicals.

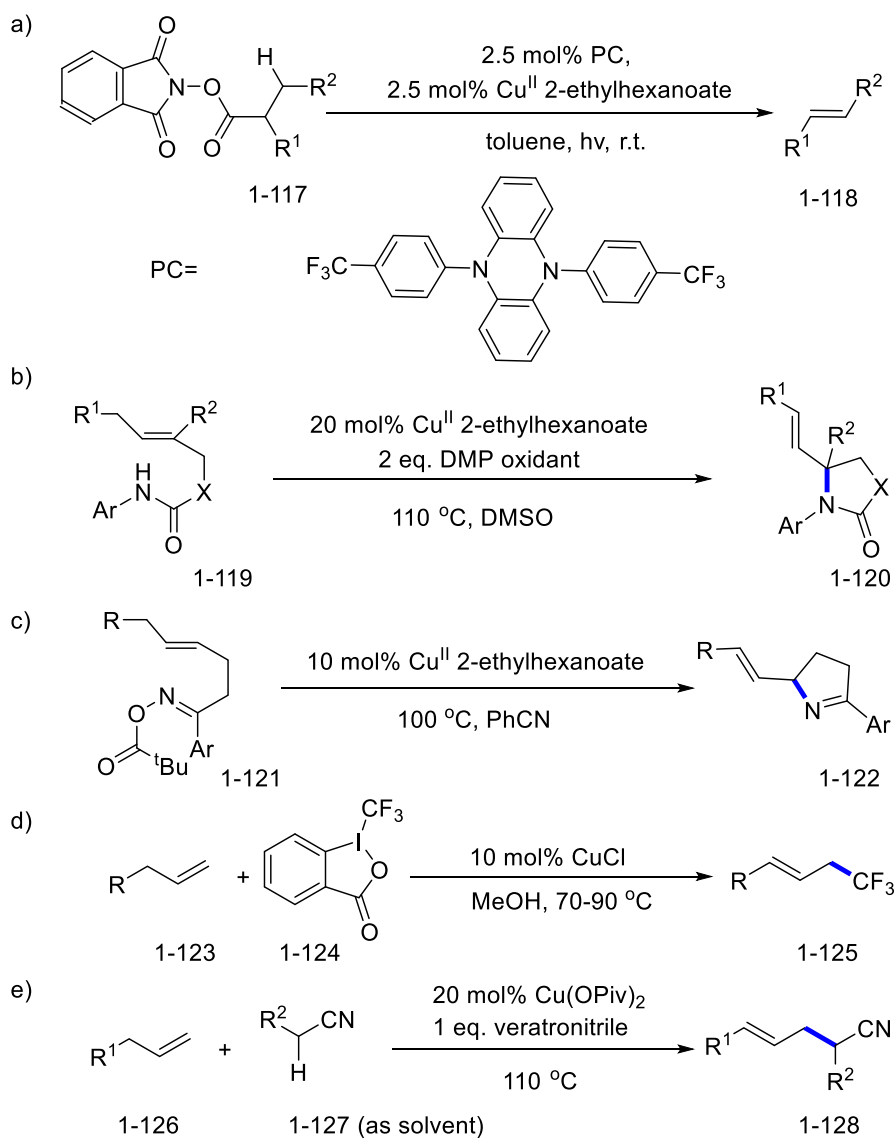
1.6.1 Oxidative elimination

C=C bond is one of the most useful functional groups for organic synthesis because numerous organic conversions are based on C=C bonds. In this regard, the Cu-catalyzed oxidative elimination is very important, because it transforms alkyl radicals, which can be generated in various manners, into alkenes. Indeed, many synthetic methods for alkenes have been developed based on this old chemistry.

In 2018, the Glorius utilized NHPI esters for the synthesis of alkenes via dual photo- and copper catalysis (Scheme 1.24a).^[108] The organic photocatalyst converts NHPI esters 1-117 into alkyl radicals under radiation. Then, the radicals are transformed into alkenes 1-118 by the Cu-catalyzed oxidative elimination. This method avoids the elevated temperature generally required by the existing methods and the isomerization problem (from terminal alkenes to internal alkenes) in the presence of transition metals. A wide range of inexpensive synthetic and biomass-derived carboxylic acids were applied in the reaction, showcasing good tolerance for functional groups.

Xu and co-workers took advantage of the amidyl radical cyclization process to generate alkyl radicals.^[109] With the incorporation of copper catalyst, the net result was the synthesis of a set of N-containing 5-member rings with pendant C=C bonds (Scheme 1.24b). Unfortunately, this reaction required a high reaction temperature (110 °C) and a strong Dess-Martin Periodinane to oxidize the N-H in 1-117 into an amidyl radical. In contrast, Bower and co-workers used N-acyloxyimine as a precursor for iminyl radical with copper catalysis under 100 °C (Scheme 1.24c).^[110] Their reaction provided an efficient approach to cyclic imines with pendant C=C bonds (1-122).

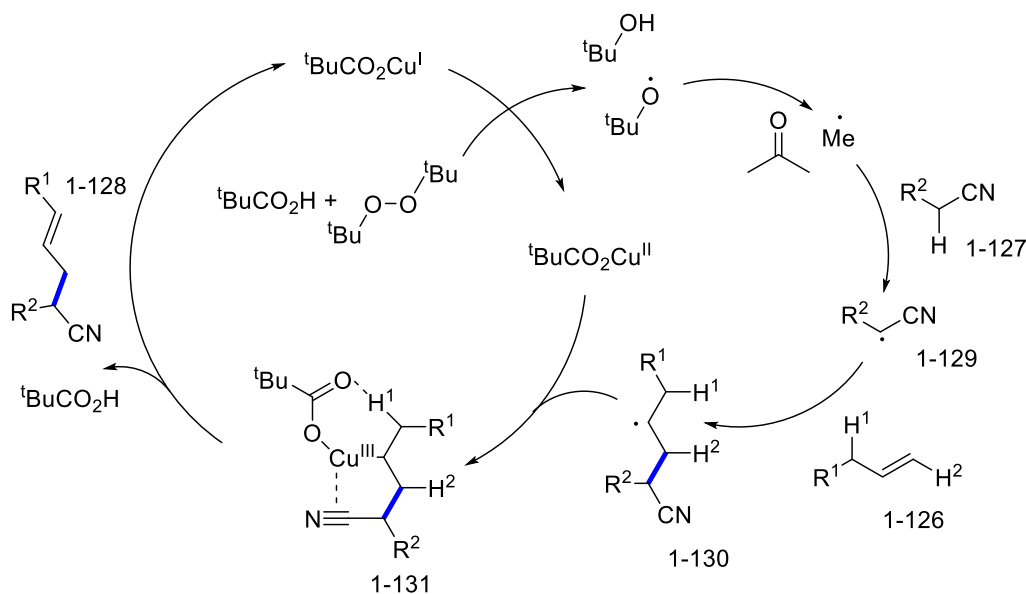
The trap of carboradicals generated by intermolecular radical addition is also possible with a copper catalyst for the oxidative elimination process. With different sources of trifluoromethyl radical, Liu, Wang and Buchwald respectively reported the copper-catalyzed allylic trifluoromethylation of unactivated alkenes.^[111-113] For example, the Buchwald group used the Togni reagent 1-124 as a source of trifluoromethyl radical to add to unactivated alkenes 1-123 (Scheme 1.24d).^[111] The copper catalyst is bifunctional in this reaction, activating 1-124 to release the trifluoromethyl radical and also mediating the oxidative elimination for the formation of a new C=C bond. This method allows the efficient preparation of allyl-CF₃ products that were difficult to access previously. Numerous functional groups could be tolerated under the mild reaction conditions.



Scheme 1.24 copper-catalyzed oxidative elimination of alkyl radicals generated in various ways.

In 2017, Dong and co-worker combined copper catalysis and addition of cyanoalkyl radicals to transform unactivated alkenes 1-126 into homoallylic nitriles 1-128 (Scheme 1.24e).^[114] A plausible reaction mechanism was proposed (Scheme 1.25), involving multiple radical intermediates. First, the O-O bond of the peroxide (DTBP) is cleaved with Cu^I to obtain a *tert*-butoxy radical, which can then fragment into acetone and methyl radical. The methyl radical is an active nucleophilic radical which can abstract hydrogen from the nitrile 1-127 to form an electrophilic cyanoalkyl radical 1-129. The intermediate 1-129 readily adds to olefin to give a new carboradical 1-130, which then leads to

the final product 1-128 via oxidative elimination. Notably, γ,δ -unsaturated nitriles 1-128 were exclusively obtained instead of β,γ -unsaturated nitriles. The coordination of cyano group to copper in 1-131 was considered as the reason behind this selectivity. As illustrated in the structure, the coordination makes the hydrogen H^2 at β position not accessible to the copper catalyst and thus the elimination of H^1 was privileged.



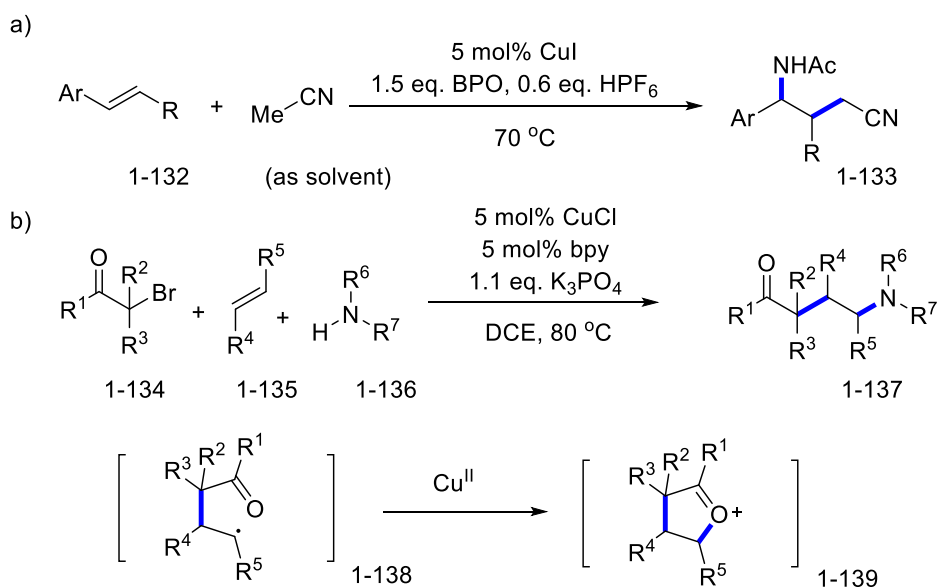
Scheme 1.25 The proposed mechanism for copper catalysis synthesis of γ,δ -unsaturated nitriles.

1.6.2 Oxidative substitution

Apart from oxidative elimination, the copper-mediated oxidative substitution of alkyl radicals is also used to construct useful reactions. This process requires the carboradicals which can lead to relatively stable cationic intermediates.^[115, 116] For example in Scheme 1.26a, Bao and co-workers also used the addition of cyanoalkyl radicals to olefins as in Scheme 1.24e.^[115] However, after radical addition to styrenes 1-132, the obtained benzyl radicals could readily be oxidized by Cu^{II} to benzyl cation. Then, the Ritter reaction with acetonitrile led to the synthesis of γ -amino butyronitriles 1-133.

In 2019, Hull and co-workers reported an procedure which realized the oxidative substitution of unactivated alkyl radicals (Scheme 1.26b).^[117] In their reaction, α -bromocarbonyl compounds were used to generate the electrophilic carbonylalkyl radicals, which can add to unactivated alkenes

to form 1-138. Although there are no strong stabilizing substituents adjacent to the radical, the carbonyl was believed to stabilize the carbocation by forming a cyclic oxonium intermediate 1-139. This enables a facile oxidation of 1-138 by the Cu^{II} . Then, 1-139 is quenched by an amine to finish this three-component assembly. This reaction is applicable to a broad scope of all the three reaction substrates. It works for both primary and secondary amines as nucleophiles, and it works also for activated alkenes in addition to unactivated alkenes.



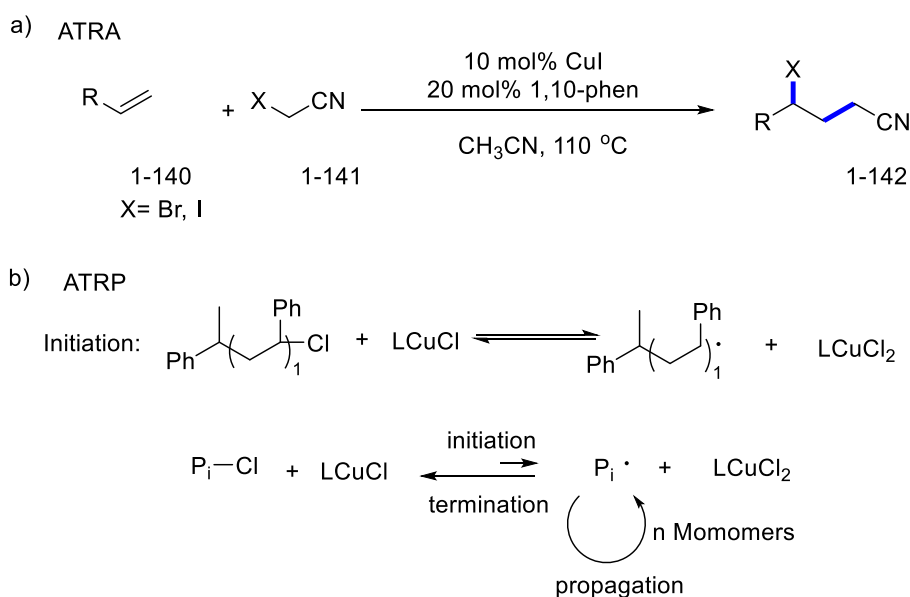
Scheme 1.26 copper-catalyzed oxidative substitution.

1.6.3 Atom transfer

Copper can mediate the formation of carbon-halogen bond through the atom transfer from $\text{Cu}^{\text{II}}\text{-X}$ ($\text{X} = \text{Cl}, \text{Br}, \text{I}$) to the alkyl radical. This method uses stable and easily available halides as a source of halogen atoms instead of electrophilic halogen reagents such as NBS. Because of these features, copper has been widely used in atom transfer radical reactions (ATRA).^[118, 119] For example in Scheme 1.27a, copper was used to catalyze the addition of α -halonitriles to alkenes.^[118] Cu^{I} abstracts a halogen atom from 1-141 to form $\text{Cu}^{\text{II}}\text{-X}$ and a cyanoalkyl radical. After the addition of the cyanoalkyl radical to olefins, $\text{Cu}^{\text{II}}\text{-X}$ quenches the formed alkyl radicals to obtain 1-142.

This reactivity of copper has a more significant application in the scenario of atom transfer radical polymerization (ATRP, Scheme 1.27b).^[120, 121] As was reported in the seminal work of the Matyjaszewski group,^[120] the Cu catalytic system delivered polystyrene with a narrow molecular

weight distribution $M_w/M_n < 1.5$. During the reaction, the molecular weight of the polymer increased in a linear manner with the reaction time or reaction conversion, indicating a controlled / 'living' radical polymerization process. The key reason contributing to the success of this reaction is the reversible initiation process, in which Cu^{I} abstracts Cl from a resting polymer chain to form the alkyl radical (Scheme 1.27b, top). The equilibrium is in favor of termination instead of initiation, thus the concentration of alkyl radical can be maintained at a low level and homocoupling of radical can be greatly suppressed (Scheme 1.27b, bottom). For each polymer-chain radical, it is able to incorporate several styrene monomers before being 'capped' by $\text{Cu}^{\text{II}}\text{-Cl}$, and later the capped polymer-chain can be activated by Cu^{I} and start incorporating monomers again. During the whole reaction course, one polymer-chain will be activated and deactivated multiple times, and in the end the number of monomers incorporated in one polymer-chain will be averaged statistically. This controlled radical polymerization process has been widely applied for synthesizing well-defined polymeric structures including block polymers.



Scheme 1.27 Copper-catalyzed atom transfer reactions

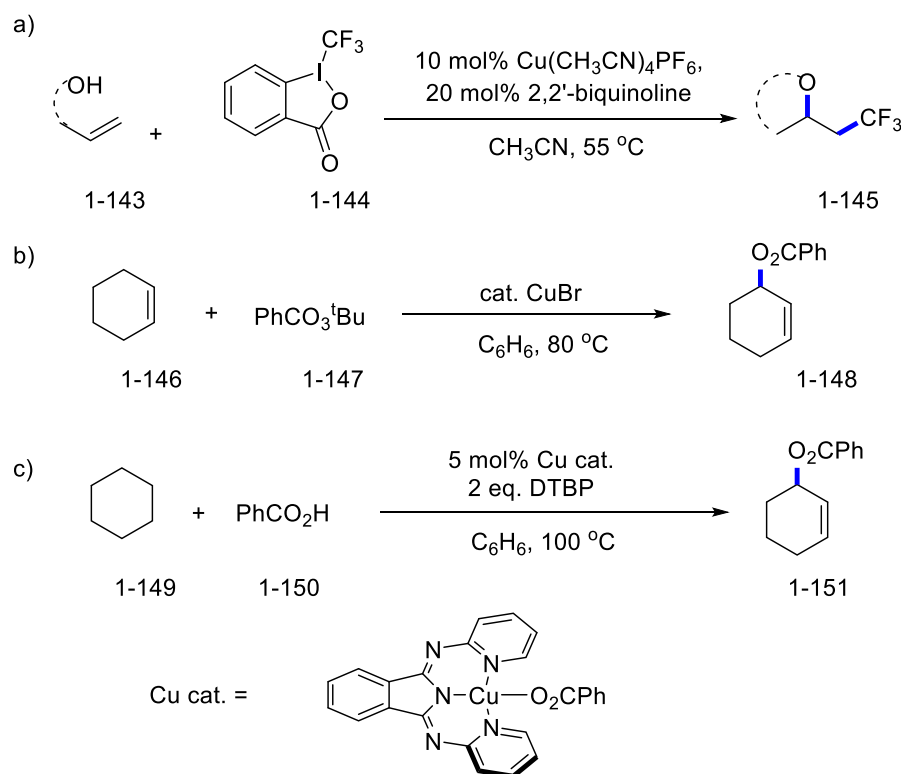
1.6.4 C(sp³)-O bond formation

Following the previous work of allylic trifluoromethylation of alkenes (Scheme 1.24d), Buchwald and co-workers further developed an oxytrifluoromethylation protocol for the synthesis of CF_3 -containing O-heterocycles (Scheme 1.28a).^[122] After the addition of CF_3 radical to the double bond, a carboradical could be formed. Then, the copper catalyst mediates the reaction of radical with the

intramolecular –OH for the formation of O-heterocycles, presumably via a Cu^{III} intermediate. This reaction was successfully applied to alcohols, phenols and acids as nucleophiles for the construction of 3 or 5-member rings. β -Lactone was also accessible, yet with obviously less efficiency than α -Lactones or γ -Lactones. Later, the enantioselective version of this reaction was reported with certain 4-pantenoic acids for the construction of optically pure γ -lactones.^[123]

Intermolecular formation of C-O from alkyl radicals was also realized in many reactions with copper catalysis.^[124] The seminal work in this regard was reported by Kharasch and Sosnovsky in 1959. They showed that the allylic oxidation of alkenes, e.g. cyclohexene (Scheme 1.28b), could be catalyzed by CuBr using *tert*-butyl perester as oxidant.^[125] Mechanistically, this reaction relied on the hydrogen abstraction by *tert*-butoxy radical to form an allylic radical. Then, copper mediated the construction of the C-O bond between the radical and nucleophilic benzoate. When an aliphatic acid was added to the reaction, the ester of this acid would be obtained instead of benzoate. Later in 1995, Pfaltz and co-workers discovered that the use of chiral bisoxazoline ligands in this system would lead to an enantioselective allylic oxidation reaction.^[126] This discovery not only increased the utility of the allylic oxidation process, but it also verified the role of copper catalyst for the formation of C-O bond.

In 2014, the Hartwig group reported that, using DTBP as oxidant, cyclohexane could be converted to allylic ester 1-151 (Scheme 1.28c).^[127] Detailed mechanistic studies were conducted for this reaction. Cyclohexene was considered as an intermediate obtained by sequential hydrogen abstraction by *tert*-butoxy radical and Cu-mediated oxidative elimination. Then, *tert*-butoxy radical transforms cyclohexane into allyl radical, which combines $\text{Cu}^{\text{II}}\text{-O}_2\text{CPh}$ to give 1-151. Competition experiments showed that the complex of Cu^{II} with more electron-rich carboxylate has a higher reaction rate with allyl radicals, and that the reaction of Cu^{II} -amidate is generally faster than that of Cu^{II} -benzoate. Unfortunately, this reaction did not work well for acyclic alkanes.



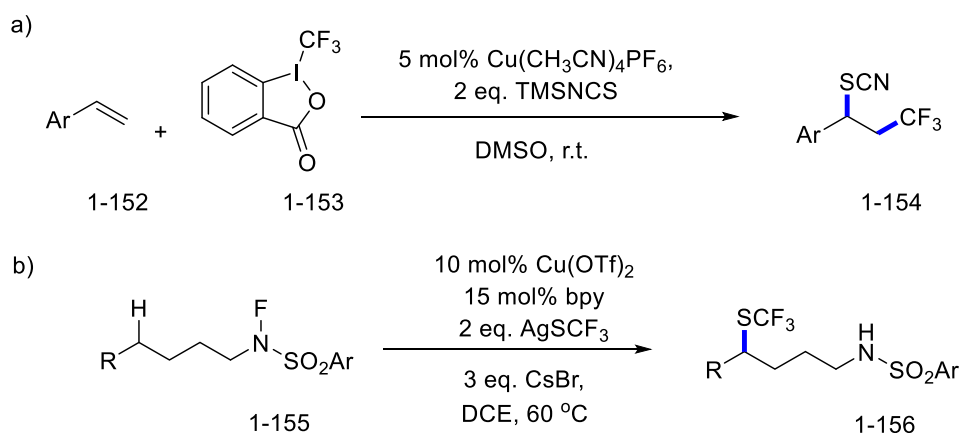
Schemes 1.28. Copper-catalyzed C-O formation with alkyl radicals

1.6.5 C(sp³)-S bond formation

Copper is also an effective catalyst promoting the C-S bond formation from alkyl radicals. In 2015, Liu and co-workers reported a protocol for the trifluoromethylthiocyanation of styrenes (Scheme 1.29a).^[128] The Togni reagent 1-153 was again used as a source of trifluoromethyl radical for the addition to styrenes. Then, a Cu^{II}-SCN species could trap the formed benzyl radicals to afford the final product 1-154. Interestingly, though trimethylsilyl isothiocyanide was used, the thiocyanides were exclusively obtained instead of isothiocyanides. This suggests that the copper catalyst possibly has a higher affinity to S than N in isothiocyanide anion. Later in 2020, the Studer group realized a copper-catalyzed benzylic C-H thiocyanation with NFSI as oxidant and also trimethylsilyl isothiocyanide.^[129] This reaction verified the viability of the functionalization of benzylic radicals by Cu^{II}-SCN.

Functionalization of unactivated alkyl radicals is possible with trifluoromethylsulfide reagents (Scheme 1.29b).^[130] Cook and co-workers took advantage of N-F reagents 1-155 for remote C-H abstraction via sulfonamidyl radical to generate an alkyl radical. Then, capture of the radical by Cu^{II}-SCF₃ led to the trifluoromethylthiolation product 1-156. AgSCF₃ was used as a stable source of

SCF₃ and CsBr acted as an activating reagent to combine Ag⁺ and release ⁻SCF₃. The same conditions could also be applied for the trifluoromethylselenation. This reaction took place under mild conditions and showed very good tolerance for different functional groups.



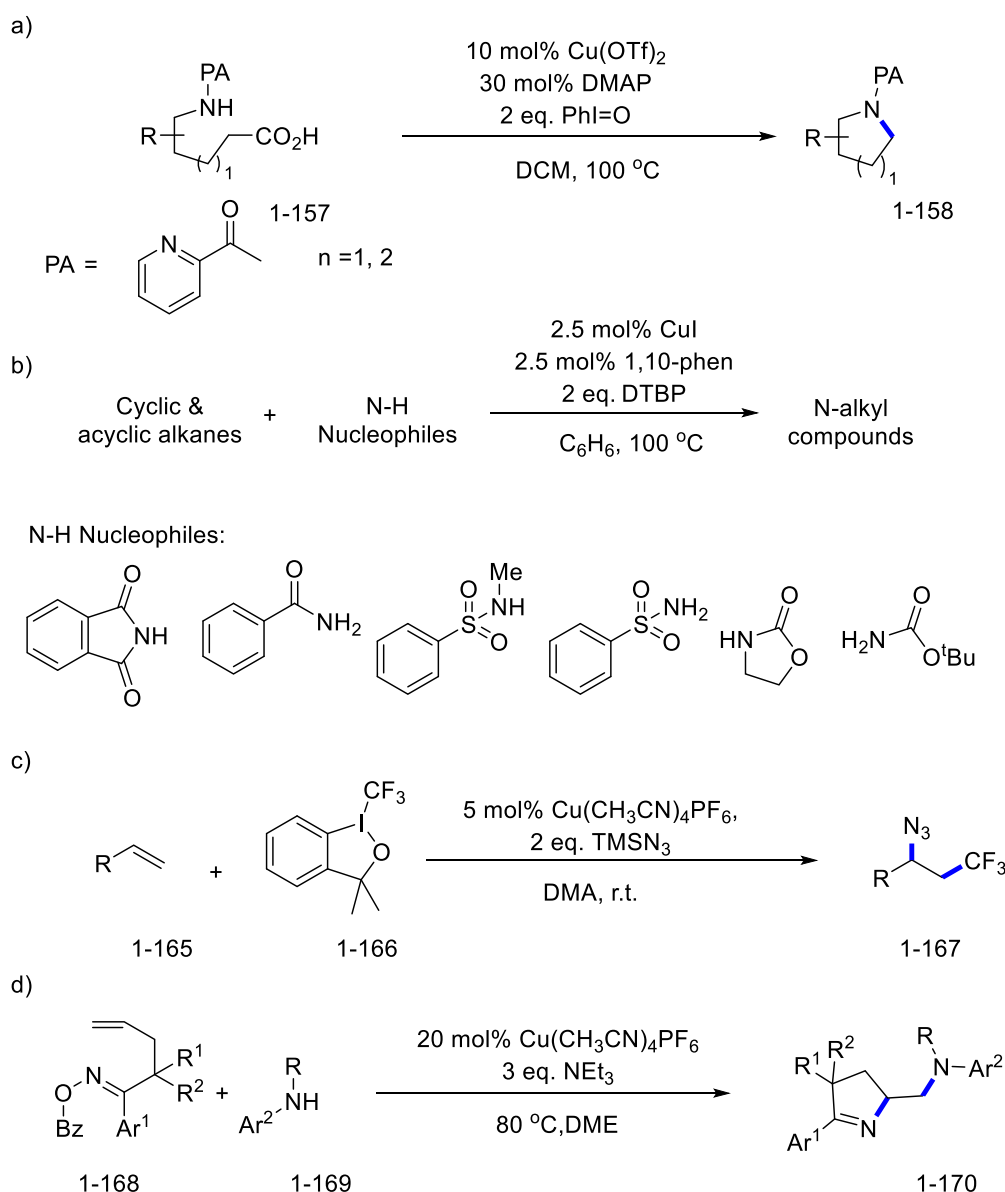
Schemes 1.29 Copper-catalyzed C-S formation with alkyl radicals.

1.6.6 C(sp³)-N bond formation

Copper-catalyzed functionalization of alkyl radicals with N-nucleophiles is a good method to forge C(sp³)-N bonds. Various nucleophiles could be applied. In 2016, the Y. Fu group reported an elegant reaction, using an intramolecular N-H to trap the alkyl radical intermediates for the synthesis of pyrrolidine and piperidine derivatives 1-158 (Scheme 1.30a).^[131] The picolinoyl (PA) as a directing group to strengthen the affinity of copper to N nucleophile was indispensable in the reaction. The use of benzoyl protected amines would lead to only trace amount of the product. This reaction relied on the PhI=O to oxidize the acid for the generation of the alkyl radical, which was then trapped by the Cu^{II} on the directing group to give a Cu^{III} intermediate. The reductive elimination furnished N-heterocycles as products. Liu and co-workers used urethane as an intramolecular nucleophile. In combination with a chiral phosphoric acid, multiple interactions were established between the urethane and copper catalyst in the resting state.^[132] The intramolecular trapping of the alkyl radical by the copper catalyst led to an enantioselective aminotrifluoromethylation reaction.

For intermolecular reactions, amides can also be used as nucleophiles. The Hartwig group applied the conditions of the C-O coupling (Scheme 1.28c) to N-nucleophiles, and found that many N-H reagents, including benzamides, sulfonamides, carbamates and phthalimide, could be used for the efficient oxidative coupling with cyclic & acyclic alkanes.^[133] Both (phen)Cu^I(phth) 1-159 and

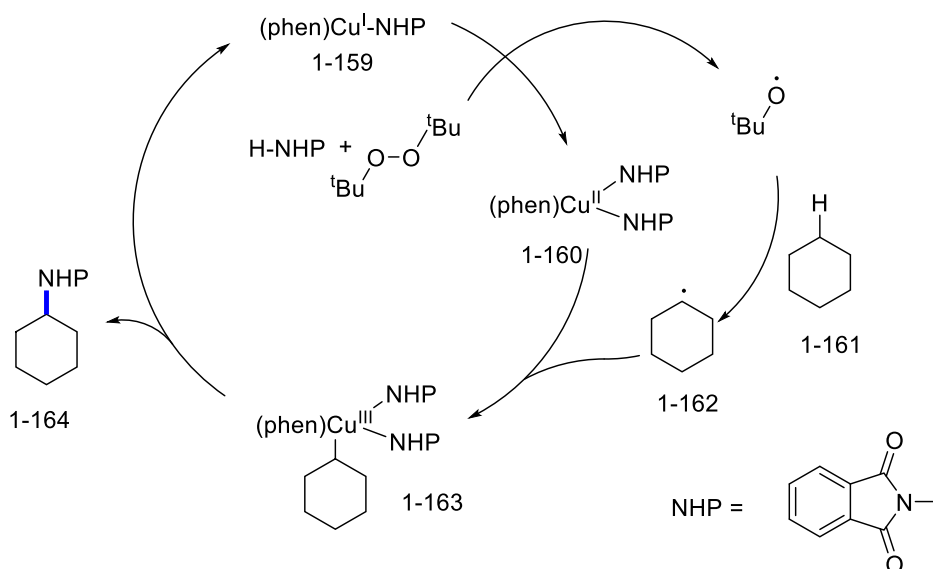
(phen)Cu^{II}(phth)₂ 1-160 were synthesized and were found as potential intermediates in the reaction (Scheme 1.31). In this reaction, 1-159 induces the generation of *tert* butoxy radical which activates the C-H in alkane to give alkyl radical 1-162. 1-160 acts as a trap for alkyl radicals, and leads to the C-N coupling product via a Cu^{III} intermediate 1-163. Notably, the preference for C-H bond in the reaction is secondary > primary > tertiary. Despite the lowest bond strength of tertiary C-H, the obtained tertiary alkyl radical is too hindered to combine efficiently with the copper catalyst. Actually, this hindrance effect can be observed in most reactions involving copper-catalyzed alkyl radical functionalization.



Schemes 1.30 Copper-catalyzed C-N formation with alkyl radicals.

By using trimethylsilyl azide as a nucleophile, Liu and co-workers extended the trifluoromethylthiocyanation in Scheme 1.29a to a trifluoromethylazidation reaction (Scheme 1.30c).^[134] Notably, in this case not only activated alkenes but also unactivated alkenes could be applied. The Studer group and the Zhu group also managed to use trimethylsilyl azide in other azidation reactions of alkyl radicals.^[135, 136]

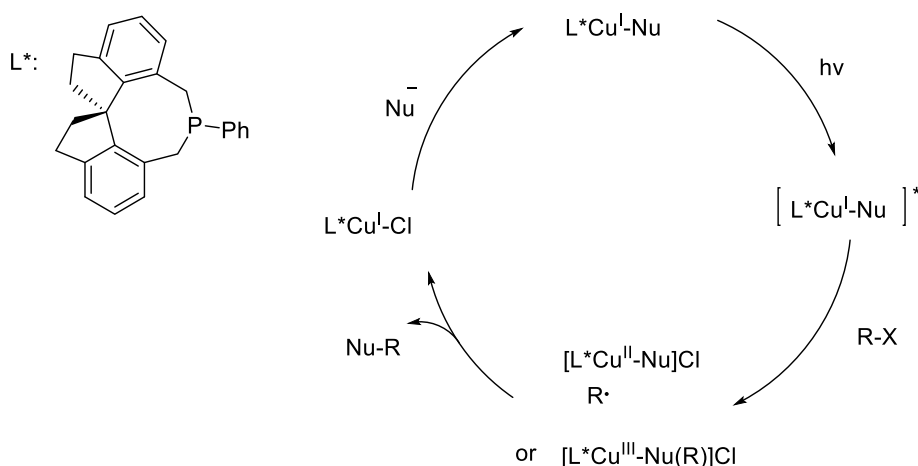
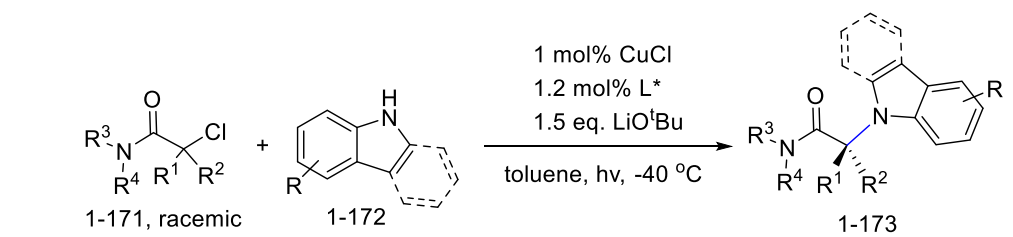
Compared to nitrogen in amides or imides, the nitrogen in aniline is more electron rich and have very different reactivities. Fortunately, this copper-catalyzed reaction is general enough to be also applied to anilines as nucleophiles, as is already demonstrated in Scheme 1.21. Wang and co-workers used iminyl radical cyclization to form an alkyl radical, which was also successful coupled to an aniline and led to the diamination product 1-170 (Scheme 1.30d).^[137] Besides, our group reported one example using imines as nucleophiles,^[97] but so far simple amines have not been applied in this reaction.



Schemes 1.31 The proposed mechanism of Copper-catalyzed oxidative coupling between alkanes and amides.

In 2016, Fu and co-workers reported an asymmetric copper-catalyzed C-N cross-coupling reaction, which is worth special attention (Scheme 1.32).^[138] Almost all the reactions in Section 1.6 involve nucleophilic alkyl radicals for copper-mediated functionalization. However, in this reaction electrophilic alkyl radicals were used and the bulk of the tertiary alkyl radical is also out of norm. The proposed mechanism is shown (Scheme 1.32 bottom). After the ligand substitution with the nucleophile, the $\text{Cu}^{\text{I}}\text{-Nu}$ can be excited with light absorption, which makes it reducing enough to

transform the chloride 1-171 into a radical intermediate. Then, the recombination of the alkyl radical with the $\text{Cu}^{\text{I}}\text{-Nu}$ complex leads to the C-N coupling product. The radical pathway enables the use of racemic substrates to convergently synthesize optically pure product 1-173. The capability to use an electrophilic alkyl radical is possibly related to the use of indoles or carbazoles as coupling partners, which are relatively electron-rich N-nucleophiles.



Schemes 1.32 Copper-catalyzed C-N formation with electrophilic alkyl radicals.

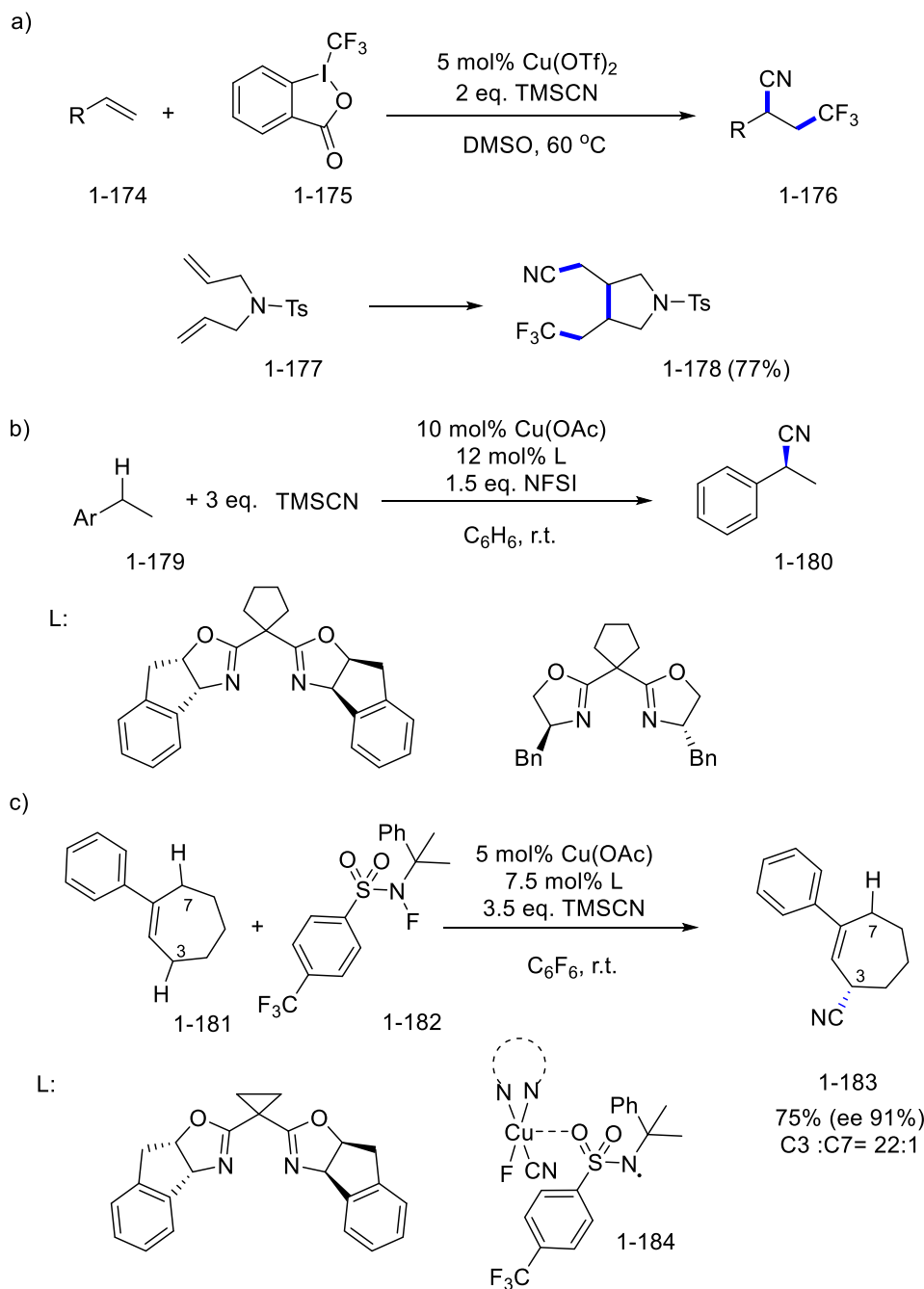
1.6.7 $\text{C}(\text{sp}^3)\text{-C}(\text{sp})$ bond formation, cyanation and alkynylation

Copper catalysts not only mediate the carbon-heteroatom bond formation of alkyl radicals, they can also forge carbon-carbon bonds. The initial effort in this regard was the cyanation reaction with trimethylsilylcyanide as nucleophile. In 2013, Liang and co-workers reported a trifluoromethylcyanation reaction of olefins with Togni reagent (Scheme 1.33a).^[139] This reaction converted a set of activated & unactivated alkenes 1-174 to useful CF_3 -containing nitriles 1-176. In the proposed mechanism, the reaction relied on the addition of CF_3 radical to alkenes to form a new alkyl radical. Then, oxidation by Cu^{II} formed a carbocation which was later trapped by the cyanide as a nucleophile (oxidative substitution mechanism). In my opinion, the direct trap of alkyl radical by $\text{Cu}^{\text{II}}\text{-CN}$ is also a plausible pathway, because 1-177 also led to the product 178 in good yield. The CF_3 radical

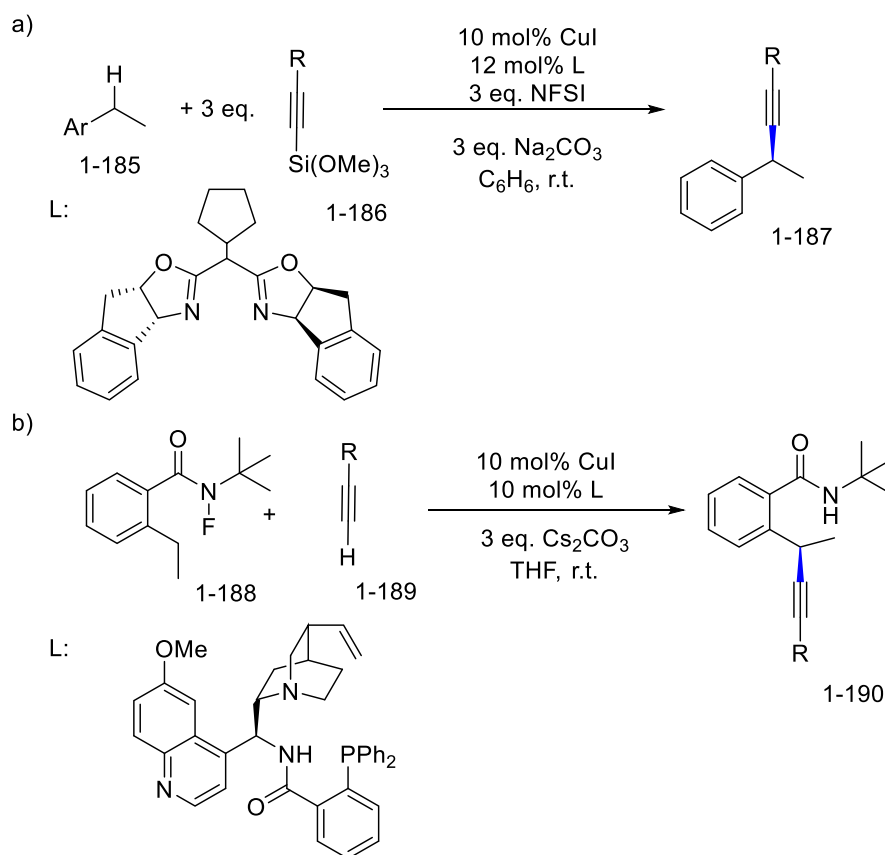
addition to 1-77 and then cyclization gives a primary carboradical, which is, in principle, difficult for a direct oxidation to carbocation.

Later in 2016, Liu, Stahl and co-workers made a groundbreaking report on the enantioselective cyanation of alkyl radicals (Scheme 1.33b).^[140] Benzylic C-H was transformed into benzylic radical with NFSI. Then, the addition to a chiral Cu^{II}-CN complex led to Cu^{III} intermediate, which reductively eliminated to obtain the chiral alkyl cyanides. The bisoxazoline ligands were the best ligands to induce the chirality in the products. Two representative ligands are displayed (Scheme 1.34b bottom), which led the opposite enantioselectivity for the product formation. In 2019, the Liu group further extended this protocol for a site-specific enantioselective allylic C-H bond functionalization, which is a state of art (Scheme 1.34c).^[44] In the substrate containing several allyl C-Hs, for example in 1-181, the ratio of cyanation at C3 and C7 can be up to 22:1, with a carefully selected hindered N-F reagent 1-182. In the meantime, good enantioselectivity was also realized. Mechanistic experiments and DFT studies revealed a Cu-bound N-centered radical for the abstraction of allylic C-H, which was very sensitive to electronic and steric factors. Besides these two reports, some other copper-catalyzed cyanations of alkyl radicals were also reported, with different ways of radical generation.^[141-143]

Alkynes are isoelectronic to cyanides. The enantioselective alkynylation of benzylic radicals was independently realized by the G. Liu group and the X. Liu group. The G. Liu group used alkynyl silanes 1-186 and similar conditions as in Scheme 1.33b, though 3 equivalent of base was necessary for the activation of the 1-186 (Scheme 1.34a).^[144] A *gem*-monosubstitution on the center carbon of the bisoxazoline ligand was found to provide better enantioselectivity than *gem*-disubstitution. The X. Liu group, on the other hand, took advantage of a chiral cinchona alkaloid-based N,N,P-ligand for the enantioselective introduction of alkynyl on benzylic C-H (Scheme 1.34b).^[145] Their reaction relied on an intramolecular hydrogen abstraction for the generation of benzylic radicals. A range of alkyl and (hetero)aryl alkynes, propargylic C(sp³)-H and (hetero)benzylic C-H bonds were all applicable.



Schemes 1.33 Copper-catalyzed cyanation of alkyl radicals.



Schemes 1.34 Copper-catalyzed alkylation of alkyl radicals.

1.6.8 C(sp³)-C(sp²) bond formation, arylation and polyfluoroarylation

The G. Liu group also extended the copper catalytic system to C(sp³)-C(sp²) coupling reactions of alkyl radicals. In 2014, they applied aryl boronic acids as nucleophiles for the trifluoromethylarylation of both activated and unactivated alkenes (Scheme 1.35a).^[146] A mutual activation of the ether-type Togni reagent 1-192 and aryl boronic acids was disclosed to be essential. The transmetalation of the aryl boronic acids might be the rate-determining step of this reaction. In order to match with the relatively slow transmetalation step, the use of a less active Togni reagent 1-192 was necessary to provide effective conversions. Later in 2017, an enantioselective version of this reaction was realized with an oxazoline ligand by the same group.^[147] This was the first enantioselective arylation reaction of benzyl radicals. However, the application to unactivated alkyl radicals was still challenging. Besides, the Liu group also used other methods to generate the benzyl radical, such as hydrogen abstraction with the use of NFSI (Scheme 1.35b).^[148] The benzyl radicals

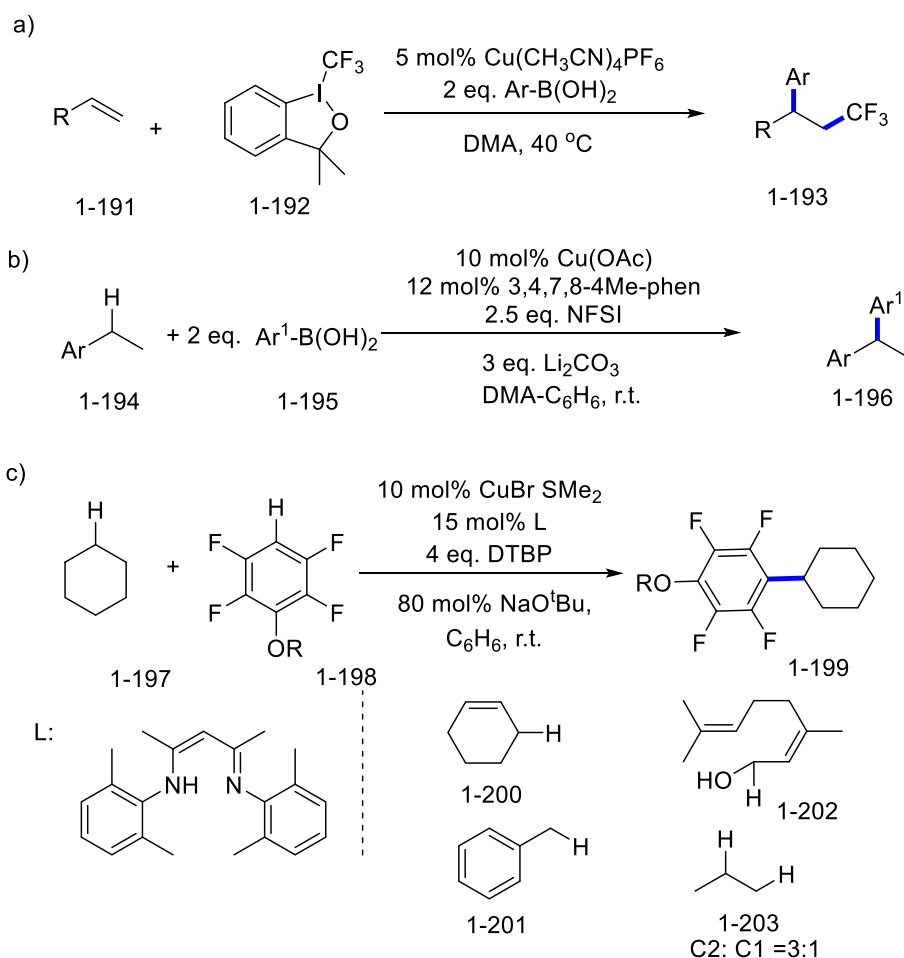
formed under these conditions were arylated to give 1,1-diarylalkanes 1-196 in the presence of a phenanthroline ligand. The chiral oxazoline ligands showed low efficiency in this reaction.

Polyfluoroarenes are important organic structures for their applications in the field of pharmaceuticals and materials. Compared to simple aryls, polyfluoroaryls displayed very different reactivity due to the fluoro substitutions. In organometallic compounds, the electron-withdrawing effect of fluoro substitutions renders a relative strong M-Ar_F bond which is reluctant to break to form organic products. As a result, in a conventional metal-catalyzed arylation reaction, the reaction scope has hardly been seen to extend to polyfluoroaryls. Copper could be a good candidate as catalyst in this scenario. In 2020, Chang and co-workers reported an oxidative coupling between alkanes and polyfluoroarenes (Scheme 1.35c).^[149] The DBTP was used as a source of *tert*-butoxy radical for generation of alkyl radicals via hydrogen abstraction of alkanes. The sodium *tert*-butoxide was used to activate the C-H on Ar_F-H to form the Ar_F-Cu species. Then, the trap of the alkyl radical by the Cu^{II}-Ar_F led to a Cu^{III} intermediate, which gave the coupling product 1-199 via reductive elimination. The β-diketimine ligand was found to be the only ligand to effectively suppress the homocoupling of the polyfluoroarenes. The scope of this reaction was very broad in terms of alkanes. In addition to cyclic unactivated alkanes 1-197, the benzylic C-H 1-200 and allylic C-H 1-201 are also suitable reaction sites. Interestingly, the C-H adjacent to heteroatoms, e.g. 1-202, can also be selectively coupled to polyfluoroarenes. Several acyclic alkanes were applied, yet the site selectivity of C-H activation turned out to be a problem. For example, with propane 1-203 as substrate, the ratio of reaction on C2 versus C1 was 3:1. Based on the same strategy, Chang and co-workers also utilized silyl-protected enols (derived from ketones) as providers of sp³ C-H to couple with polyfluoroarenes. The net result was the formation of β-aryl carbonyl products from ketones.^[150]

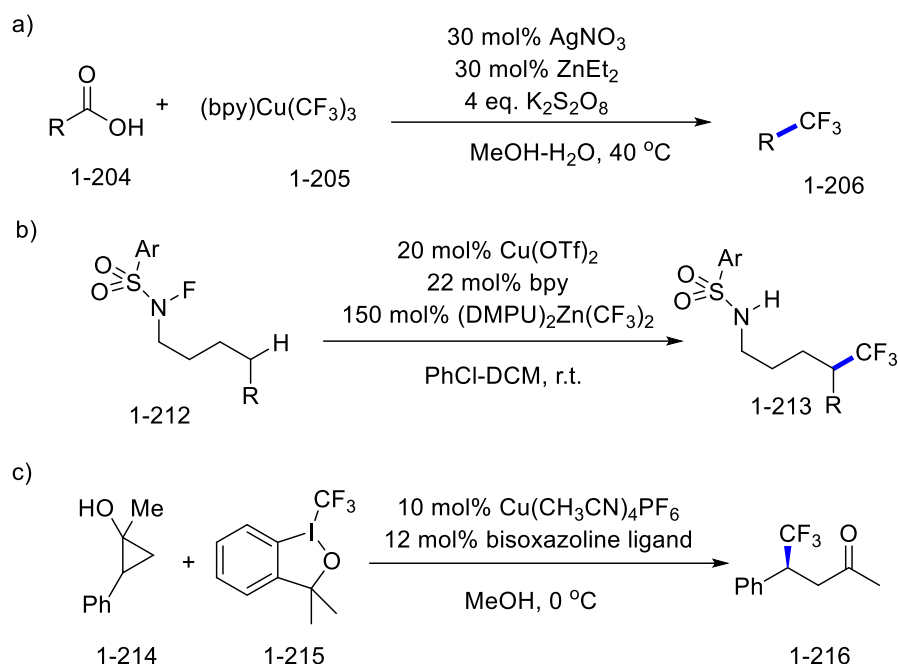
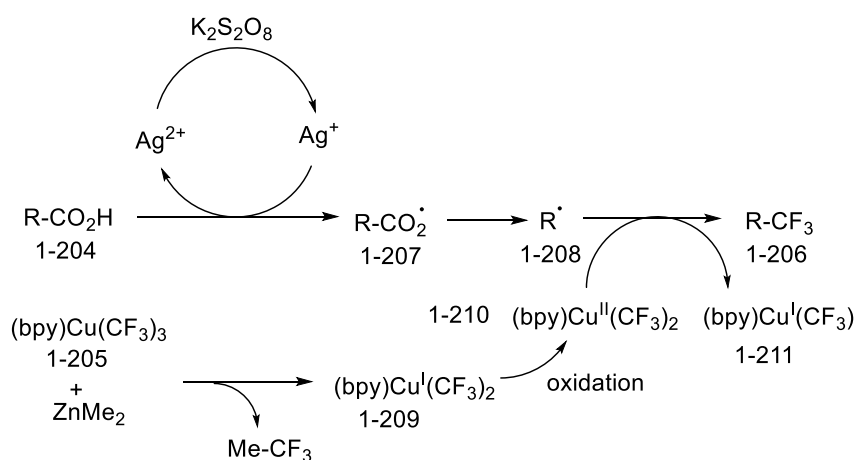
1.6.9 C(sp³)-C(sp³) bond formation, polyfluoroalkylation

The copper-mediated C(sp³)-C(sp³) bond formation of alkyl radicals is so far limited to polyfluoroalkylation. In Scheme 1.19c, a difluoromethylation process is already described. For trifluoromethylation, the Li group has pioneered in using nucleophilic CF₃ reagents for the functionalization of alkyl radicals. In 2017, they used (bpy)Cu(CF₃)₃ as a source of CF₃ for the decarboxylative trifluoromethylation of aliphatic acids 1-204 (Scheme 1.36a).^[151] Copper was used as a stoichiometric reagent instead of a catalyst, but still it played a central role in the C-C bond formation. The proposed mechanism of this reaction is shown in Scheme 1.37. AgNO₃ acts as a catalyst for oxidizing the acids to form alkyl radicals 1-208 with K₂S₂O₈ as terminal oxidant. On the other hand,

(bpy)Cu^{III}(CF₃)₃ can react with ZnMe₂ to give (bpy)Cu^I(CF₃)₂ with the release of Me-CF₃. Then, (bpy)Cu^I(CF₃)₂ is oxidized to (bpy)Cu^{II}(CF₃)₂, which traps the alkyl radical 1-208 for the formation of 1-206. Later in 2019, the same group used the zinc reagent (DMPU)₂Zn(CF₃)₂ to replace the copper reagent 1-205, and thus copper could be used in catalytic amount (Scheme 1.36b).^[152] A set of δ -trifluoromethylated sulfonamides were synthesized by sequential 1,5-hydrogen abstraction of N-radicals and Cu-mediated CF₃-transfer to alkyl radicals.

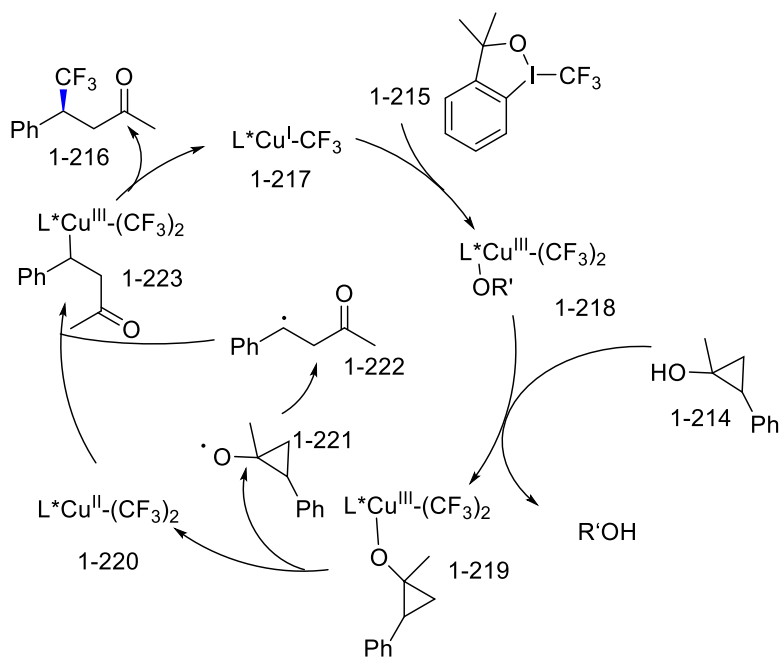


Schemes 1.35 Copper-catalyzed C(sp³)-C(sp²) bond formation of alkyl radicals.

**Schemes 1.36** Copper-catalyzed trifluoromethylation of alkyl radicals**Schemes 1.37** The proposed mechanism of decarboxylative trifluoromethylation with (bpy)Cu(CF₃)₃

Apart from nucleophilic CF₃ reagents, electrophilic CF₃ reagents were also used for CF₃ transfer to alkyl radicals.^[153, 154] In 2020, Liu and co-workers used ether-type Togni reagent 1-215 to react with cyclopropyl alcohols 1-214, leading to an enantioselective ring-opening trifluoromethylation reaction (Scheme 1.36c). In the proposed mechanism (Scheme 1.38), the Togni reagent 1-215 can oxidatively add to the Cu^I to form the Cu^{III} intermediate. The Cu^{III} intermediate 218 undergoes ligand exchange with alcohol 1-214, and then the homolysis of the Cu^{III}-O bond leads to Cu^{II}-CF₃ and alkoxy

radical 1-221 in the meantime. 1-221, after radical ring opening, recombines $\text{Cu}^{\text{II}}\text{-CF}_3$ for the generation of 1-216. Despite the opposite polarity of CF_3 reagents, $\text{Cu}^{\text{II}}\text{-CF}_3$ was always considered as the key intermediate for the functionalizations of alkyl radicals.



Schemes 1.38 The proposed mechanism for enantioselective ring-opening trifluoromethylation of cyclopropanols.

1.7 The goal of the thesis

In recent 10 years, electrochemical and photochemical methods have become more and more popular in organic synthesis. They can incorporate photoenergy or electric energy into the reaction system, so as to transform stable functional groups into active radical species in a mild and controllable manner (Section 1.2&1.3). A diverse set of radicals could be generated with these methods without strong oxidants or reductants. Copper is a versatile transition metal that can mediate the formation of various chemical bonds from alkyl radical (Section 1.6). However, so far the reactions combining electrochemistry and photochemistry with copper-catalyzed carboradical functionalization are still highly underdeveloped. Therefore, we have aimed to explore the chemical space lying within the intersection of electrochemistry and photochemistry with the copper chemistry, to discover interesting and useful reactions.

Due to the importance of nitrogen-containing compounds, the addition of N-centered radical to alkenes has attracted substantial attention as an approach to aminating alkenes. Electrochemical oxidation readily generates N-radical from N-H for cyclization to intramolecular double bonds (Section 1.4.2.1). The resultant carboradical has never been functionalized with a transition metal catalyst, which possibly leads to various products. Herein, we want to use copper to mediate the oxidative elimination of this radical (Section 1.6.1). If successful, a formal aza-Wacker reaction could be developed which potentially has different reaction features with the conventional palladium-catalyzed methods.

The combination of intermolecular N-centered radical addition to alkenes (Section 1.4.3&1.4.4) with copper catalysis is even more interesting than the intramolecular version, because it assembles more molecules together for building up complex structures. So far, copper-catalyzed aminocyclization (Scheme 1.14c), aminoarylation (Scheme 1.14d) and aminotrifluoromethylation (Scheme 1.17e) were reported for alkenes, and among these reactions only $\text{Cu}^{\text{II}}\text{-CF}_3$ was reported to functionalize the less stable carboradicals from the addition of N-radical to the unactivated alkenes. Without a stabilizing group, the alkyl radicals have a shorter lifetime and thus entail a more effective trapping by copper catalyst. We want to combine the addition of N-radical to unactivated alkenes with copper catalyzed oxidative elimination. This strategy would potentially provide a new approach from unactivated alkenes to allylamines. The radical nature would enable this reaction to have very good functional group tolerance.

Apart from oxidative elimination, copper has also been reported to mediate the coupling of alkyl radicals with many other nucleophiles (Section 1.6.3-1.6.9). We also want to develop some new nucleophiles in this radical coupling reaction. Polyfluoroarenes are important organic molecules, which are the targets of Chang's work via C-H oxidative coupling (Scheme 1.35c). Despite being more atom- and step-economic, the C-H oxidation methods suffer from the problem of C-H site-selectivity. Additionally, the use of strong oxidant (DTBP) and strong base (sodium *tert*-butoxide) largely limited the tolerance for functional groups. We seek to develop some polyfluoroaryl metallic reagents for coupling with the alkyl radicals from the facile photoreduction of NHPI esters. The use of preformed polyfluoroaryl metal reagents would allow incorporation of polyfluoroaryls with variable fluorine content and fluorine substitution patterns, without the assistance of strong base. The use of NHPI esters, derived from easily available aliphatic acids, can avoid the use strong oxidant and has no need to face the site selectivity problem as in the case of C-H oxidation.

References:

- [1] Zard, S. Z. *Radical Reactions in Organic Synthesis*; Oxford University Press: Oxford, 2003.
- [2] Jasperse, C. P.; Curran, D. P.; Fevig, T. L. Radical Reactions in Natural Product Synthesis. *Chem. Rev.* **1991**, *91*, 1237-1286.
- [3] Pitre, S. P.; Weires, N. A.; Overman, L. E. Forging C(sp³)-C(sp³) Bonds with Carbon-Centered Radicals in the Synthesis of Complex Molecules. *J. Am. Chem. Soc.* **2019**, *141*, 2800-2813.
- [4] Wang, K.; Kong, W. Q. Recent Advances in Transition Metal-Catalyzed Asymmetric Radical Reactions. *Chin. J. Chem.* **2018**, *36*, 247-256.
- [5] Yi, H.; Zhang, G. T.; Wang, H. M.; Huang, Z. Y.; Wang, J.; Singh, A. K.; Lei, A. W. Recent Advances in Radical C-H Activation/Radical Cross-Coupling. *Chem. Rev.* **2017**, *117*, 9016-9085.
- [6] Hung, K.; Hu, X. R.; Maimone, T. J. Total synthesis of complex terpenoids employing radical cascade processes. *Nat. Prod. Rep.* **2018**, *35*, 174-202.
- [7] Studer, A.; Curran, D. P. Catalysis of Radical Reactions: A Radical Chemistry Perspective. *Angew. Chem. Int. Ed.* **2016**, *55*, 58-102.
- [8] Nicewicz, D. A.; MacMillan, D. W. C. Merging photoredox catalysis with organocatalysis: The direct asymmetric alkylation of aldehydes. *Science* **2008**, *322*, 77-80.
- [9] Arias-Rotondo, D. M.; McCusker, J. K. The photophysics of photoredox catalysis: a roadmap for catalyst design. *Chem. Soc. Rev.* **2016**, *45*, 5803-5820.
- [10] Prier, C. K.; Rankic, D. A.; MacMillan, D. W. C. Visible Light Photoredox Catalysis with Transition Metal Complexes: Applications in Organic Synthesis. *Chem. Rev.* **2013**, *113*, 5322-5363.
- [11] Shaw, M. H.; Twilton, J.; MacMillan, D. W. C. Photoredox Catalysis in Organic Chemistry. *J. Org. Chem.* **2016**, *81*, 6898-6926.
- [12] Shang, T. Y.; Lu, L. H.; Cao, Z.; Liu, Y.; He, W. M.; Yu, B. Recent advances of 1,2,3,5-tetrakis(carbazol-9-yl)-4,6-dicyanobenzene (4CzIPN) in photocatalytic transformations. *Chem. Commun.* **2019**, *55*, 5408-5419.
- [13] Romero, N. A.; Nicewicz, D. A. Organic Photoredox Catalysis. *Chem. Rev.* **2016**, *116*, 10075-10166.
- [14] McNally, A.; Prier, C. K.; MacMillan, D. W. C. Discovery of an alpha-Amino C-H Arylation Reaction Using the Strategy of Accelerated Serendipity. *Science* **2011**, *334*, 1114-1117.
- [15] Jiang, H.; An, X. D.; Tong, K.; Zheng, T. Y.; Zhang, Y.; Yu, S. Y. Visible-Light-Promoted Iminyl-Radical Formation from Acyl Oximes: A Unified Approach to Pyridines, Quinolines, and Phenanthridines. *Angew. Chem. Int. Ed.* **2015**, *54*, 4055-4059.
- [16] Nguyen, T. M.; Nicewicz, D. A. Anti-Markovnikov Hydroamination of Alkenes Catalyzed by an Organic Photoredox System. *J. Am. Chem. Soc.* **2013**, *135*, 9588-9591.

- [17] Margrey, K. A.; Nicewicz, D. A. A General Approach to Catalytic Alkene Anti-Markovnikov Hydrofunctionalization Reactions via Acridinium Photoredox Catalysis. *Acc. Chem. Res.* **2016**, *49*, 1997-2006.
- [18] Yan, M.; Kawamata, Y.; Baran, P. S. Synthetic Organic Electrochemical Methods Since 2000: On the Verge of a Renaissance. *Chem. Rev.* **2017**, *117*, 13230-13319.
- [19] Wiebe, A.; Gieshoff, T.; Mohle, S.; Rodrigo, E.; Zirbes, M.; Waldvogel, S. R. Electrifying Organic Synthesis. *Angew. Chem. Int. Ed.* **2018**, *57*, 5594-5619.
- [20] Moeller, K. D. Using Physical Organic Chemistry To Shape the Course of Electrochemical Reactions. *Chem. Rev.* **2018**, *118*, 4817-4833.
- [21] Bard, A. J.; Faulkner, L. R. *Electrochemical Methods: Fundamentals and Applications*, Chapter 1; John Wiley & Sons Inc (Verlag), 2001.
- [22] Roth, H. G.; Romero, N. A.; Nicewicz, D. A. Experimental and Calculated Electrochemical Potentials of Common Organic Molecules for Applications to Single-Electron Redox Chemistry. *Synlett* **2016**, *27*, 714-723.
- [23] Horn, E. J.; Rosen, B. R.; Chen, Y.; Tang, J. Z.; Chen, K.; Eastgate, M. D.; Baran, P. S. Scalable and sustainable electrochemical allylic C-H oxidation. *Nature* **2016**, *533*, 77-81.
- [24] Kawamata, Y.; Yan, M.; Liu, Z. Q.; Bao, D. H.; Chen, J. S.; Starr, J. T.; Baran, P. S. Scalable, Electrochemical Oxidation of Unactivated C-H Bonds. *J. Am. Chem. Soc.* **2017**, *139*, 7448-7451.
- [25] Nutting, J. E.; Rafiee, M.; Stahl, S. S. Tetramethylpiperidine N-Oxyl (TEMPO), Phthalimide N-Oxyl (PINO), and Related N-Oxyl Species: Electrochemical Properties and Their Use in Electrocatalytic Reactions. *Chem. Rev.* **2018**, *118*, 4834-4885.
- [26] Yan, M.; Kawamata, Y.; Baran, P. S. Synthetic Organic Electrochemistry: Calling All Engineers. *Angew. Chem. Int. Ed.* **2018**, *57*, 4149-4155.
- [27] Schäfer, H.-J. In *Electrochemistry IV*; Steckhan, E., Ed.; Springer Berlin Heidelberg: Berlin, Heidelberg, 1990, p 91-151.
- [28] Sperry, J. B.; Wright, D. L. The application of cathodic reductions and anodic oxidations in the synthesis of complex molecules. *Chem. Soc. Rev.* **2006**, *35*, 605-621.
- [29] Trowbridge, A.; Walton, S. M.; Gaunt, M. J. New Strategies for the Transition-Metal Catalyzed Synthesis of Aliphatic Amines. *Chem. Rev.* **2020**, *120*, 2613-2692.
- [30] Huang, L. B.; Arndt, M.; Goossen, K.; Heydt, H.; Goossen, L. J. Late Transition Metal-Catalyzed Hydroamination and Hydroamidation. *Chem. Rev.* **2015**, *115*, 2596-2697.
- [31] Davies, J.; Morcillo, S. P.; Douglas, J. J.; Leonori, D. Hydroxylamine Derivatives as Nitrogen-Radical Precursors in Visible-Light Photochemistry. *Chem.-Eur. J.* **2018**, *24*, 12154-12163.
- [32] Minatti, A.; Muniz, K. Intramolecular aminopalladation of alkenes as a key step to pyrrolidines and related heterocycles. *Chem. Soc. Rev.* **2007**, *36*, 1142-1152.
- [33] Kotov, V.; Scarborough, C. C.; Stahl, S. S. Palladium-catalyzed aerobic oxidative amination of alkenes: Development of intra- and intermolecular Aza-Wacker reactions. *Inorg. Chem.* **2007**, *46*, 1910-1923.
- [34] Jiang, H.; Studer, S. Intermolecular radical carboamination of alkenes. *Chem. Soc. Rev.* **2020**, *49*, 1790-1811.

- [35] Zard, S. Z. Recent progress in the generation and use of nitrogen-centred radicals. *Chem. Soc. Rev.* **2008**, *37*, 1603-1618.
- [36] Xiong, P.; Xu, H. C. Chemistry with Electrochemically Generated N-Centered Radicals. *Acc. Chem. Res.* **2019**, *52*, 3339-3350.
- [37] Cowley, B. R.; Waters, W. A. 240. Some reactions of the dimethylamino radical, $\cdot\text{NMe}_2$. *J. Chem. Soc.* **1961**, 1228-1231.
- [38] Angelina, L.; Davies, J.; Simonetti, M.; Sanz, L. M.; Sheikh, N. S.; Leonori, D. Reaction of Nitrogen-Radicals with Organometallics Under Ni-Catalysis: N-Arylations and Amino-Functionalization Cascades. *Angew. Chem. Int. Ed.* **2019**, *58*, 5003-5007.
- [39] Li, Y.; Liang, Y. J.; Dong, J. C.; Deng, Y.; Zhao, C. Y.; Su, Z. M.; Guan, W.; Bi, X. H.; Liu, Q.; Fu, J. K. Directed Copper-Catalyzed Intermolecular Aminative Difunctionalization of Unactivated Alkenes. *J. Am. Chem. Soc.* **2019**, *141*, 18475-18485.
- [40] Ganley, J. M.; Murray, P. R. D.; Knowles, R. R. Photocatalytic Generation of Aminium Radical Cations for C-N Bond Formation. *ACS Catal.* **2020**, *10*, 11712-11738.
- [41] Musacchio, A. J.; Lainhart, B. C.; Zhang, X.; Naguib, S. G.; Sherwood, T. C.; Knowles, R. R. Catalytic intermolecular hydroaminations of unactivated olefins with secondary alkyl amines. *Science* **2017**, *355*, 727-730.
- [42] Zhang, Z. X.; Stateman, L. M.; Nagib, D. A. δ C-H (hetero)arylation via Cu-catalyzed radical relay. *Chem. Sci.* **2019**, *10*, 1207-1211.
- [43] Stateman, L. M.; Nakafuku, K. M.; Nagib, D. A. Remote C-H Functionalization via Selective Hydrogen Atom Transfer. *Synthesis* **2018**, *50*, 1569-1586.
- [44] Li, J. Y.; Zhang, Z. H.; Wu, L. Q.; Zhang, W.; Chen, P. H.; Lin, Z. Y.; Liu, G. S. Site-specific allylic C-H bond functionalization with a copper-bound N-centred radical. *Nature* **2019**, *574*, 516-+.
- [45] Zheng, G.; Li, Y.; Han, J.; Xiong, T.; Zhang, Q. Radical cascade reaction of alkynes with N-fluoroarylsulfonimides and alcohols. *Nat. Commun.* **2015**, *6*, 7011.
- [46] Rossler, S. L.; Jelier, B. J.; Magnier, E.; Dagousset, G.; Carreira, E. M.; Togni, A. Pyridinium Salts as Redox-Active Functional Group Transfer Reagents. *Angew. Chem. Int. Ed.* **2020**, *59*, 9264-9280.
- [47] Allen, L. J.; Cabrera, P. J.; Lee, M.; Sanford, M. S. N-Acyloxyphthalimides as Nitrogen Radical Precursors in the Visible Light Photocatalyzed Room Temperature C-H Amination of Arenes and Heteroarenes. *J. Am. Chem. Soc.* **2014**, *136*, 5607-5610.
- [48] Jiang, H.; Studer, A. Chemistry With N-Centered Radicals Generated by Single-Electron Transfer-Oxidation Using Photoredox Catalysis. *CCS Chem.* **2019**, *1*, 38-49.
- [49] Nicolaou, K. C.; Baran, P. S.; Zhong, Y. L.; Barluenga, S.; Hunt, K. W.; Kranich, R.; Vega, J. A. Iodine(V) reagents in organic synthesis. Part 3. New routes to heterocyclic compounds via o-iodoxybenzoic acid-mediated cyclizations: Generality, scope, and mechanism. *J. Am. Chem. Soc.* **2002**, *124*, 2233-2244.
- [50] Zhuang, S. J.; Liu, K.; Li, C. Z. Stereoselective 6-Exo Cyclization of Amidyl Radicals. An Experimental and Theoretical Study. *J. Org. Chem.* **2011**, *76*, 8100-8106.
- [51] Horner, J. H.; Musa, O. M.; Bouvier, A.; Newcomb, M. Absolute kinetics of amidyl radical reactions. *J. Am. Chem. Soc.* **1998**, *120*, 7738-7748.

- [52] Zhu, L.; Xiong, P.; Mao, Z. Y.; Wang, Y. H.; Yan, X. M.; Lu, X.; Xu, H. C. Electrocatalytic Generation of Amidyl Radicals for Olefin Hydroamidation: Use of Solvent Effects to Enable Anilide Oxidation. *Angew. Chem. Int. Ed.* **2016**, *55*, 2226-2229.
- [53] Long, H.; Song, J. S.; Xu, H. C. Electrochemical synthesis of 7-membered carbocycles through cascade 5-exo-trig/7-endo-trig radical cyclization. *Org. Chem. Front.* **2018**, *5*, 3129-3132.
- [54] Xu, H. C.; Moeller, K. D. Intramolecular anodic olefin coupling reactions: The use of a nitrogen trapping group. *J. Am. Chem. Soc.* **2008**, *130*, 13542.
- [55] Xiong, P.; Xu, H. H.; Xu, H. C. Metal- and Reagent-Free Intramolecular Oxidative Amination of Tri- and Tetrasubstituted Alkenes. *J. Am. Chem. Soc.* **2017**, *139*, 2956-2959.
- [56] Miller, D. C.; Choi, G. J.; Orbe, H. S.; Knowles, R. R. Catalytic Olefin Hydroamidation Enabled by Proton-Coupled Electron Transfer. *J. Am. Chem. Soc.* **2015**, *137*, 13492-13495.
- [57] Choi, G. J.; Knowles, R. R. Catalytic Alkene Carboaminations Enabled by Oxidative Proton-Coupled Electron Transfer. *J. Am. Chem. Soc.* **2015**, *137*, 9226-9229.
- [58] Zhu, Q. L.; Graff, D. E.; Knowles, R. R. Intermolecular Anti-Markovnikov Hydroamination of Unactivated Alkenes with Sulfonamides Enabled by Proton-Coupled Electron Transfer. *J. Am. Chem. Soc.* **2018**, *140*, 741-747.
- [59] Jia, J. Q.; Ho, Y. A.; Buelow, R. F.; Rueping, M. Bronsted Base Assisted Photoredox Catalysis: Proton Coupled Electron Transfer for Remote C-C Bond Formation via Amidyl Radicals. *Chem.-Eur. J.* **2018**, *24*, 14054-14058.
- [60] Zhang, S.; Gutierrez-Bonet, A.; Molander, G. A. Merging Photoredox PCET with Ni-Catalyzed Cross-Coupling: Cascade Amidoarylation of Unactivated Olefins. *Chem* **2019**, *5*, 339-352.
- [61] Davies, J.; Booth, S. G.; Essafi, S.; Dryfe, R. A. W.; Leonori, D. Visible-Light-Mediated Generation of Nitrogen-Centered Radicals: Metal-Free Hydroimination and Iminohydroxylation Cyclization Reactions. *Angew. Chem. Int. Ed.* **2015**, *54*, 14017-14021.
- [62] Davies, J.; Svejstrup, T. D.; Reina, D. F.; Sheikh, N. S.; Leonori, D. Visible-Light-Mediated Synthesis of Amidyl Radicals: Transition Metal-Free Hydroamination and N-Arylation Reactions. *J. Am. Chem. Soc.* **2016**, *138*, 8092-8095.
- [63] Shen, X.; Huang, C. C.; Yuan, X. A.; Yu, S. Y. Diastereoselective and Stereodivergent Synthesis of 2-Cinnamylpyrrolines Enabled by Photoredox-Catalyzed Iminoalkenylation of Alkenes. *Angew. Chem. Int. Ed.* **2021**, *60*, 9672-9679.
- [64] Jiang, H.; Studer, A. Iminyl-Radicals by Oxidation of α -Imino-oxy Acids: Photoredox-Neutral Alkene Carboimination for the Synthesis of Pyrrolines. *Angew. Chem. Int. Ed.* **2017**, *56*, 12273-12276.
- [65] Davies, J.; Sheikh, N. S.; Leonori, D. Photoredox Imino Functionalizations of Olefins. *Angew. Chem. Int. Ed.* **2017**, *56*, 13361-13365.
- [66] Cecere, G.; Konig, C. M.; Alleva, J. L.; MacMillan, D. W. C. Enantioselective Direct α -Annulation of Aldehydes via a Photoredox Mechanism: A Strategy for Asymmetric Amine Fragment Coupling. *J. Am. Chem. Soc.* **2013**, *135*, 11521-11524.
- [67] An, X. D.; Jiao, Y. Y.; Zhang, H.; Gao, Y. X.; Yu, S. Y. Photoredox-Induced Radical Relay toward Functionalized β -Amino Alcohol Derivatives. *Org. Lett.* **2018**, *20*, 401-404.

- [68] Miyazawa, K.; Koike, T.; Akita, M. Regiospecific Intermolecular Aminohydroxylation of Olefins by Photoredox Catalysis. *Chem.-Eur. J.* **2015**, *21*, 11677-11680.
- [69] Mo, J. N.; Yu, W. L.; Chen, J. Q.; Hu, X. Q.; Xu, P. F. Regiospecific Three-Component Aminofluorination of Olefins via Photoredox Catalysis. *Org. Lett.* **2018**, *20*, 4471-4474.
- [70] Chen, J. Q.; Yu, W. L.; Wei, Y. L.; Li, T. H.; Xu, P. F. Photoredox-Induced Functionalization of Alkenes for the Synthesis of Substituted Imidazolines and Oxazolidines. *J. Org. Chem.* **2017**, *82*, 243-249.
- [71] Yu, W. L.; Chen, J. Q.; Wei, Y. L.; Wang, Z. Y.; Xu, P. F. Alkene functionalization for the stereospecific synthesis of substituted aziridines by visible-light photoredox catalysis. *Chem. Commun.* **2018**, *54*, 1948-1951.
- [72] Guo, W. S.; Wang, Q.; Zhu, J. P. Selective 1,2-Aminoisothiocyanation of 1,3-Dienes Under Visible-Light Photoredox Catalysis. *Angew. Chem. Int. Ed.* **2021**, *60*, 4085-4089.
- [73] Zhang, H. W.; Pu, W. Y.; Xiong, T.; Li, Y.; Zhou, X.; Sun, K.; Liu, Q.; Zhang, Q. Copper-Catalyzed Intermolecular Aminocyanation and Diamination of Alkenes. *Angew. Chem. Int. Ed.* **2013**, *52*, 2529-2533.
- [74] Wang, D. H.; Wang, F.; Chen, P. H.; Lin, Z. Y.; Liu, G. S. Enantioselective Copper-Catalyzed Intermolecular Amino- and Azidocyanation of Alkenes in a Radical Process. *Angew. Chem. Int. Ed.* **2017**, *56*, 2054-2058.
- [75] Wang, D. H.; Wu, L. Q.; Wang, F.; Wan, X. L.; Chen, P. H.; Lin, Z. Y.; Liu, G. S. Asymmetric Copper-Catalyzed Intermolecular Aminoarylation of Styrenes: Efficient Access to Optical 2,2-Diarylethylamines. *J. Am. Chem. Soc.* **2017**, *139*, 6811-6814.
- [76] Day, J. C.; Katsaros, M. G.; Kocher, W. D.; Scott, A. E.; Skell, P. S. Addition-Reactions of Imidyl Radicals with Olefins and Arenes. *J. Am. Chem. Soc.* **1978**, *100*, 1950-1951.
- [77] Guin, J.; Frohlich, R.; Studer, A. Thiol-catalyzed stereoselective transfer hydroamination of olefins with N-aminated dihydropyridines. *Angew. Chem. Int. Ed.* **2008**, *47*, 779-782.
- [78] Lardy, S. W.; Schmidt, V. A. Intermolecular Radical Mediated Anti-Markovnikov Alkene Hydroamination Using N-Hydroxyphthalimide. *J. Am. Chem. Soc.* **2018**, *140*, 12318-12322.
- [79] Zhang, Y.; Liu, H. D.; Tang, L. N.; Tang, H. J.; Wang, L.; Zhu, C.; Feng, C. Intermolecular Carboamination of Unactivated Alkenes. *J. Am. Chem. Soc.* **2018**, *140*, 10695-10699.
- [80] Jiang, H.; Studer, A. Amidyl Radicals by Oxidation of alpha-Amido-oxy Acids: Transition-Metal-Free Amidofluorination of Unactivated Alkenes. *Angew. Chem. Int. Ed.* **2018**, *57*, 10707-10711.
- [81] Jiang, H.; Seidler, G.; Studer, A. Carboamination of Unactivated Alkenes through Three-Component Radical Conjugate Addition. *Angew. Chem. Int. Ed.* **2019**, *58*, 16528-16532.
- [82] Jiang, H.; Studer, A. Transition-Metal-Free Three-Component Radical 1,2-Amidoalkynylation of Unactivated Alkenes. *Chem.-Eur. J.* **2019**, *25*, 516-520.
- [83] Xiao, H. W.; Shen, H. G.; Zhu, L.; Li, C. Z. Copper-Catalyzed Radical Aminotrifluoromethylation of Alkenes. *J. Am. Chem. Soc.* **2019**, *141*, 11440-11445.
- [84] Gooßen, L. J.; Rodríguez, N.; Gooßen, K. Carboxylic Acids as Substrates in Homogeneous Catalysis. *Angew. Chem. Int. Ed.* **2008**, *47*, 3100-3120.

- [85] Anderson, J. M.; Kochi, J. K. Silver(I)-Catalyzed Oxidative Decarboxylation of Acids by Peroxydisulfate - Role of Silver(II). *J. Am. Chem. Soc.* **1970**, *92*, 1651.
- [86] Johnson, R. G.; Ingham, R. K. The Degradation of Carboxylic Acid Salts by Means of Halogen - the Hunsdiecker Reaction. *Chem. Rev.* **1956**, *56*, 219-269.
- [87] Noble, A.; McCarver, S. J.; MacMillan, D. W. C. Merging Photoredox and Nickel Catalysis: Decarboxylative Cross-Coupling of Carboxylic Acids with Vinyl Halides. *J. Am. Chem. Soc.* **2015**, *137*, 624-627.
- [88] Till, N. A.; Smith, R. T.; MacMillan, D. W. C. Decarboxylative Hydroalkylation of Alkynes. *J. Am. Chem. Soc.* **2018**, *140*, 5701-5705.
- [89] Okada, K.; Okamoto, K.; Oda, M. A New and Practical Method of Decarboxylation - Photosensitized Decarboxylation of N-Acyloxyphthalimides Via Electron-Transfer Mechanism. *J. Am. Chem. Soc.* **1988**, *110*, 8736-8738.
- [90] Ishii, T.; Kakeno, Y.; Nagao, K.; Ohmiya, H. N-Heterocyclic Carbene-Catalyzed Decarboxylative Alkylation of Aldehydes. *J. Am. Chem. Soc.* **2019**, *141*, 3854-3858.
- [91] Qin, T.; Cornella, J.; Li, C.; Malins, L. R.; Edwards, J. T.; Kawamura, S.; Maxwell, B. D.; Eastgate, M. D.; Baran, P. S. A general alkyl-alkyl cross-coupling enabled by redox-active esters and alkylzinc reagents. *Science* **2016**, *352*, 801-805.
- [92] Cornella, J.; Edwards, J. T.; Qin, T.; Kawamura, S.; Wang, J.; Pan, C. M.; Gianatassio, R.; Schmidt, M.; Eastgate, M. D.; Baran, P. S. Practical Ni-Catalyzed Aryl-Alkyl Cross-Coupling of Secondary Redox-Active Esters. *J. Am. Chem. Soc.* **2016**, *138*, 2174-2177.
- [93] Toriyama, F.; Cornella, J.; Wimmer, L.; Chen, T. G.; Dixon, D. D.; Creech, G.; Baran, P. S. Redox-Active Esters in Fe-Catalyzed C-C Coupling. *J. Am. Chem. Soc.* **2016**, *138*, 11132-11135.
- [94] Li, C.; Wang, J.; Barton, L. M.; Yu, S.; Tian, M. Q.; Peters, D. S.; Kumar, M.; Yu, A. W.; Johnson, K. A.; Chatterjee, A. K.; Yan, M.; Baran, P. S. Decarboxylative borylation. *Science* **2017**, *356*.
- [95] Zeng, X. J.; Yan, W. H.; Zacate, S. B.; Chao, T. H.; Sun, X. D.; Cao, Z.; Bradford, K. G. E.; Paeth, M.; Tyndall, S. B.; Yang, K. D.; Kuo, T. C.; Cheng, M. J.; Liu, W. Copper-Catalyzed Decarboxylative Difluoromethylation. *J. Am. Chem. Soc.* **2019**, *141*, 11398-11403.
- [96] Mao, R. Z.; Frey, A.; Balon, J.; Hu, X. L. Decarboxylative C(sp³)-N cross-coupling via synergetic photoredox and copper catalysis. *Nat. Catal.* **2018**, *1*, 120-126.
- [97] Mao, R. Z.; Balon, J.; Hu, X. L. Cross-Coupling of Alkyl Redox-Active Esters with Benzophenone Imines: Tandem Photoredox and Copper Catalysis. *Angew. Chem. Int. Ed.* **2018**, *57*, 9501-9504.
- [98] Mao, R. Z.; Balon, J.; Hu, X. L. Decarboxylative C(sp³)-O Cross-Coupling. *Angew. Chem. Int. Ed.* **2018**, *57*, 13624-13628.
- [99] Okada, K.; Okamoto, K.; Morita, N.; Okubo, K.; Oda, M. Photosensitized Decarboxylative Michael Addition through N-(Acyloxy)Phthalimides Via an Electron-Transfer Mechanism. *J. Am. Chem. Soc.* **1991**, *113*, 9401-9402.
- [100] Schnermann, M. J.; Overman, L. E. A Concise Synthesis of (-)-Aplyviolene Facilitated by a Strategic Tertiary Radical Conjugate Addition. *Angew. Chem. Int. Ed.* **2012**, *51*, 9576-9580.

- [101] Cheng, W. M.; Shang, R.; Fu, Y. Photoredox/Bronsted Acid Co-Catalysis Enabling Decarboxylative Coupling of Amino Acid and Peptide Redox-Active Esters with N-Heteroarenes. *Acs. Catal.* **2017**, *7*, 907-911.
- [102] Webb, E. W.; Park, J. B.; Cole, E. L.; Donnelly, D. J.; Bonacorsi, S. J.; Ewing, W. R.; Doyle, A. G. Nucleophilic (Radio)Fluorination of Redox-Active Esters via Radical-Polar Crossover Enabled by Photoredox Catalysis. *J. Am. Chem. Soc.* **2020**, *142*, 9493-9500.
- [103] Kochi, J. K. Mechanisms of Organic Oxidation and Reduction by Metal Complexes. *Science* **1967**, *155*, 415.
- [104] Iqbal, J.; Bhatia, B.; Nayyar, N. K. Transition Metal-Promoted Free-Radical Reactions in Organic-Synthesis - the Formation of Carbon-Carbon Bonds. *Chem. Rev.* **1994**, *94*, 519-564.
- [105] Wang, F.; Chen, P. H.; Liu, G. S. Copper-Catalyzed Radical Relay for Asymmetric Radical Transformations. *Acc. Chem. Res.* **2018**, *51*, 2036-2046.
- [106] Kochi, J. K. Decomposition of Peroxides Catalyzed by Copper Compounds and Oxidation of Alkyl Radicals by Cupric Salts. *J. Am. Chem. Soc.* **1963**, *85*, 1958.
- [107] Kochi, J. K.; Bemis, A.; Jenkins, C. L. Mechanism of Electron Transfer Oxidation of Alkyl Radicals by Copper(2) Complexes. *J. Am. Chem. Soc.* **1968**, *90*, 4616.
- [108] Tlahuext-Aca, A.; Candish, L.; Garza-Sanchez, R. A.; Glorius, F. Decarboxylative Olefination of Activated Aliphatic Acids Enabled by Dual Organophotoredox/Copper Catalysis. *Acs. Catal.* **2018**, *8*, 1715-1719.
- [109] Xiong, P.; Xu, F.; Qian, X. Y.; Yohannes, Y.; Song, J. S.; Lu, X.; Xu, H. C. Copper-Catalyzed Intramolecular Oxidative Amination of Unactivated Internal Alkenes. *Chem.-Eur. J.* **2016**, *22*, 4379-4383.
- [110] Faulkner, A.; Race, N. J.; Scott, J. S.; Bower, J. F. Copper catalyzed Heck-like cyclizations of oxime esters. *Chem. Sci.* **2014**, *5*, 2416-2421.
- [111] Parsons, A. T.; Buchwald, S. L. Copper-Catalyzed Trifluoromethylation of Unactivated Olefins. *Angew. Chem. Int. Ed.* **2011**, *50*, 9120-9123.
- [112] Xu, J.; Fu, Y.; Luo, D. F.; Jiang, Y. Y.; Xiao, B.; Liu, Z. J.; Gong, T. J.; Liu, L. Copper-Catalyzed Trifluoromethylation of Terminal Alkenes through Allylic C-H Bond Activation. *J. Am. Chem. Soc.* **2011**, *133*, 15300-15303.
- [113] Wang, X.; Ye, Y. X.; Zhang, S. N.; Feng, J. J.; Xu, Y.; Zhang, Y.; Wang, J. B. Copper-Catalyzed C(sp³)-C(sp³) Bond Formation Using a Hypervalent Iodine Reagent: An Efficient Allylic Trifluoromethylation. *J. Am. Chem. Soc.* **2011**, *133*, 16410-16413.
- [114] Wu, X. S.; Riedel, J.; Dong, V. M. Transforming Olefins into gamma,delta-Unsaturated Nitriles through Copper Catalysis. *Angew. Chem. Int. Ed.* **2017**, *56*, 11589-11593.
- [115] Zhu, N. B.; Wang, T.; Ge, L.; Li, Y. J.; Zhang, X. H.; Bao, H. L. gamma-Amino Butyric Acid (GABA) Synthesis Enabled by Copper-Catalyzed Carboamination of Alkenes. *Org. Lett.* **2017**, *19*, 4718-4721.
- [116] Hu, H. Y.; Chen, S. J.; Mandal, M.; Pratik, S. M.; Buss, J. A.; Krska, S. W.; Cramer, C. J.; Stahl, S. S. Copper-catalysed benzylic C-H coupling with alcohols via radical relay enabled by redox buffering. *Nat. Catal.* **2020**, *3*, 358-367.

- [117] Gockel, S. N.; Buchanan, T. L.; Hull, K. L. Cu-Catalyzed Three-Component Carboamination of Alkenes. *J. Am. Chem. Soc.* **2018**, *140*, 58-61.
- [118] Pu, W. Y.; Sun, D. N.; Fan, W. Y.; Pan, W. W.; Chai, Q. H.; Wang, X. X.; Lv, Y. H. Cu-Catalyzed atom transfer radical addition reactions of alkenes with α -bromoacetonitrile. *Chem. Commun.* **2019**, *55*, 4821-4824.
- [119] Udding, J. H.; Tuijp, K. C. J. M.; Vanzanden, M. N. A.; Hiemstra, H.; Speckamp, W. N. Transition-Metal-Catalyzed, Chlorine-Transfer Radical Cyclizations of 2-(3-Alken-1-Oxy)-2-Chloroacetates - Formal Total Synthesis of Avenaciolide and Isoavenaciolide. *J. Org. Chem.* **1994**, *59*, 1993-2003.
- [120] Wang, J. S.; Matyjaszewski, K. Controlled Living Radical Polymerization - Atom-Transfer Radical Polymerization in the Presence of Transition-Metal Complexes. *J. Am. Chem. Soc.* **1995**, *117*, 5614-5615.
- [121] Matyjaszewski, K.; Xia, J. Atom Transfer Radical Polymerization. *Chem. Rev.* **2001**, *101*, 2921-2990.
- [122] Zhu, R.; Buchwald, S. L. Copper-Catalyzed Oxytrifluoromethylation of Unactivated Alkenes. *J. Am. Chem. Soc.* **2012**, *134*, 12462-12465.
- [123] Zhu, R.; Buchwald, S. L. Enantioselective Functionalization of Radical Intermediates in Redox Catalysis: Copper-Catalyzed Asymmetric Oxytrifluoromethylation of Alkenes. *Angew. Chem. Int. Ed.* **2013**, *52*, 12655-12658.
- [124] Eames, J.; Watkinson, M. Catalytic allylic oxidation of alkenes using an asymmetric Kharasch-Sosnovsky reaction. *Angew. Chem. Int. Ed.* **2001**, *40*, 3567.
- [125] Kharasch, M. S.; Sosnovsky, G.; Yang, N. C. Reactions of *Tert*-Butyl Peresters .1. The Reaction of Peresters with Olefins. *J. Am. Chem. Soc.* **1959**, *81*, 5819-5824.
- [126] Gokhale, A. S.; Minidis, A. B. E.; Pfaltz, A. Enantioselective Allylic Oxidation Catalyzed by Chiral Bisoxazoline-Copper Complexes. *Tetrahedron Lett.* **1995**, *36*, 1831-1834.
- [127] Tran, B. L.; Driess, M.; Hartwig, J. F. Copper-Catalyzed Oxidative Dehydrogenative Carboxylation of Unactivated Alkanes to Allylic Esters via Alkenes. *J. Am. Chem. Soc.* **2014**, *136*, 17292-17301.
- [128] Liang, Z. L.; Wang, F.; Chen, P. H.; Liu, G. S. Copper-Catalyzed Intermolecular Trifluoromethylthiocyanation of Alkenes: Convenient Access to CF₃-Containing Alkyl Thiocyanates. *Org. Lett.* **2015**, *17*, 2438-2441.
- [129] Jiang, C.; Chen, P.; Liu, G. Copper-Catalyzed Benzylic C-H Bond Thiocyanation: Enabling Late-Stage Diversifications. *CCS Chem.* **2020**, *2*, 1884-1893.
- [130] Modak, A.; Pinter, E. N.; Cook, S. P. Copper-Catalyzed, N-Directed Csp(3)-H Trifluoromethylthiolation (-SCF₃) and Trifluoromethylselenation (-SeCF₃). *J. Am. Chem. Soc.* **2019**, *141*, 18405-18410.
- [131] Liu, Z. J.; Lu, X.; Wang, G.; Li, L.; Jiang, W. T.; Wang, Y. D.; Xiao, B.; Fu, Y. Directing Group in Decarboxylative Cross-Coupling: Copper-Catalyzed Site-Selective C-N Bond Formation from Nonactivated Aliphatic Carboxylic Acids. *J. Am. Chem. Soc.* **2016**, *138*, 9714-9719.

- [132] Lin, J. S.; Dong, X. Y.; Li, T. T.; Jiang, N. C.; Tan, B.; Liu, X. Y. A Dual-Catalytic Strategy To Direct Asymmetric Radical Aminotrifluoromethylation of Alkenes. *J. Am. Chem. Soc.* **2016**, *138*, 9357-9360.
- [133] Tran, B. L.; Li, B. J.; Driess, M.; Hartwig, J. F. Copper-Catalyzed Intermolecular Amidation and Imidation of Unactivated Alkanes. *J. Am. Chem. Soc.* **2014**, *136*, 2555-2563.
- [134] Wang, F.; Qi, X. X.; Liang, Z. L.; Chen, P. H.; Liu, G. S. Copper-Catalyzed Intermolecular Trifluoromethylazidation of Alkenes: Convenient Access to CF₃-Containing Alkyl Azides. *Angew. Chem. Int. Ed.* **2014**, *53*, 1881-1886.
- [135] Bao, X.; Wang, Q.; Zhu, J. P. Dual Photoredox/Copper Catalysis for the Remote C(sp³)-H Functionalization of Alcohols and Alkyl Halides by N-Alkoxy pyridinium Salts. *Angew. Chem. Int. Ed.* **2019**, *58*, 2139-2143.
- [136] Zhang, B.; Studer, A. Copper-Catalyzed Intermolecular Aminoazidation of Alkenes. *Org. Lett.* **2014**, *16*, 1790-1793.
- [137] Wang, L.; Wang, C. Copper-Catalyzed Diamination of Oxime Ester-Tethered Unactivated Alkenes with Unprotected Amines. *J. Org. Chem.* **2019**, *84*, 6547-6556.
- [138] Kainz, Q. M.; Matier, C. D.; Bartoszewicz, A.; Zultanski, S. L.; Peters, J. C.; Fu, G. C. Asymmetric copper-catalyzed C-N cross-couplings induced by visible light. *Science* **2016**, *351*, 681-684.
- [139] He, Y. T.; Li, L. H.; Yang, Y. F.; Zhou, Z. Z.; Hua, H. L.; Liu, X. Y.; Liang, Y. M. Copper-Catalyzed Intermolecular Cyanotrifluoromethylation of Alkenes. *Org. Lett.* **2014**, *16*, 270-273.
- [140] Zhang, W.; Wang, F.; McCann, S. D.; Wang, D. H.; Chen, P. H.; Stahl, S. S.; Liu, G. S. Enantioselective cyanation of benzylic C-H bonds via copper-catalyzed radical relay. *Science* **2016**, *353*, 1014-1018.
- [141] Zhou, S.; Zhang, G. Y.; Fu, L.; Chen, P. H.; Li, Y. B.; Liu, G. S. Copper-Catalyzed Asymmetric Cyanation of Alkenes via Carbonyl-Assisted Coupling of Alkyl-Substituted Carbon-Centered Radicals. *Org. Lett.* **2020**, *22*, 6299-6303.
- [142] Wang, D. H.; Zhu, N.; Chen, P. H.; Lin, Z. Y.; Liu, G. S. Enantioselective Decarboxylative Cyanation Employing Cooperative Photoredox Catalysis and Copper Catalysis. *J. Am. Chem. Soc.* **2017**, *139*, 15632-15635.
- [143] Song, L.; Fu, N. K.; Ernst, B. G.; Lee, W. H.; Frederick, M. O.; DiStasio, R. A.; Lin, S. Dual electrocatalysis enables enantioselective hydrocyanation of conjugated alkenes. *Nat. Chem.* **2020**, *12*.
- [144] Fu, L.; Zhang, Z. H.; Chen, P. H.; Lin, Z. Y.; Liu, G. S. Enantioselective Copper-Catalyzed Alkynylation of Benzylic C-H Bonds via Radical Relay. *J. Am. Chem. Soc.* **2020**, *142*, 12493-12500.
- [145] Zhang, Z. H.; Dong, X. Y.; Du, X. Y.; Gu, Q. S.; Li, Z. L.; Liu, X. Y. Copper-catalyzed enantioselective Sonogashira-type oxidative cross-coupling of unactivated C(sp³)-H bonds with alkynes. *Nat. Commun.* **2019**, *10*.
- [146] Wang, F.; Wang, D. H.; Mu, X.; Chen, P. H.; Liu, G. S. Copper-Catalyzed Intermolecular Trifluoromethylarylation of Alkenes: Mutual Activation of Arylboronic Acid and CF₃+ Reagent. *J. Am. Chem. Soc.* **2014**, *136*, 10202-10205.

- [147] Wu, L. Q.; Wang, F.; Wan, X. L.; Wang, D. H.; Chen, P. H.; Liu, G. S. Asymmetric Cu-Catalyzed Intermolecular Trifluoromethylation of Styrenes: Enantioselective Arylation of Benzylic Radicals. *J. Am. Chem. Soc.* **2017**, *139*, 2904-2907.
- [148] Zhang, W.; Chen, P. H.; Liu, G. S. Copper-Catalyzed Arylation of Benzylic C-H bonds with Alkylarenes as the Limiting Reagents. *J. Am. Chem. Soc.* **2017**, *139*, 7709-7712.
- [149] Xie, W.; Heo, J.; Kim, D.; Chang, S. Copper-Catalyzed Direct C-H Alkylation of Polyfluoroarenes by Using Hydrocarbons as an Alkylating Source. *J. Am. Chem. Soc.* **2020**, *142*, 7487-7496.
- [150] Xie, W. L.; Kim, D.; Chang, S. Copper-Catalyzed Formal Dehydrogenative Coupling of Carbonyls with Polyfluoroarenes Leading to beta-C-H Arylation. *J. Am. Chem. Soc.* **2020**, *142*, 20588-20593.
- [151] Tan, X. Q.; Liu, Z. L.; Shen, H. G.; Zhang, P.; Zhang, Z. Z.; Li, C. Z. Silver-Catalyzed Decarboxylative Trifluoromethylation of Aliphatic Carboxylic Acids. *J. Am. Chem. Soc.* **2017**, *139*, 12430-12433.
- [152] Liu, Z. L.; Xiao, H. W.; Zhang, B. X.; Shen, H. G.; Zhu, L.; Li, C. Z. Copper-Catalyzed Remote C(sp³)-H Trifluoromethylation of Carboxamides and Sulfonamides. *Angew. Chem. Int. Ed.* **2019**, *58*, 2510-2513.
- [153] Jiang, C.; Wang, L.; Zhang, H. G.; Chen, P. H.; Guo, Y. L.; Liu, G. S. Enantioselective Copper-Catalyzed Trifluoromethylation of Benzylic Radicals via Ring Opening of Cyclopropanols. *Chem* **2020**, *6*, 2407-2419.
- [154] Kautzky, J. A.; Wang, T.; Evans, R. W.; MacMillan, D. W. C. Decarboxylative Trifluoromethylation of Aliphatic Carboxylic Acids. *J. Am. Chem. Soc.* **2018**, *140*, 6522-6526.

Chapter 2 Formal aza-Wacker cyclization by dual electrooxidation and copper catalysis

The work described in this chapter has been published: (Yi, X. L.; Hu, X. L. Formal Aza-Wacker Cyclization by Tandem Electrochemical Oxidation and Copper Catalysis. *Angew. Chem. Int. Ed.* **2019**, 58, 4700-4704). The license number for reprint of the materials: 5074881115922.

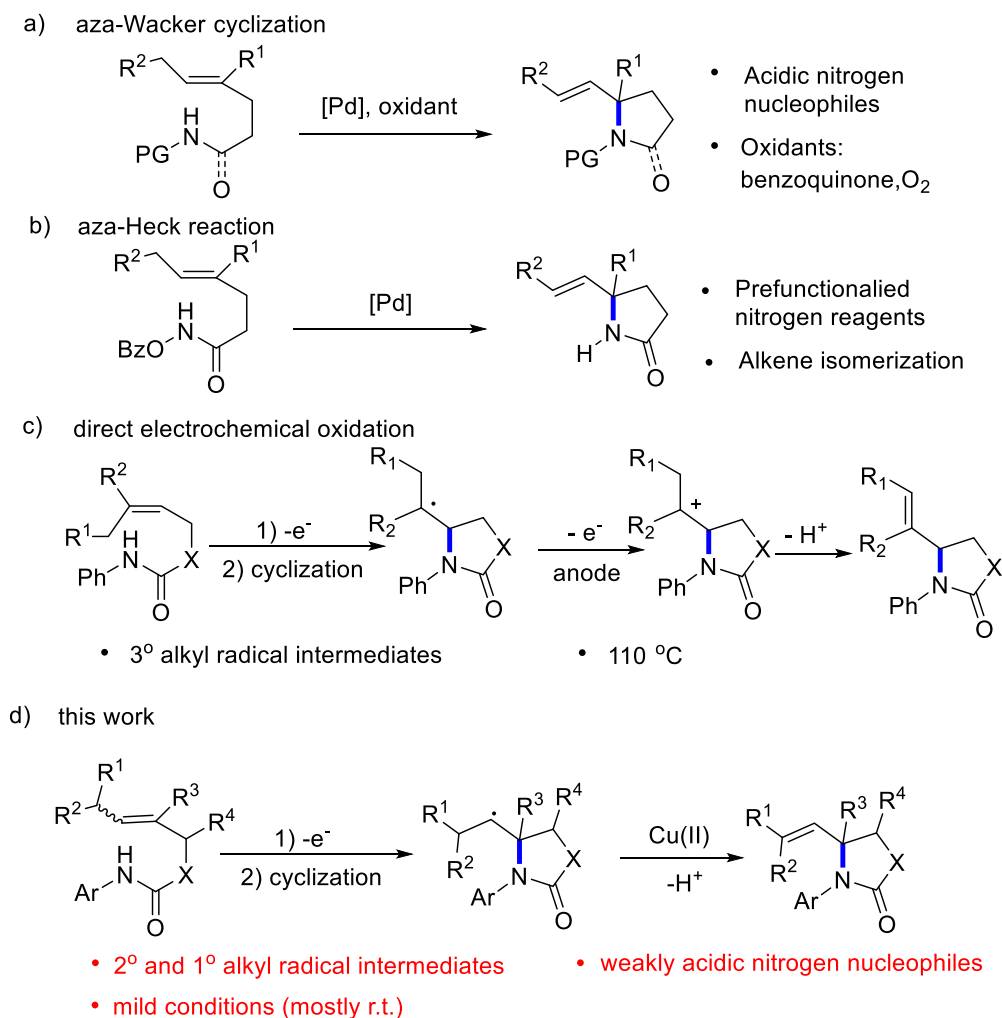
2.1 Background

Nitrogen-containing five-membered heterocycles, such as pyrrolidinones and oxazolidinones, are ubiquitous in many natural products and synthetic bio-active compounds.^[1,2] Pd-catalyzed aza-Wacker cyclization is an attractive method to generate these structures, via intramolecular aminopalladation of alkenes and β -hydrogen elimination (Scheme 2.1a).^[3-7] The olefin functionality was retained in the products, making it suitable for diversity-oriented synthesis. However, this method usually works for acidic nitrogen nucleophiles such as sulfonamides (e.g. pK_a = 12.9 for *N*-phenylmethanesulfonamide), while less acidic substrates like carbamates (e.g. pK_a = 20.0 for allyl phenylcarbamate) and amides (e.g. pK_a = 21.5 for *N*-phenyl acetamide) are sluggish reaction partners.^[8,9] Pd-catalyzed aza-Heck uses hydroxylamine-derived electrophiles for the cyclization to obtain similar products (Scheme 2.1b).^[9,10] This reaction avoids the use of external oxidants and has less requirements on the substituents on nitrogen, though in some cases alkene isomerizations occurs in the products. This is a general concern for Pd-catalyzed reactions because of their capability to mediate the chain-walking of carbon-carbon double bonds.

A Cu-catalyzed method was developed for the intramolecular cyclization of carbamates and ureas, but a high reaction temperature and a strong oxidant (Dess–Martin periodinane) were required (Scheme 1.24b).^[11] In 2017, the group of Xu developed an electrochemical protocol of intramolecular oxidative amination of alkenes (Scheme 2.1c).^[12] It was proposed that electrochemical oxidation generated an amidyl radical, which underwent intramolecular cyclization to give an alkyl radical. The latter was oxidized by the electrode to afford alkene moiety upon proton loss. Despite the elegant concept, this method relied on having tertiary alkyl radical intermediates, probably due

to inefficient direct oxidation of secondary and primary alkyl radicals at the electrode. Additionally, this method still required an elevated temperature (110 °C).

Considering that copper is a good catalyst to mediate oxidative transformation of alkyl radicals into alkenes (Section 1.6.1),^[13,14] we incorporated Cu catalysis into the electrochemical oxidative amination process (Scheme 2.1d). This approach enabled, for the first time, the transformation of secondary and even primary alkyl radical intermediates, leading to a broad-scope methodology for formal aza-Wacker cyclization. The Cu catalysis also enabled the reactions at room temperature.

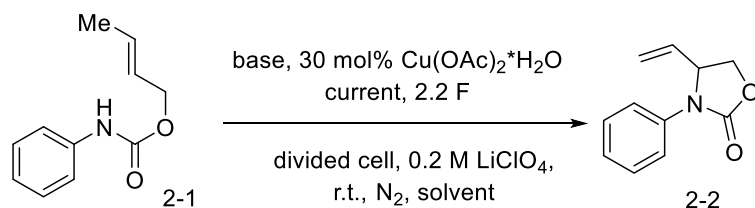


Scheme 2.1 aza-Wacker cyclization and its alternatives leading to the similar products.

2.2 Reaction optimizations

We began by investigating the electrochemical oxidative amination of crotyl N-phenylcarbamate 2-1 in the presence of a Cu catalyst (Table 2.1). After initial exploration of conditions, we found that in a divided cell with MeOH as solvent, carbon fiber as working electrode, 0.2 M LiClO₄ as electrolyte, Cu(OAc)₂ (30 mol%) as catalyst, 2 eq. of NaOAc as base, and under constant current (3 mA, $j = 0.19 \text{ mA/cm}^2$), the desired product 2-2 could be obtained in a yield of 33% after passing 2.2 F electron at room temperature (Entry 1). Different solvents were tested (Entries 2-4). EtOH and acetone gave relatively lower yield, while DMF was not suited for this reaction. Increasing the amount of base to 3 or 4 equivalent improved the reaction yield to 46% and 51%, respectively (Entries 5 & 6). Without base, the reaction could hardly proceed (Entry 7). The use of NaHCO₃ or LiO^tBu as base led to precipitation of Cu salts and low yields (Entries 8&9). The use of NaOPiv (OPiv= pivalate) or NaOBz (OBz= benzoate), however, could improve the yield to 64% and 62%, respectively (Entries 10&11). When the reaction was conducted with a lower current 1.5 mA, the yield was further increased to 70% (Entry 12).

Then, some other metal catalysts were applied. CuCl₂ could still offer a yield of 56% (Entry 13), while FeCl₃, Ni(OAc)₂, Co(OAc)₂ and Pd(OAc)₂ were not effective catalysts (Entries 14-17). The yields of about 10% of the product possibly arisen from the background reaction, because a similar yield was observed when no metal catalyst was used (Entry 18). Besides, different electrodes provided distinctive performance (Entries 19-20). Using reticulated vitreous carbon (RVC) in place of carbon fiber as working electrode decreased the yield to 35% (Entry 19), probably due to the higher current density (0.25 vs 0.10 mA/cm²). Pt working electrode was also tried and was found to be completely incompetent for this reaction. The use of NBu₄OTs as electrolyte slightly reduced the yield (Entry 21). As solvent of lower polarity was reported to facilitate Cu-mediated oxidative elimination,^[13] some mixed solvents were tried. A 1:1 mixture of MeOH and dichloromethane (DCM) was the best solvent, giving a yield of 80% for the product 2-2 (Entry 22).

Table 2.1 Optimization of conditions for the electrochemical formal aza-Wacker cyclization.

entry	solvent	catalyst	base	<i>i</i> / mA	yield ^[a] / %
1	MeOH	Cu(OAc) ₂ H ₂ O	2 eq. NaOAc	3	33
2	EtOH	Cu(OAc) ₂ H ₂ O	2 eq. NaOAc	3	22
3	acetone	Cu(OAc) ₂ H ₂ O	2 eq. NaOAc	3	15
4	DMF	Cu(OAc) ₂ H ₂ O	2 eq. NaOAc	3	0
5	MeOH	Cu(OAc) ₂ H ₂ O	3 eq. NaOAc	3	46
6	MeOH	Cu(OAc) ₂ H ₂ O	4 eq. NaOAc	3	51
7	MeOH	Cu(OAc) ₂ H ₂ O	--	3	trace
8	MeOH	Cu(OAc) ₂ H ₂ O	4 eq. NaHCO ₃	3	10
9	MeOH	Cu(OAc) ₂ H ₂ O	4 eq. LiO ^t Bu	3	10
10	MeOH	Cu(OAc) ₂ H ₂ O	4 eq. NaOPiv	3	64
11	MeOH	Cu(OAc) ₂ H ₂ O	4 eq. NaOBz	3	62
12	MeOH	Cu(OAc) ₂ H ₂ O	4 eq. NaOPiv	1.5	70
13	MeOH	CuCl ₂ 2H ₂ O	4 eq. NaOPiv	1.5	56
14	MeOH	FeCl ₃ 6H ₂ O	4 eq. NaOPiv	1.5	13
15	MeOH	Ni(OAc) ₂ 4H ₂ O	4 eq. NaOPiv	1.5	13
16	MeOH	Co(OAc) ₂ 4H ₂ O	4 eq. NaOPiv	1.5	10
17	MeOH	Pd(OAc) ₂	4 eq. NaOPiv	1.5	8
18	MeOH	--	4 eq. NaOPiv	1.5	13
19 ^[b]	MeOH	Cu(OAc) ₂ H ₂ O	4 eq. NaOPiv	1.5	0
20 ^[c]	MeOH	Cu(OAc) ₂ H ₂ O	4 eq. NaOPiv	1.5	35
21 ^[d]	MeOH	Cu(OAc) ₂ H ₂ O	4 eq. NaOPiv	1.5	66
22 ^[e]	MeOH-DCM	Cu(OAc) ₂ H ₂ O	4 eq. NaOPiv	1.5	80

Reaction conditions: 0.2 mmol scale, carbon fiber (geometric area 15.8 cm²) as anode, Pt foil (1 cm²) as cathode 8 mL solvent in each cell; 2-1, base and catalyst in anodic cell; 0.4 mL additional H₂O in cathodic cell. ^a GC yield ^b 1 cm² Pt foil as anode. ^c RVC cube (geometric area 6 cm²) as anode. ^d 0.1 M NBu₄OTs as electrolyte. ^e The ratio of MeOH:DCM is 1:1.

2.3 Reaction scope studies

The optimized conditions (Entry 22, Table 2.1) were applied to explore the substrate scope of this transformation (Figure 2.1). First, substrates with different substituents on the aryl group were tested. *Ortho*-methyl group was tolerated, giving 2-3 in 62% yield. Substrates with an electron-withdrawing group at the *para*-position, such as -Cl (2-4), -CF₃ (2-5) and -CN (2-6), were transformed into the corresponding products in good yields. The strongly electron-withdrawing nitro group decreased the yield to 55% (2-7). With an electron-donating methoxy group at the *para* position, oxidation of the arene dominated under the standard conditions to give the side product 2-8', and the cyclization product 2-8 was obtained in less than 10% yield. Interestingly, by using NBu₄OTs as electrolyte, the arene oxidation was suppressed and 2-9 was obtained in 48% yield. This could be related to the relatively hydrophobic electric double layer formed by the organic electrolyte.^[15] The hydrophobic environment repulses the polar methanol which is a reactant for the side reaction. Besides, the presence of electron-withdrawing -NO₂ could also suppress the oxidation of aryl part. A substrate with 2-methoxy-5-nitrophenyl led to the cyclization product (2-9) in 58% yield under the standard conditions.

Next, variations on the crotyl part of the substrates were explored. When there was a methyl substituent at the C4 position (Figure 2.1), an oxazolidinone containing an internal alkene moiety (2-10) was obtained in 58% yield (E: Z= 10:1). A phenyl group at the C4 position was also tolerated to give the exclusive E-product (2-11) in 56% yield. When there were two methyl groups on C4, 2-12 was formed under the standard conditions, yet with substantial amount of the hydroamination product 2-12', which is hard to be separated from the product. This problem was solved by using an increased temperature (75 °C), leading to 2-12 in a decent yield (65%). Substitutions at the C1 position were also tested using *n*-Pr, *i*-Pr, and the N-methyl-2-pyrrolidone group. All three substrates gave good yields (2-13, 2-14 and 2-15). The diastereoselectivity (trans over cis) increases with the steric bulk of the substituent: 2.6:1 for *n*-Pr, 6.6:1 for *i*-Pr, and > 20:1 for the N-methyl-2-pyrrolidone. When there was a substituent at the C2 position, a quaternary carbon center could be formed during cyclization (2-16 to 2-19). Gratifyingly, this protocol enabled the synthesis of spiro structures containing 6-membered (2-17, 55%) and 5-membered (2-18, 77%) cyclic alkene. Bicyclic (2-20), and multicyclic structures (2-19) were also successfully constructed.

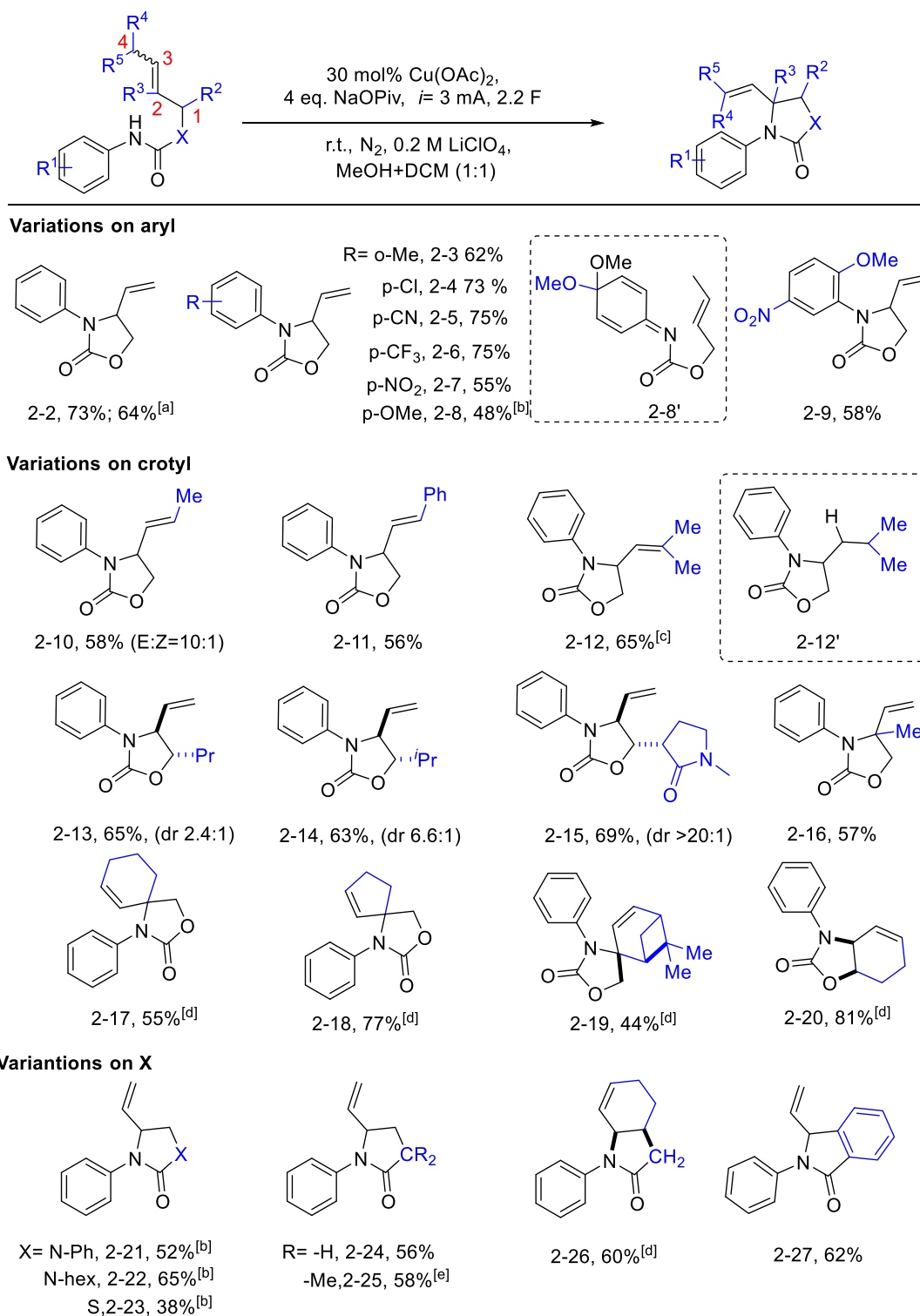


Figure 2.1 Scope of the electrochemical formal aza-Wacker cyclization. Reaction conditions: 0.2 mmol scale, carbon fiber (geometric area 15.8 cm²) as anode, Pt foil (1 cm²) as cathode; 8 mL solvent in each cell; 1, base and catalyst in anodic cell; 0.4 mL additional H₂O in cathodic cell. ^[a] In 6 mmol scale. ^[b] 0.1 M NBu₄OTs as electrolyte. ^[c] MeOH-PhCl(1:3)

as solvent, 0.1 M NBu₄OTs as electrolyte, 4 eq. NaOAc as base, 75 °C. ^[d] MeOH-PhCl (1:1) as solvent, 0.1 M NBu₄OTs as electrolyte, 4 eq. NaOAc as base, 65 °C. ^[e] 6 eq. NaOPiv as base, 5 F.

The substrate scope could be extended beyond carbamates. The ureas as providers of N-H led to the synthesis of imidazolidinones. Both phenyl (2-21, 52%) and alkyl (2-22) on the other nitrogen atom were tolerated. Using a carbamothioate and amides as substrates provided thiazolidinone (2-23) and γ -lactams (2-24 to 2-25). γ -Lactam contained in a bicyclic structure (2-26) could be synthesized as well. Additionally, the amide and alkene units in the substrate could be connected by a benzene linker, giving rise to isoindolinone (2-26) in 62% yield. It was noted that the cyclization was insensitive to the configuration of the alkenes. Thus, the use of substrates as E/Z mixture was possible (for 2-21, 2-23, 2-25 and 2-26).

While the reactions in Figure 2.1 were conducted at a scale of 0.2 mmol, the reaction of 2-1 was scaled to 6 mmol using a larger setup, and with a reduced amount of copper catalyst (10 mol%). The target product 2-2 was obtained in 64% yield (0.73 g).

2.4 Mechanistic investigations

A few experiments were conducted to probe the mechanism of the transformation. For a substrate (2-28) containing a cyclopropyl group which acts as a radical clock, the product from ring-opening and elimination (2-29) was obtained in 62% yield under the standard conditions (Figure 2.2a). This result is consistent with the formation of an alkyl radical after the amidyl radical intramolecular cyclization. For a bulky substrate 2-30, the double cyclization product 2-31 was obtained as the major product in 32% yield (Figure 2.2b), which presumably originated from the addition of the alkyl radical into the aryl group.^[15, 16]

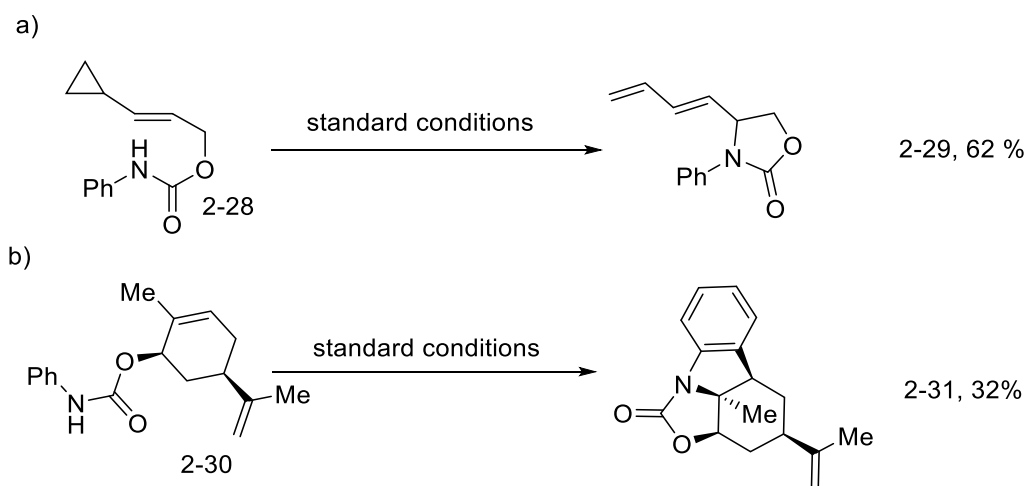


Figure 2.2 Evidences for a radical reaction pathway.

To probe the role of the Cu catalyst, reactions of several representative substrates were conducted with and without the $\text{Cu}(\text{OAc})_2$ catalyst. For substrate 2-1, which forms a secondary alkyl radical in the reaction, 80% yield of 2-2, but no 2-2' (formed from a hydrogen abstraction reaction by the alkyl radical)^[17] was obtained in the presence of $\text{Cu}(\text{OAc})_2$ (Figure 2.3a). In the absence of $\text{Cu}(\text{OAc})_2$, however, 2-2 was obtained only in 28% yield, and the reaction also gave 12% of 2-2'. For substrate 2-28, which forms a primary alkyl radical in the reaction, 62% of elimination product 2-29 but no product 2-29' was obtained in the presence of $\text{Cu}(\text{OAc})_2$ (Figure 2.3b). In the absence of $\text{Cu}(\text{OAc})_2$, no 2-29 was obtained. Only 2-29' was formed in a yield of 25%. These results indicate that the Cu catalyst is essential for the efficient oxidative elimination of secondary and primary alkyl radical intermediates to form alkenes. Interestingly, for reactions involving tertiary alkyl radicals (Figure 2.3c), for example, for 2-32 and 2-34, two products were obtained, the alkenes (2-33 & 2-35) and the methoxylated products (2-33' & 2-35'). Regardless of the existence of the copper, these

products were obtained in almost the same yields. This result indicates that the oxidation of tertiary alkyl radicals occurs readily at the electrode even without a Cu catalyst, consistent with the work of Xu and co-workers.^[12]

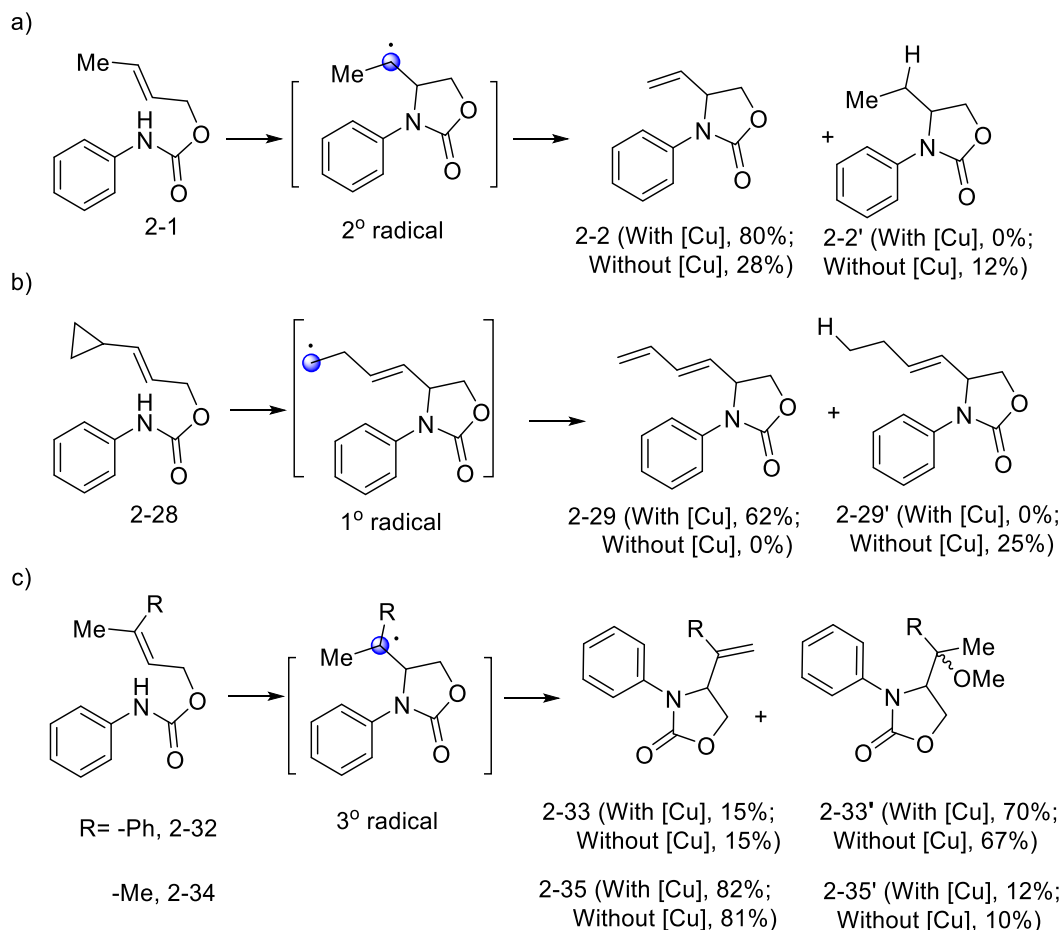


Figure 2.3 Conversion of primary, secondary and tertiary alkyl intermediates in the presence or in the absence of $\text{Cu}(\text{OAc})_2$ catalyst.

Cyclic voltammetry (CV) was used to probe the oxidation process at the electrode (Figure 2.4). The direct oxidation of 2-1 started only at potentials higher than 1.0 V vs the Fc^+/Fc couple. Addition of 1 eq. of NaOPiv generated a new oxidation peak at about 0.83 V. The oxidation of NaOPiv occurred only at potentials higher than 0.9 V. Thus, NaOPiv facilitated the oxidation of 2-1. We tentatively attributed this promotion to the formation of a substrate-base complex 2-33. A substrate without double bond (2-34) gave an oxidation peak at a similar potential, while adding -OMe to the phenyl of the substrate 2-1 shifted the oxidation to 0.56 V (for 2-35). These results indicate that the

initial oxidation event occurs at the N-containing part and is not related to the alkene part. We further mixed $\text{Cu}(\text{OAc})_2$ (20 mol%) with 2-1 and NaOPiv, the CV curve remained largely intact. This result shows that the Cu catalyst does not have obvious influence on the initial oxidation step.

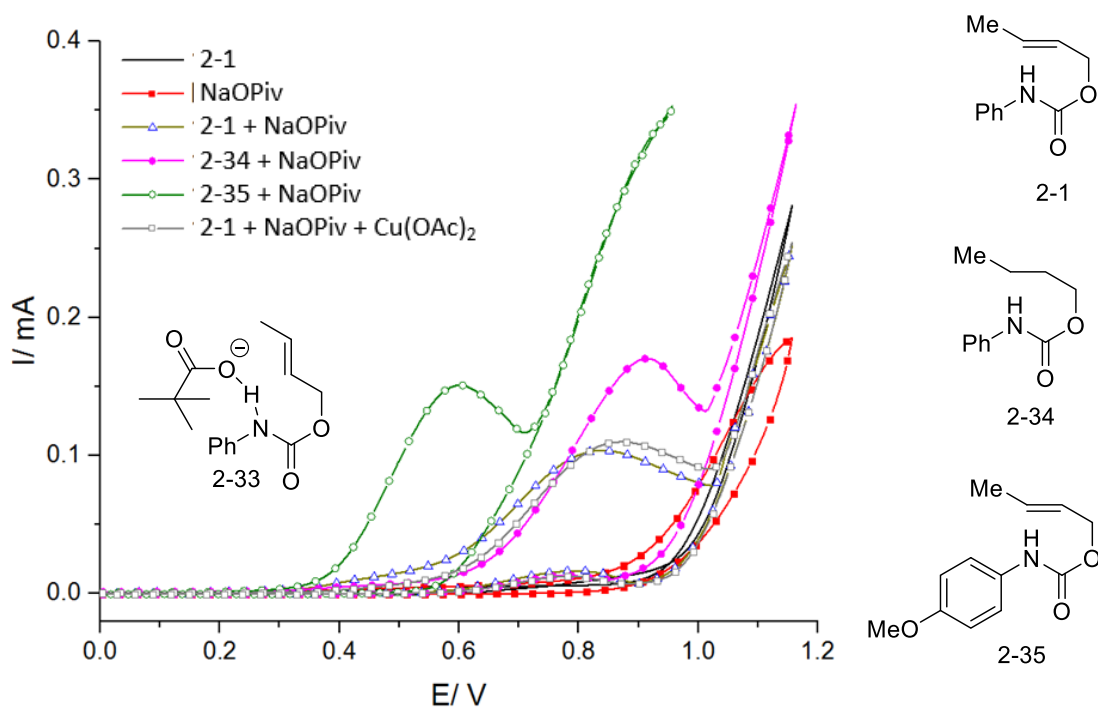
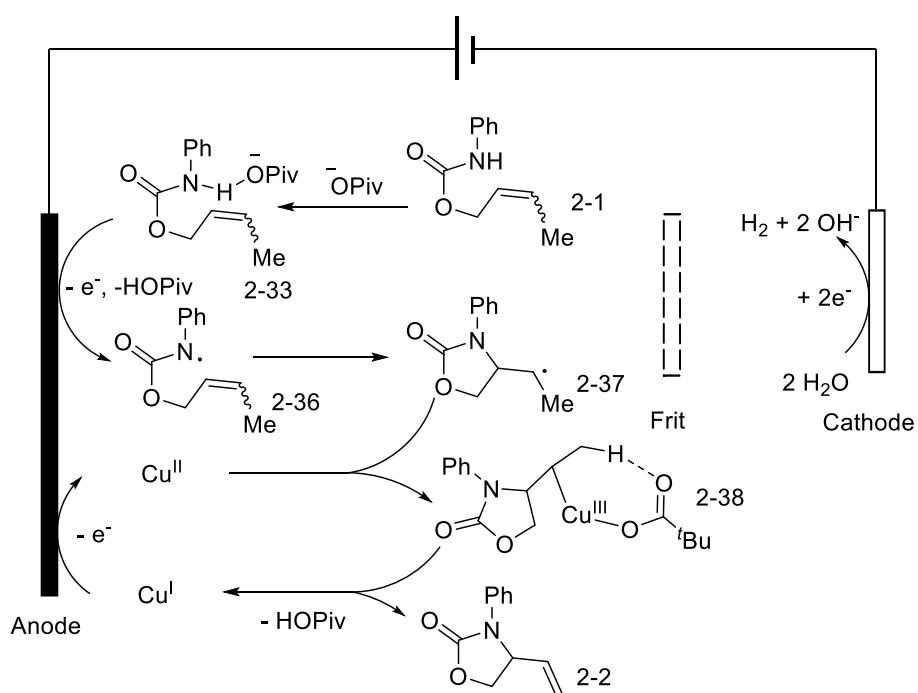


Figure 2.4 Cyclic voltammetry of the reagents in the reaction. The potential is versus Fc/Fc^+ . Concentration of reagents (if applicable): 0.01 M 2-1 (or 2-34, 2-35) 0.01 M NaOPiv, 0.002 M $\text{Cu}(\text{OAc})_2$. 0.1 M NBu_4BF_4 as electrolyte. Conditions: DCM+MeOH (1:1) as solvent, scan rate 100 mV/s.

2.5 The proposed reaction mechanism

Based on the above results, we propose the following mechanism for the electrochemical formal aza-Wacker cyclization (Scheme 2.2). First, the substrate 2-1 associates with the pivalate to give an adduct 2-33, which is easier to be oxidized at the anode to give an amidyl radical 2-36 with the release of pivalic acid. The N-centered radical undergoes 5-exo-trig cyclization to afford the alkyl radical 2-37, which is captured by Cu^{II} to generate a formal Cu^{III} alkyl intermediate 2-38. Subsequent elimination, assisted by the pivalate, furnishes the alkene product 2-2 and yields a Cu^{I} species. The latter is oxidized at the electrode to Cu^{II} to re-enter the catalytic cycle.



Scheme 2.2 A plausible mechanism for the electrochemical formal aza-Wacker cyclization.

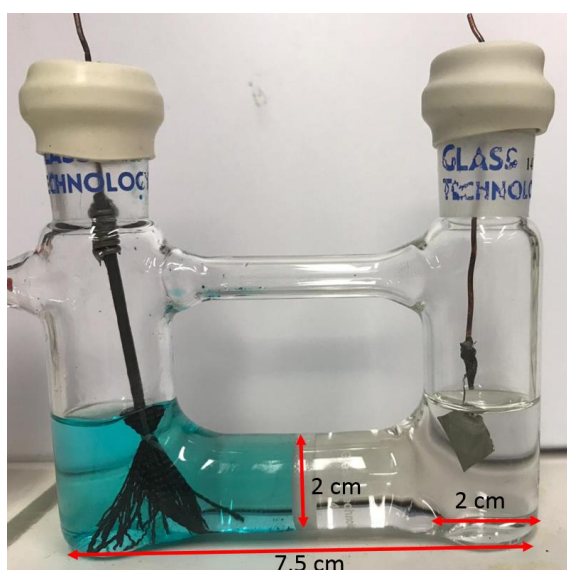
2.6 Conclusion

By integrating electrochemical oxidation with Cu catalysis, we have developed a formal aza-Wacker cyclization method. This tandem process relies on the cyclization of amidyl radical to generate an alkyl radical, which is converted to an alkene with copper-mediated oxidative elimination. Mechanistic studies revealed that primary and secondary alkyl radical intermediates couldn't be efficiently oxidized on the electrode directly and the assistance of copper was indispensable. A wide range of 5-membered N-containing heterocycles bearing a pendant, functionalizable alkene moiety can be synthesized under mild conditions.

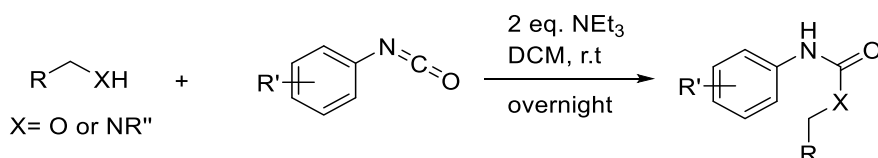
2.7 Experiments

2.7.1 General consideration

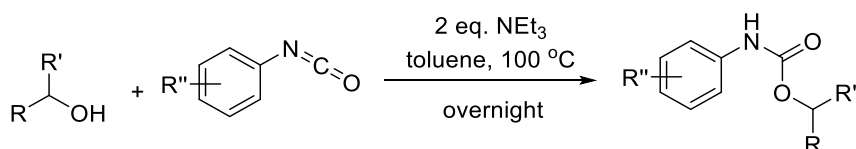
Commercially available solvents (DCM and chlorobenzene) and reagents were used without purification. Methanol was purged with N_2 overnight to remove oxygen. A divided H cell with a C4 frit was used for electrolysis (parameters shown in the picture below). Carbon fiber anode was fabricated by dissecting 4 cm² carbon cloth (hydrophilic carbon cloth, supplied by FuelCellsEtc) to fibers (68 fibers on average, $d = 0.37$ mm, $l = 2$ cm) and tying up the fibers on the end of a carbon rod ($d = 2$ mm). The distance between anode and cathode is around 5.5 cm. All electrolysis experiments were carried out with IVIUMSTAT potential station. Cyclic voltammograms (CV) were recorded on BIO-LOGIC VSP potential station. Gas chromatography-mass spectrometer (GCMS) was used for product analysis and identification. Gas chromatography (GC) with flame ionization detector (FID) was used for reaction optimization (1,3,5-trimethoxylbenzene as internal standard) and determination of ratio of diastereoisomers. Separations were conducted on silica gel column with hexane-ethylacetate (EA) as eluent. NMR spectra were recorded with Bruker Avance 400 MHz instruments. Chemical shifts are reported in ppm relative to residual signal of $CHCl_3$ (7.26 ppm) for 1H and $CDCl_3$ (77.16 ppm) for ^{13}C . Descriptions of multiplicities are abbreviated as follows: s = singlet, d = doublet, t = triplet, q = quartet, m = multiplet, b = broad. Determinations of high resolution mass spectra (HRMS) by electrospray ionization (ESI) were performed with Micro Mass QTOF Ultima spectrometer at the EPFL Mass Spectrometry Center. Infrared spectra were collected using Varian 800 FT-IR. Description of the intensity of the peaks: s= strong, m= medium.



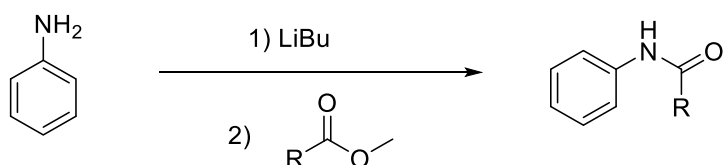
2.7.2 Procedures for substrate synthesis



Synthesis of carbamates and ureas: To a solution of 1 eq. of alcohol or amine in CH_2Cl_2 (0.5 M) was added 1.0 eq. of phenyl isocyanate and then 2 eq. of NEt_3 . The reaction was maintained at room temperature overnight to complete. The resultant solution was concentrated and the residue was separated by silica gel column chromatography with ethyl acetate/hexanes to provide the products.



Synthesis of carbamates with relatively hindered alcohols: To a solution of 1 eq. of alcohol in toluene (0.1 M) was added 1.2 eq. of phenyl isocyanate and then 2 eq. of NEt_3 . The reaction was heated at 100°C overnight to complete. The resultant solution was concentrated and the residue was separated by silica gel column chromatography with ethyl acetate/hexanes to provide the product.



Synthesis of amides: To a N_2 -protected Schlenk flask were added aniline (2 eq.) and Et_2O (0.8 M). The solution was cooled down to -78°C , and 2 eq. of Li^nBu (2.5 M in hexane) was slowly added to the solution. After 5 min, the solution was warmed to room temperature and the ester (1 eq., 1 M in Et_2O) was added dropwise to the solution. The reaction was stirred at room temperature for 2 h.

The reaction was quenched with saturated NH_4Cl solution. The organic phase were collected and the aqueous phase was extracted by EtOAc twice. The organic solutions were combined and then concentrated. Purification on silica gel column afforded the products.

2.7.3 Procedures for electrochemical reaction setup

General procedure 1 (2-GP1):

0.2 mmol substrate, 0.8 mmol NaOPiv, 0.06 mmol $\text{Cu}(\text{OAc})_2 \cdot \text{H}_2\text{O}$ and 1.6 mmol LiClO_4 were added to the anodic compartment, and 1.6 mmol LiClO_4 was added to the cathodic compartment. Anode and cathode (1 cm^2 Pt foil) with rubber septa were installed on the H-cell, which was then vacuumized and refilled with N_2 for 3 times. 4 mL MeOH and 4 mL DCM were added to both anodic and cathodic cells, and 0.4 mL H_2O was further added to the cathodic cell. The solution in the anodic cell was purged with N_2 for 5 min. 1.5 mA of constant current was imposed for 28000 s (about 2.2 F). The solution in anodic cell was collected and evaporated, and the residual was diluted by 15 mL Et_2O . 2 mL H_2O and 3 drop of 15% aqueous ammonia were added to remove the electrolyte and Cu species. The organic phase was collected, evaporated and then subjected to column separation to afford the final products.

Note: After electrolysis, no significant crossover of product (or substrate) to cathodic cell was observed (same for the procedures below).

General procedure 2 (2-GP2):

0.2 mmol substrate, 0.8 mmol NaOAc, 0.06 mmol $\text{Cu}(\text{OAc})_2 \cdot \text{H}_2\text{O}$ and 0.8 mmol NBu_4OTf were added to the anodic cell, and 0.8 mmol NBu_4OTf was added to the cathodic cell. Anode and cathode (1 cm^2 Pt foil) with rubber septa were installed on the H-cell, which was then vacuumized and refilled with N_2 for 3 times. 4 mL MeOH and 4 mL PhCl were added to both anodic and cathodic cells, and 0.4 mL H_2O was further added to the cathodic cell. The solution in anodic cell was purged with N_2 for 5 min. The H-cell was heated at 65 $^\circ\text{C}$ in an oil bath, and 1.5 mA of constant current was imposed for 28000 s (2.2 F). The product separation procedures are the same as in 2-GP1.

Scale-up electrolysis:

A large H cell was used for the scale-up electrolysis (height: 13 cm; length: 10 cm; diameter of C4 frit: 3 cm). 6 mmol 2-1, 24 mmol NaOPiv, 0.6 mmol $\text{Cu}(\text{OAc})_2 \cdot \text{H}_2\text{O}$ and 8 mmol LiClO_4 were added to the anodic cell, and 8 mmol LiClO_4 was added to the cathodic cell. Anode (made from 36 cm^2 carbon cloth, geometric area 142 cm^2) and cathode (1 cm^2 Pt foil) with rubber septum were installed on the H-cell, which was then vacuumized and refilled with N_2 for 3 times. 40 mL MeOH and 40 mL PhCl were both added to anodic and cathodic cells, and 1 mL HOAc was further added to the cathodic cell. The solution in anodic cell was purged with N_2 for 15 min. 10 mA ($j = 0.07 \text{ mA}/\text{cm}^2$)

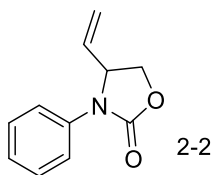
of constant current was imposed for 35 h (about 2.2 F). The product separation procedures are the same as in 2-4-GP1, and 0.73 g product 2-2 was isolated as yellowish oil (yield 64%).

2.7.4 Procedures for cyclic voltammetry

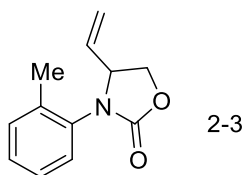
The cyclic voltammograms were recorded in a DCM-MeOH solvent (1:1, 4 mL) in a four-neck flask, with Bu_4NBF_4 (0.1 M) as electrolyte, glassy carbon disk as working electrode (diameter, 3 mm), Pt wire as counter electrode, $\text{Ag}^+|\text{Ag}$ [0.01 M, in CH_3CN , with Bu_4NBF_4 (0.1 M) as electrolyte] as reference electrode. The scan rate was 100 mV/s. Concentration of reagents (if applicable): 0.01 M **1**, 0.01 M NaOPiv, 0.002 M $\text{Cu}(\text{OAc})_2$.

$E(\text{Fc}^+/\text{Fc})$ comparing to the reference electrode was 0.143 V (determined with 0.003 M Ferrocene).

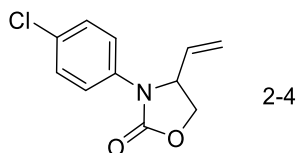
2.7.5 Characterization data for the products



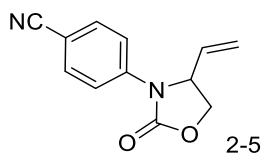
3-phenyl-4-vinyloxazolidin-2-one, synthesized via 2-GP1, colorless oil, 27.6 mg (Yield = 73%). ^1H NMR (400 MHz, CDCl_3) δ 7.48 – 7.40 (m, 2H), 7.40 – 7.31 (m, 2H), 7.20 – 7.11 (m, 1H), 5.80 (ddd, J = 17.7, 10.1, 7.8 Hz, 1H), 5.41 – 5.29 (m, 2H), 4.91 – 4.82 (m, 1H), 4.59 (t, J = 8.7 Hz, 1H), 4.11 (dd, J = 8.7, 6.4 Hz, 1H). ^{13}C NMR (101 MHz, CDCl_3) δ 155.7, 137.1, 134.8, 129.0, 125.1, 121.5, 120.6, 67.2, 59.7. The spectra match well with the reported data.^[18] GC-MS 189.



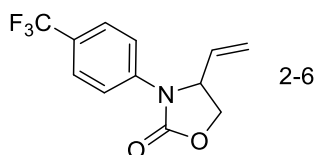
3-(o-tolyl)-4-vinyloxazolidin-2-one, synthesized via 2-GP1, colorless oil, 25.1 mg (Yield = 62%). ^1H NMR (400 MHz, CDCl_3) δ 7.30 – 7.18 (m, 3H), 7.15 – 7.09 (m, 1H), 5.82 – 5.68 (m, 1H), 5.22 – 5.13 (m, 2H), 4.74 – 4.60 (m, 2H), 4.22 – 4.13 (m, 1H), 2.30 (s, 3H). ^{13}C NMR (101 MHz, CDCl_3) δ 156.3, 136.7, 134.6, 134.4, 131.4, 128.3, 127.6, 126.8, 121.6, 67.7, 62.3, 18.2. The spectra match well with the reported data.^[19] GC-MS 203.



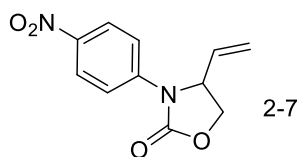
3-(4-chlorophenyl)-4-vinyloxazolidin-2-one, synthesized via 2-GP1, yellowish oil, 32.5 mg (Yield = 73%). ^1H NMR (400 MHz, CDCl_3) δ 7.39 (d, J = 9.0 Hz, 2H), 7.31 (d, J = 9.0 Hz, 2H), 5.78 (ddd, J = 17.1, 10.2, 7.8 Hz, 1H), 5.40 – 5.31 (m, 2H), 4.88 – 4.77 (m, 1H), 4.59 (t, J = 8.7 Hz, 1H), 4.11 (dd, J = 8.7, 6.2 Hz, 1H). ^{13}C NMR (101 MHz, CDCl_3) δ 155.5, 135.7, 134.5, 130.3, 129.1, 122.6, 120.9, 67.2, 59.6. The spectra match well with the reported data. GC-MS 223.



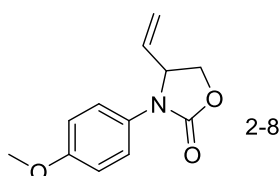
4-(2-oxo-4-vinyloxazolidin-3-yl)benzonitrile, synthesized via 2-GP1, colorless oil, 32.4 mg (Yield = 75%). ^1H NMR (400 MHz, CDCl_3) δ 7.62 (s, 4H), 5.81 (ddd, J = 17.5, 10.2, 7.5 Hz, 1H), 5.46 – 5.36 (m, 2H), 4.96–4.85 (m, 1H), 4.62 (t, J = 8.7 Hz, 1H), 4.15 (dd, J = 8.7, 5.6 Hz, 1H). ^{13}C NMR (101 MHz, CDCl_3) δ 154.8, 141.3, 134.0, 133.1, 121.0, 120.2, 118.7, 107.6, 67.3, 58.8. The spectra match well with the reported data.^[18] GC-MS 214.



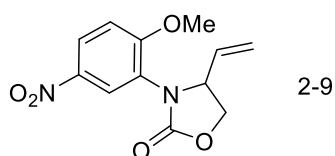
3-(4-(trifluoromethyl)phenyl)-4-vinyloxazolidin-2-one, synthesized via 2-GP1, colorless oil, 38.3 mg (Yield = 75%). ^1H NMR (400 MHz, CDCl_3) δ 7.60 (s, 4H), 5.87 – 5.76 (m, 1H), 5.44 – 5.36 (m, 2H), 4.95 – 4.87 (m, 1H), 4.62 (t, J = 8.7 Hz, 1H), 4.15 (dd, J = 8.7, 5.9 Hz, 1H). ^{13}C NMR (101 MHz, CDCl_3) δ 155.2, 140.3, 134.3, 126.5 (q, J = 33.0 Hz), 126.2 (q, J = 3.9 Hz), 124.1 (q, J = 271.6 Hz), 121.0, 120.4, 67.3, 59.1. The spectra match well with the reported data.^[18] GC-MS 257.



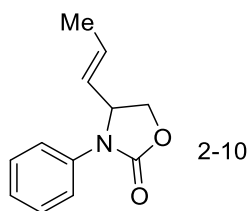
3-(4-nitrophenyl)-4-vinyloxazolidin-2-one, synthesized via 2-GP1, yellowish oil, 25.8 mg (Yield = 55%). ^1H NMR (400 MHz, CDCl_3) δ 8.27 – 8.18 (m, 2H), 7.73 – 7.65 (m, 2H), 5.84 (ddd, J = 17.4, 10.2, 7.5 Hz, 1H), 5.48 – 5.40 (m, 2H), 4.99 – 4.90 (m, 1H), 4.65 (t, J = 8.7 Hz, 1H), 4.18 (dd, J = 8.7, 5.4 Hz, 1H). ^{13}C NMR (101 MHz, CDCl_3) δ 154.8, 143.7, 143.1, 133.9, 124.8, 121.1, 119.7, 67.4, 59.0. The spectra match well with the reported data. ^[18] GC-MS 234.



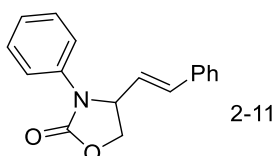
3-(4-methoxyphenyl)-4-vinyloxazolidin-2-one, synthesized via modified 2-GP1 (using 0.1 M NBu_4OTf as electrolyte), colorless oil, 21.0 mg (Yield = 48%). ^1H NMR (400 MHz, CDCl_3) δ 7.33 – 7.27 (m, 2H), 6.92 – 6.85 (m, 2H), 5.78 (ddd, J = 17.1, 10.1, 8.1 Hz, 1H), 5.35 – 5.26 (m, 2H), 4.81–4.70 (m, 1H), 4.58 (t, J = 8.6 Hz, 1H), 4.09 (dd, J = 8.7, 6.7 Hz, 1H), 3.78 (s, 3H). ^{13}C NMR (101 MHz, CDCl_3) δ 157.4, 156.2, 135.0, 129.8, 124.2, 120.9, 114.4, 67.2, 60.6, 55.6. The spectra match well with the reported data. ^[18] GC-MS 219.



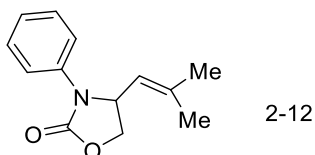
3-(2-methoxy-5-nitrophenyl)-4-vinyloxazolidin-2-one, synthesized via 2-GP1, white solid, m.p. 163–164 °C, 30.7 mg (Yield = 58%). ^1H NMR (400 MHz, CDCl_3) δ 8.22 (dd, J = 9.1, 2.8 Hz, 1H), 8.16 (d, J = 2.8 Hz, 1H), 7.03 (d, J = 9.1 Hz, 1H), 5.80 – 5.66 (m, 1H), 5.25 – 5.15 (m, 2H), 4.87 – 4.75 (m, 1H), 4.65 (t, J = 8.6 Hz, 1H), 4.23 – 4.11 (m, 1H), 3.98 (s, 3H). ^{13}C NMR (101 MHz, CDCl_3) δ 160.5, 156.5, 141.3, 134.2, 126.0, 125.4, 125.2, 122.0, 111.7, 68.0, 61.0, 56.7. GC-MS 264. ESI HRMS m/z ($\text{M}+\text{H}$)⁺ calcd 265.0825, obsd 265.0831. IR: 1735 cm^{-1} (s).



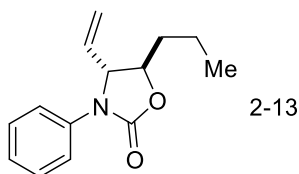
3-phenyl-4-(prop-1-en-1-yl)oxazolidin-2-one, synthesized via 2-GP1, colorless oil, 23.5 mg (Yield = 58%, E:Z = 10:1). ^1H NMR (400 MHz, CDCl_3) δ 7.45 – 7.30 (m, 4H), 7.15 (t, J = 7.3 Hz, 1H), 5.79 (dt, J = 14.0, 7.2 Hz, 1H), 5.47 – 5.28 (m, 1H), 4.85–4.77 (m, 1H), 4.55 (t, J = 8.7 Hz, 1H), 4.26 – 3.98 (m, 1H), 1.76 – 1.62 (d, J = 5.0 Hz, 3H). ^{13}C NMR (101 MHz, CDCl_3) δ 155.9, 137.2, 132.3, 129.0, 127.8, 125.0, 121.8, 67.6, 59.3, 17.8. GC-MS 203. ESI HRMS m/z ($\text{M}+\text{Na}$) $^+$ calcd 226.0844, obsd 226.0847. IR: 1744 cm^{-1} (s).



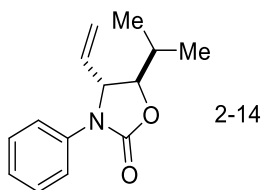
(E)-3-phenyl-4-styryloxazolidin-2-one, synthesized via 2-GP1, sticky liquid, 29.7 mg (Yield = 56 %). ^1H NMR (400 MHz, CDCl_3) δ 7.54 – 7.46 (m, 2H), 7.40 – 7.27 (m, 7H), 7.14 (t, J = 7.3 Hz, 1H), 6.66 (d, J = 15.9 Hz, 1H), 6.13 (dd, J = 15.9, 8.2 Hz, 1H), 5.03 (td, J = 8.3, 6.3 Hz, 1H), 4.65 (t, J = 8.6 Hz, 1H), 4.20 (dd, J = 8.7, 6.4 Hz, 1H). ^{13}C NMR (101 MHz, CDCl_3) δ 155.8, 137.1, 135.4, 135.3, 129.1, 128.9, 128.8, 126.8, 125.7, 125.2, 121.6, 67.5, 59.6. GC-MS 265. ESI HRMS m/z ($\text{M}+\text{Na}$) $^+$ calcd 288.1000, obsd 288.1004. IR: 1752 cm^{-1} (s).



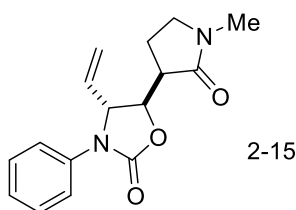
4-(2-methylprop-1-en-1-yl)-3-phenyloxazolidin-2-one, synthesized via modified 2-GP2 (MeOH: PhCl = 1:3, 75 $^\circ\text{C}$), white crystal, 28.0 mg (Yield = 65%). ^1H NMR (400 MHz, CDCl_3) δ 7.41 – 7.30 (m, 4H), 7.15 (t, J = 6.6 Hz, 1H), 5.17 – 5.03 (m, 2H), 4.56 (t, J = 8.2 Hz, 1H), 4.01 (dd, J = 8.5, 6.8 Hz, 1H), 1.73 (d, J = 1.2 Hz, 3H), 1.71 (d, J = 1.3 Hz, 3H). ^{13}C NMR (101 MHz, CDCl_3) δ 156.0, 139.0, 137.3, 129.0, 125.0, 122.3, 121.6, 67.8, 55.4, 25.9, 18.4. GC-MS 217.



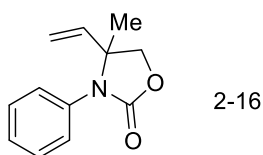
3-phenyl-5-propyl-4-vinyloxazolidin-2-one, synthesized via 2-GP1, colorless oil, separated as diastereoisomers, 30.1 mg (Yield = 65%, dr = 3.2:1). The major isomer could be obtained in small quantity by careful separation, whose NMR data are displayed below. ^1H NMR (400 MHz, CDCl_3) δ 7.45 – 7.37 (m, 2H), 7.39 – 7.30 (m, 2H), 7.19 – 7.10 (m, 1H), 5.76 (ddd, J = 17.1, 10.2, 8.0 Hz, 1H), 5.41 – 5.28 (m, 2H), 4.46 – 4.37 (m, 1H), 4.33 – 4.15 (m, 1H), 1.87 – 1.70 (m, 2H), 1.66 – 1.46 (m, 2H), 0.99 (t, J = 7.3 Hz, 3H). ^{13}C NMR (101 MHz, CDCl_3) δ 155.5, 137.3, 135.2, 129.0, 125.0, 121.7, 120.7, 79.0, 65.5, 36.0, 18.4, 13.9. GC-MS 231. ESI HRMS m/z ($\text{M}+\text{Na}$) $^+$ calcd 254.1157, obsd 254.1160. IR: 1745 cm^{-1} (s), 1378 cm^{-1} (s).



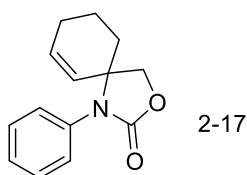
5-isopropyl-3-phenyl-4-vinyloxazolidin-2-one, synthesized via 2-GP1, yellowish oil, separated as diastereoisomers, 29.2 mg (Yield = 63%, dr = 6.7:1). NMR data of the major isomer are displayed below. ^1H NMR (400 MHz, CDCl_3) δ 7.44 (d, J = 8.2 Hz, 2H), 7.38 – 7.28 (m, 2H), 7.17 – 7.11 (m, 1H), 5.85 – 5.73 (m, 1H), 5.35 – 5.26 (m, 2H), 4.52 (t, J = 6.8 Hz, 1H), 4.09 – 4.01 (m, 1H), 2.08 – 1.91 (m, 1H), 1.10–1.01 (m, 6H). ^{13}C NMR (101 MHz, CDCl_3) δ 155.3, 137.2, 135.9, 129.0, 125.0, 121.6, 120.2, 83.5, 62.7, 32.2, 17.8, 17.1. GC-MS 231. ESI HRMS m/z ($\text{M}+\text{Na}$) $^+$ calcd 254.1157, obsd 254.1161. IR: 1744 cm^{-1} (s), 1386 cm^{-1} (s).



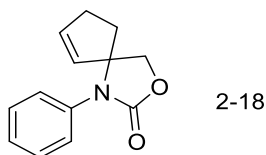
5-(1-methyl-2-oxopyrrolidin-3-yl)-3-phenyl-4-vinyloxazolidin-2-one, synthesized via 2-GP1, colorless oil, 39.6 mg (Yield = 69%). ^1H NMR (400 MHz, CDCl_3) δ 7.51 – 7.39 (m, 2H), 7.36 – 7.27 (m, 2H), 7.15 (t, J = 7.4 Hz, 1H), 5.74 (ddd, J = 17.6, 10.1, 8.0 Hz, 1H), 5.50 – 5.33 (m, 2H), 5.30 (d, J = 10.1 Hz, 1H), 4.44 (dd, J = 6.8, 2.5 Hz, 1H), 3.48-3.42 (m, 1H), 3.37-3.30 (m, 1H), 2.87-2.81 (m, 4H), 2.33-2.27 (m, 1H), 2.19 – 2.01 (m, 1H). ^{13}C NMR (101 MHz, CDCl_3) δ 171.5, 155.2, 137.0, 135.0, 129.0, 125.4, 122.5, 121.1, 79.3, 61.4, 47.6, 42.6, 29.9, 21.9. GC-MS 286. ESI HRMS m/z ($\text{M}+\text{H}$) $^+$ calcd 287.1396, obsd 287.1398. IR: 1747 cm^{-1} (s), 1678 cm^{-1} (s), 1390 cm^{-1} (s).



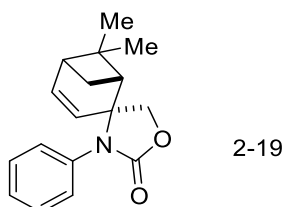
4-methyl-3-phenyl-4-vinyloxazolidin-2-one, synthesized via 2-GP1, white solid, 23.2 mg (Yield = 57%). ^1H NMR (400 MHz, CDCl_3) δ 7.39 – 7.33 (m, 2H), 7.30 – 7.24 (m, 3H), 6.08 (dd, J = 17.4, 10.7 Hz, 1H), 5.31 (d, J = 10.7 Hz, 1H), 5.23 (d, J = 17.4 Hz, 1H), 4.26 (d, J = 8.5 Hz, 1H), 4.15 (d, J = 8.5 Hz, 1H), 1.47 (s, 3H). ^{13}C NMR (101 MHz, CDCl_3) δ 156.7, 139.7, 135.5, 129.1, 127.3, 127.1, 117.3, 74.4, 63.7, 21.6. GC-MS 203.



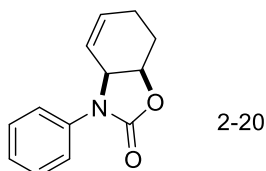
1-phenyl-3-oxa-1-azaspiro[4.5]dec-6-en-2-one, synthesized via 2-GP2, colorless oil, 25.4 mg (Yield = 55%). ^1H NMR (400 MHz, CDCl_3) δ 7.47 – 7.18 (m, 5H), 6.02-5.96 (m, 1H), 5.82 (d, J = 10.1 Hz, 1H), 4.24 (d, J = 8.6 Hz, 1H), 4.16 (d, J = 8.6 Hz, 1H), 2.03 – 1.77 (m, 4H), 1.74 – 1.60 (m, 1H), 1.59 – 1.40 (m, 1H). ^{13}C NMR (101 MHz, CDCl_3) δ 157.0, 135.9, 133.4, 129.3, 129.1, 127.6, 127.4, 73.6, 63.1, 31.6, 24.1, 19.6. GC-MS 229. ESI HRMS m/z ($\text{M}+\text{Na}$) $^+$ calcd 252.1001, obsd 252.1004. IR: 1753 cm^{-1} (s), 1397 cm^{-1} (m).



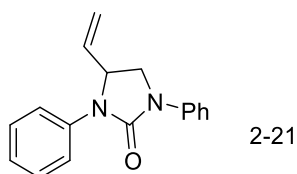
1-phenyl-3-oxa-1-azaspiro[4.4]non-6-en-2-one, synthesized via 2-GP2, white solid, m.p. 94-96 °C, 33.0 mg (Yield = 77%). ^1H NMR (400 MHz, CDCl_3) δ 7.38 – 7.31 (m, 2H), 7.28 – 7.23 (m, 3H), 5.98 (dt, J = 5.5, 2.3 Hz, 1H), 5.82 (dt, J = 5.5, 2.1 Hz, 1H), 4.35 – 4.26 (m, 2H), 2.32-2.24 (m, 1H), 2.23 – 2.15 (m, 1H), 2.13-2.06 (m, 1H), 2.05-1.97 (m, 1H). ^{13}C NMR (101 MHz, CDCl_3) δ 156.6, 137.3, 135.6, 132.2, 129.1, 127.7, 127.4, 75.7, 73.7, 33.6, 30.9. GC-MS 215. ESI HRMS m/z ($\text{M}+\text{Na}$) $^+$ calcd 238.0844, obsd 238.0848. IR: 1744 cm^{-1} (s), 1387 cm^{-1} (m).



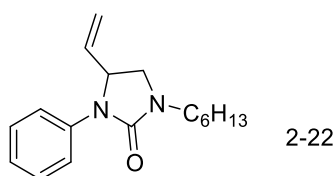
6,6-dimethyl-3'-phenylspiro[bicyclo[3.1.1]heptane-2,4'-oxazolidin]-3-en-2'-one, synthesized via 2-GP2, white crystal, m.p. 117-118 °C, 24.2 mg (Yield = 44%). ^1H NMR (400 MHz, CDCl_3) δ 7.40-7.30 (m, 3H), 7.18 (d, J = 7.5 Hz, 2H), 6.47-6.42 (m, 1H), 5.81 (d, J = 8.7, 1H), 4.44 (d, J = 9.0 Hz, 1H), 4.29 (d, J = 9.0 Hz, 1H), 2.50-2.42 (m, 1H), 2.04-1.98 (m, 2H), 1.33 (s, 3H), 0.95 (s, 3H), 0.69-0.65 (m, 1H). ^{13}C NMR (101 MHz, CDCl_3) δ 157.1, 141.5, 136.5, 129.8, 129.4, 128.4, 125.3, 73.0, 68.6, 51.9, 47.4, 40.9, 30.6, 26.8, 23.9. GC-MS 269. ESI HRMS m/z ($\text{M}+\text{Na}$) $^+$ calcd 292.1313, obsd 292.1320. IR: 1752 cm^{-1} (s).



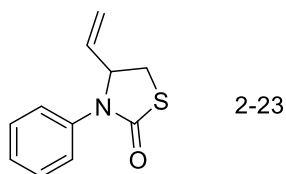
3-phenyl-3a,6,7,7a-tetrahydrobenzo[d]oxazol-2(3H)-one, synthesized via 2-GP2, colorless oil, 34.7 mg (Yield = 81%). ^1H NMR (400 MHz, CDCl_3) δ 7.52 (d, J = 8.1 Hz, 2H), 7.40-7.32 (m, 2H), 7.19 – 7.11 (m, 1H), 6.15 – 5.95 (m, 1H), 5.75 (d, J = 10.4 Hz, 1H), 4.94 – 4.83 (m, 1H), 4.76-4.70 (m, 1H), 2.38 – 2.17 (m, 2H), 2.09-2.01 (m, 1H), 1.93 – 1.76 (m, 1H). ^{13}C NMR (101 MHz, CDCl_3) δ 155.4, 137.4, 132.8, 129.3, 124.8, 121.3, 120.9, 72.3, 54.0, 24.5, 19.6. GC-MS 215.



1,3-diphenyl-4-vinylimidazolidin-2-one, synthesized via modified 2-GP1 (using 0.1 M NBu₄OTs as electrolyte), colorless oil, 27.4 mg (Yield = 52%). ¹H NMR (400 MHz, CDCl₃) δ 7.64 – 7.57 (m, 2H), 7.51 – 7.44 (m, 2H), 7.41-7.31 (m, 4H), 7.14-7.06 (m, 2H), 5.87 (ddd, *J* = 17.5, 10.2, 7.6 Hz, 1H), 5.39 (d, *J* = 17.2 Hz, 1H), 5.31 (d, *J* = 10.2 Hz, 1H), 4.83-4.77 (m, 1H), 4.13 (t, *J* = 9.0 Hz, 1H), 3.66 (dd, *J* = 9.0, 6.2 Hz, 1H). ¹³C NMR (101 MHz, CDCl₃) δ 155.3, 140.0, 138.7, 136.3, 129.0, 128.8, 124.1, 123.2, 121.6, 119.5, 118.2, 56.2, 48.9. GC-MS 264.

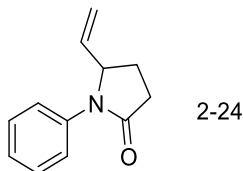


1-hexyl-3-phenyl-4-vinylimidazolidin-2-one, synthesized via modified 2-GP1 (using 0.1 M NBu₄OTs as electrolyte), colorless oil, 35.3 mg (Yield = 65%). ¹H NMR (400 MHz, CDCl₃) δ 7.46 (d, *J* = 8.1 Hz, 2H), 7.34 – 7.25 (m, 2H), 7.03 (t, *J* = 7.4 Hz, 1H), 5.81 (ddd, *J* = 17.4, 10.2, 7.3 Hz, 1H), 5.30 (d, *J* = 17.2 Hz, 1H), 5.23 (d, *J* = 10.3 Hz, 1H), 4.70 – 4.60 (m, 1H), 3.65 (t, *J* = 8.9 Hz, 1H), 3.33 – 3.25 (m, 2H), 3.19 – 3.02 (m, 1H), 1.57-1.51 (m, 2H), 1.39 – 1.24 (m, 6H), 0.97 – 0.83 (m, 3H). ¹³C NMR (101 MHz, CDCl₃) δ 158.1, 139.5, 136.8, 128.7, 123.1, 120.4, 118.5, 56.6, 48.8, 44.0, 31.7, 27.6, 26.5, 22.7, 14.2. GC-MS 272. ESI HRMS *m/z* (*M*+H)⁺ calcd 273.1967, obsd 273.1970. IR: 1709 cm⁻¹(s), 1357 cm⁻¹(s).

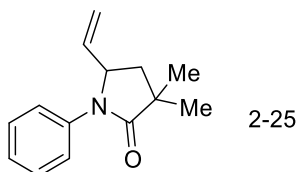


3-phenyl-4-vinylthiazolidin-2-one, synthesized via modified 2-GP1 (using 0.1 M NBu₄OTs as electrolyte), colorless oil, 15.6 mg (Yield = 38%). ¹H NMR (400 MHz, CDCl₃) δ 7.36 (t, *J* = 7.7 Hz, 2H), 7.29 (d, *J* = 7.6 Hz, 2H), 7.24-7.17 (m, 1H), 5.88 (ddd, *J* = 17.5, 10.2, 7.6 Hz, 1H), 5.32 – 5.19 (m, 2H), 4.83-4.75 (m, 1H), 3.60 (dd, *J* = 11.1, 7.3 Hz, 1H), 3.16 (dd, *J* = 11.0, 6.1 Hz, 1H). ¹³C NMR (101 MHz, CDCl₃)

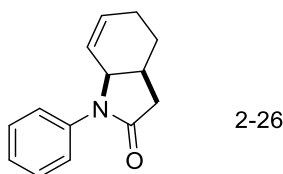
δ 171.4, 138.2, 135.6, 129.1, 126.5, 125.1, 119.6, 64.7, 32.2. GC-MS 205. ESI HRMS m/z (M+H)⁺ calcd 206.0640, obsd 206.0639. IR: 1669 cm⁻¹(s).



1-phenyl-5-vinylpyrrolidin-2-one, synthesized via 2-GP1, yellowish oil, 20.8 mg (Yield = 56%). ¹H NMR (400 MHz, CDCl₃) δ 7.57 – 7.41 (m, 2H), 7.39 – 7.29 (m, 2H), 7.20 – 7.07 (m, 1H), 5.76 (ddd, J = 17.3, 10.3, 7.1 Hz, 1H), 5.23 – 5.08 (m, 2H), 4.70-4.64 (m, 1H), 2.68-2.62(m, 1H), 2.57-2.50 (m, 1H), 2.42-2.36 (m, 1H), 1.96-1.86 (m, 1H). ¹³C NMR (101 MHz, CDCl₃) δ 174.5, 138.2, 137.5, 128.8, 125.3, 123.0, 117.5, 62.7, 31.2, 26.1. GC-MS 187. ESI HRMS m/z (M+H)⁺ calcd 188.1075, obsd 188.1077. IR: 1694 cm⁻¹(s), 1498 cm⁻¹(m), 1380 cm⁻¹(s).

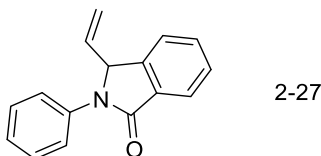


3,3-dimethyl-1-phenyl-5-vinylpyrrolidin-2-one, synthesized via modified 2-GP1 (using 6 eq. NaOPiv as base, 5 F), colorless oil, 25.1 mg (Yield = 58%). ¹H NMR (400 MHz, CDCl₃) δ 7.40 (d, J = 8.6, 2H), 7.34 (dd, J = 8.7, 7.1 Hz, 2H), 7.18 – 7.12 (m, 1H), 5.65 (ddd, J = 17.2, 10.2, 7.8 Hz, 1H), 5.22 (d, J = 17.1, 1H), 5.13 (d, J = 10.2, 1H), 4.61 (q, J = 7.5 Hz, 1H), 2.23 (dd, J = 12.8, 7.3 Hz, 1H), 1.79 (dd, J = 12.8, 7.5 Hz, 1H), 1.31 (s, 3H), 1.23 (s, 3H). ¹³C NMR (101 MHz, CDCl₃) δ 179.2, 138.7, 138.2, 128.7, 125.3, 123.6, 118.0, 59.3, 41.8, 41.1, 25.8, 25.0. The spectra match well with the reported data.^[19] GC-MS 215.

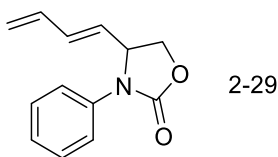


1-phenyl-1,3,3a,4,5,7a-hexahydro-2H-indol-2-one, synthesized via 2-GP2, yellowish oil, 25.4 mg (Yield = 60%). ¹H NMR (400 MHz, CDCl₃) δ 7.46 – 7.35 (m, 4H), 7.19 (t, J = 7.2, 1H), 6.00 – 5.89 (m, 1H), 5.75 – 5.64 (m, 1H), 4.63 – 4.51 (m, 1H), 2.67 – 2.57 (m, 2H), 2.47-2.41 (m, 1H), 2.23 – 1.98 (m,

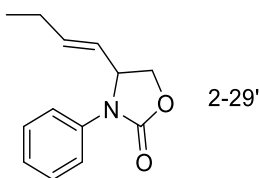
2H), 1.87 – 1.76 (m, 1H), 1.75-1.65 (m, 1H). ^{13}C NMR (101 MHz, CDCl_3) δ 173.8, 137.9, 131.7, 129.1, 125.7, 123.7, 123.5, 57.2, 36.9, 31.0, 24.0, 22.3. GC-MS 213. ESI HRMS m/z ($\text{M}+\text{Na}$) $^+$ calcd 236.1051, obsd 236.1055. IR: 1696 cm^{-1} (s), 1379 cm^{-1} (m).



2-phenyl-3-vinylisoindolin-1-one, synthesized via 2-GP1, white solid, 28.7mg (Yield = 61%). ^1H NMR (400 MHz, CDCl_3) δ 7.94 (d, J = 7.6 Hz, 1H), 7.74 – 7.56 (m, 3H), 7.52 (t, J = 7.5 Hz, 1H), 7.48 – 7.36 (m, 3H), 7.25 – 7.16 (m, 1H), 5.63 – 5.50 (m, 3H), 5.38 – 5.31 (m, 1H). ^{13}C NMR (101 MHz, CDCl_3) δ 167.4, 143.6, 137.8, 135.4, 132.4, 131.9, 129.0, 128.9, 125.3, 124.2, 123.2, 123.1, 120.4, 65.0. The spectra match well with the reported data.^[20] GC-MS 235.

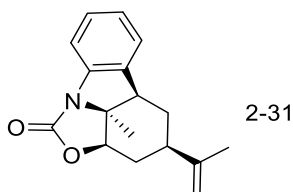


(E)-4-(buta-1,3-dien-1-yl)-3-phenyloxazolidin-2-one, synthesized via 2-GP1, colorless oil, 26.7 mg (Yield = 62%). ^1H NMR (400 MHz, CDCl_3) δ 7.50 – 7.39 (m, 2H), 7.40 – 7.29 (m, 2H), 7.20 – 7.07 (m, 1H), 6.40 – 6.18 (m, 2H), 5.70 – 5.55 (m, 1H), 5.34 – 5.21 (m, 1H), 5.18 (d, J = 8.1 Hz, 1H), 4.98 – 4.81 (m, 1H), 4.58 (t, J = 8.6 Hz, 1H), 4.11 (dd, J = 8.7, 6.5 Hz, 1H). ^{13}C NMR (101 MHz, CDCl_3) δ 155.7, 137.1, 135.8, 135.2, 129.5, 129.1, 125.1, 121.6, 120.1, 67.4, 59.0. GC-MS 215. ESI HRMS m/z ($\text{M}+\text{H}$) $^+$ calcd 216.1024, obsd 216.1027.

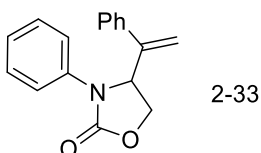


(E)-4-(but-1-en-1-yl)-3-phenyloxazolidin-2-one, synthesized via modified 2-GP1 (Without $\text{Cu}(\text{OAc})_2$), colorless oil, 11.5 mg (Yield = 26%). ^1H NMR (400 MHz, CDCl_3) δ 7.48 – 7.39 (m, 2H), 7.38 – 7.31 (m, 2H), 7.22 – 7.07 (m, 1H), 5.83 (dt, J = 15.3, 6.4 Hz, 1H), 5.37 (dd, J = 15.4, 8.3, 1H), 4.93 –

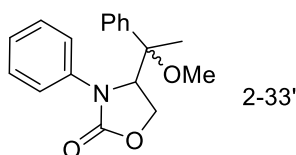
4.74 (m, 1H), 4.56 (t, $J = 8.6$ Hz, 1H), 4.08 (dd, $J = 8.6, 6.7$ Hz, 1H), 2.09 – 1.92 (m, 2H), 0.93 (t, $J = 7.5$ Hz, 3H). ^{13}C NMR (101 MHz, CDCl_3) δ 155.9, 139.2, 137.2, 128.9, 125.6, 125.0, 121.9, 67.7, 59.5, 25.3, 13.2. The spectra match well with the reported data. GC-MS 217. IR: 1743 cm^{-1} (s), 1392 cm^{-1} (s).



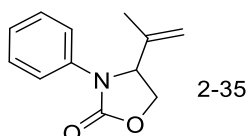
(4R)-2a1-methyl-4-(prop-1-en-2-yl)-2a,2a1,3,4,5,5a-hexahydro-1H-oxazolo[5,4,3-jk]carbazol-1-one, synthesized via 2-GP2, white crystal, m.p. 174-176 °C, 17.0 mg (Yield = 32%). ^1H NMR (400 MHz, CDCl_3) δ 7.45 (d, $J = 7.8$ Hz, 1H), 7.27 (td, $J = 7.7, 1.3$ Hz, 1H), 7.18 (d, $J = 7.6$ Hz, 1H), 7.07 (td, $J = 7.5, 1.1$ Hz, 1H), 4.77 – 4.70 (m, 1H), 4.69 – 4.66 (m, 1H), 4.61 (dd, $J = 9.1, 7.9$ Hz, 1H), 3.03 (dd, $J = 11.1, 8.1$ Hz, 1H), 2.34 – 2.23 (m, 1H), 2.20 – 2.08 (m, 1H), 2.07 – 1.98 (m, 1H), 1.68 (s, 3H), 1.50 – 1.40 (m, 4H), 1.19 – 1.04 (m, 1H). ^{13}C NMR (101 MHz, CDCl_3) δ 154.0, 147.4, 138.6, 137.2, 128.5, 125.0, 124.6, 115.2, 110.4, 82.0, 66.0, 48.2, 40.1, 37.2, 35.2, 28.1, 20.4. GC-MS 269. ESI HRMS m/z ($\text{M}+\text{H}$) $^+$ calcd 292.1313, obsd 292.1318. IR: 1744 cm^{-1} (s), 1390 cm^{-1} (m).



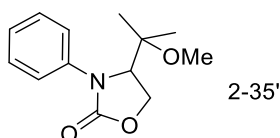
3-phenyl-4-(1-phenylvinyl)oxazolidin-2-one, obtained together with **5ac** via 2-GP1, yellowish oil, 7.1 mg (Yield = 13%). ^1H NMR (400 MHz, CDCl_3) δ 7.55 (d, $J = 8.1$ Hz, 2H), 7.43 – 7.31 (m, 7H), 7.14 (t, $J = 7.4$ Hz, 1H), 5.52 (s, 1H), 5.34 – 5.23 (m, 2H), 4.63 (t, $J = 8.6$ Hz, 1H), 4.16 (dd, $J = 8.5, 4.4$ Hz, 1H). ^{13}C NMR (101 MHz, CDCl_3) δ 155.6, 144.2, 137.6, 137.5, 129.2, 129.1, 128.8, 126.6, 124.5, 119.9, 115.8, 67.8, 59.6. GC-MS 265.



4-(1-methoxy-1-phenylethyl)-3-phenyloxazolidin-2-one, obtained together with **2ac** via 2-GP1, sticky liquid (dr= 1:1), 38.8 mg (Yield = 65%). ^1H NMR (400 MHz, CDCl_3) δ 7.52 – 7.28 (4H), 7.22 – 6.71 (6H), 4.73 – 4.34 (2H), 4.11 (1H), 2.94 (3H), 1.55 (3H). ^{13}C NMR (101 MHz, CDCl_3) δ 156.8, 156.8, 141.1, 139.4, 138.6, 137.3, 128.7, 128.7, 128.4, 128.4, 128.2, 127.7, 127.1, 125.5, 125.0, 124.0, 123.4, 81.8, 80.4, 65.1, 64.8, 64.5, 63.8, 50.1, 50.0, 17.4, 15.7. GC-MS 297. ESI HRMS m/z ($\text{M}+\text{Na}$) $^+$ calcd 320.1263, obsd 320.1263. IR: 1747 cm^{-1} (s), 1398 cm^{-1} (s).

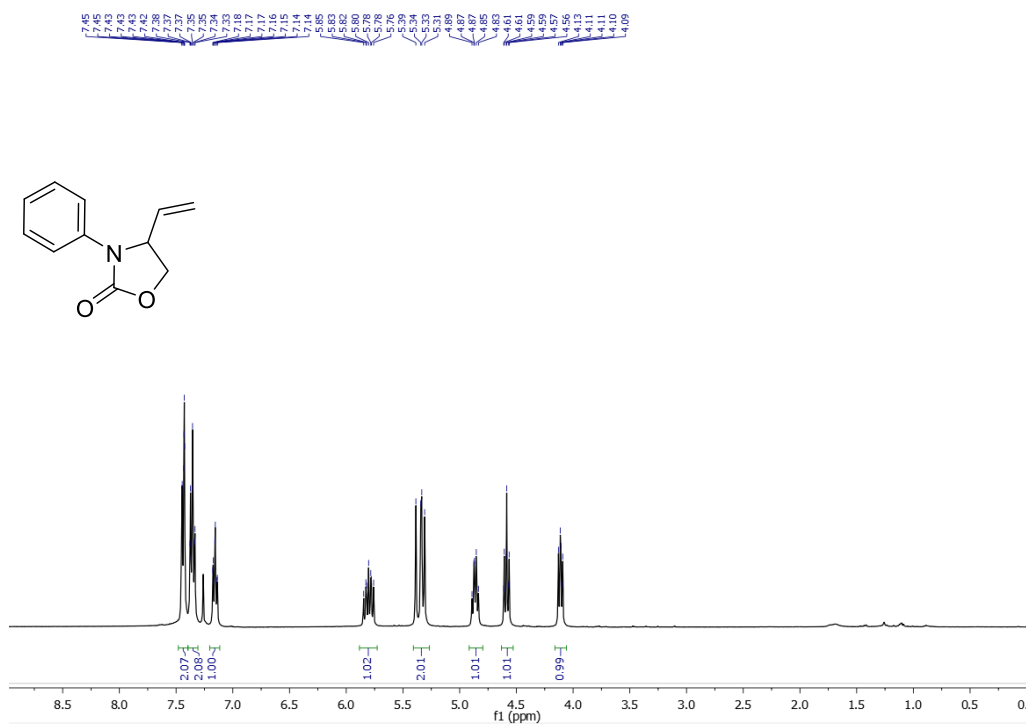
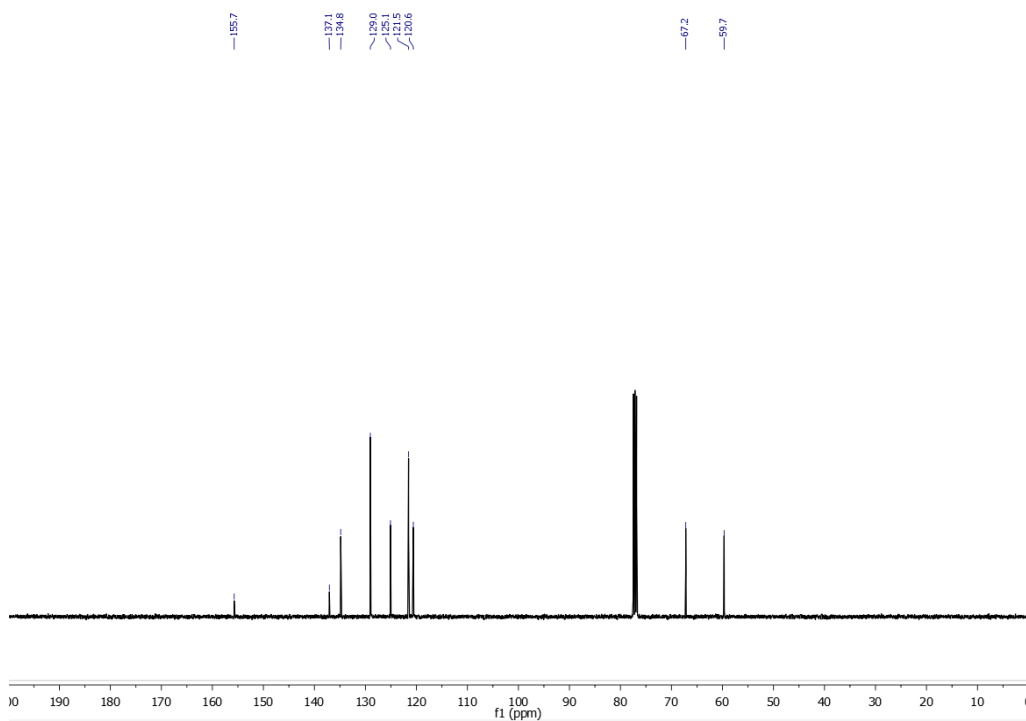


3-phenyl-4-(prop-1-en-2-yl)oxazolidin-2-one, obtained together with **5ad** via 2-GP1, white solid, 30.2 mg (Yield = 74%). ^1H NMR (400 MHz, CDCl_3) δ 7.54 – 7.46 (m, 2H), 7.39 – 7.25 (m, 2H), 7.13 (t, J = 7.5 Hz, 1H), 5.08 (s, 1H), 5.02 (s, 1H), 4.88 (dd, J = 9.1, 5.5 Hz, 1H), 4.55 (t, J = 8.9 Hz, 1H), 4.11 (dd, J = 8.8, 5.5 Hz, 1H), 1.68 (s, 3H). ^{13}C NMR (101 MHz, CDCl_3) δ 155.8, 141.4, 137.4, 129.0, 124.7, 120.4, 116.3, 66.3, 62.1, 16.6. GC-MS 203.



4-(2-methoxypropan-2-yl)-3-phenyloxazolidin-2-one, obtained together with **2ad** via 2-GP1, colorless oil, 5.0 mg (Yield = 11%). ^1H NMR (400 MHz, CDCl_3) δ 7.46 – 7.33 (m, 4H), 7.26 – 7.16 (m, 1H), 4.56 – 4.35 (m, 3H), 3.12 (s, 3H), 1.12 (s, 3H), 0.94 (s, 3H). ^{13}C NMR (101 MHz, CDCl_3) δ 157.0, 138.3, 129.2, 126.2, 124.4, 77.0, 64.3, 63.5, 49.3, 22.6, 19.0. GC-MS 235. ESI HRMS m/z ($\text{M}+\text{Na}$) $^+$ calcd 258.1106, obsd 258.1108. IR: 1754 cm^{-1} (s).

2.7.6 NMR spectra of 2-2 (an example of the products)

¹H-NMR spectrum of 2-2¹³C-NMR spectrum of 2-2

References :

- [1] Pritchett, B. P.; Stoltz, B. M. Enantioselective palladium-catalyzed allylic alkylation reactions in the synthesis of Aspidosperma and structurally related monoterpene indole alkaloids. *Nat. Prod. Rep.* **2018**, *35*, 559-574.
- [2] Mukhtar, T. A.; Wright, G. D. Streptogramins, oxazolidinones, and other inhibitors of bacterial protein synthesis. *Chem. Rev.* **2005**, *105*, 529-542.
- [3] Kotov, V.; Scarborough, C. C.; Stahl, S. S. Palladium-catalyzed aerobic oxidative amination of alkenes: Development of intra- and intermolecular Aza-Wacker reactions. *Inorg. Chem.* **2007**, *46*, 1910-1923.
- [4] Minatti, A.; Muniz, K. Intramolecular aminopalladation of alkenes as a key step to pyrrolidines and related heterocycles. *Chem. Soc. Rev.* **2007**, *36*, 1142-1152.
- [5] Fix, S. R.; Brice, J. L.; Stahl, S. S. Efficient intramolecular oxidative amination of olefins through direct dioxygen-coupled palladium catalysis. *Angew. Chem. Int. Ed.* **2002**, *41*, 164-166.
- [6] Joosten, A.; Persson, A. K. A.; Millet, R.; Johnson, M. T.; Backvall, J. E. Palladium(II)-Catalyzed Oxidative Cyclization of Allylic Tosylcarbamates: Scope, Derivatization, and Mechanistic Aspects. *Chem.-Eur. J.* **2012**, *18*, 15151-15157.
- [7] Weinstein, A. B.; Stahl, S. S. Reconciling the Stereochemical Course of Nucleopalladation with the Development of Enantioselective Wacker-Type Cyclizations. *Angew. Chem. Int. Ed.* **2012**, *51*, 11505-11509.
- [8] <https://www.chem.wisc.edu/areas/reich/pkatable/> for Bordwell pKa Table (in DMSO).
- [9] Shuler, S. A.; Yin, G. Y.; Krause, S. B.; Vesper, C. M.; Watson, D. A. Synthesis of Secondary Unsaturated Lactams via an Aza-Heck Reaction. *J. Am. Chem. Soc.* **2016**, *138*, 13830-13833.
- [10] Hazelden, I. R.; Ma, X. F.; Langer, T.; Bower, J. F. Diverse N-Heterocyclic Ring Systems via Aza-Heck Cyclizations of N-(Pentafluorobenzoyloxy)sulfonamides. *Angew. Chem. Int. Ed.* **2016**, *55*, 11198-11202.
- [11] Xiong, P.; Xu, F.; Qian, X. Y.; Yohannes, Y.; Song, J. S.; Lu, X.; Xu, H. C. Copper-Catalyzed Intramolecular Oxidative Amination of Unactivated Internal Alkenes. *Chem.-Eur. J.* **2016**, *22*, 4379-4383.
- [12] Xiong, P.; Xu, H. H.; Xu, H. C. Metal- and Reagent-Free Intramolecular Oxidative Amination of Tri- and Tetrasubstituted Alkenes. *J. Am. Chem. Soc.* **2017**, *139*, 2956-2959.
- [13] Kochi, J. K.; Bemis, A.; Jenkins, C. L. Mechanism of Electron Transfer Oxidation of Alkyl Radicals by Copper(2) Complexes. *J. Am. Chem. Soc.* **1968**, *90*, 4616.
- [14] Wu, X. S.; Riedel, J.; Dong, V. M. Transforming Olefins into gamma,delta-Unsaturated Nitriles through Copper Catalysis. *Angew. Chem. Int. Ed.* **2017**, *56*, 11589-11593.
- [15] Jiang, Y. Y.; Dou, G. Y.; Xu, K.; Zeng, C. C. Bromide-catalyzed electrochemical trifluoromethylation/cyclization of N-arylacrylamides with low catalyst loading. *Org. Chem. Front.* **2018**, *5*, 2573-2577.

- [16] Sherman, E. S.; Fuller, P. H.; Kasi, D.; Chemler, S. R. Pyrrolidine and piperidine formation via copper(II) carboxylate-promoted intramolecular carboamination of unactivated olefins: Diastereoselectivity and mechanism. *J. Org. Chem.* **2007**, *72*, 3896-3905.
- [17] Davies, J.; Svejstrup, T. D.; Reina, D. F.; Sheikh, N. S.; Leonori, D. Visible-Light-Mediated Synthesis of Amidyl Radicals: Transition Metal-Free Hydroamination and N-Arylation Reactions. *J. Am. Chem. Soc.* **2016**, *138*, 8092-8095.
- [18] Moreno-Manas, M.; Morral, L.; Pleixats, R.; Villarroya, S. Palladium(0)-catalyzed reaction of acidic anilines with (Z)-2-Butene-1,4-diyl dicarbonate - Preparation of n-aryl-4-vinyloxazolidin-2-ones. *Eur J. Org. Chem.* **1999**, *1999*, 181-186.
- [19] Khan, A.; Xing, J. X.; Zhao, J. M.; Kan, Y. H.; Zhang, W. B.; Zhang, Y. J. Palladium-Catalyzed Enantioselective Decarboxylative Cycloaddition of Vinylethylene Carbonates with Isocyanates. *Chem.-Eur. J.* **2015**, *21*, 120-124.
- [20] Yang, G. Q.; Zhang, W. B. Regioselective Pd-Catalyzed Aerobic Aza-Wacker Cyclization for Preparation of Isoindolinones and Isoquinolin-1(2H)-ones. *Org. Lett.* **2012**, *14*, 268-271.

Chapter 3 Intermolecular oxidative amination of unactivated alkenes by dual photoredox and copper catalysis

The work described in this chapter has been published: (Yi, X. L.; Hu, X. L. Intermolecular oxidative amination of unactivated alkenes by dual photoredox and copper catalysis. *Chem. Sci.* **2021**, *12*, 1901-1906). Reprint of the materials is allowed by the Royal Society of Chemistry.

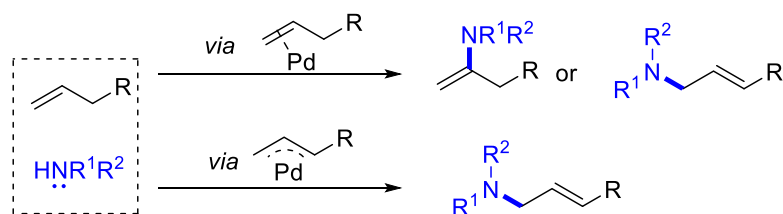
3.1 Background

Oxidative amination of alkenes^[1-3] is a versatile method to synthesize allylic amines and related nitrogen-containing compounds, which are prevalent bioactive molecules and organic materials.^[4-6] Pd catalysis via aminopalladation is a good way for oxidative amination of alkenes (Scheme 3.1a, top).^[7-9] However, in most cases it leads to enamines instead of allylic amines as products, from the Makovnikov addition of the amino group to the alkenes. Pd-catalyzed allylic C-H activation, developed independently by the Liu group and the White group, is an alternative approach which gives linear allylic amines as products via an allyl palladium intermediate (Scheme 3.1a, bottom).^[10-12] So far, only mono-substituted terminal alkenes are suitable substrates. Besides, allylic amines can also be prepared by allylic C-H insertion of metal-nitrenoid of alkenes typically with a branch selectivity (Scheme 3.1b).^[13-15] These methods have generally limited tolerance for substrates containing highly polar or nucleophilic moieties. The addition of amidyl radical to an alkene followed by elimination of β -H provides another possible strategy to effect the oxidative amination (Scheme 3.1c). This strategy could have intrinsic anti-Makovnikov selectivity and is potentially suitable for internal alkenes. The radical nature of the reaction is compatible with polar substrates, which are important for industrial applications.^[16]

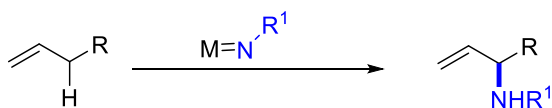
Amidyl radical addition to alkenes for intramolecular cyclization (Section 1.4.2) and the intermolecular addition to activated alkenes (Section 1.4.3) have been well explored. Compared to activated alkenes, the C-radical intermediate from amidyl radical addition to unactivated alkenes is not stabilized by aryl or heteroatom, and it's relatively harder to be selectively reacted because of a

shorter lifetime. In Section 1.4.4, several radical aminations of unactivated alkenes have already been described, which relied on trapping the C-radical intermediates by a hydrogen donor or a SOMOphile for further functionalization. Li and co-workers reported the only example to trap the C-radical intermediates with a metallic species $[\text{Cu}^{\text{II}}\text{-CF}_3]$ to realize an aminotrifluoromethylation reaction (Scheme 1.17e). During our preparation for the publication of this work, Ritter and co-workers reported an elegant metal-free allylic amination reaction through addition of aminium radicals, which were generated from the energy transfer between an excited photocatalyst and iminothianthrenes, to alkenes (Scheme 3.1d).^[17] Radical–radical cross-coupling between the resulting carbon radical and persistent thianthrenium radical followed by elimination furnishes alkyl allyl amines as the products.

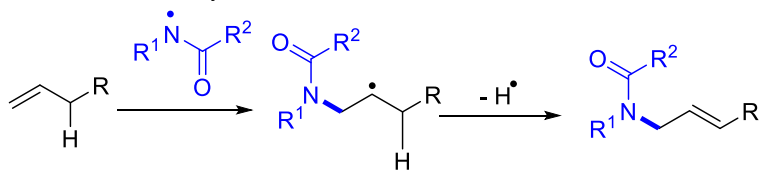
a) Pd catalyzed oxidative amination



b) Oxidative amination via metal nitrenoid

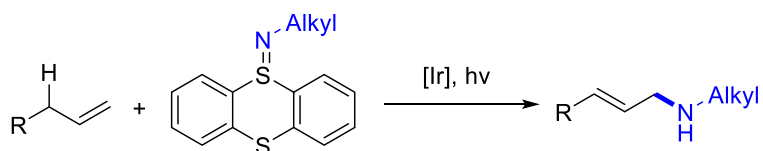


c) Oxidative amination via amidyl radical addition



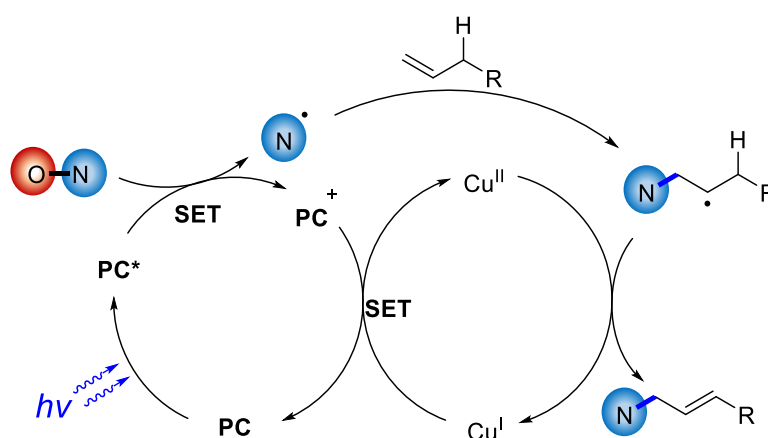
- Intrinsic anti-Markovnikov selectivity
- Tolerance for polar substrates
- Terminal & Internal alkenes

d) Oxidative amination via aminium radical addition (Ritter et. al.)



Scheme 3.1 Different methods of oxidative amination for the synthesis of allylic amines.

Here in this work, we describe an alternative approach based on synergetic photoredox and Cu catalysis. Cu has been reported to mediate β -H elimination of alkyl radicals to produce alkenes (Section 1.6.1). Recent reports described facile generation of amidyl radicals via reduction of hydroxylamine precursors by an excited state of a photoredox catalyst.^[18, 19] In this context, we envisioned a synergetic photoredox and Cu catalysis for oxidative amination of unactivated alkenes (Scheme 3.2). The photochemically generated amidyl radical adds to an alkene to give an alkyl radical, which is trapped by a Cu species. The latter undergoes β -H elimination to give the desired allylic amine.



Scheme 3.2 Reaction design: intermolecular oxidative amination of unactivated alkenes via tandem photoredox and Cu catalysis.

3.2 Reaction optimizations

We started our exploration with different sources of amidyl radicals (Figure 3.1). In light of the precedent work of Studer and co-workers, we thought that Troc-protection N radical could be a good candidate for addition to unactivated alkenes.^[20, 21] By using 3-2 as a N radical source, the alkene 3-1 could be converted to allylic amine derivative in 24% yield, when 1 mol% of Ir(ppy)₃ was used as a photocatalyst, 15 mol% of Cu(2-ethylhexanoate)₂ was used as a metal catalyst and 1 equivalent of NaOPiv was added. Troc-NH₂ was obtained as the main side product and no diamination was observed. When less electron-deficient N reagents were used (3-3 to 3-5), only trace amount of the target product was observed. Other electron-deficient N reagents with different substituents on the benzoyl (2,6-difluoro for 3-6, 4-CF₃ for 3-7, 3,5-diCF₃ for 3-8, 4-CO₂Me for 3-9) also led to the product, albeit in relatively lower yield (10%-20%). However, the electron-deficient

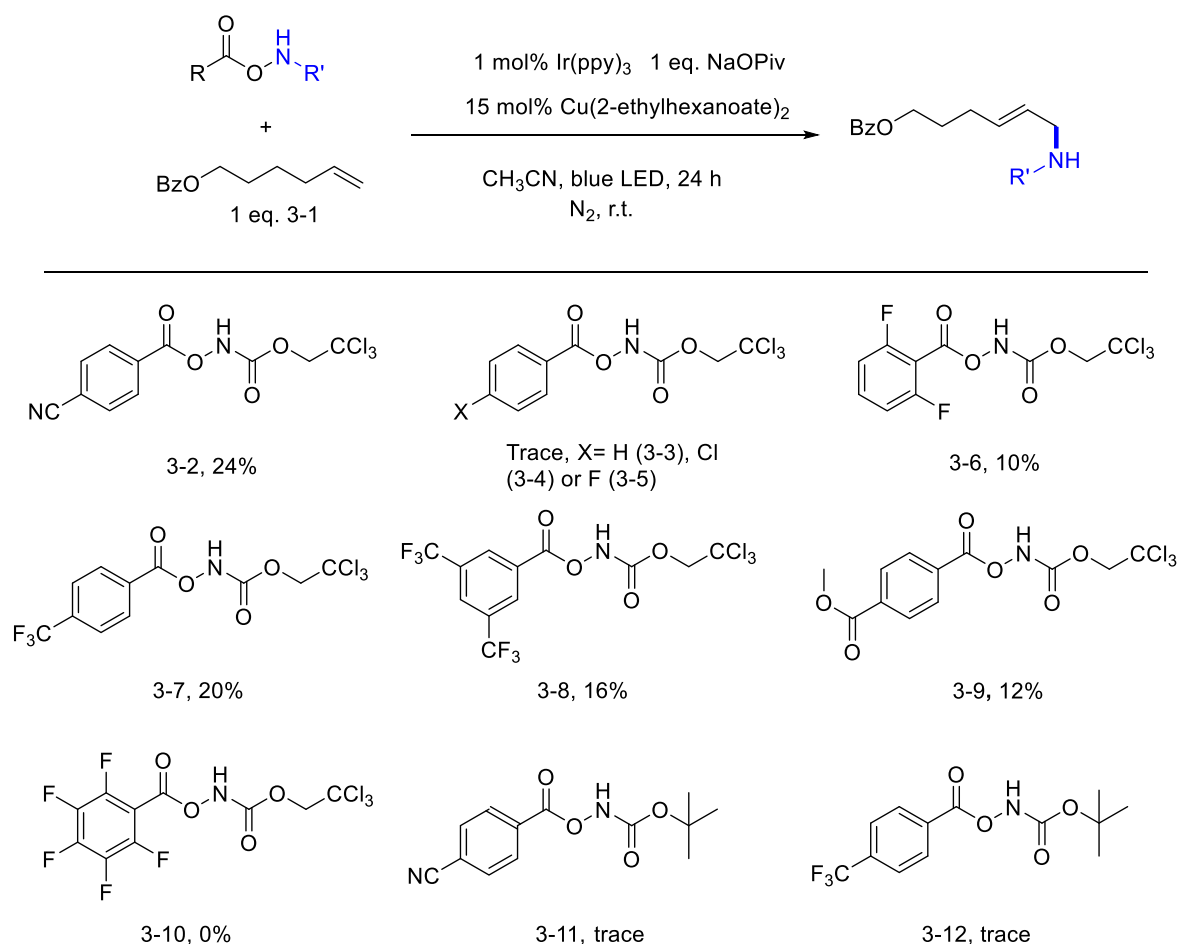
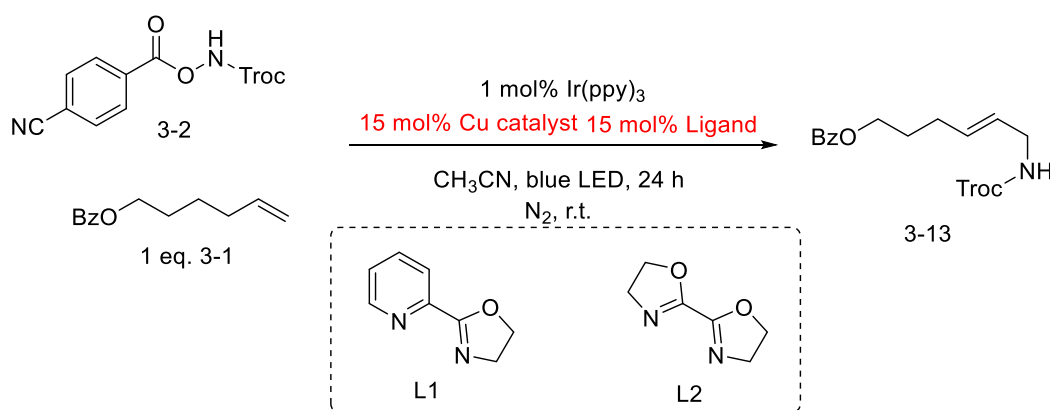


Figure 3.1 Screening of amidyl radical sources. Conditions: All reagents of indicated amount dissolved in 1 mL CH₃CN, blue LED radiation for 24 h.

N reagent derived from pentafluorobenzoic acid did not work at all for this reaction. We also tested 3-11 and 3-12 as a source of Boc-protected N radical, and only trace amount of the target product from oxidative amination was observed. Thus, 3-2 was selected as the N radical source.

Then, the copper catalyst was optimized (Table 3.1). The use of Cu(OPiv)₂ as metal catalyst improved the yield to 42% (Entry 2), in contrast to 38% when Cu(2-ethylhexanoate)₂ was used (Entry 1). CuOAc could give a yield of 21% (Entry 3), while Cu(OTf)₂ was completely inactive for this reaction (Entry 4). When copper catalyst was removed from the conditions, 7% of 3-13 was observed (Entry 5). We tried to add some ligands to the reaction conditions (Entries 6-9). The addition of bipyridine or 1,10-phenanthroline completely suppressed the reaction. The use of L1 or L2 led to the target product yet was not helpful for the improvement of the yield.

Table 3.1 Screening of Cu catalysts.



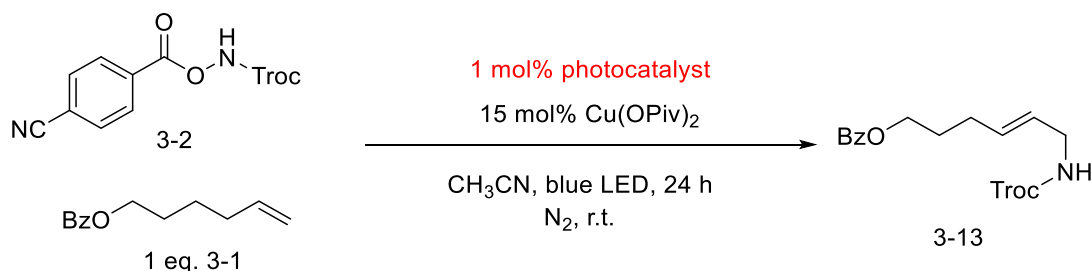
Entry	Cu catalyst	ligand	Yield/ %
1	Cu(2-Ethyl hexanoate) ₂	-	38
2	Cu(OPiv) ₂	-	42
3	Cu(OAc)	-	21
4	Cu(OTf) ₂	-	0
5	-	-	7
6	Cu(2-Ethyl hexanoate) ₂	bipyridine	0
7	Cu(2-Ethyl hexanoate) ₂	1,10-phenanthroline	0
8	Cu(2-Ethyl hexanoate) ₂	L1	10
9	Cu(2-Ethyl hexanoate) ₂	L2	39

Conditions: All reagents of indicated amount dissolved in 1 mL CH₃CN, blue LED radiation for 24 h.

Different photocatalysts were used for this reaction (Table 3.2). It was found that only the Ir(ppy)₃ type photocatalysts with a very reducing excited state (Table 1.1) could mediate this

conversion. The cationic Ir^{III} catalyst (Entry 1), the organophotocatalyst 4CzIPN (Entry 2) and Ru catalyst (Entry 3) were all inactive under the conditions. Ir(dfppy)₃, Ir(dfppy)₂(ppy), Ir(dfppy)(ppy)₂ and Ir(ppy)₃ gave the product 3-13 in similar yields (Entries 4-7, 39-42%).

Table 3.2 optimization of photocatalysts.



Entry	Photocatalyst	Yield/ %
1	Ir(ppy) ₂ (dbbpy) BF ₄	trace
2	4CzIPN	trace
3	Ru(bpy) ₃ (BF ₄) ₂	0
4	Ir(dfppy) (ppy) ₂	40
5	Ir(dfppy) ₂ (ppy)	39
6	Ir(ppy) ₃	42
7	Ir(dfppy) ₃	41

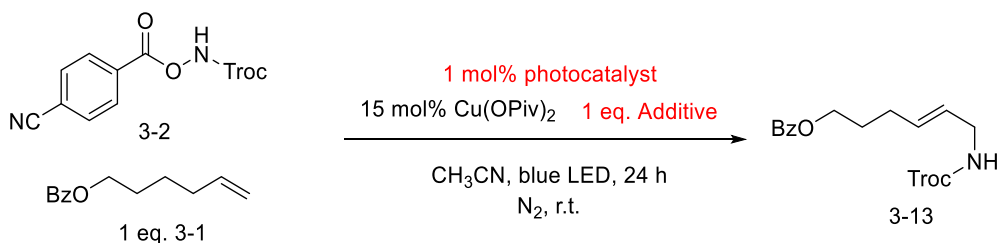
Conditions: All reagents of indicated amount dissolved in 1 mL CH₃CN, blue LED radiation for 24 h.

Some additives were tentatively added to the reaction, with a potential role of neutralizing the acid generated in the course of the reaction (Table 3.3). The addition of NEt₃ completely disabled the reaction (Entry 1). Other organic bases, such as pyridine and 2,6-lutidine, also led to lower yields (Entries 2&3). Different metal pivalates were tried, and, unluckily, none of them could increase the reaction yield (Entries 4-8). However, 1 equivalent of Mg(OPiv)₂ and H₂O slightly increased the yield to 44% (Entry 9). The replacement of Ir(ppy)₃ by Ir(dfppy)₂(ppy) based on Entry 9 further increased the yield to 49% (Entry 10). Notably, the addition of H₂O resulted in a precipitate during the reaction, which was analyzed as mainly Mg(4-cyanobenzoate)₂·xH₂O.

Finally, we tried to increase the reaction yield by increasing the amount of alkene 3-1 (Table 3.4). 2 equivalent and 3 equivalent of 3-1 respectively increased the reaction yield to 59% and 64% (Entry 2, 3). A slow generation of the amidyl radical by controlling the addition rate of 3-2 to the reaction mixture improved further the yield of 3-13 to 76%, when 3 equivalent of 3-2 were used

(Entry 5). With these conditions, the amount of copper catalyst could be reduced to 10 mol% without affecting the yield (77%, Entry 6). 70% yield of 3-13 was obtained after isolation.

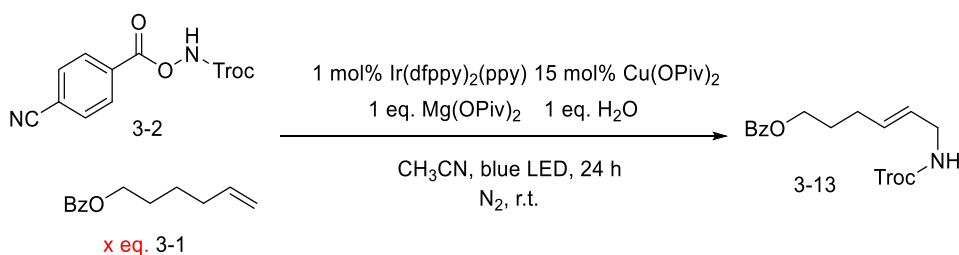
Table 3.3 Screening of additives.



Entry	photocatalyst	additive	Yield/ %
1	Ir(ppy) ₃	NEt ₃	0
2	Ir(ppy) ₃	pyridine	27
3	Ir(ppy) ₃	2,6-dimethylpyridine	35
4	Ir(ppy) ₃	NaOPiv	24
5	Ir(ppy) ₃	Zn(OPiv) ₂	21
6	Ir(ppy) ₃	Mg(OPiv) ₂	38
7	Ir(ppy) ₃	LiOPiv	34
8	Ir(ppy) ₃	Al(OPiv) ₃	30
9	Ir(ppy) ₃	Mg(OPiv) ₂ , H ₂ O	44
10	Ir(dfppy) ₂ (ppy)	Mg(OPiv) ₂ , H ₂ O	49

Conditions: All reagents of indicated amount dissolved in 1 mL CH₃CN, blue LED radiation for 24 h.

Table 3.4 Optimization of the amount of alkene and addition procedure.



Entry	Amount of alkene	Variations	Yield/ %
1	1 eq.	-	49
2	2 eq.	-	59
3	3 eq.	-	64
4 ^a	2 eq.	Slow addition of 3-2	67
5 ^a	3 eq.	Slow addition of 3-2	76
6 ^a	3 eq.	10% Cu(OPiv) ₂ , Slow addition of 3-2	77(70) ^b

Conditions: All reagents of indicated amount dissolved in 1 mL CH₃CN blue LED radiation for 24 h. ^a Slow addition procedure: 0.02 mmol 3-2 and all other reagents were dissolved in 0.2 mL CH₃CN; the rest of 3-2 (0.08 mmol) was dissolved in 0.4 mL CH₃CN; the latter was added at 1.2 μ L/min to the former after reaction starts. ^b Yield after isolation.

3.3 Scope investigations

Based on the optimal conditions (Table 3.4, Entry 6), we examined the scope of terminal alkenes (Figure 3.2). Remote electrophilic functionalities such as bromide, iodide, and terminal epoxide were all tolerated to afford the corresponding products in good yields (3-14 to 3-16, 66-77%). Alcohol (3-17) and amide (3-18) were also compatible. A range of alkenes containing a terminal carboxylic acid group were tested. 9-Decenoic acid (for 3-19), 5-hexenoic acid (for 3-20) and 4-pentenoic acid (for 3-21), but not 3-butenic acid, were successfully aminated. The products were isolated after methylation as methyl esters in moderate yields (50-53%). Polar substrates (3-22 and 3-23), derived from L-phenylalanine and L-threonine, respectively, were also viable for this reaction. When a more electron-deficient alkenyl group was present in an internal position (for 3-24 and 3-25), amination of the terminal double bond was dominant, which is consistent with electrophilic nature of the amidyl radical.^[19]

Next, alkenes with various substitutions at the C3 position were examined. Bulky substituents, such as cyclohexyl (for 3-26), *tert*-butyl (for 3-27) and 1-hydroxycyclohexyl (for 3-28), didn't deteriorate the reaction yield (59-74%). However, double substitutions at C3 dramatically decreased the yield (3-29, 23%). In the case of a phenyl substitution, 3-30 was obtained in 40% yield. *Cis*-alkene was obtained as the major isomer (Z:E = 4:1), possibly because of the isomerization of styrene-type compounds under radiation.^[22] Although 3-butenic acid was not a suitable substrate, the esters of 3-butenic acid could be used for the generation of α,β -unsaturated esters (3-31 to 3-34). 4-hydroxyl (3-33) and 2-iodo (3-34) groups on the phenyl substituent were tolerated against the potential oxidation or dehalogenation reactions. The use of 1,1-disubstituted alkenes led to lower yield of the target product (48% for 3-35, < 10% for 3-36). This could have resulted from the side reactions associated with the direct oxidation of the tertiary radical intermediate to carbocation (Section 1.6.2). The reaction of 3-37, derived from L-menthol, was successfully scaled up to 2.5 mmol, giving 0.63 g of 3-38 as product (61% yield). The latter can be easily deprotected to give the primary amine 3-39 in 85% yield. Notably, the majority of the excess alkene could be recovered after the reaction (1.23 g, 2.2 equivalent).

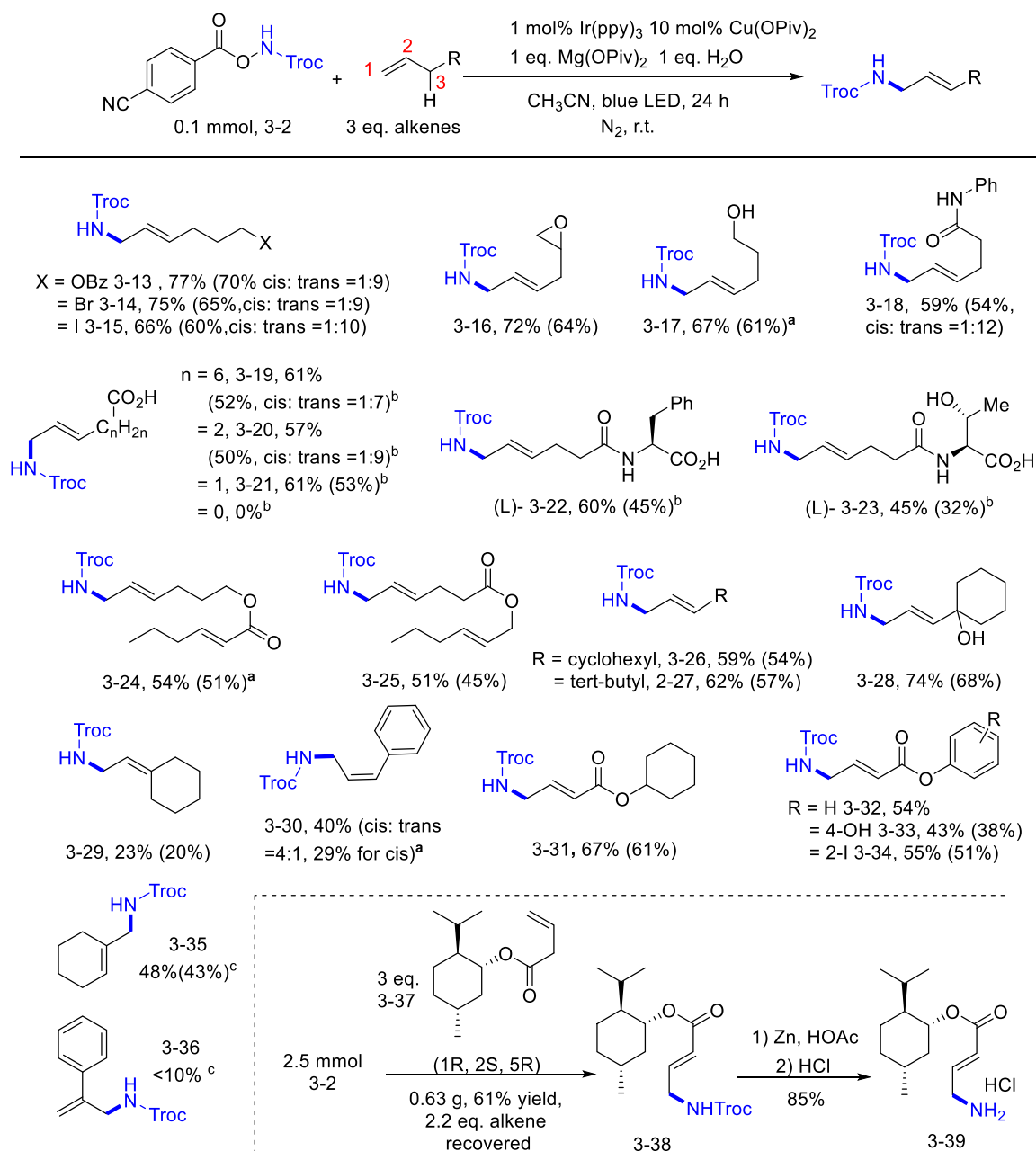


Figure 3.2 Scope studies of terminal alkenes for the oxidative amination. Reaction conditions: Same as Table 3.4, Entry 6. NMR yields and isolation yields (in the bracket) are shown. ^a Reaction conditions: Same as Table 3.4, Entry 3. ^b Reaction conditions: Based on Table 3.4, Entry 3, without addition of Mg(OPiv)₂ or H₂O. Products were isolated as esters after methylation. ^c Reaction conditions: Based on Table 3.4, Entry 3, with acetone as solvent.

The oxidative amination method was then applied to internal alkenes (Figure 3.3). This transformation was effective when the alkenes were symmetrically substituted, such as cyclohexene (3-40), cyclopentene (3-41), and 4-octene (3-42). *Trans*-4-octene and *cis*-4-octene led to similar yields of 3-43. The reaction of an unsymmetrically substituted alkene, 2-octene, had a good yield but poor

regioselectivity (3-43-1: 3-43-2= 1.4:1). When 2-hexen-1-ol was used as the substrate, amination at the C2 position (3-44) was dominant (58% yield) compared to amination at the C3 position, which led to an epoxyl product 3-44' (16%). Analogous allylic alcohols (3-45 to 3-47) were aminated, with modest to good yields (33% to 61%). The diastereoselectivity was low despite having a bulky substituent adjacent to the alcohol group. A trisubstituted alkene led to 3-48 in 51% yield. A tosyl-protected allylamine reacted with 3-2 to give 3-49 in 60% yield. Allylic esters reacted with 3-2 to give both allylic amines (3-50 and 3-51) and aziridines (3-50' and 3-51') in similar yields.

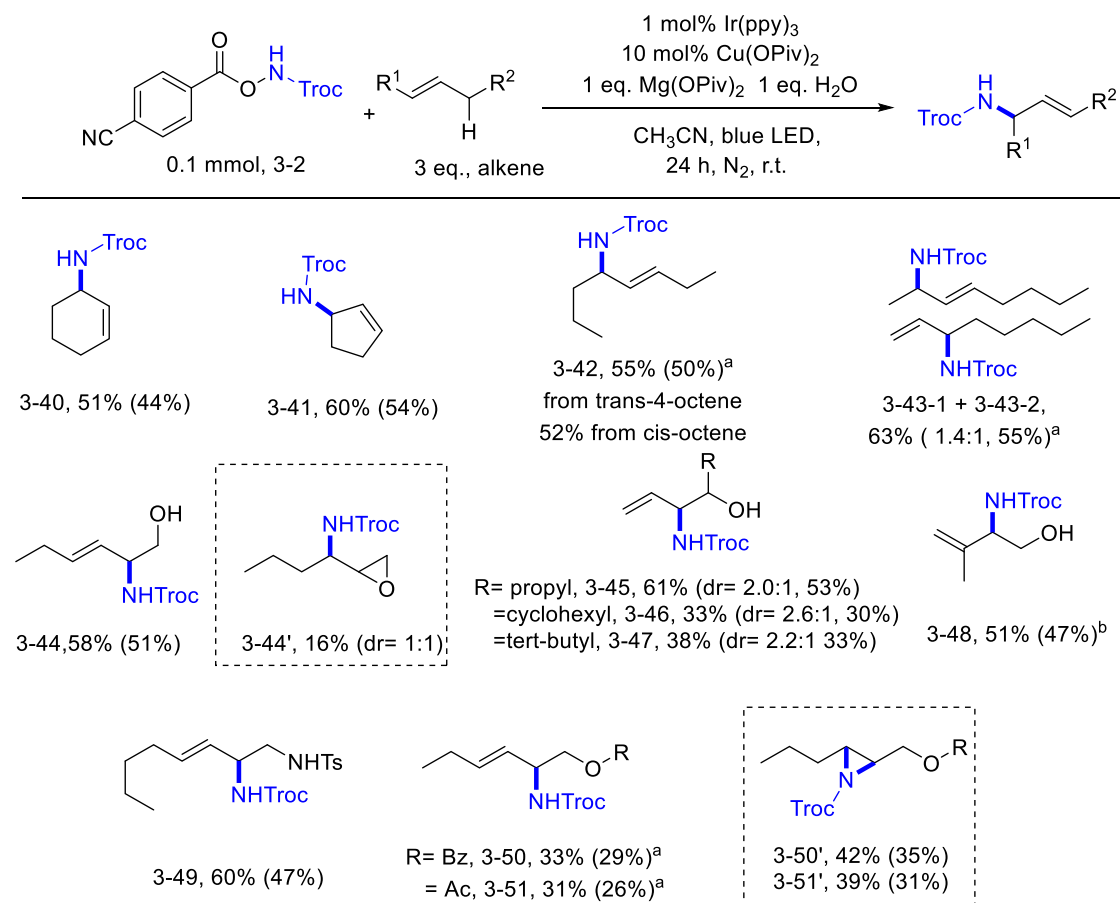


Figure 3.3 Scope studies of internal alkenes for oxidative amination. Reaction conditions: Same as Table 3.4, Entry 6. NMR yields and isolation yields (in the bracket) are shown. ^a Reaction conditions: Same as Table 3.4, Entry 3. ^b Reaction conditions: Based on Table 3.4, Entry 3, with acetone as solvent.

3.4 Mechanistic studies

3.4.1 Photochemical studies

The Stern-Volmer quenching of Ir(dfppy)₂(ppy) by different reagents was probed (Figure 3.4). Among all reagents used in the reaction, only 3-2 and Cu(OPiv)₂ could significantly quench the excited photocatalyst. A less electron-deficient N radical source 3-3 was also not able to quench the

excited photocatalyst. In the corresponding Stern-Volmer plots, the slopes, which are proportional to the quenching coefficients, are 9955 M^{-1} and 2438 M^{-1} for 3-2 and Cu(OPiv)_2 , respectively, suggesting 3-2 as a more efficient quencher than Cu(OPiv) . Additionally, cyclic voltammetry was used to measure the redox potentials of the reagents. The reduction potential of 3-2 ($E_{\text{red}}(3-2) = -1.43 \text{ V}$ vs SCE) is less negative than the oxidation potential of the excited photocatalyst ($E(\text{Ir}^{\text{IV}}/\text{Ir}^*) = -1.56 \text{ V}$), indicating that oxidative quenching of the excited state of $\text{Ir}(\text{dfppy})_2(\text{ppy})$ by 3-2 is thermodynamically downhill. Meanwhile, the reduction potential of 3-3 ($E_{\text{red}}(3-3) = -1.82 \text{ V}$ vs SCE) is more negative, which explains why 3-3 was not a suitable substrate for the reaction.

To probe the possibility of a quenching process by energy transfer, we tested several photocatalysts with a similar triplet energy to $\text{Ir}(\text{dfppy})_2(\text{ppy})$ (Figure 3.5). Neither $\text{Ir}(\text{dfCF}_3\text{ppy})_2(\text{dtbbpy}) \text{PF}_6$ or 4CzIPN was active for the reaction, despite having a similar or slightly higher triplet energy. This implies that energy transfer mechanism is not very likely in our case. Notably, these two catalysts have less reducing excited states ($-0.89 \text{ V}^{[23]}$ for $\text{Ir}(\text{dfCF}_3\text{ppy})_2(\text{dtbbpy}) \text{PF}_6$ and $-1.04 \text{ V}^{[24]}$ for 4CzIPN), meaning that they are not able to reduce 3-2 with their exciting states. This is consistent with a SET oxidative quenching mechanism.

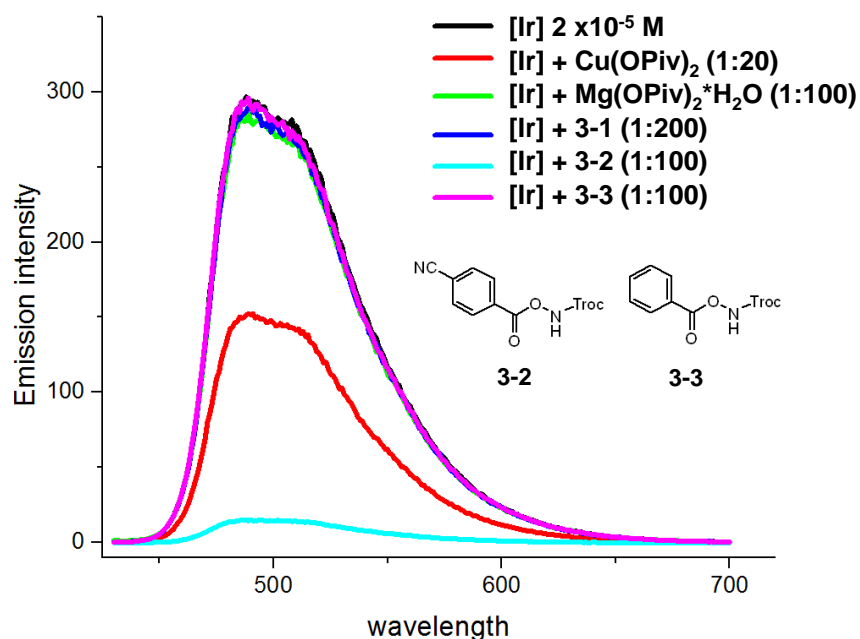


Figure 3.4 Stern-Volmer quenching of different reagents in this reaction.

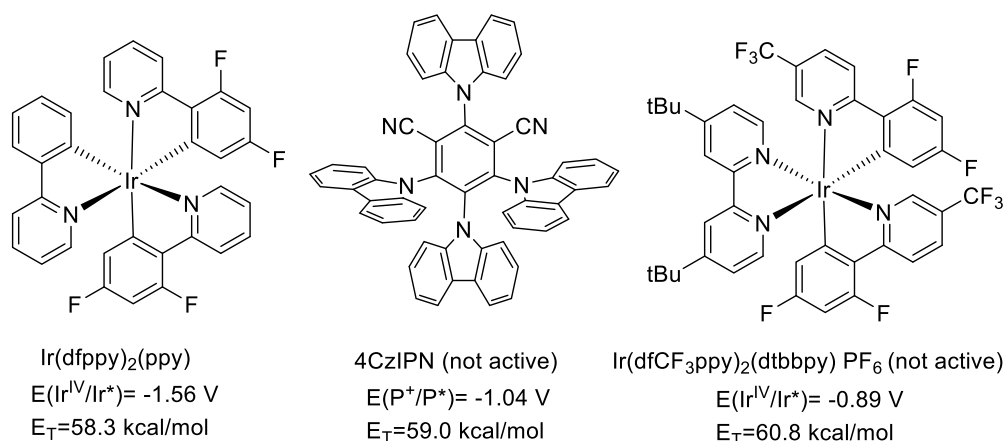


Figure 3.5 Comparison of oxidative quenching potentials and triplet energies of several photocatalysts.

3.4.2 Radical process

To verify the radical nature of this reaction, 1 equivalent of TEMPO was added to the reaction mixture of 3-1 and 3-2 (Figure 3.6a). The oxidative amination product 3-13 was not obtained, but the TEMPO adduct 3-52 was isolated in 17% yield. Additionally, the reaction of substrate 3-53 containing a cyclopropyl substituent, which served as a radical clock, yielded product 3-54 in which the cyclopropyl ring was opened (Figure 3.6b). These results confirm the involvement of amidyl radical addition in this reaction.

3.4.3 The role of copper

During the investigation of reaction scope, we observed a competition between elimination of β -H and cyclization for substrates with a pendant nucleophilic group (-OH or -NHTs; Figure 3.7), which helps to profile the role of copper in the reaction. When there is one carbon between the alkene and nucleophilic groups, only cyclization was observed (for 3-60 and 3-63). When there are two carbons, only elimination was observed (for 3-61 and 3-64). When there are 3 carbons, cyclization was favored (for 3-62 and 3-65), yet the product of elimination (3-65', 22% yield compared to 68% yield for 3-65) was still obtained if the nucleophilic group was -OH. Cu^{II} species have been reported to both mediate oxidative elimination of alkyl radical to form alkene (Section 1.6.1) and cyclization of alkyl radical with a nucleophile (Section 1.6.4 and 1.6.6). For the copper mediated oxidative elimination, a Cu^{III}-alkyl species has always invoked as intermediate, yet few direct evidences have been reported. In the present case, if a Cu^{III}-alkyl intermediate 3-66 is formed, the nucleophilic group would be able to coordinate to copper. The observation of cyclization products supports the

formation of such a Cu^{III}-alkyl intermediate which could reductively eliminate to form the cyclic products.

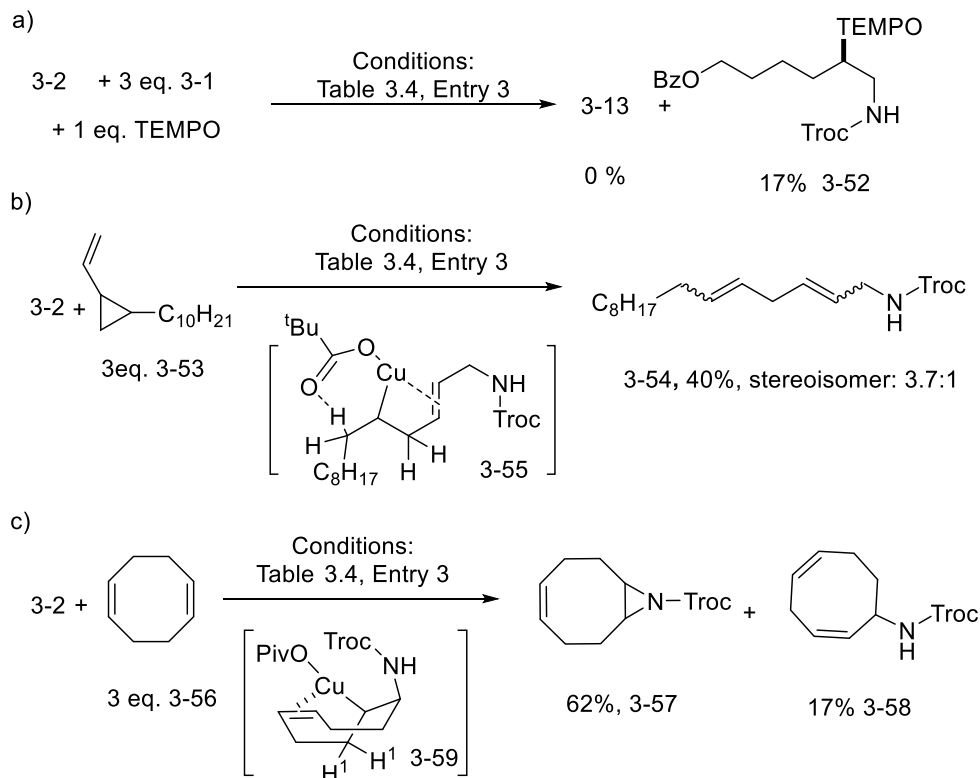


Figure 3.6 Several reactions for mechanistic studies.

Interestingly, when cyclooctadiene 3-56 was applied as a substrate (Figure 3.6c), aziridine 3-57 was obtained as the main product (62%) instead of 3-58 (17%). This result might be rationalized by the coordination of Cu in 3-59 by the alkene moiety. The coordination could shield H¹ from accessing the Cu center so that elimination of H¹ was suppressed. Consequently, C-N reductive elimination to give the aziridine product 3-57 was favored. This rational might be applicable to explain the generation of 3-50' and 3-51', as in these cases the ester group of the alkenes could act as a coordinating group. Besides, the coordination of Cu by the double bond (Figure 3.6b, intermediate 3-55) could also be used to rationalize the generation of a skipped diene 3-54 as the main product instead of a conjugated diene, which would be thermodynamically more stable.

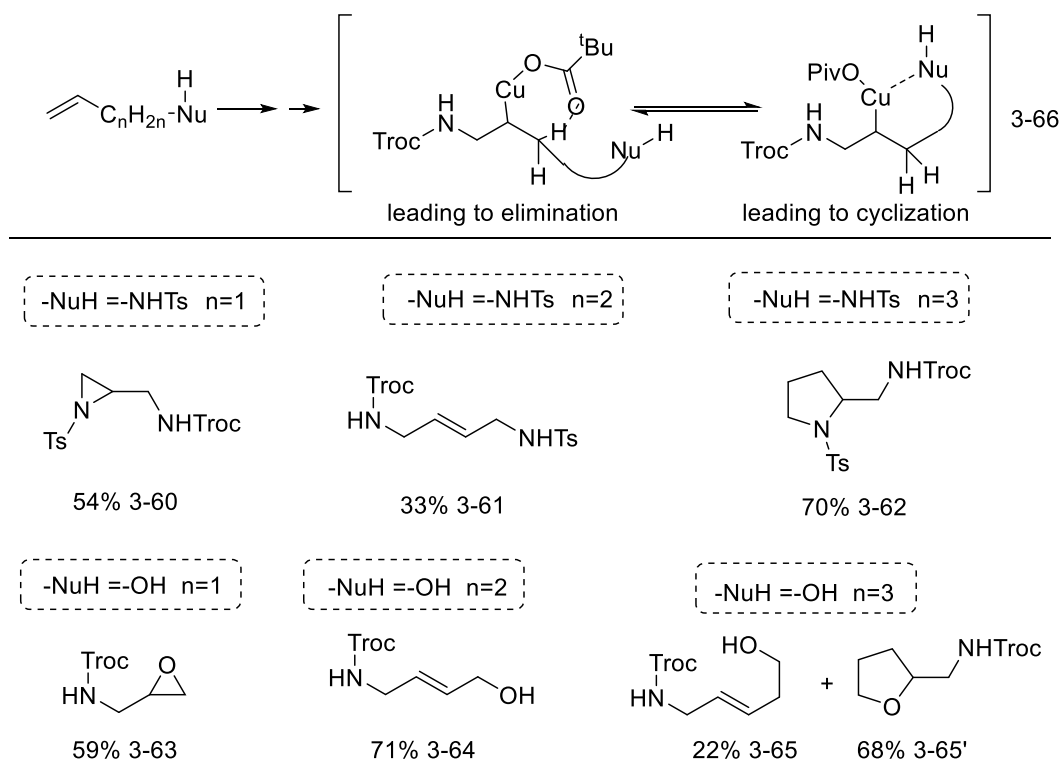
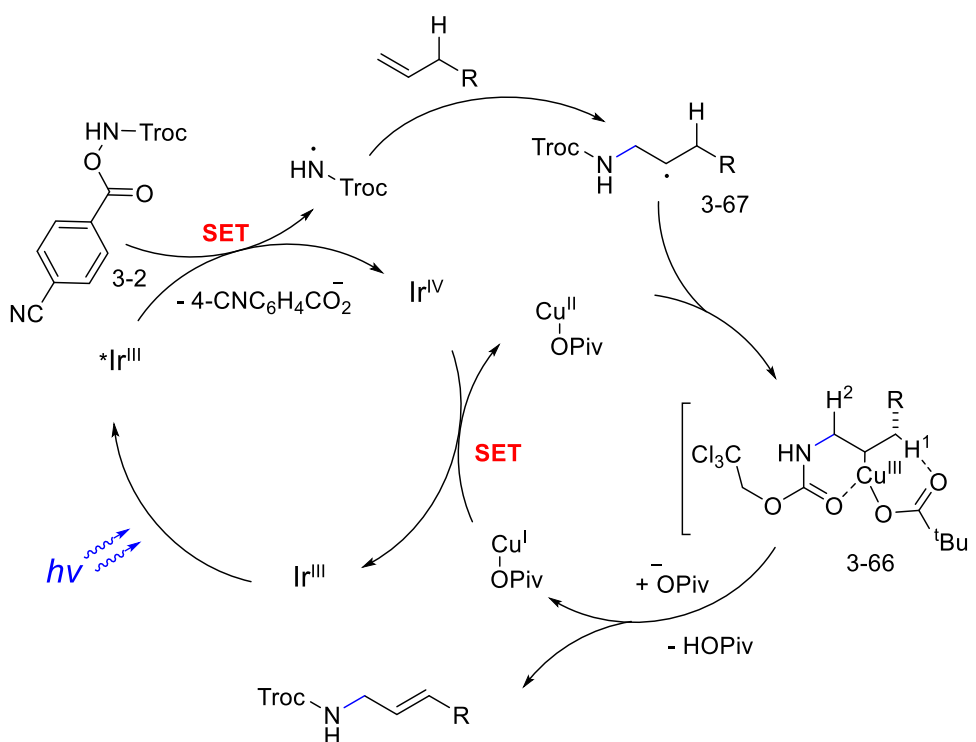


Figure 3.7 Reactions of substrates with a tethered nucleophilic group: Competition between cyclization and elimination.
 Conditions: same as Table 3.4, Entry 3.

3.5 The proposed reaction Mechanism

Taking into account the results above, we proposed a plausible catalytic cycle (Scheme 3.3). The reaction starts from the oxidative quenching of the excited photocatalyst by 3-2, which generates the Troc-protected N radical while releasing a carboxylate. The addition of N radical to the alkene leads to the alkyl radical 3-67, which is then trapped by a Cu^{II} -pivalate species to give a Cu^{III} -alkyl species 3-66. The latter undergoes elimination of β -H to form the allylic amine and a Cu^{I} species which is then oxidized back to Cu^{II} by Ir^{IV} . To explain the regioselectivity for H elimination in 3-66, we propose that the coordination of the Troc group to Cu^{III} prevents the H^2 to be accessed by the carboxylate so that elimination of H^1 dominates.^[25] The influence of intramolecular coordination to the reaction selectivity was evidenced by the products of several substrates (e.g., for 3-50' and 3-57).



Scheme 3.3 The proposed reaction mechanism.

3.6 Conclusion

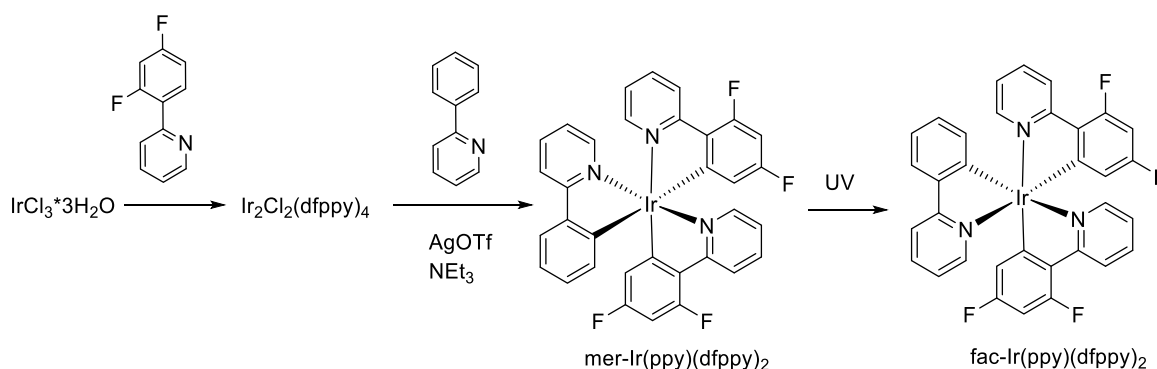
In conclusion, by integrating photochemical generation of amidyl radicals with Cu-mediated β -H elimination of alkyl radical, we developed an intermolecular oxidative amination of unactivated alkenes. The method can be used to synthesize a wide range of allylic amines, from readily available alkenes, with high functional group tolerance. The mechanistic studies provided evidence for a Cu^{III}-alkyl intermediate in the copper mediated oxidative elimination process.

3.7 Experiments

3.7.1 General consideration

Solvents (DCM, anhydrous acetonitrile and DMSO) and commercially available reagents were used without purification. H₂O was purged with N₂ for 2 h to remove oxygen before use. 15 mL Teflon-screw capped vials (d = 2 cm) were used for the setup of oxidative amination reaction. Blue LEDs (From Kessil Co., Ltd., 40 W max., wavelength centered at 460 nm, product No. A160WE) was used as the radiation source and a cooling fan was used to keep the reaction temperature from going up during photolysis. After the reaction workup, ¹H- NMR spectra of crude products were recorded with 1,3,5-trimethylbenzene as an internal standard to determine the NMR yields. Silica gel columns were used for reaction separation, with hexane- ethyl acetate (EA) as eluent unless otherwise noted. NMR spectra were recorded with a Bruker Avance 400 MHz instrument. Chemical shifts are reported in ppm after being referenced to residual signal of CHCl₃ for ¹H (7.26 ppm) and CDCl₃ for ¹³C (77.16 ppm). Descriptions of multiplicities are abbreviated as follows: s = singlet, d = doublet, t = triplet, q = quartet, m = multiplet, b = broad. Determinations of high resolution mass spectra (HRMS) of unknown compounds by electrospray ionization (ESI) were performed with a Micro Mass QTOF Ultima spectrometer at the EPFL Mass Spectrometry Center. Fluorescence quenching were examined with a Varian Cary Eclipse fluorescence spectrophotometer. Cyclic voltammograms (CV) were recorded on a BIO-LOGIC VSP.

3.7.2 Procedures for synthesis of substrates, catalysts and additives

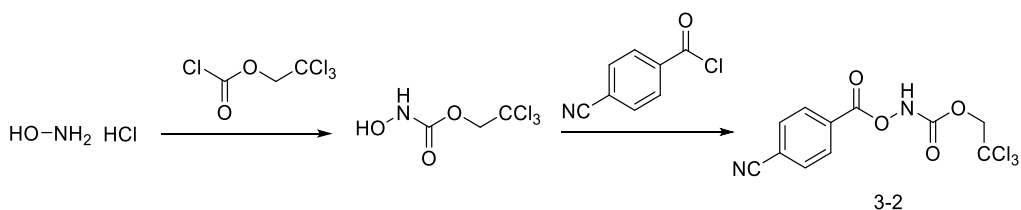


fac-Ir(ppy)(dfppy)₂: 0.5 mmol IrCl₃·3H₂O and 1.75 mmol 2-(2,4-difluorophenyl)pyridine were added to a 50 mL flask containing 15 mL 2-ethoxyethanol and 5 mL H₂O. The mixture was heated to 135 °C under nitrogen for 24 h, and then the reaction was quenched by addition of 20 mL H₂O.

Filtration and subsequent wash with EtOH and Et₂O gave chloride-bridged iridium dimer IrCl₂(dfppy)₄ as a bright yellow powder in 66% yield.

0.04 mmol IrCl₂(dfppy)₄, 0.2 mmol AgOTf, 0.16 mmol 2-phenylpyridine, 0.16 mmol NEt₃ were added to 6 mL DCE.^[26] The mixture was refluxed under nitrogen for 6 h. *mer*-Ir(dfppy)₂(ppy) was obtained by chromatography on silica gel with DCM-hexane as eluent, as a yellow powder in 50% yield. ¹H NMR (400 MHz, CDCl₃) δ 8.20 (dd, *J* = 15.0, 8.6 Hz, 2H), 8.09 (d, *J* = 5.9 Hz, 1H), 7.94 (d, *J* = 8.2 Hz, 1H), 7.87 (d, *J* = 5.6 Hz, 1H), 7.78 – 7.74 (m, 1H), 7.65 (td, *J* = 7.6, 1.8 Hz, 1H), 7.61 – 7.51 (m, 2H), 7.50 (t, *J* = 7.9 Hz, 1H), 7.07 – 6.96 (m, 2H), 6.99 – 6.87 (m, 2H), 6.79 – 6.69 (m, 2H), 6.50 – 6.35 (m, 2H), 6.08 – 6.00 (m, 1H), 5.84 (dd, *J* = 9.2, 2.4 Hz, 1H).

0.04 mmol *mer*-Ir(dfppy)₂(ppy) was dissolved in 3 mL DMSO and radiated by UV (254 nm) overnight under nitrogen.^[27] A precipitate was formed. The solution was diluted by DCM until the precipitate was dissolved. The solution mixture was washed with water to remove DMSO. Evaporation of the organic phase afforded a yellow solid, which was then washed twice by DCM-hexane (1:10). *fac*-Ir(dfppy)₂(ppy) was obtained in 88% yield. ¹H NMR (400 MHz, DMSO-*d*₆) δ 8.32 – 8.18 (m, 3H), 7.99 – 7.79 (m, 4H), 7.63 – 7.53 (m, 2H), 7.47 – 7.41 (m, 1H), 7.32 – 7.16 (m, 3H), 6.89 (td, *J* = 7.5, 1.5 Hz, 1H), 6.80 (td, *J* = 7.3, 1.4 Hz, 1H), 6.71 – 6.60 (m, 2H), 6.55 (dd, *J* = 7.5, 1.4 Hz, 1H), 6.15 – 6.05 (m, 2H).



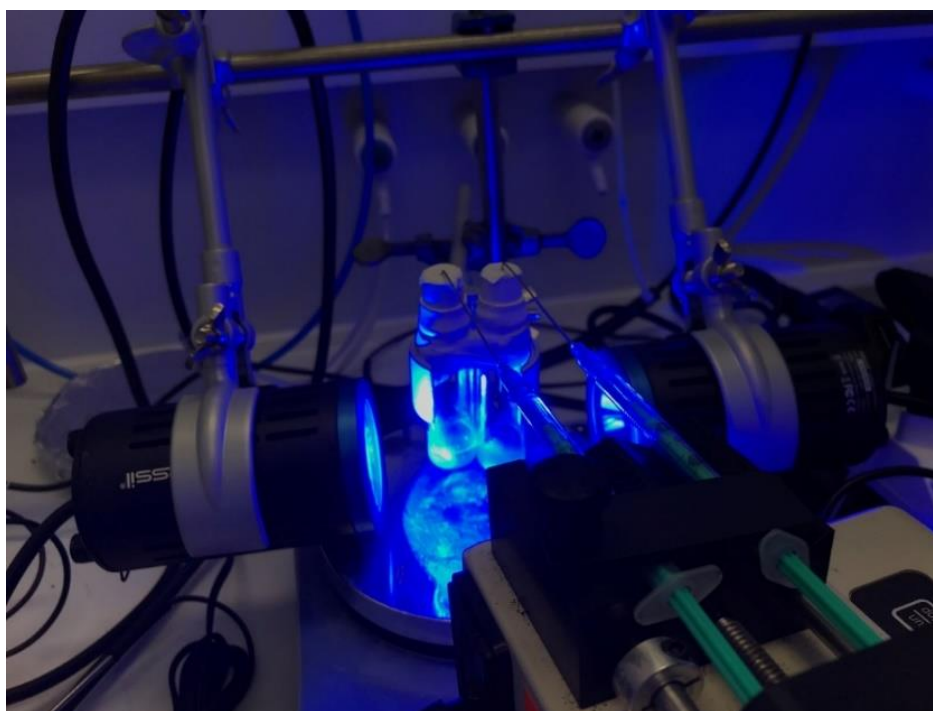
The synthesis of 3-2 and the analogous amidyl radical sources followed the procedure reported in literature, with minor modifications.^[28] NEt₃ (2.8 mL, 20 mmol) and hydroxylamine hydrochloride (0.77g, 11 mmol) were added into 10 mL DCM, and the reaction mixture was stirred at room temperature for 5 min. Then, the suspension was cooled to 0 °C, and Troc-Cl (10 mmol, in 20 mL DCM) was added over 30 min by a syringe pump. The mixture was stirred at room temperature for 30 min and 1.4 mL NEt₃ (10 mmol) was added. Next, the suspension was cooled again to 0 °C, followed by the addition of 4-cyanobenzoyl chloride (7 mmol, in 10 mL of DCM) over 30 min. The mixture was then warmed to room temperature and left for 30 min. The product was separated by

chromatography on silica gel to afford 3-2 as a white solid in 60% yield. ^1H NMR (400 MHz, CDCl_3) δ 8.70 – 8.59 (s, 1H), 8.25 – 8.17 (m, 2H), 7.85 – 7.77 (m, 2H), 4.84 (s, 2H).

3.7.3 Procedures for the photochemical reaction

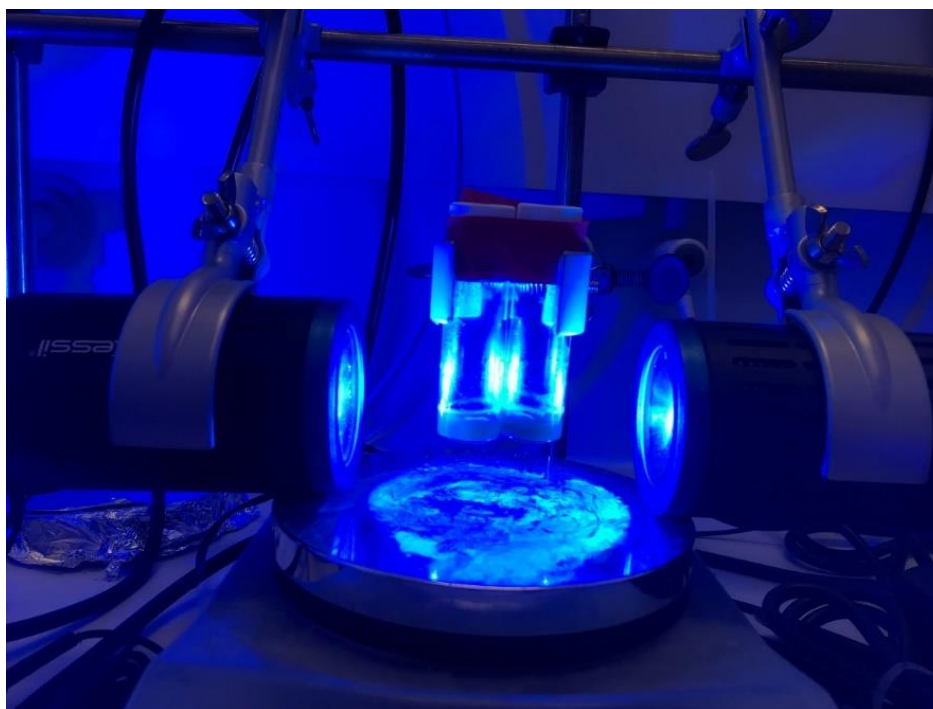
General procedure 1 (3-GP1):

0.01 mmol $\text{Cu}(\text{OPiv})_2$ and 0.001 mmol $\text{Ir}(\text{dfppy})_2(\text{ppy})$ were added to a glass vial ($d=2$ cm), which was then transferred to the glovebox. 0.1 mmol $\text{Mg}(\text{OPiv})_2$, 0.3 mmol alkene (3 equiv.), 0.1 mL acetonitrile solution of water (1 M H_2O) and 0.1 mL acetonitrile solution of 3-2 (0.2 M, 20% of the total amount) were added to the vial. The vial was sealed with a rubber septum and placed under blue LED radiation. The rest solution of 3-2 (0.4 mL, 0.2 M) was added to the vial at a rate of $1.2\ \mu\text{L}/\text{min}$ by a syringe pump. The setup is illustrated in the picture below. After 24 h, the reaction was stopped. To the reaction solution were added 4 mL ethyl acetate, 1 mL water and 2 drops of 15% ammonia solution, and then the organic phase was collected after sufficient mixing. The organic phase was concentrated. The residue was subsequently analyzed by NMR to obtain the NMR yield and was separated on silica gel column to give the final product.



General procedure 2 (3-GP2):

0.01 mmol $\text{Cu}(\text{OPiv})_2$, 0.001 mmol $\text{Ir}(\text{dfppy})_2(\text{ppy})$ and 0.1 mmol 3-2 were added to a glass vial (d=2 cm), which was then transferred to the glovebox. 0.1 mmol $\text{Mg}(\text{OPiv})_2$, 0.3 mmol alkene (3 equiv.), 0.1 mL acetonitrile solution of water (1 M H_2O) and 0.9 mL acetonitrile were added to the vial. The vial was sealed with a plastic cap and placed under blue LED radiation for 24 h. The setup is illustrated in the picture below. When the reaction completed, to the reaction solution were added 4 mL ethyl acetate, 1 mL water and 2 drops of 15% ammonia solution, and then the organic phase was collected after sufficient mixing. The organic phase was concentrated. The residue subsequently was analyzed by NMR to obtain the NMR yield and was separated on silica gel column to give the final product.

**General procedure 3 (3-GP3):**

0.01 mmol $\text{Cu}(\text{OPiv})_2$, 0.001 mmol $\text{Ir}(\text{dfppy})_2(\text{ppy})$ and 0.1 mmol 3-2 were added to a glass vial (d=2 cm), which was then transferred to the glovebox. 0.3 mmol alkene (3 equiv.), 1 mL acetonitrile were added to the vial. The vial was sealed with a plastic cap and placed under blue LED radiation for 24 h (the setup is the same as in GP2). When the reaction completed, 0.6 mmol MeI and 1 mmol K_2CO_3 were added to the reaction, and the vial was heated for 12 h at 60 °C. To the reaction

solution were added 4 mL ethyl acetate, 1 mL water and 2 drops of 15% ammonia solution, and then the organic phase was collected after sufficient mixing. The organic phase was concentrated. The residue was subsequently analyzed by NMR to obtain the NMR yield and was separated on silica gel column to give the final product.

Scale-up procedure:

10% Cu(OPiv)₂ (67.5 mg), 0.5% Ir(dfppy)₂(ppy) (10 mg), 1equiv. Mg(OPiv)₂ (0.58 g) and 3 equiv. alkene 3-37 (1.70 g) were added to a 50 mL Schlenk tube, in which the atmosphere was then changed to nitrogen. Next, 3 mL CH₃CN, 45 μ L H₂O and 2 mL solution of 3-2 (0.25 M in CH₃CN) was added and the reaction vessel was placed under radiation of blue LED. 8 mL of solution of 3-2 (0.25 M in CH₃CN) was added at a rate of 0.01 mL/min by a syringe pump. After the addition, the reaction was maintained for another 20 h for completion. A substantial amount of precipitate was obtained.

Filtering the reaction mixture gave a white solid, which was then washed twice with diethyl ether. Drying under vacuum led to 0.328 g white powder, which was analyzed with NMR to be Mg(4-cyanobenzoate)₂·xH₂O.

To the filtrate were added 30 mL ethyl acetate, 2 mL water and 1 mL 15% ammonia solution, and then the organic phase was collected after sufficient mixing. The organic phase was concentrated. The residue was separated on silica gel column to recover the alkene (1.232 g, 2.20 equiv.) and give the final product 3-38 (0.632 g, 61%).

3.7.4 Experimental details for mechanistic studies

Stern-Volmer quenching

All solutions and samples were prepared under nitrogen. Stock solutions of Ir(dfppy)₂(bpy) (2.9 mg in 20.0 mL CH₃CN, 2.0×10⁻⁴ M), Cu(OPiv)₂ (10.6 mg in 20.0 mL CH₃CN, 2.0×10⁻³ M), CuOAc (2.5 mg in 10.0 mL CH₃CN, 2.0×10⁻³ M) Mg(OPiv)₂·H₂O (45.3 mg Mg(OPiv)₂ and 3.6 μ L H₂O in 20.0 mL CH₃CN, 1.0×10⁻² M), 3-2 (81.6 mg in 20.0 mL CH₃CN, 2.0×10⁻² M), 3-1 (135 mg in 20.0 mL CH₃CN, 2.0×10⁻² M) and 3-3 (62.5 mg in 10.0 mL CH₃CN, 2.0×10⁻² M) were prepared. The sample solutions were prepared by mixing given amounts of certain stock solutions, and then diluted to 5.0 mL in a volumetric flask under nitrogen. The sample solution was transfer to a cuvette with screw cap for further measurements on a fluorescence spectrometer. Parameters: exciting (420 nm, slit 2.5 nm), emission measurement (430 nm-700 nm).

Figure 3.8 shows an example of Stern-Volmer plotting (Cu(OPiv)_2 as quencher).

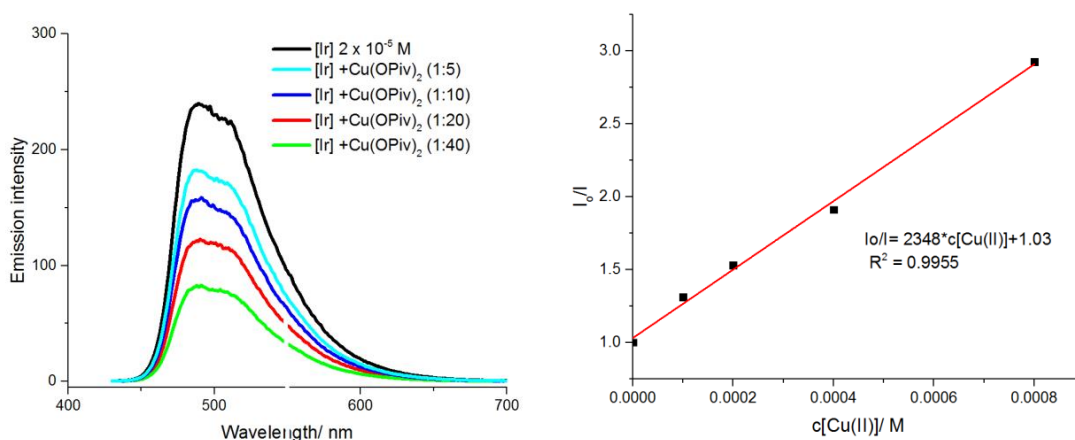


Figure 3.8 Emission quenching by Cu(OPiv)_2 at different concentrations and the corresponding Stern-Volmer Plot.

Measurement of redox potentials of reagents with CV

The CVs were recorded in CH_3CN , with Bu_4NBF_4 (0.05 M) as electrolyte, glassy carbon disk as working electrode (diameter, 3 mm), Pt wire as counter electrode, $\text{Ag}|\text{AgCl}$, KCl(aq) as reference electrode. The scan rate was 100 mV/s. Concentration of reagents (if applicable): 0.0001 M Fc , 0.0001 M $\text{Ir(dfppy)}_2(\text{ppy})$, 0.001 M Cu(OPiv)_2 , 0.01 M 3-2, 0.01 M 3-3.

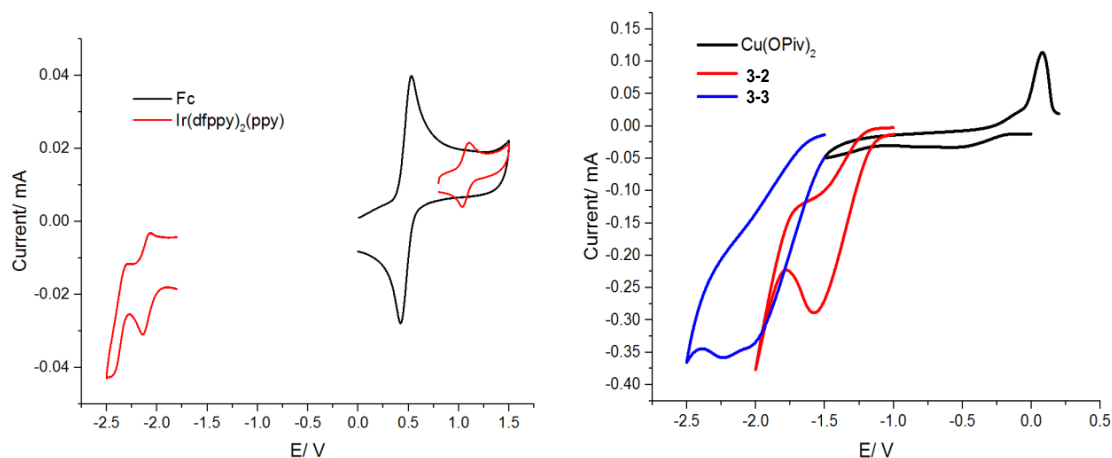
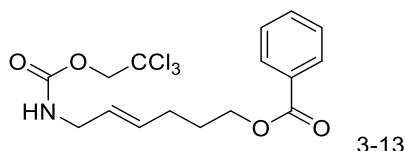


Figure 3.9 CVs of reaction reagents.

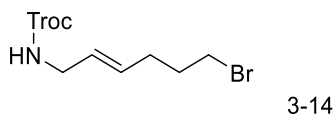
$E(\text{Fc}^+/\text{Fc})$ is 0.477 V vs the reference electrode in our system. $E(\text{Fc}^+/\text{Fc})$ in CH_3CN is 0.380 V vs. SCE. The potentials vs $E(\text{Fc}^+/\text{Fc})$ above are converted to potentials vs SCE: $E(\text{Ir}^{\text{III}}/\text{Ir}^{\text{II}}) = -2.22$ V, $E(\text{Ir}^{\text{IV}}/\text{Ir}^{\text{III}}) = 0.97$ V, $E_{\text{ox}}(\text{Cu}^{\text{I}}) = -0.10$ V, $E_{\text{red}}(3-2) = -1.43$ V, $E_{\text{red}}(3-3) = -1.82$ V.

Based on the emission spectrum (Figure 3.8), $\lambda_{\max} = 490$ nm, which corresponds to a triplet energy $E_0 = 2.53$ eV. The oxidation potential of the excited state can be estimated:^[29] $E(\text{Ir}^*/\text{Ir}^{\text{IV}}) = E(\text{Ir}^{\text{III}}/\text{Ir}^{\text{IV}}) - E_0 = -1.56$ V.

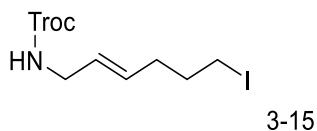
3.7.5 Characterization data for the products



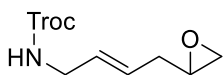
(E)-6-((Troc-amino)hex-4-en-1-yl benzoate, synthesized via 3-CP1, colorless oil, 27.4 mg (Yield = 70%), trans: cis = 9:1. For trans-isomer, ^1H NMR (400 MHz, CDCl_3) δ 8.03 (d, $J = 7.8$ Hz, 2H), 7.55 (t, $J = 6.9$ Hz, 1H), 7.43 (t, $J = 7.6$ Hz, 2H), 5.77 – 5.62 (m, 1H), 5.59 – 5.44 (m, 1H), 5.13 (b, 1H), 4.72 (s, 2H), 4.32 (td, $J = 6.5, 2.5$ Hz, 2H), 3.79 (t, $J = 6.7$ Hz, 2H), 2.29 – 2.09 (m, 2H), 1.93 – 1.79 (m, 2H). ^{13}C NMR (101 MHz, CDCl_3) δ 166.7, 154.5, 133.0, 132.4, 130.4, 129.6, 128.5, 126.5, 95.7, 74.6, 64.3, 43.2, 28.7, 28.1. HRMS (ESI/QTOF) m/z : $[\text{M} + \text{Na}]^+$ Calcd for $\text{C}_{16}\text{H}_{18}\text{Cl}_3\text{NNaO}_4^+$ 416.0194; Found 416.0193.



2,2,2-Trichloroethyl (E)-6-bromohex-2-en-1-yl carbamate, synthesized via 3-CP1, colorless oil, 23.0 mg (Yield = 65%), trans: cis = 9:1. For trans-isomer, ^1H NMR (400 MHz, CDCl_3) δ 5.68 – 5.49 (m, 2H), 5.01 (b, 1H), 4.73 (s, 2H), 3.81 (t, $J = 5.7$ Hz, 2H), 3.39 (t, $J = 6.6$ Hz, 3H), 2.20 (q, $J = 6.9$ Hz, 2H), 1.98 – 1.88 (m, 3H). ^{13}C NMR (101 MHz, CDCl_3) δ 154.5, 131.7, 127.1, 95.7, 74.7, 43.2, 33.1, 32.0, 30.6. HRMS (ESI/QTOF) m/z : $[\text{M} + \text{Na}]^+$ Calcd for $\text{C}_9\text{H}_{13}\text{BrCl}_3\text{NNaO}_2^+$ 373.9087; Found 373.9081.

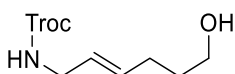


2,2,2-Trichloroethyl (E)-6-iodohex-2-en-1-yl carbamate, synthesized via 3-CP1, colorless oil, 24.0 mg (Yield = 60%), trans: cis = 10:1. For trans-isomer, ^1H NMR (400 MHz, CDCl_3) δ 5.67 – 5.48 (m, 2H), 5.01 (b, 1H), 4.73 (s, 2H), 3.80 (t, $J = 5.5$ Hz, 2H), 3.17 (t, $J = 6.8$ Hz, 3H), 2.15 (q, $J = 6.6$ Hz, 2H), 1.89 (p, $J = 6.9$ Hz, 2H). ^{13}C NMR (101 MHz, CDCl_3) δ 154.5, 131.5, 127.1, 95.7, 74.7, 43.2, 32.8, 32.6, 6.3. HRMS (ESI/QTOF) m/z : $[\text{M} + \text{Na}]^+$ Calcd for $\text{C}_9\text{H}_{13}\text{Cl}_3\text{INNaO}_2^+$ 421.8949; Found 421.8958.



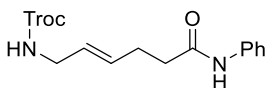
3-16

2,2,2-Trichloroethyl (E)-(4-(oxiran-2-yl)but-2-en-1-yl)carbamate, synthesized via 3-CP1, colorless oil, 18.5 mg (Yield = 64%). ^1H NMR (400 MHz, CDCl_3) δ 5.75 – 5.58 (m, 2H), 5.07 (b, 1H), 4.73 (s, 2H), 3.83 (t, J = 5.5 Hz, 2H), 3.02 – 2.92 (m, 1H), 2.81 – 2.71 (t, J = 4.4 Hz, 1H), 2.50 (dd, J = 4.9, 2.7 Hz, 1H), 2.42 – 2.22 (m, 2H). ^{13}C NMR (101 MHz, CDCl_3) δ 154.5, 128.7, 127.8, 95.7, 74.7, 51.3, 46.7, 43.1, 35.1. HRMS (ESI/QTOF) m/z : $[\text{M} + \text{Na}]^+$ Calcd for $\text{C}_9\text{H}_{12}\text{Cl}_3\text{NNaO}_3^+$ 309.9775; Found 309.9781.



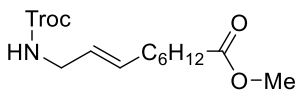
3-17

2,2,2-Trichloroethyl (E)-(6-hydroxyhex-2-en-1-yl)carbamate, synthesized via 3-CP2, colorless oil, 17.7 mg (Yield = 61%), ^1H NMR (400 MHz, CDCl_3) δ 5.67 (dt, J = 14.7, 6.6, 1.4 Hz, 1H), 5.50 (dt, J = 15.3, 6.1, 1.5 Hz, 1H), 5.08 (b, 1H), 4.72 (s, 2H), 3.79 (td, J = 5.9, 1.1 Hz, 2H), 3.64 (t, J = 6.5 Hz, 2H), 2.13 (q, J = 6.7 Hz, 2H), 1.68 – 1.61 (m, 3H). ^{13}C NMR (101 MHz, CDCl_3) δ 154.5, 133.3, 126.1, 95.7, 74.7, 62.4, 43.3, 32.1, 28.6. HRMS (ESI/QTOF) m/z : $[\text{M} + \text{Na}]^+$ Calcd for $\text{C}_9\text{H}_{14}\text{Cl}_3\text{NNaO}_3^+$ 311.9931; Found 311.9935.



3-18

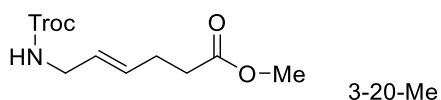
2,2,2-Trichloroethyl (E)-(6-oxo-6-(phenylamino)hex-2-en-1-yl)carbamate, synthesized via 3-CP1, white solid, 20.4 mg (Yield = 54%). trans: cis = 12:1. For trans-isomer, ^1H NMR (400 MHz, CDCl_3) δ 7.51 (d, J = 7.9 Hz, 2H), 7.31 (m, 3H), 7.10 (t, J = 7.4 Hz, 1H), 5.71 (dt, J = 15.8, 6.0 Hz, 1H), 5.56 (dt, J = 15.8, 6.0 Hz, 1H), 5.08 (b, 1H), 4.69 (s, 2H), 3.79 (t, J = 6.0 Hz, 2H), 2.56 – 2.35 (m, 4H). ^{13}C NMR (101 MHz, CDCl_3) δ 170.5, 154.6, 137.9, 131.7, 129.2, 127.1, 124.5, 120.0, 95.7, 74.6, 43.1, 37.2, 28.0. HRMS (ESI/QTOF) m/z : $[\text{M} + \text{Na}]^+$ Calcd for $\text{C}_{15}\text{H}_{17}\text{Cl}_3\text{N}_2\text{NaO}_3^+$ 401.0197; Found 401.0202.



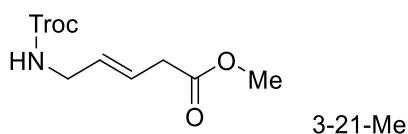
3-19-Me

(E)-Methyl 10-(Troc-amino)dec-8-enoate, synthesized via 3-CP3, isolated as methylated product, colorless oil, 19.4 mg (Yield = 52%), trans: cis = 7:1. For trans-isomer, ^1H NMR (400 MHz, CDCl_3) δ 5.63 (dt, J = 14.1, 6.8 Hz, 1H), 5.45 (dt, J = 14.1, 6.2 Hz, 1H), 5.04 (b, 1H), 4.72 (s, 2H), 3.78 (t, J = 6.1

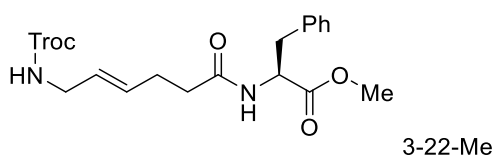
Hz, 2H), 3.66 (s, 3H), 2.29 (t, $J = 7.5$ Hz, 2H), 2.01 (m, 2H), 1.60 (m, 2H), 1.43 – 1.18 (m, 6H). ^{13}C NMR (101 MHz, CDCl_3) δ 174.4, 154.5, 134.1, 125.4, 95.8, 74.6, 51.6, 43.3, 34.2, 32.2, 29.0, 28.9, 28.8, 25.0. HRMS (ESI/QTOF) m/z : $[\text{M} + \text{Na}]^+$ Calcd for $\text{C}_{14}\text{H}_{22}\text{Cl}_3\text{NNaO}_4^+$ 396.0507; Found 396.0501.



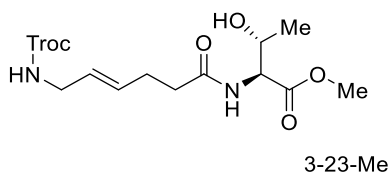
(E)-Methyl 6-(Troc-amino)hex-4-enoate, synthesized via 3-CP3, isolated as methylated product, colorless oil, 15.8 mg (Yield = 50%), trans: cis = 9:1. For trans-isomer, ^1H NMR (400 MHz, CDCl_3) δ 5.70 – 5.59 (m, 1H), 5.57 – 5.45 (m, 1H), 5.02 (b, 1H), 4.72 (s, 2H), 3.79 (t, $J = 5.6$ Hz, 2H), 3.67 (s, 3H), 2.44 – 2.29 (m, 4H). ^{13}C NMR (101 MHz, CDCl_3) δ 173.4, 154.5, 131.6, 126.8, 95.7, 74.7, 51.8, 43.1, 33.6, 27.5. HRMS (ESI/QTOF) m/z : $[\text{M} + \text{Na}]^+$ Calcd for $\text{C}_{10}\text{H}_{14}\text{Cl}_3\text{NNaO}_4^+$ 339.9881; Found 339.9877.



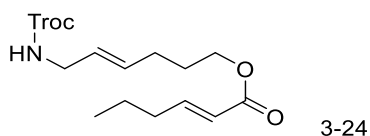
(E)-Methyl 5-(Troc-amino)pent-3-enoate, synthesized via 3-CP3, isolated as methylated product, colorless oil, 16.1 mg (Yield = 53%). ^1H NMR (400 MHz, CDCl_3) δ 5.77 (dt, $J = 15.2, 6.8$ Hz, 1H), 5.62 (dt, $J = 15.4, 5.9$ Hz, 1H), 5.10 (b, 1H), 4.72 (s, 2H), 3.85 (t, $J = 5.4$ Hz, 2H), 3.68 (s, 3H), 3.09 (d, $J = 6.9$ Hz, 2H). ^{13}C NMR (101 MHz, CDCl_3) δ 172.0, 154.5, 129.8, 124.9, 95.7, 74.7, 52.1, 42.9, 37.4. HRMS (ESI/QTOF) m/z : $[\text{M} + \text{Na}]^+$ Calcd for $\text{C}_9\text{H}_{12}\text{Cl}_3\text{NNaO}_4^+$ 325.9724; Found 325.9731.



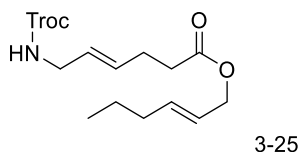
Methyl (S,E)-3-phenyl-2-(6-(Troc-amino)hex-4-enamido)propanoate, synthesized via 3-CP3, isolated as methylated product, sticky gel, 20.9 mg (Yield = 45%). ^1H NMR (400 MHz, CDCl_3) δ 7.37 – 7.23 (m, 3H), 7.12 – 7.04 (m, 2H), 5.95 (d, $J = 7.9$ Hz, 1H), 5.64 – 5.54 (m, 1H), 5.44 (dt, $J = 15.2, 6.1$ Hz, 1H), 5.23 (b, 1H), 4.95 – 4.83 (m, 1H), 4.80 – 4.66 (m, 2H), 3.75 (m, 5H), 3.16 (dd, $J = 13.9, 5.8$ Hz, 1H), 3.08 (dd, $J = 13.9, 5.8$ Hz, 1H), 2.42 – 2.21 (m, 4H). ^{13}C NMR (101 MHz, CDCl_3) δ 172.5, 171.8, 154.5, 135.9, 131.8, 129.4, 128.7, 128.7, 127.3, 95.8, 74.7, 53.1, 52.6, 43.2, 37.9, 35.7, 28.0. HRMS (ESI/QTOF) m/z : $[\text{M} + \text{Na}]^+$ Calcd for $\text{C}_{19}\text{H}_{23}\text{Cl}_3\text{N}_2\text{NaO}_5^+$ 487.0565; Found 487.0578.



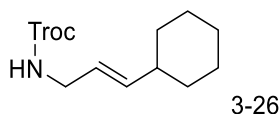
Methyl ((E)-6-(Troc-amino)hex-4-en-1-yl)-L-threoninate, synthesized via 3-CP3, isolated as methylated product, sticky gel, 13.5 mg (Yield = 32%). ^1H NMR (400 MHz, CDCl_3) δ 6.35 (d, J = 9.0 Hz, 1H), 5.75 – 5.63 (m, 1H), 5.57 (dt, J = 15.4, 5.8 Hz, 1H), 5.46 (s, 1H), 4.71 (s, 2H), 4.59 (dd, J = 8.8, 2.5 Hz, 1H), 4.35 (qd, J = 6.4, 2.5 Hz, 1H), 3.86 – 3.75 (m, 5H), 2.49 – 2.35 (m, 4H), 2.19 (m, 1H), 1.23 (d, J = 6.4 Hz, 3H). ^{13}C NMR (101 MHz, CDCl_3) δ 173.0, 171.8, 154.6, 131.7, 127.4, 95.8, 74.7, 68.2, 57.3, 52.8, 43.2, 36.0, 28.2, 20.3. HRMS (ESI/QTOF) m/z : $[\text{M} + \text{Na}]^+$ Calcd for $\text{C}_{14}\text{H}_{21}\text{Cl}_3\text{N}_2\text{NaO}_6^+$ 441.0357; Found 441.0352.



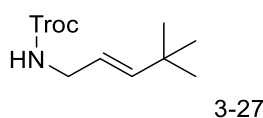
(E)-(E)-6-(Troc-amino)hex-4-en-1-yl hex-2-enoate, synthesized via 3-CP2, colorless oil, 19.7 mg (Yield = 51%). ^1H NMR (400 MHz, CDCl_3) δ 6.96 (dt, J = 15.5, 6.9 Hz, 1H), 5.81 (dt, J = 15.6, 1.7 Hz, 1H), 5.65 (dt, J = 14.8, 6.6 Hz, 1H), 5.50 (dt, J = 15.1, 6.1 Hz, 1H), 5.02 (b, 1H), 4.72 (s, 2H), 4.12 (t, J = 6.5 Hz, 2H), 3.80 (t, J = 6.0 Hz, 2H), 2.25 – 2.07 (m, 4H), 1.74 (p, J = 6.8 Hz, 2H), 1.57 – 1.46 (m, 2H), 0.93 (t, J = 7.3 Hz, 3H). ^{13}C NMR (101 MHz, CDCl_3) δ 166.9, 154.5, 149.6, 132.6, 126.4, 121.4, 95.7, 74.7, 63.5, 43.2, 34.4, 28.7, 28.2, 21.4, 13.8. HRMS (ESI/QTOF) m/z : $[\text{M} + \text{Na}]^+$ Calcd for $\text{C}_{15}\text{H}_{22}\text{Cl}_3\text{NNaO}_4^+$ 408.0507; Found 408.0507.



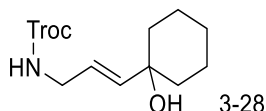
(E)-Hex-2-en-1-yl (E)-6-(Troc-amino)hex-4-enoate, synthesized via 3-CP1, colorless oil, 17.4 mg (Yield = 45%). ^1H NMR (400 MHz, CDCl_3) δ 5.80 – 5.71 (m, 1H), 5.70 – 5.61 (m, 1H), 5.60 – 5.46 (m, 2H), 5.00 (s, 1H), 4.72 (s, 2H), 4.51 (dq, J = 6.4, 1.1 Hz, 2H), 3.79 (t, J = 6.0, 2H), 2.42 – 2.29 (m, 4H), 2.03 (qt, J = 6.7, 1.4 Hz, 2H), 1.48 – 1.34 (m, 2H), 0.90 (t, J = 7.4 Hz, 3H). ^{13}C NMR (101 MHz, CDCl_3) δ 172.8, 154.5, 136.7, 131.7, 126.8, 124.0, 95.7, 74.7, 65.5, 43.1, 34.4, 33.8, 27.5, 22.2, 13.8. HRMS (ESI/QTOF) m/z : $[\text{M} + \text{Na}]^+$ Calcd for $\text{C}_{15}\text{H}_{22}\text{Cl}_3\text{NNaO}_4^+$ 408.0507; Found 408.0505.



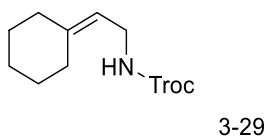
2,2,2-Trichloroethyl (E)- (3-cyclohexylallyl)carbamate, synthesized via 3-CP1, colorless oil, 17.0 mg (Yield = 54%). ^1H NMR (400 MHz, CDCl_3) δ 5.59 (dd, J = 15.5, 6.6 Hz, 1H), 5.41 (dt, J = 15.5, 5.9 Hz, 1H), 4.98 (b, 1H), 4.72 (s, 2H), 3.79 (t, J = 6.0 Hz, 2H), 1.98 – 1.88 (m, 1H), 1.80 – 1.59 (m, 5H), 1.34 – 0.97 (m, 5H). ^{13}C NMR (101 MHz, CDCl_3) δ 154.5, 140.0, 122.8, 95.8, 74.7, 43.5, 40.4, 32.9, 26.2, 26.1. HRMS (ESI/QTOF) m/z : $[\text{M} + \text{H}]^+$ Calcd for $\text{C}_{12}\text{H}_{19}\text{Cl}_3\text{NO}_2^+$ 314.0476; Found 314.0475.



2,2,2-Trichloroethyl (E)- (4,4-dimethylpent-2-en-1-yl)carbamate, synthesized via 3-CP1, white solid, 16.5 mg (Yield = 57%). ^1H NMR (400 MHz, CDCl_3) δ 5.66 (dt, J = 15.7, 1.4 Hz, 1H), 5.37 (dt, J = 15.6, 6.2 Hz, 1H), 4.96 (b, 1H), 4.73 (s, 2H), 3.80 (td, J = 6.0, 1.4 Hz, 2H), 1.00 (s, 9H). ^{13}C NMR (101 MHz, CDCl_3) δ 154.5, 145.1, 120.2, 95.8, 74.7, 43.6, 33.1, 29.6. HRMS (ESI/QTOF) m/z : $[\text{M} + \text{H}]^+$ Calcd for $\text{C}_{10}\text{H}_{17}\text{Cl}_3\text{NO}_2^+$ 288.0319; Found 288.0313.

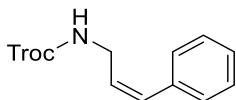


2,2,2-Trichloroethyl (E)- (3-(1-hydroxycyclohexyl)allyl)carbamate, synthesized via 3-CP1, colorless liquid, 22.4 mg (Yield = 68%). ^1H NMR (400 MHz, CDCl_3) δ 5.83 – 5.64 (m, 2H), 5.10 (s, 1H), 4.73 (s, 2H), 3.85 (t, J = 5.6 Hz, 2H), 1.69 – 1.44 (m, 10H), 1.33 – 1.22 (m, 1H). ^{13}C NMR (101 MHz, CDCl_3) δ 154.5, 140.6, 123.2, 95.7, 74.7, 71.3, 43.0, 37.9, 25.5, 22.1. HRMS (ESI/QTOF) m/z : $[\text{M} + \text{Na}]^+$ Calcd for $\text{C}_{12}\text{H}_{18}\text{NCl}_3\text{NaO}_3^+$ 352.0244; Found 352.0249.



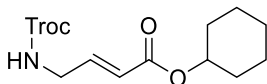
2,2,2-Trichloroethyl (2-cyclohexylideneethyl)carbamate, synthesized via 3-CP2, colorless oil, 6.0 mg (Yield = 20%). ^1H NMR (400 MHz, CDCl_3) δ 5.16 (t, J = 7.2 Hz, 1H), 4.87 (b, 1H), 4.72 (s, 2H), 3.83 (t, J = 6.3 Hz, 2H), 2.17 (m, 2H), 2.09 (m, 2H), 1.61 – 1.40 (m, 6H). ^{13}C NMR (101 MHz, CDCl_3) δ 154.5,

145.1, 116.5, 95.8, 74.7, 38.4, 37.1, 29.0, 28.5, 27.9, 26.8. HRMS (ESI/QTOF) m/z : $[M + H]^+$ Calcd for $C_{11}H_{17}Cl_3NO_2^+$ 300.0319; Found 300.0319.



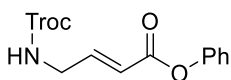
3-30

2,2,2-Trichloroethyl (Z)-(3-phenylallyl)carbamate, synthesized via 3-CP2, colorless oil, 8.9 mg (Yield = 29%). 1H NMR (400 MHz, $CDCl_3$) δ 7.36 (t, J = 7.4 Hz, 2H), 7.32 – 7.26 (m, 1H), 7.22 (d, J = 7.3 Hz, 2H), 6.61 (d, J = 11.6 Hz, 1H), 5.77 – 5.59 (m, 1H), 5.07 (b, 1H), 4.74 (s, 2H), 4.15 (t, J = 6.2 Hz, 2H). ^{13}C NMR (101 MHz, $CDCl_3$) δ 154.6, 136.2, 132.2, 128.8, 128.5, 127.7, 127.6, 95.7, 74.7, 39.7. HRMS (ESI/QTOF) m/z : $[M + H]^+$ Calcd for $C_{12}H_{13}Cl_3NO_2^+$ 308.0006; Found 308.0005.



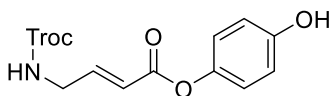
3-31

Cyclohexyl 4-(E)-(Troc-amino)but-2-enoate, synthesized via 3-CP1, colorless liquid, 21.9 mg (Yield = 61%). 1H NMR (400 MHz, $CDCl_3$) δ 6.83 (dt, J = 15.8, 4.9 Hz, 1H), 5.90 (d, J = 15.6 Hz, 1H), 5.17 (b, 1H), 4.81 – 4.71 (m, 1H), 4.70 (s, 2H), 3.96 (m, 2H), 1.85 – 1.74 (m, 2H), 1.66 (m, 2H), 1.51 – 1.11 (m, 6H). ^{13}C NMR (101 MHz, $CDCl_3$) δ 165.4, 154.6, 142.9, 122.7, 95.5, 74.8, 73.1, 42.0, 31.7, 25.5, 23.9. HRMS (ESI/QTOF) m/z : $[M + Na]^+$ Calcd for $C_{13}H_{18}Cl_3NNaO_4^+$ 380.0194; Found 380.0195.



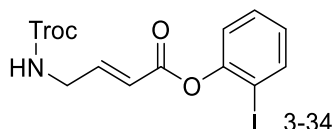
3-32

(E)-Phenyl 4-(Troc-amino)but-2-enoate, synthesized via 3-CP1, colorless oil, 18.0 mg (Yield = 51%). 1H NMR (400 MHz, $CDCl_3$) δ 7.43 – 7.36 (m, 2H), 7.27 – 7.22 (m, 1H), 7.16 – 7.07 (m, 3H), 6.19 (dt, J = 15.8, 2.1 Hz, 1H), 5.28 (s, 1H), 4.78 (s, 2H), 4.15 – 4.06 (m, 2H). ^{13}C NMR (101 MHz, $CDCl_3$) δ 164.3, 154.6, 150.7, 145.7, 129.6, 126.1, 121.6, 121.3, 95.5, 74.9, 42.1. HRMS (ESI/QTOF) m/z : $[M + Na]^+$ Calcd for $C_{13}H_{12}Cl_3NNaO_4^+$ 373.9724; Found 373.9728.

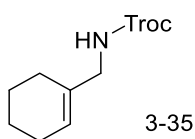


3-33

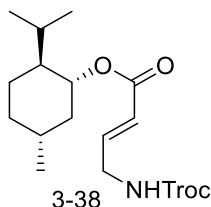
(E)-4-Hydroxyphenyl 4-(Troc-amino)but-2-enoate, synthesized via 3-CP1, sticky gel, 14.0 mg (Yield = 38%). ^1H NMR (400 MHz, CDCl_3) δ 7.09 (dt, J = 15.7, 4.8 Hz, 1H), 7.00 – 6.89 (m, 2H), 6.82 – 6.73 (m, 2H), 6.16 (dt, J = 15.7, 1.9 Hz, 1H), 5.42 (s, 1H), 5.33 (t, J = 6.3 Hz, 1H), 4.77 (s, 2H), 4.14 – 4.06 (m, 2H). ^{13}C NMR (101 MHz, CDCl_3) δ 165.0, 154.7, 153.7, 145.7, 144.0, 122.5, 121.3, 116.2, 95.4, 74.9, 42.1. HRMS (ESI/QTOF) m/z : $[\text{M} + \text{Na}]^+$ Calcd for $\text{C}_{13}\text{H}_{12}\text{Cl}_3\text{NNaO}_5^+$ 389.9673; Found 389.9679.



(E)-2-Iodophenyl 4-(Troc-amino)but-2-enoate, synthesized via 3-CP1, colorless oil, 24.4 mg (Yield = 51%). ^1H NMR (400 MHz, CDCl_3) δ 7.84 (dd, J = 7.9, 1.5 Hz, 1H), 7.37 (ddd, J = 8.9, 6.2, 1.5 Hz, 1H), 7.20 (dt, J = 15.7, 4.8 Hz, 1H), 7.14 (dd, J = 8.1, 1.5 Hz, 1H), 6.98 (td, J = 7.6, 1.5 Hz, 1H), 6.23 (dt, J = 15.8, 2.0 Hz, 1H), 5.27 (s, 1H), 4.79 (s, 2H), 4.14 (ddd, J = 6.6, 4.9, 2.0 Hz, 2H). ^{13}C NMR (101 MHz, CDCl_3) δ 163.3, 154.6, 151.2, 146.5, 139.6, 129.6, 127.8, 123.1, 121.1, 95.6, 90.4, 75.0, 42.2. HRMS (ESI/QTOF) m/z : $[\text{M} + \text{Na}]^+$ Calcd for $\text{C}_{13}\text{H}_{11}\text{Cl}_3\text{INNaO}_4^+$ 499.8691; Found 499.8693.

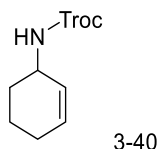


2,2,2-trichloroethyl (cyclohex-1-en-1-ylmethyl)carbamate, synthesized via modified 3-CP2 (acetone as solvent), white solid, 12.1 mg (Yield = 43%). ^1H NMR (400 MHz, CDCl_3) δ 5.61 (m, 1H), 4.98 (b, 1H), 4.73 (s, 2H), 3.72 (d, J = 6.1 Hz, 2H), 2.05 – 1.92 (m, 4H), 1.71 – 1.52 (m, 4H). ^{13}C NMR (101 MHz, CDCl_3) δ 154.8, 134.2, 123.8, 95.8, 74.6, 47.6, 26.4, 25.1, 22.6, 22.4. HRMS (ESI/QTOF) m/z : $[\text{M} + \text{Na}]^+$ Calcd for $\text{C}_{10}\text{H}_{14}\text{Cl}_3\text{NNaO}_2^+$ 307.9982; Found 307.9983.

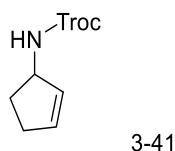


(1R,2S,5R)-2-Isopropyl-5-methylcyclohexyl (E)-4-(Troc-amino)but-2-enoate, synthesized via scale-up procedure (section 4), sticky gel, 0.632 g (Yield = 61%). ^1H NMR (400 MHz, CDCl_3) δ 6.87 (dt, J = 15.7, 4.9 Hz, 1H), 5.94 (dq, J = 15.8, 1.9 Hz, 1H), 5.45 (s, 1H), 4.78 – 4.61 (m, 3H), 4.01 (td, J = 6.5, 1.7 Hz, 2H), 2.00 – 1.93 (m, 1H), 1.82 (m, 1H), 1.72 – 1.62 (m, 2H), 1.47 (m, 1H), 1.41 – 1.33 (m, 1H), 1.11

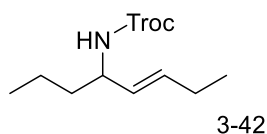
– 0.95 (m, 2H), 0.89 – 0.83 (m, 7H), 0.72 (dd, $J = 6.9, 1.3$ Hz, 3H). ^{13}C NMR (101 MHz, CDCl_3) δ 165.6, 154.6, 143.1, 122.5, 95.5, 74.8, 74.6, 47.2, 42.0, 41.0, 34.3, 31.5, 27.2, 26.4, 23.5, 22.1, 20.8, 16.4. HRMS (ESI/QTOF) m/z : $[\text{M} + \text{Na}]^+$ Calcd for $\text{C}_{17}\text{H}_{26}\text{Cl}_3\text{NNaO}_4^+$ 436.0820; Found 436.0821.



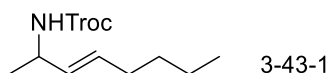
2,2,2-Trichloroethyl cyclohex-2-en-1-ylcarbamate, synthesized via 3-CP1, white solid, 12.0 mg (Yield = 44%). ^1H NMR (400 MHz, CDCl_3) δ 5.94 – 5.80 (m, 1H), 5.69 – 5.57 (m, 1H), 4.97 (b, 1H), 4.72 (s, 2H), 4.29 – 4.15 (m, 1H), 2.10 – 1.88 (m, 3H), 1.81 – 1.54 (m, 3H). ^{13}C NMR (101 MHz, CDCl_3) δ 153.9, 131.5, 127.3, 95.8, 74.6, 46.8, 29.7, 24.9, 19.7. HRMS (ESI/QTOF) m/z : $[\text{M} + \text{H}]^+$ Calcd for $\text{C}_9\text{H}_{13}\text{Cl}_3\text{NO}_2^+$ 272.0006; Found 272.0012.



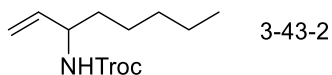
2,2,2-Trichloroethyl cyclopent-2-en-1-ylcarbamate, synthesized via 3-CP1, white solid, 13.9 mg (Yield = 54%). ^1H NMR (400 MHz, CDCl_3) δ 6.00 – 5.93 (m, 1H), 5.75 – 5.67 (m, 1H), 4.95 (b, 1H), 4.85 – 4.75 (m, 1H), 4.73 (s, 2H), 2.51 – 2.27 (m, 3H), 1.69 – 1.57 (m, 1H). ^{13}C NMR (101 MHz, CDCl_3) δ 154.0, 135.3, 130.7, 95.8, 74.6, 57.8, 31.5, 31.2. HRMS (ESI/QTOF) m/z : $[\text{M} + \text{H}]^+$ Calcd for $\text{C}_8\text{H}_{11}\text{Cl}_3\text{NO}_2^+$ 257.9850; Found 257.9849.



(E)-2,2,2-Trichloroethyl oct-5-en-4-ylcarbamate, synthesized via 3-CP2, colorless oil, 15.1 mg (Yield = 50%). ^1H NMR (400 MHz, CDCl_3) δ 5.60 (dt, $J = 15.3, 6.3$ Hz, 1H), 5.26 (dd, $J = 15.5, 6.5$ Hz, 1H), 4.78 (d, $J = 8.6$ Hz, 1H), 4.65 (m, 2H), 4.06 (p, $J = 7.2$ Hz, 1H), 1.97 (p, $J = 7.1$ Hz, 2H), 1.44 (m, 2H), 1.36 – 1.24 (m, 2H), 0.91 (t, $J = 7.4$ Hz, 3H), 0.86 (t, $J = 7.3$ Hz, 3H). ^{13}C NMR (101 MHz, CDCl_3) δ 154.0, 133.6, 128.9, 95.9, 74.6, 53.2, 37.8, 25.4, 19.1, 14.0, 13.6. HRMS (ESI/QTOF) m/z : $[\text{M} + \text{H}]^+$ Calcd for $\text{C}_{11}\text{H}_{18}\text{Cl}_3\text{NNaO}_2^+$ 324.0295; Found 324.0299.

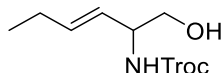


3-43-1



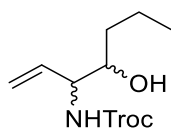
3-43-2

(E)-2,2,2-Trichloroethyl oct-3-en-2-ylcarbamate+ 2,2,2-trichloroethyl oct-1-en-3-ylcarbamate , synthesized via 3-CP2, colorless oil, 16.6 mg (Yield =55%), **3aa-1:3aa-2** = 1.4:1. For alkenyl hydrogen of **3aa-1**, ^1H NMR (400 MHz, CDCl_3) δ 5.68 – 5.58 (m, 1H), 5.41 (dd, J = 15.5, 5.8 Hz, 1H). For alkenyl hydrogen of **3aa-2**, ^1H NMR (400 MHz, CDCl_3) δ 5.83 – 5.71 (m, 1H), 5.20 (d, J = 17.1 Hz, 1H), 5.13 (d, J = 10.4 Hz, 1H). For the details of ^1H NMR, Please refer to the attached spectrum. ^{13}C NMR (101 MHz, CDCl_3) δ 154.1, 153.8, 138.3, 131.6, 130.8, 115.1, 95.8, 74.6, 53.8, 48.8, 35.1, 32.0, 31.6, 31.4, 25.4, 22.7, 22.3, 21.2, 14.1, 14.1. HRMS (ESI/QTOF) m/z : $[\text{M} + \text{H}]^+$ Calcd for $\text{C}_{11}\text{H}_{19}\text{Cl}_3\text{NO}_2^+$ 302.0476; Found 302.0484.



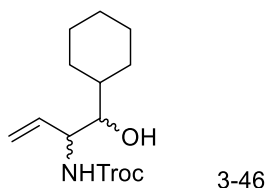
3-44

(E)-2,2,2-Trichloroethyl (1-hydroxyhex-3-en-2-yl)carbamate, synthesized via 3-CP1, white solid, 14.9 mg (Yield =51%). ^1H NMR (400 MHz, CDCl_3) δ 5.79 (dt, J = 15.6, 6.3 Hz, 1H), 5.41 (dd, J = 15.5, 6.1 Hz, 1H), 5.32 (b, 1H), 4.73 (s, 2H), 4.29 (m, 1H), 3.70 (m, 2H), 2.08 (p, J = 7.4, 2H), 1.84 (b, 1H), 1.00 (t, J = 7.4 Hz, 3H). ^{13}C NMR (101 MHz, CDCl_3) δ 154.6, 136.0, 125.0, 95.7, 74.8, 65.3, 54.9, 25.5, 13.5. HRMS (ESI/QTOF) m/z : $[\text{M} + \text{Na}]^+$ Calcd for $\text{C}_9\text{H}_{14}\text{Cl}_3\text{NNaO}_3^+$ 311.9931; Found 311.9935.

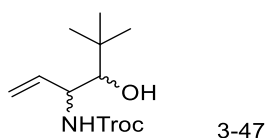


3-45

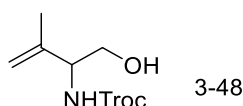
2,2,2-Trichloroethyl (4-hydroxyhept-1-en-3-yl)carbamate, synthesized via 3-CP1, colorless liquid, 16.1 mg (Yield =53%), dr= 2.0:1. ^1H NMR (400 MHz, CDCl_3) δ 5.87 – 5.72 (m, 1H), 5.70-5.30(d, J =9.0 Hz, 1H), 5.30 – 5.10 (m, 2H), 4.68 (d, J = 7.8 Hz, 2H), 4.32 – 4.09 (m, 1H), 3.69 (m, 1H), 1.70 (s, 1H), 1.52 – 1.27 (m, 4H), 0.87 (td, J = 6.8, 3.7 Hz, 3H). ^{13}C NMR (101 MHz, CDCl_3) δ 154.8, 154.3, 136.3, 132.8, 118.6, 116.8, 91.7, 74.7, 74.6, 73.4, 72.7, 57.9, 57.2, 36.4, 35.8, 19.1, 19.0, 14.1, 14.1. HRMS (ESI/QTOF) m/z : $[\text{M} + \text{Na}]^+$ Calcd for $\text{C}_{10}\text{H}_{16}\text{Cl}_3\text{NNaO}_3^+$ 326.0088; Found 326.0086.



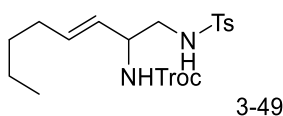
2,2,2-Trichloroethyl (1-cyclohexyl-1-hydroxybut-3-en-2-yl)carbamate, synthesized via 3-CP1, colorless liquid, 11.6 mg (Yield =34%), dr= 2.6:1. ^1H NMR (400 MHz, CDCl_3) δ 5.86 (m, 1H), 5.70 – 5.44 (m, 1H), 5.38 – 5.23 (m, 2H), 4.83 – 4.62 (m, 2H), 4.49 – 4.35 (m, 1H), 3.38 (m, 1H), 1.99 (m, 1H), 1.85 – 1.09 (m, 9H), 0.98 (m, 2H). ^{13}C NMR (101 MHz, CDCl_3) δ 154.6, 154.1, 136.9, 132.5, 118.5, 116.6, 95.9, 78.1, 77.4, 74.7, 74.6, 55.1, 54.5, 40.9, 40.0, 29.4, 29.0, 28.7, 26.4, 26.3, 26.1, 25.9, 25.9, 25.8. HRMS (ESI/QTOF) m/z : $[\text{M} + \text{Na}]^+$ Calcd for $\text{C}_{13}\text{H}_{20}\text{Cl}_3\text{NNaO}_3^+$ 366.0401; Found 366.0402.



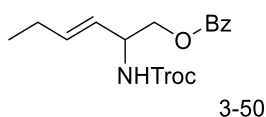
2,2,2-Trichloroethyl (1-*t*-butyl-1-hydroxybut-3-en-2-yl)carbamate, synthesized via 3-CP1, colorless liquid, 11.4 mg (Yield =36%), dr= 2.2:1. ^1H NMR (400 MHz, CDCl_3) δ 6.03 – 5.80 (m, 1H), 5.61 (m, 1H), 5.39 – 5.15 (m, 2H), 4.88 – 4.61 (m, 2H), 4.52 – 4.36 (m, 1H), 3.30-3.50 (s, 1H), 1.83 (s, 1H), 0.99 (s, 9H). ^{13}C NMR (101 MHz, CDCl_3) δ 154.0, 153.8, 138.4, 134.0, 118.4, 115.5, 95.8, 81.5, 79.7, 74.7, 74.6, 55.6, 53.3, 35.2, 34.9, 26.7, 26.5. HRMS (ESI/QTOF) m/z : $[\text{M} + \text{Na}]^+$ Calcd for $\text{C}_{11}\text{H}_{18}\text{Cl}_3\text{NNaO}_3^+$ 340.0244; Found 340.0240.



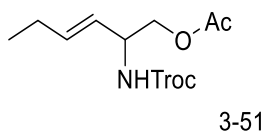
2,2,2-trichloroethyl (1-hydroxy-3-methylbut-3-en-2-yl)carbamate, synthesized via modified 3-CP2 (acetone as solvent), white solid, 13.0 mg (Yield =47%). ^1H NMR (400 MHz, CDCl_3) δ 5.65 – 5.43 (m, 1H), 5.06 – 5.02 (s, 1H), 5.01 – 4.96 (s, 1H), 4.77 (d, J = 12.0 Hz, 1H), 4.70 (d, J = 12.1 Hz, 1H), 4.21 (m, 1H), 3.77 (m, 2H), 1.82 (s, 3H), 1.73 (b, 1H). ^{13}C NMR (101 MHz, CDCl_3) δ 154.5, 141.9, 113.0, 95.6, 74.7, 63.1, 57.9, 20.5. HRMS (ESI/QTOF) m/z : $[\text{M} + \text{Na}]^+$ Calcd for $\text{C}_8\text{H}_{12}\text{Cl}_3\text{NNaO}_3^+$ 297.9775; Found 297.9779.



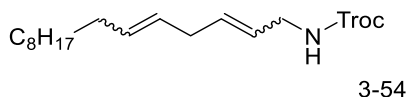
2,2,2-Trichloroethyl (E)-(1-((4-methylphenyl)sulfonamido)oct-3-en-2-yl)carbamate, synthesized via 3-CP1, yellowish oil, 22.2 mg (Yield = 47%). ^1H NMR (400 MHz, CDCl_3) δ 7.74 (d, J = 8.4 Hz, 2H), 7.31 (d, J = 8.2 Hz, 2H), 5.66 (dtd, J = 15.1, 6.7, 1.4 Hz, 1H), 5.34 – 5.22 (m, 2H), 4.95 – 4.83 (m, 1H), 4.80 – 4.56 (m, 2H), 4.26 – 4.18 (m, 1H), 3.15 (ddd, J = 11.7, 7.0, 4.8 Hz, 1H), 3.05 (dt, J = 12.9, 6.3 Hz, 1H), 2.43 (s, 3H), 2.00 (q, J = 6.8 Hz, 2H), 1.38 – 1.20 (m, 4H), 0.91 – 0.83 (m, 3H). ^{13}C NMR (101 MHz, CDCl_3) δ 154.4, 143.8, 136.9, 135.2, 130.0, 127.2, 125.7, 95.6, 74.7, 52.6, 47.0, 32.0, 31.1, 22.3, 21.7, 14.0. HRMS (ESI/QTOF) m/z : $[\text{M} + \text{Na}]^+$ Calcd for $\text{C}_{18}\text{H}_{25}\text{Cl}_3\text{N}_2\text{NaSO}_4^+$ 493.0493; Found 493.0499.



(E)-2-(Troc-amino)hex-3-en-1-yl benzoate, synthesized via 3-CP2, colorless oil, 11.4 mg (Yield = 29%). ^1H NMR (400 MHz, CDCl_3) δ 8.02 (d, J = 7.6 Hz, 2H), 7.57 (t, J = 7.4 Hz, 1H), 7.44 (t, J = 7.7 Hz, 2H), 5.94 – 5.78 (m, 1H), 5.46 (dd, J = 15.5, 6.2, 1H), 5.25 (s, 1H), 4.82 – 4.59 (m, 3H), 4.39 (d, J = 5.8 Hz, 2H), 2.08 (p, J = 7.1 Hz, 2H), 0.98 (t, J = 7.4 Hz, 3H). ^{13}C NMR (101 MHz, CDCl_3) δ 166.5, 154.0, 136.1, 133.3, 129.7, 128.5, 124.3, 95.5, 74.5, 66.2, 52.4, 25.4, 13.3. HRMS (ESI/QTOF) m/z : $[\text{M} + \text{Na}]^+$ Calcd for $\text{C}_{16}\text{H}_{18}\text{Cl}_3\text{NNaO}_4^+$ 416.0194; Found 416.0194.

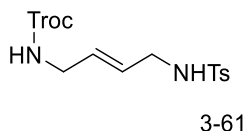


(E)-2-(Troc-amino)hex-3-en-1-yl acetate, synthesized via 3-CP2, colorless oil, 8.7 mg (Yield = 26%). ^1H NMR (400 MHz, CDCl_3) δ 5.78 (dt, J = 16.5, 6.5 Hz, 1H), 5.37 (dd, J = 15.6, 6.2 Hz, 1H), 5.21 – 5.12 (m, 1H), 4.73 (s, 2H), 4.45 (m, 1H), 4.13 (d, J = 5.4 Hz, 2H), 2.07 (m, 5H), 0.98 (t, J = 7.4 Hz, 3H). ^{13}C NMR (101 MHz, CDCl_3) δ 171.1, 154.1, 136.0, 124.4, 95.7, 74.7, 65.9, 52.4, 25.4, 20.9, 13.4. HRMS (ESI/QTOF) m/z : $[\text{M} + \text{Na}]^+$ Calcd for $\text{C}_{11}\text{H}_{16}\text{Cl}_3\text{NNaO}_4^+$ 354.0037; Found 354.0039.

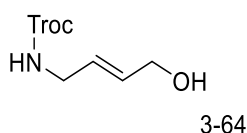


2,2,2-Trichloroethyl pentadeca-2,5-dien-1-ylcarbamate, synthesized via 3-CP2, colorless oil, 16.1 mg (Yield = 40%), as mixture of stereoisomers 3.7:1. ^1H NMR (400 MHz, CDCl_3) δ 5.72 – 5.55 (m, 1H), 5.53 – 5.31 (m, 3H), 4.97 (s, 1H), 4.73 (s, 2H), 3.93 – 3.77 (m, 2H), 2.82 – 2.68 (m, 2H), 1.98 (m, 2H), 1.38 – 1.24 (m, 14H), 0.92 – 0.84 (m, 3H). For the major isomer, ^{13}C NMR (101 MHz, CDCl_3) δ 154.5,

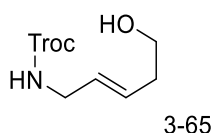
132.7, 132.3, 127.3, 125.8, 95.8, 74.7, 43.3, 35.3, 32.7, 32.1, 29.7, 29.7, 29.7, 29.6, 29.5, 29.4, 22.8, 14.3. HRMS (ESI/QTOF) m/z : $[M + Na]^+$ Calcd for $C_{18}H_{30}Cl_3NNaO_2^+$ 420.1234; Found 420.1244.



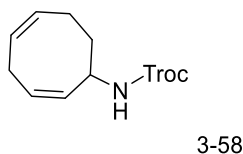
2,2,2-Trichloroethyl (E)-4-((4-methylphenyl)sulfonamido)but-2-en-1-yl carbamate, synthesized via 3-CP2, colorless oil, 11.6 mg (Yield = 28%). 1H NMR (400 MHz, $CDCl_3$) δ 7.77 – 7.71 (m, 2H), 7.35 – 7.28 (m, 2H), 5.67 – 5.49 (m, 2H), 5.01 (s, 1H), 4.71 (s, 2H), 4.61 (s, 1H), 3.76 (t, J = 5.6 Hz, 2H), 3.60 (t, J = 6.4 Hz, 2H), 2.44 (s, 3H). ^{13}C NMR (101 MHz, $CDCl_3$) δ 154.5, 143.8, 137.1, 129.9, 129.4, 127.6, 127.3, 95.6, 74.7, 44.7, 42.5, 21.7. HRMS (ESI/QTOF) m/z : $[M + H]^+$ Calcd for $C_{14}H_{18}Cl_3N_2O_4S^+$ 415.0047; Found 415.0052.



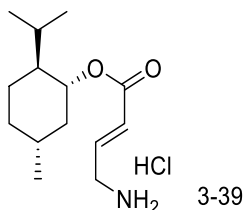
2,2,2-Trichloroethyl (E)-4-hydroxybut-2-en-1-yl carbamate, synthesized via 3-CP2, colorless oil, 18.5 mg (Yield = 70%). 1H NMR (400 MHz, $CDCl_3$) δ 5.83 (dt, J = 15.8, 5.1 Hz, 1H), 5.74 (dt, J = 15.6, 5.5 Hz, 1H), 5.22 (s, 1H), 4.72 (s, 2H), 4.15 (d, J = 5.0 Hz, 2H), 3.85 (d, J = 5.8 Hz, 2H), 1.83 (s, 1H). ^{13}C NMR (101 MHz, $CDCl_3$) δ 154.6, 131.6, 127.1, 95.7, 74.7, 62.8, 42.7. HRMS (ESI/QTOF) m/z : $[M + Na]^+$ Calcd for $C_7H_{10}Cl_3NNaO_3^+$ 283.9618; Found 283.9628.



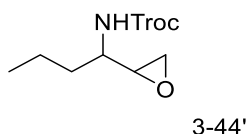
2,2,2-Trichloroethyl (E)-5-hydroxypent-2-en-1-yl carbamate, synthesized via 3-CP2, colorless oil, 4.0 mg (Yield = 14%). 1H NMR (400 MHz, $CDCl_3$) δ 5.63 (m, 2H), 5.09 (s, 1H), 4.73 (s, 2H), 3.83 (t, J = 5.7 Hz, 2H), 3.67 (t, J = 6.2 Hz, 2H), 2.31 (q, J = 6.3 Hz, 2H), 1.57 (s, 1H). ^{13}C NMR (101 MHz, $CDCl_3$) δ 154.6, 129.8, 128.6, 95.7, 74.7, 61.9, 43.2, 35.7. HRMS (ESI/QTOF) m/z : $[M + Na]^+$ Calcd for $C_8H_{12}Cl_3NNaO_3^+$ 297.9775; Found 297.9784.



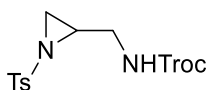
2,2,2-Trichloroethyl (E)-(5-hydroxypent-2-en-1-yl)carbamate, synthesized via 3-CP1, colorless oil, 3.2 mg (Yield = 11%). ^1H NMR (400 MHz, CDCl_3) δ 5.82 – 5.64 (m, 2H), 5.59 – 5.43 (m, 1H), 5.22 – 5.12 (m, 1H), 5.00 (s, 1H), 4.88 (m, 1H), 4.71 (s, 2H), 3.04 – 2.78 (m, 2H), 2.66 – 2.52 (m, 1H), 2.06 (m, 1H), 1.85 (m, 1H), 1.40 – 1.28 (m, 1H). HRMS (ESI/QTOF) m/z : $[\text{M} + \text{H}]^+$ Calcd for $\text{C}_{11}\text{H}_{15}\text{Cl}_3\text{NO}_2^+$ 298.0163; Found 298.0168.



(1R,2S,5R)-2-Isopropyl-5-methylcyclohexyl (E)-4-aminobut-2-enoate hydrochloride. 0.2 mmol **3w** and 2 mmol Zn powder were added to 2 mL acetic acid. The reaction was stirred for 24 h at room temperature. The reaction solution was filtered on a thin paddle of celite, which was then washed with MeOH. The collected filtrate was evaporated, redissolved with Et_2O and washed with a K_2CO_3 aqueous solution. The organic phase was dried and evaporated to 2 mL, and then 0.2 mL HCl (4 M in dioxane) was added. **4w** was obtained as a white solid, 46.8 mg, 85%. ^1H NMR (400 MHz, CDCl_3) δ 8.75 – 8.47 (b, 3H), 7.01 (dt, $J = 15.8, 5.9$ Hz, 1H), 6.20 (d, $J = 15.8$ Hz, 1H), 4.78 – 4.67 (m, 1H), 3.89 (m, 2H), 2.02 – 1.93 (m, 1H), 1.84 (pd, $J = 7.1, 2.7$ Hz, 1H), 1.73 – 1.61 (m, 2H), 1.53 – 1.33 (m, 2H), 1.12 – 0.96 (m, 2H), 0.92 – 0.84 (m, 7H), 0.73 (dd, $J = 7.0, 2.0$ Hz, 3H). ^{13}C NMR (101 MHz, CDCl_3) δ 165.5, 138.0, 126.4, 75.2, 47.1, 41.0, 40.5, 34.3, 31.5, 26.3, 23.5, 22.2, 20.9, 16.5. HRMS (ESI/QTOF) m/z : $[\text{M} + \text{H}]^+$ Calcd for $\text{C}_{14}\text{H}_{26}\text{NO}_2^+$ 240.1958; Found 240.1955.

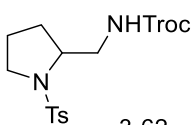


2,2,2-Trichloroethyl (1-(oxiran-2-yl)butyl)carbamate, synthesized via 3-CP1, colorless oil, dr= 1:1. ^1H NMR (400 MHz, CDCl_3) δ 5.05 – 4.81 (m, 1H), 4.80 – 4.59 (m, 2H), 1.77 – 1.58 (m, 2H), 1.47 (m, 2H), 0.95 (t, $J = 7.2$ Hz, 3H). For the details of hydrogens on epoxy group please see the attached spectrum. ^{13}C NMR (101 MHz, CDCl_3) δ 154.7, 154.5, 95.7, 74.7, 74.6, 53.9, 53.5, 52.8, 50.0, 46.0, 44.4, 35.6, 33.7, 19.1, 18.9, 14.0, 13.9. HRMS (ESI/QTOF) m/z : $[\text{M} + \text{H}]^+$ Calcd for $\text{C}_9\text{H}_{14}\text{Cl}_3\text{NNaO}_3^+$ 311.9931; Found 311.9928.



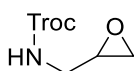
3-60

2,2,2-Trichloroethyl ((1-tosylaziridin-2-yl)methyl)carbamate, synthesized via 3-CP2, colorless oil, 18.0 mg (Yield = 45%). ^1H NMR (400 MHz, CDCl_3) δ 7.82 (d, J = 7.9 Hz, 2H), 7.36 (d, J = 7.9 Hz, 2H), 5.00 (t, J = 6.2 Hz, 1H), 4.68 (m, 2H), 3.60 (ddd, J = 14.7, 6.4, 3.6 Hz, 1H), 3.18 (dt, J = 14.6, 6.1 Hz, 1H), 2.96 (tt, J = 7.0, 4.0 Hz, 1H), 2.66 (d, J = 7.0 Hz, 1H), 2.45 (s, 3H), 2.21 (d, J = 4.5 Hz, 1H). ^{13}C NMR (101 MHz, CDCl_3) δ 154.6, 145.1, 134.6, 130.0, 128.1, 95.5, 74.7, 41.5, 38.4, 31.7, 21.8. HRMS (ESI/QTOF) m/z : $[\text{M} + \text{H}]^+$ Calcd for $\text{C}_{13}\text{H}_{16}\text{Cl}_3\text{N}_2\text{O}_4\text{S}^+$ 400.9891; Found 400.9889.



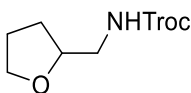
3-62

2,2,2-Trichloroethyl ((1-tosylpyrrolidin-2-yl)methyl)carbamate, synthesized via 3-CP2, colorless oil, 28.0 mg (Yield = 65%). ^1H NMR (400 MHz, CDCl_3) δ 7.72 (dd, J = 8.3, 2.0 Hz, 2H), 7.33 (d, J = 7.8 Hz, 2H), 5.79 (t, J = 6.0 Hz, 1H), 4.84 – 4.67 (m, 2H), 3.74 – 3.63 (m, 1H), 3.51 – 3.32 (m, 3H), 3.27 – 3.08 (m, 1H), 2.43 (s, 3H), 1.86 – 1.57 (m, 3H), 1.47 (dt, J = 12.4, 6.2 Hz, 1H). ^{13}C NMR (101 MHz, CDCl_3) δ 155.3, 144.0, 133.9, 130.0, 127.8, 95.8, 74.6, 59.8, 49.9, 45.6, 29.7, 24.2, 21.7. HRMS (ESI/QTOF) m/z : $[\text{M} + \text{H}]^+$ Calcd for $\text{C}_{15}\text{H}_{20}\text{Cl}_3\text{N}_2\text{O}_4\text{S}^+$ 429.0204; Found 429.0205.



3-63

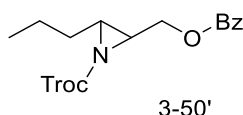
2,2,2-Trichloroethyl (oxiran-2-yl)methyl carbamate, synthesized via 3-CP2, colorless oil, 12.7 mg (Yield = 51%). ^1H NMR (400 MHz, CDCl_3) δ 5.20 (s, 1H), 4.83 – 4.66 (m, 2H), 3.67 (ddd, J = 14.8, 6.1, 3.0 Hz, 1H), 3.33 (ddd, J = 14.7, 6.3, 5.1 Hz, 1H), 3.14 (ddt, J = 5.4, 3.8, 2.8 Hz, 1H), 2.82 (t, J = 4.3 Hz, 1H), 2.64 (dd, J = 4.6, 2.6 Hz, 1H). ^{13}C NMR (101 MHz, CDCl_3) δ 154.9, 95.6, 74.8, 50.5, 45.1, 42.4. HRMS (ESI/QTOF) m/z : $[\text{M} + \text{Na}]^+$ Calcd for $\text{C}_6\text{H}_8\text{Cl}_3\text{NNaO}_3^+$ 269.9462; Found 269.9463.



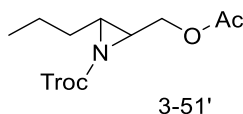
3-65'

2,2,2-Trichloroethyl ((tetrahydrofuran-2-yl)methyl)carbamate, synthesized via 3-CP2, colorless oil, 17.2mg (Yield = 62%). ^1H NMR (400 MHz, CDCl_3) δ 5.41 (s, 1H), 4.81 – 4.62 (m, 2H), 3.99 (qd, J = 6.9,

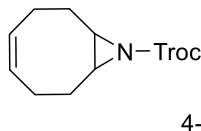
3.3 Hz, 1H), 3.92 – 3.82 (m, 1H), 3.80 – 3.70 (m, 1H), 3.48 (ddd, $J = 13.9, 6.7, 3.4$ Hz, 1H), 3.18 (ddd, $J = 13.1, 7.1, 5.3$ Hz, 1H), 2.11 – 1.83 (m, 3H), 1.64 – 1.49 (m, 1H). ^{13}C NMR (101 MHz, CDCl_3) δ 154.9, 95.7, 77.7, 74.7, 68.3, 45.1, 28.6, 26.0. HRMS (ESI/QTOF) m/z : $[\text{M} + \text{Na}]^+$ Calcd for $\text{C}_8\text{H}_{12}\text{Cl}_3\text{NNaO}_3^+$ 297.9775; Found 297.9783.



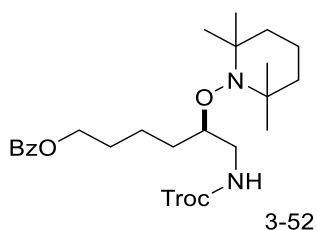
2,2,2-Trichloroethyl 2-((benzyloxy)methyl)-3-propylaziridine-1-carboxylate, synthesized via 3-CP2, colorless oil, 13.7mg (Yield = 35%). ^1H NMR (400 MHz, CDCl_3) δ 8.15 – 7.99 (m, 2H), 7.62 – 7.53 (m, 1H), 7.45 (t, $J = 7.8$ Hz, 2H), 4.78 – 4.65 (m, 2H), 4.61 – 4.44 (m, 2H), 2.78 (q, $J = 4.5$ Hz, 1H), 2.68 (td, $J = 6.3, 3.3$ Hz, 1H), 1.82 (ddt, $J = 14.3, 8.9, 5.6$ Hz, 1H), 1.61 – 1.49 (m, 2H), 1.42 – 1.31 (m, 1H), 0.98 (t, $J = 7.4$ Hz, 3H). ^{13}C NMR (101 MHz, CDCl_3) δ 166.1, 159.6, 133.5, 129.9, 129.6, 128.6, 94.9, 63.0, 42.2, 41.9, 33.0, 20.3, 13.8. HRMS (ESI/QTOF) m/z : $[\text{M} + \text{H}]^+$ Calcd for $\text{C}_{16}\text{H}_{19}\text{Cl}_3\text{NO}_4^+$ 394.0374; Found 394.0373.



2,2,2-Trichloroethyl 2-(acetoxymethyl)-3-propylaziridine-1-carboxylate, synthesized via 3-CP2, colorless oil, 10.6 mg (Yield = 32%). ^1H NMR (400 MHz, CDCl_3) δ 4.74 (s, 2H), 4.33 – 4.16 (m, 2H), 2.64 (td, $J = 5.0, 3.3$ Hz, 1H), 2.54 (ddd, $J = 6.9, 5.6, 3.3$ Hz, 1H), 2.07 (s, 3H), 1.79 (ddt, $J = 14.4, 8.8, 5.6$ Hz, 1H), 1.60 – 1.43 (m, 2H), 1.35 – 1.24 (m, 1H), 0.97 (t, $J = 7.4$ Hz, 3H). ^{13}C NMR (101 MHz, CDCl_3) δ 170.6, 159.6, 94.9, 75.7, 63.0, 42.5, 41.6, 32.9, 20.9, 20.3, 13.8. HRMS (ESI/QTOF) m/z : $[\text{M} + \text{Na}]^+$ Calcd for $\text{C}_{11}\text{H}_{16}\text{Cl}_3\text{NNaO}_4^+$ 354.0037; Found 354.0039.

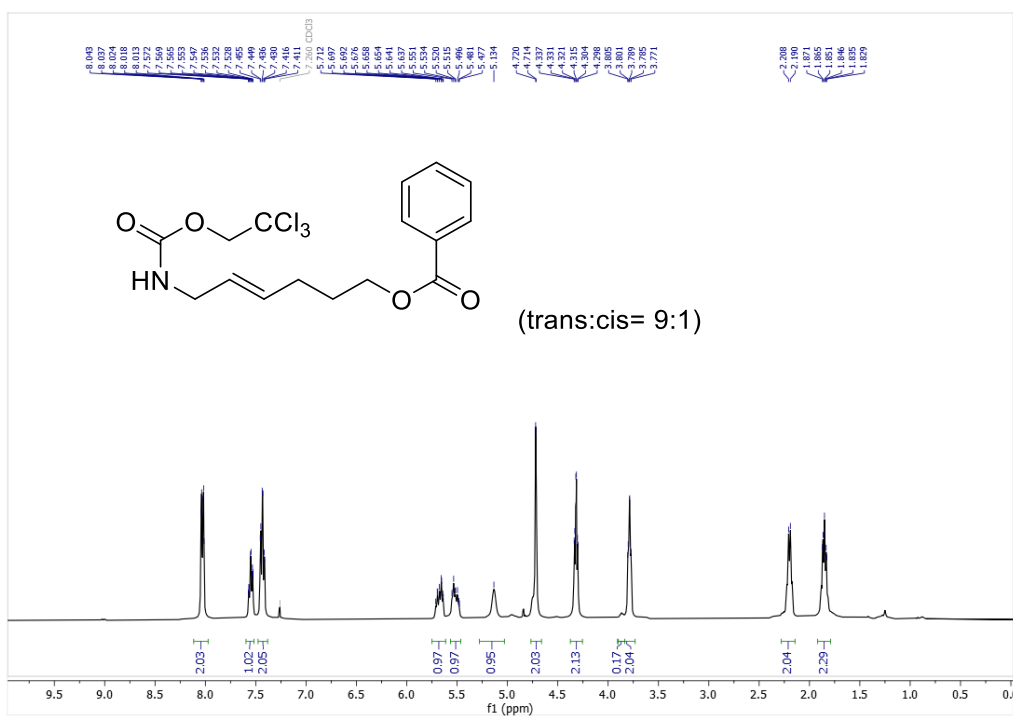
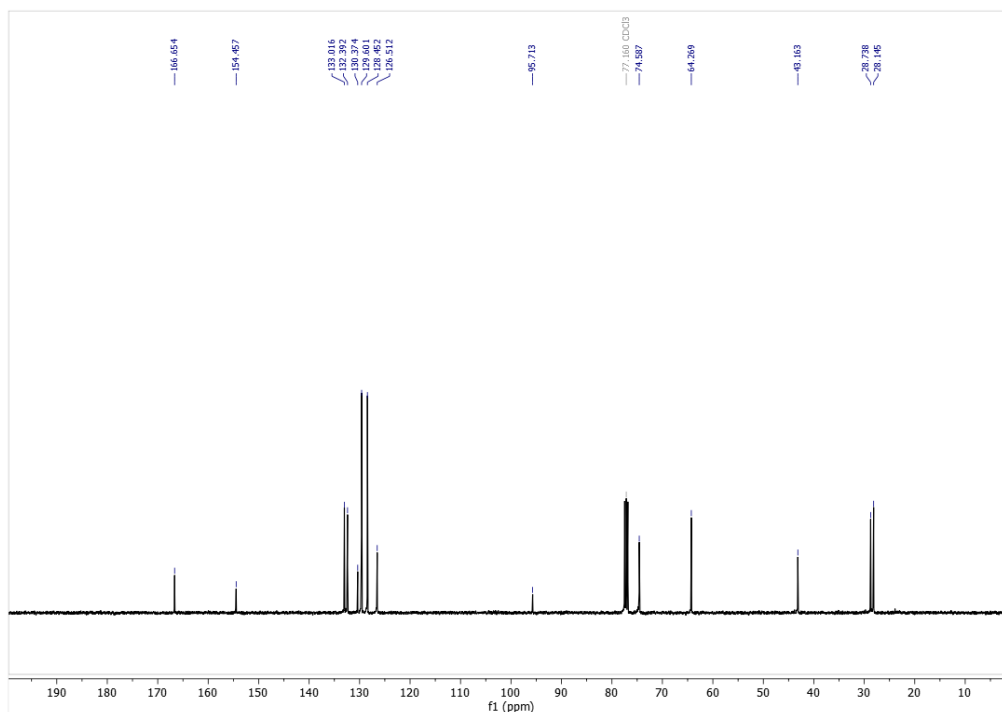


2,2,2-Trichloroethyl 2-(acetoxymethyl)-3-propylaziridine-1-carboxylate, synthesized via 3-CP1, colorless oil, 17.0 mg (Yield = 57%). ^1H NMR (400 MHz, CDCl_3) δ 5.79 – 5.67 (m, 2H), 4.82 (d, $J = 12.0$ Hz, 1H), 4.68 (d, $J = 11.9$ Hz, 1H), 2.42 – 2.15 (m, 8H), 1.20 – 1.06 (m, 2H). ^{13}C NMR (101 MHz, CDCl_3) δ 160.5, 130.6, 95.2, 75.4, 45.0, 27.9, 25.8. HRMS (ESI/QTOF) m/z : $[\text{M} + \text{H}]^+$ Calcd for $\text{C}_{11}\text{H}_{15}\text{Cl}_3\text{NO}_2^+$ 298.0163; Found 298.0167.



(R)-5-TEMPO-6-(Troc-amino)hexyl benzoate, synthesized via 3-CP2 (with addition of 1 equiv. of TEMPO), colorless oil, 9.3 mg (Yield = 17%). ^1H NMR (400 MHz, CDCl_3) δ 8.04 (dt, J = 7.0, 1.5 Hz, 2H), 7.60 – 7.51 (m, 1H), 6.98 – 6.81 (m, 1H), 4.80 – 4.65 (m, 2H), 4.33 (t, J = 6.5 Hz, 2H), 4.13 – 4.03 (m, 1H), 3.50 (ddd, J = 14.1, 7.8, 3.1 Hz, 1H), 3.36 (ddd, J = 14.1, 8.2, 3.1 Hz, 1H), 1.86 – 1.66 (m, 4H), 1.52 – 1.02 (m, 20H). ^{13}C NMR (101 MHz, CDCl_3) δ 166.8, 154.6, 133.0, 130.6, 129.7, 128.5, 96.0, 79.8, 74.5, 64.9, 61.1, 60.0, 46.1, 40.7, 40.3, 34.6, 33.2, 32.0, 29.1, 22.5, 20.7, 17.3. HRMS (ESI/QTOF) m/z : $[\text{M} + \text{H}]^+$ Calcd for $\text{C}_{25}\text{H}_{38}\text{Cl}_3\text{N}_2\text{O}_5^+$ 551.1841; Found 551.1849

3.7.6 NMR spectra of 3-13 (an example of the products)

 ^1H -NMR spectrum of 3-13 ^{13}C -NMR spectrum of 3-13

References

- [1] McDonald, R. I.; Liu, G. S.; Stahl, S. S. Palladium(II)-Catalyzed Alkene Functionalization via Nucleopalladation: Stereochemical Pathways and Enantioselective Catalytic Applications. *Chem. Rev.* **2011**, *111*, 2981-3019.
- [2] Chemler, S. R.; Karyakarte, S. D.; Khoder, Z. M. Stereoselective and Regioselective Synthesis of Heterocycles via Copper-Catalyzed Additions of Amine Derivatives and Alcohols to Alkenes. *J. Org. Chem.* **2017**, *82*, 11311-11325.
- [3] Lee, J. H.; Choi, S.; Hong, K. B. Alkene Difunctionalization Using Hypervalent Iodine Reagents: Progress and Developments in the Past Ten Years. *Molecules* **2019**, *24*.
- [4] Johannsen, M.; Jorgensen, K. A. Allylic amination. *Chem. Rev.* **1998**, *98*, 1689-1708.
- [5] Shen, Y.; Liang, W. J.; Shi, Y. N.; Kennelly, E. J.; Zhao, D. K. Structural diversity, bioactivities, and biosynthesis of natural diterpenoid alkaloids. *Nat. Prod. Rep.* **2020**, *37*, 763-796.
- [6] Vitaku, E.; Smith, D. T.; Njardarson, J. T. Analysis of the Structural Diversity, Substitution Patterns, and Frequency of Nitrogen Heterocycles among U.S. FDA Approved Pharmaceuticals. *J. Med. Chem.* **2014**, *57*, 10257-10274.
- [7] Qi, X. T.; Kohler, D. G.; Hull, K. L.; Liu, P. Energy Decomposition Analyses Reveal the Origins of Catalyst and Nucleophile Effects on Regioselectivity in Nucleopalladation of Alkenes. *J. Am. Chem. Soc.* **2019**, *141*, 11892-11904.
- [8] Brice, J. L.; Harang, J. E.; Timokhin, V. I.; Anastasi, N. R.; Stahl, S. S. Aerobic oxidative amination of unactivated alkenes catalyzed by palladium. *J. Am. Chem. Soc.* **2005**, *127*, 2868-2869.
- [9] Kohler, D. G.; Gockel, S. N.; Kennemur, J. L.; Waller, P. J.; Hull, K. L. Palladium-catalysed anti-Markovnikov selective oxidative amination. *Nat. Chem.* **2018**, *10*, 333-340.
- [10] Liu, G. S.; Yin, G. Y.; Wu, L. Palladium-catalyzed intermolecular aerobic oxidative amination of terminal alkenes: Efficient synthesis of linear allylamine derivatives. *Angew. Chem. Int. Ed.* **2008**, *47*, 4733-4736.
- [11] Ma, R. L.; White, M. C. C-H to C-N Cross-Coupling of Sulfonamides with Olefins. *J. Am. Chem. Soc.* **2018**, *140*, 3202-3205.
- [12] Reed, S. A.; White, M. C. Catalytic intermolecular linear allylic C-H amination via heterobimetallic catalysis. *J. Am. Chem. Soc.* **2008**, *130*, 3316.
- [13] Dolan, N. S.; Scamp, R. J.; Yang, T.; Berry, J. F.; Schomaker, J. M. Catalyst-Controlled and Tunable, Chemoselective Silver-Catalyzed Intermolecular Nitrene Transfer: Experimental and Computational Studies. *J. Am. Chem. Soc.* **2016**, *138*, 14658-14667.
- [14] Liang, C. G.; Collet, F.; Robert-Peillard, F.; Muller, P.; Dodd, R. H.; Dauban, P. Toward a synthetically useful stereoselective C-H amination of hydrocarbons. *J. Am. Chem. Soc.* **2008**, *130*, 343-350.
- [15] Knecht, T.; Mondal, S.; Ye, J. H.; Das, M.; Glorius, F. Intermolecular, Branch-Selective, and Redox-Neutral Cp*Ir-III-Catalyzed Allylic C-H Amidation. *Angew. Chem. Int. Ed.* **2019**, *58*, 7117-7121.

- [16] Blakemore, D. C.; Castro, L.; Churcher, I.; Rees, D. C.; Thomas, A. W.; Wilson, D. M.; Wood, A. Organic synthesis provides opportunities to transform drug discovery. *Nat. Chem.* **2018**, *10*, 383-394.
- [17] Cheng, Q.; Chen, J. T.; Lin, S. Y.; Ritter, T. Allylic Amination of Alkenes with Iminothianthrenes to Afford Alkyl Allylamines. *J. Am. Chem. Soc.* **2020**, *142*, 17287-17293.
- [18] An, X. D.; Jiao, Y. Y.; Zhang, H.; Gao, Y. X.; Yu, S. Y. Photoredox-Induced Radical Relay toward Functionalized beta-Amino Alcohol Derivatives. *Org. Lett.* **2018**, *20*, 401-404.
- [19] Davies, J.; Morcillo, S. P.; Douglas, J. J.; Leonori, D. Hydroxylamine Derivatives as Nitrogen-Radical Precursors in Visible-Light Photochemistry. *Chem.-Eur. J.* **2018**, *24*, 12154-12163.
- [20] Jiang, H.; Studer, A. Amidyl Radicals by Oxidation of alpha-Amido-oxy Acids: Transition-Metal-Free Amidofluorination of Unactivated Alkenes. *Angew. Chem. Int. Ed.* **2018**, *57*, 10707-10711.
- [21] Jiang, H.; Studer, A. Transition-Metal-Free Three-Component Radical 1,2-Amidoalkynylation of Unactivated Alkenes. *Chem.-Eur. J.* **2019**, *25*, 516-520.
- [22] Dai, G. L.; Lai, S. Z.; Luo, Z. Z.; Tang, Z. Y. Selective Syntheses of Z-Alkenes via Photocatalyzed Decarboxylative Coupling of N-Hydroxyphthalimide Esters with Terminal Arylalkynes. *Org. Lett.* **2019**, *21*, 2269-2272.
- [23] Zhou, Q. Q.; Zou, Y. Q.; Lu, L. Q.; Xiao, W. J. Visible-Light-Induced Organic Photochemical Reactions through Energy-Transfer Pathways. *Angew. Chem. Int. Ed.* **2019**, *58*, 1586-1604.
- [24] Shang, T. Y.; Lu, L. H.; Cao, Z.; Liu, Y.; He, W. M.; Yu, B. Recent advances of 1,2,3,5-tetrakis(carbazol-9-yl)-4,6-dicyanobenzene (4CzIPN) in photocatalytic transformations. *Chem. Commun.* **2019**, *55*, 5408-5419.
- [25] Wu, X. S.; Riedel, J.; Dong, V. M. Transforming Olefins into gamma,delta-Unsaturated Nitriles through Copper Catalysis. *Angew. Chem. Int. Ed.* **2017**, *56*, 11589-11593.
- [26] Tamura, Y.; Hisamatsu, Y.; Kumar, S.; Itoh, T.; Sato, K.; Kuroda, R.; Aoki, S. Efficient Synthesis of Tris-Heteroleptic Iridium(III) Complexes Based on the Zn²⁺-Promoted Degradation of Tris-Cyclometalated Iridium(III) Complexes and Their Photophysical Properties. *Inorg. Chem.* **2017**, *56*, 812-833.
- [27] Tamayo, A. B.; Alleyne, B. D.; Djurovich, P. I.; Lamansky, S.; Tsyba, I.; Ho, N. N.; Bau, R.; Thompson, M. E. Synthesis and characterization of facial and meridional tris-cyclometalated iridium(III) complexes. *J. Am. Chem. Soc.* **2003**, *125*, 7377-7387.
- [28] Qin, Q. X.; Han, Y. Y.; Jiao, Y. Y.; He, Y. Y.; Yu, S. Y. Photoredox-Catalyzed Diamidation and Oxidative Amidation of Alkenes: Solvent-Enabled Synthesis of 1,2-Diamides and alpha-Amino Ketones. *Org. Lett.* **2017**, *19*, 2909-2912.
- [29] Arias-Rotondo, D. M.; McCusker, J. K. The photophysics of photoredox catalysis: a roadmap for catalyst design. *Chem. Soc. Rev.* **2016**, *45*, 5803-5820.

Chapter 4 Decarboxylative coupling of aliphatic acids with polyfluoroaryl nucleophiles by dual photoredox and copper catalysis

4.1 Background

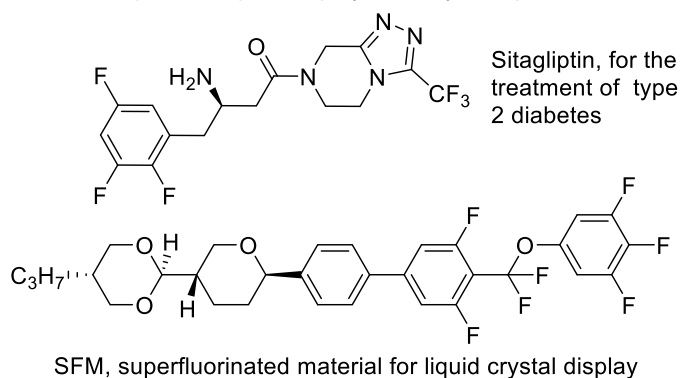
Polyfluoroarenes can form special intermolecular interactions^[1-3], such as π - π_F and anion- π_F interactions, which lead to widespread applications in pharmaceuticals^[4-5] and materials.^[1, 7, 8] For example, polyfluoroaryl structure could be found in Sitagliptin, which is used for the treatment of type 2 diabetes, and also in some materials for liquid crystal display (Scheme 4.1a). The synthesis of functionalized polyfluoroarenes from easily available simple polyfluoroarenes has drawn much recent attention. Strategies such as S_NAr reaction^[9-12] on polyfluoroarenes, reactions via polyfluoroaryl radicals,^[13-15] and radical addition to polyfluoroarenes^[16] have been reported. However, these strategies require highly electron-deficient polyfluoroarenes, which makes them unsuitable for arenes with a lower F-content. Metal catalyzed C-C cross-coupling of polyfluoroaryl reagents, on the other hand, provides a more general and versatile approach to the synthesis of polyfluoroaryl compounds (Scheme 4.1b).^[17-20] A $M-Ar_F$ species could be formed from $X-Ar_F$, $H-Ar_F$ or polyfluoroaryl metallic reagent, and subsequent reductive elimination from the metal forges a new C-C bond.

Many examples for the coupling of polyfluoroaryls with aryls,^[21-23] alkenyls,^[24-26] alkynyls,^[27] benzyls^[28-30] and allyls^[31-33] have been reported. However, the coupling of polyfluoroaryls with unactivated alkyl groups^[34-35] remains challenging, possibly due to the difficulty in the reductive elimination step as a result of a strong $M-Ar_F$ bond^[36, 37] and the facile β -H elimination reaction from many M-alkyl intermediates as an influential side reaction. In an important development, Chang and co-workers reported a Cu-catalyzed method for the oxidative coupling of polyfluoroarenes with alkanes (Scheme 4.1c).^[34] This reaction involves the *tert*-butoxide-assisted C-H metalation of a polyfluoroarene to form an $Cu^{II}-Ar_F$ species, which captured an alkyl radical to effect the coupling. Despite the advance, arenes with a low F-content (e.g. 2F and 3F) were not suitable substrates, likely

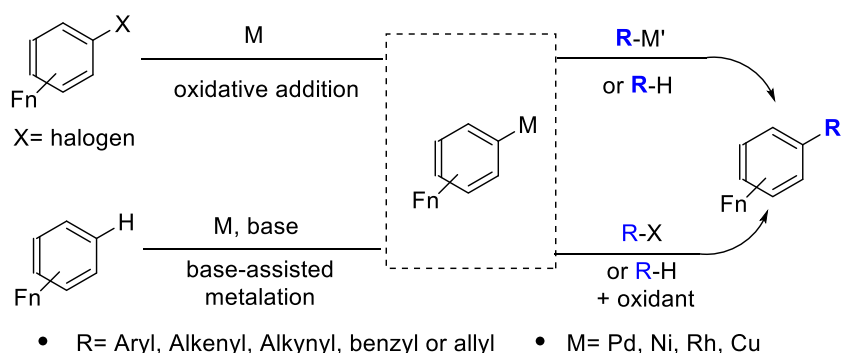
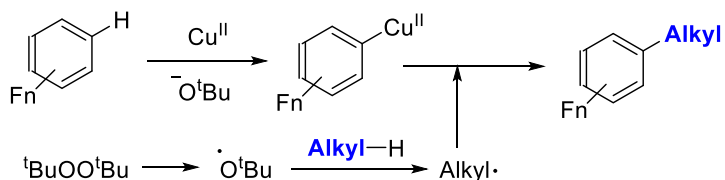
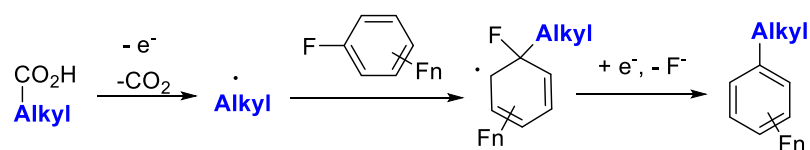
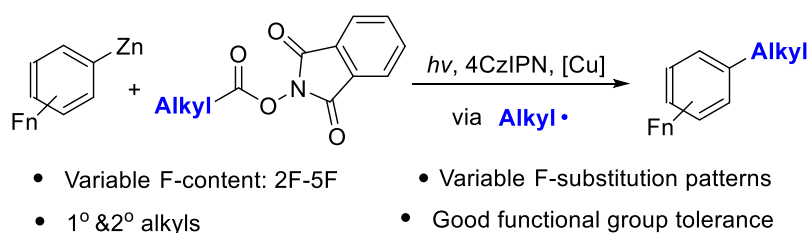
because the corresponding Ar_F-H bonds were less acidic and resistant to base-assisted C-H metalation. The use of a strong base and a peroxide oxidant also limited the tolerance for functional groups. The group of Ritter recently developed decarboxylative polyfluoroarylation of alkyl carboxylic acids based on radical addition to polyfluoroarenes followed by the elimination of ipso-fluorine (Scheme 4.1d).^[16] This novel method still has some limitations such as regioselectivity of radical addition as well as limited scope for F-substitution. The method was less efficient for polyfluoroarenes with 4F and not suitable for those with 3F or less.

Here, we describe a metallophotoredox approach ^[38-40] for the coupling of Ar_F-Zn reagents with aliphatic NHPI esters derived from alkylcarboxylic acids (Scheme 4.1e). Unlike their unstable Lithium and Grignard analogues ^[41, 42], the Ar_F-Zn reagents ^[43] are more stable and less reactive, which makes them easier to handle and makes the reaction more tolerant for functional groups. Using these preformed reagents, we were able to install Ar_F groups with a wide range of F-content (2F -5F) and with varied F-substitution patterns. Although the coupling reaction of NHPI esters is well established with many organometallic reagents,^[44-47] such coupling with weakly nucleophilic Ar_F-Zn reagents is hitherto unknown. Compared to the method of Ritter, our organometallic approach avoids the problem of regioselectivity and also leads to broader scope for F-substitution.

a) Selected examples of important polyfluoroaryl compounds



b) Metal-catalyzed coupling reaction of polyfluoroaryls

c) Cu-catalyzed coupling of polyfluoroarenes to alkanes (Chang *et.al.*)d) Decarboxylative Polyfluoroarylation via alkyl radical addition (Ritter *et.al.*)e) This work: Cu-catalyzed coupling of $\text{Ar}_\text{F}\text{-Zn}$ with NHPI esters

Scheme 4.1 Importance of polyfluoroaryl compounds and their synthesis by metal catalyzed C-C coupling of polyfluoroaryl reagents.

4.2 Reaction optimizations

We started our exploration using (diglyme)Zn(C₆F₅)₂ (4-1) as the source of -Ar_F, which could be obtained as a stable solid from a simple reaction of pentafluoriodobenzene and diethylzinc. With 1 mol% of Ir(dfppy)₂(ppy) as photocatalyst, 10 mol% of Cu(OTf)₂ as catalyst and 20 mol% of dtbbpy as ligand, NHPI ester 4-2 was converted to 4-3 in 52% yield in dichloromethane (Figure 4.1). Different ligands were tested. 4,4'-Dimethoxybipyridine (L2) and bipyridine (L3) led to slightly lower yields. The bipyridine ligand with electron-withdrawing group (L4) was not suitable for the reaction. 1,10-phenanthroline (L5) and 5,5'-bipyridine (L6) also lowered the reaction yield. When the ortho position of the ligand was occupied (L7 & L8), the reaction led to no target product. Besides, pyridinyl oxazoline (L9), bis(oxazoline) (L10), terpyridine (L11), diimine (L13) were all tried as ligands, yet no 4-3 was obtained. L12, which is the best ligand in Chang's work, was found not efficient, possibly because the deep color of the copper complex interfered with the photochemical process.

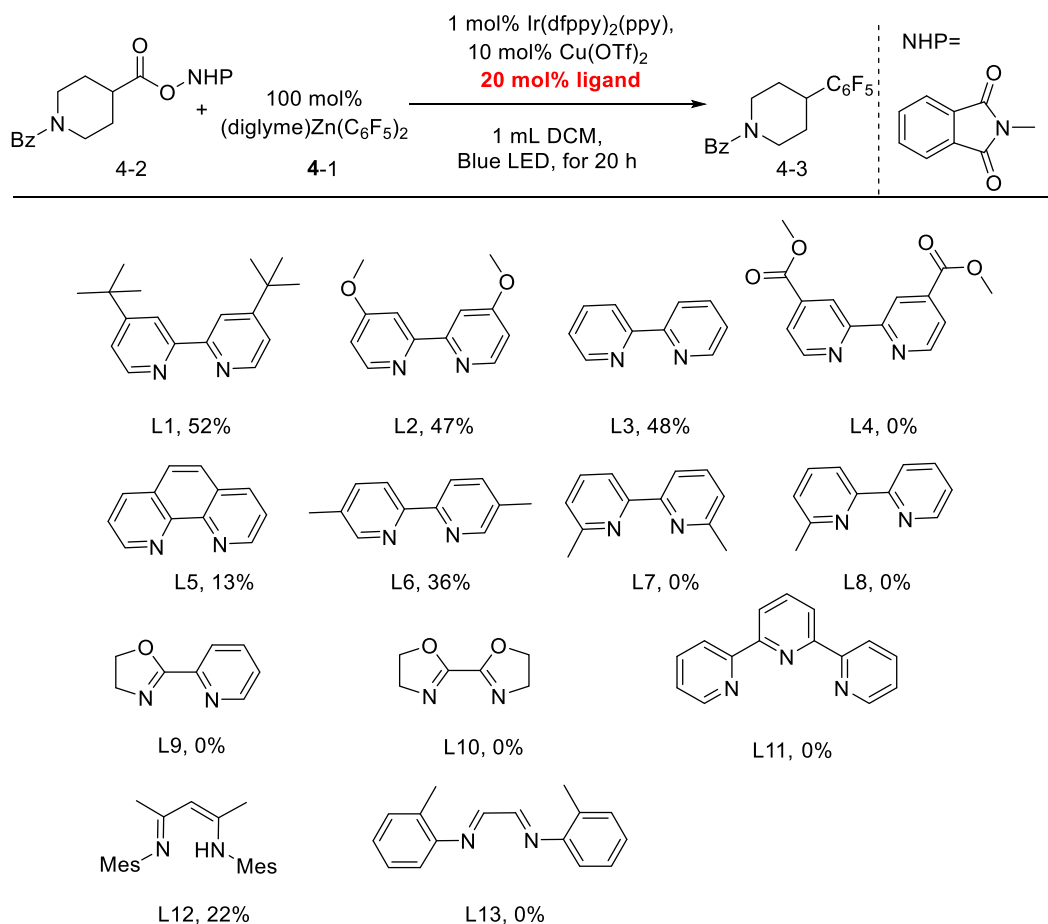
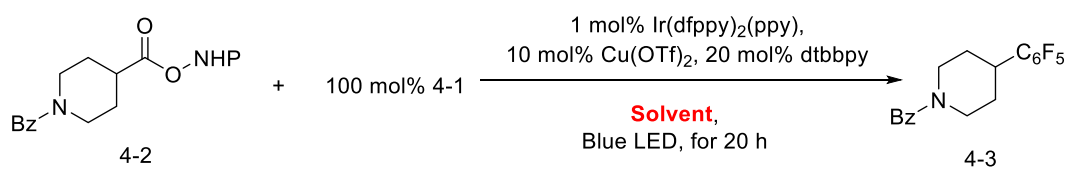


Figure 4.1 Optimization of ligands. Reaction conditions: 0.1 mmol 4-1, 0.1 mmol 4-2 and other additives in 1 mL DCM. Reaction under Blue LED for 20 h.

Then, we tried to optimize the solvent of the reaction (Table 4.1). Increasing the concentration of the solvent had a positive influence on the reaction (Entries 1-4). Decreasing the volume of DCM to 0.5 mL improved the yield to 68%. Acetone, DCM, PhCl and EtOAc were all good solvents for this reaction, while DMA was suited for this reaction. The best yield of 95% was given by EtOAc (Entry 8).

Table 4.1 Optimizations of solvents.

			
Entry	Solvent	Volume/ mL	Yield/ %
1	DCM	3	22
2	DCM	1	52
3	DCM	0.75	62
4	DCM	0.5	68
5	Acetone	0.5	84
6	PhCl	0.5	82
7	DCE	0.5	88
8	EtOAc	0.5	95
9	DMA	0.5	0

Reaction conditions: 0.1 mmol 4-1, 0.1 mmol 4-2 and other additives in the given solvent. Reaction under Blue LED for 20 h.

Based on the conditions of Entry 8 in Table 4.1, different catalysts were tried (Table 4.2). The use of Cu(OPiv)₂ also led to a high yield (94%, Entry 2). Cu^I as catalysts gave the target product in relatively lower yield (Entries 3&4). When iron (Entry 5) or nickel (Entry 6) was used as catalyst, the reaction yield was respectively 15% and 0%. In contrast, when no catalyst was added (Entry 7), only 7% of 3-3 was observed as product, confirming the importance of the copper catalyst.

Table 4.2 Test of different metal catalysts for the reaction.

$4\text{-}2 + 100 \text{ mol\% } 4\text{-}1 \xrightarrow[\text{EtOAc, Blue LED, for 20 h}]{\substack{1 \text{ mol\% Ir(dfppy)}_2(\text{ppy}), \\ 10 \text{ mol\% catalyst, 20 mol\% dtbbpy}}} 4\text{-}3$		
Entry	Metal Cat.	Yield/ %
1	Cu(OTf) ₂	95
2	Cu(OPiv) ₂	94
3	CuBr	75
4	Cu(CH ₃ CN) ₄ BF ₄	83
5	Fe(OTf) ₂	15
6	NiCl ₂ (DME)	0
7	-	8

Reaction conditions: 0.1 mmol 4-1, 0.1 mmol 4-2 and other additives in 0.5 mL EtOAc. Reaction under Blue LED for 20 h.

When the photocatalyst Ir(dfppy)₂(ppy) was replaced by Ir(dfppy)(ppy)₂ or Ir(ppy)₃, 4-3 was obtained in slightly decreased yields (Figure 4.2). However, the use of [Ir(dtbbpy)(ppy)₂] PF₆ or [Ru(bpy)₃](PF₆)₂ as photocatalyst led to much lower yields. Some organophotocatalysts were tested. The dihydrophenazine derivatized photocatalyst (OPC-1) was not very effective for this reaction. However, 4CzIPN, an easily accessible and inexpensive organophotocatalyst,^[48-51] mediated this transformation with high efficiency (93% yield). Several structurally modified 4CzIPN catalysts (OPC-2 to OPC-7) were subjected to the reaction, yet the yields were generally lower than when 4CzIPN was used. Therefore, we decided to use 4CzIPN as photocatalyst.

Finally, the Zn reagents with different ligands were used as the source of pentafluorophenyl (Table 4.3). Without the diglyme as ligand, the reaction yield was slightly lower. Pyridines as ligands would decrease the reaction yield to different extent. With the electron-rich DMAP as ligand, the target product could be obtained in 75% yield. However, the use of methyl isonicotinate as ligand would make this reaction completely unproductive. Therefore, 4-1 was still recognized as the best pentafluorophenyl reagent.

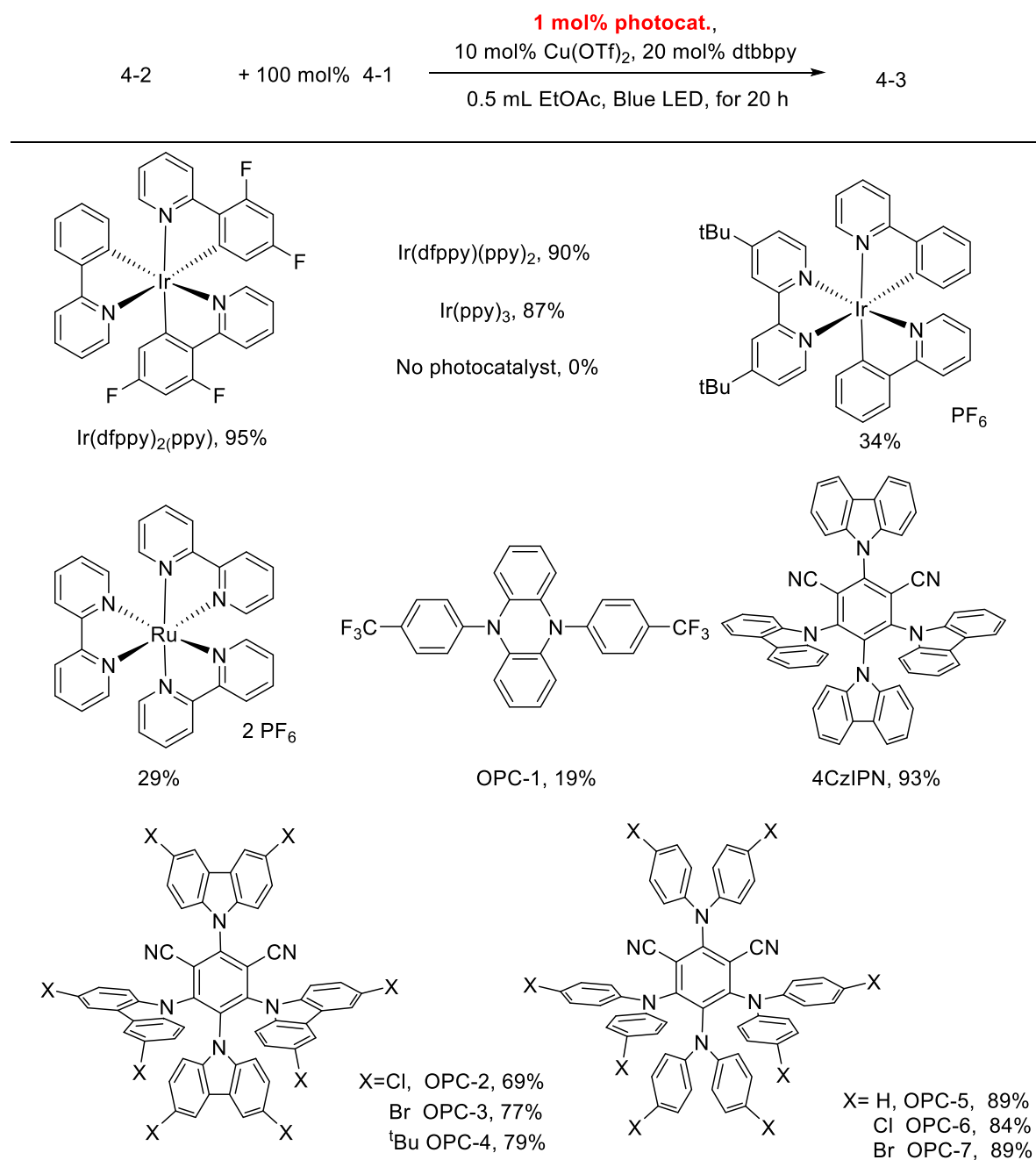
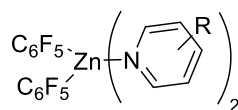
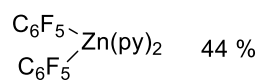
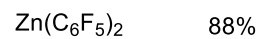
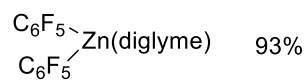
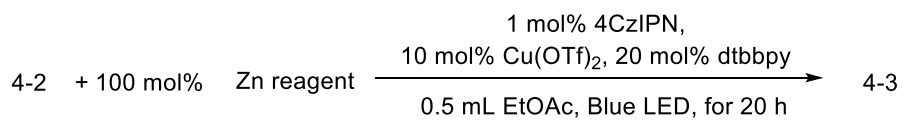


Figure 4.2 Optimizations of photocatalysts. Reaction conditions: 0.1 mmol 4-1, 0.1 mmol 4-2 and other additives in 0.5 mL EtOAc. Reaction under Blue LED for 20 h.



R= 2-Me 50%
 4-Me 22%
 4-CO₂Me trace
 4-NMe₂ 75%

Figure 4.3 Optimizations of zinc reagents. Reaction conditions: 0.1 mmol 4-1, 0.1 mmol 4-2 and other additives in 0.5 mL EtOAc. Reaction under Blue LED for 20 h.

4.3 Scope investigations

Based on the conditions, we started the evaluation of the substrate scope of NHPI esters (Figure 4.4). For secondary alkyl NHPI esters, the cyclic structures led to good yields of the polyfluoroaryl products (4-3 to 4-9, 55%-85%). Acyclic substrates were also successfully converted to the coupling products (4-10 to 4-12). Despite considerable hindrance, 4-12 with two cyclohexyls was still obtained in decent yield (64%). Sulfonamide (4-4), ether (4-5), ketone (4-7), electron-rich arene (4-11) were compatible with the reaction conditions. Several pharmaceuticals, including Ibuprofen, Ketoprofen and Naproxen, could be modified via this reaction into polyfluoroaryl compounds (4-13 to 4-15) in excellent yields. A substrate with an α -oxyalkyl group was not suitable for the reaction, with a less than 5% GC yield (4-16). This might be a result of the facile direct oxidation of α -oxyalkyl radical^[52] in relative to the trapping by copper catalyst.

A wide range of primary alkyl NHPI esters (4-17 to 4-30) were also suitable substrates for this reaction (Figure 4.4). Notably, the arylbromide (4-17), alkylbromide (4-18) and alkyl iodide (4-19), which serve as electrophiles in many coupling reactions,^[53, 54] could be tolerated in this reaction, leaving a synthetic handle for further transformations. A hindered primary radical (4-22) and primary benzyl radicals (4-23, 4-24) were also suitable for this transformation. Despite high molecular weight, some polyfluoro products could still be volatile (4-21, 4-22) and suffered from substantial loss during separation (e.g. For 4-22, 72% GC yield but 36% isolation yield). Double polyfluoroarylation on the same substrate was demonstrated, affording 4-25 in 63% yield. Again, we tried to apply some primary alkyl NHPI esters derived from natural products and pharmaceuticals (4-27 to 4-30). The products 4-27, 4-28 and 4-29 were obtained in good yields. The NHPI ester derived from structurally more complicated dehydrocholic acid led to a lower yield (4-30, 42%). For the coupling of tertiary alkyl NHPI esters, the coupling was generally not efficient (for example, 4-31 and 4-32, < 5% yield). Some specific substrates, e.g., those with a cyclopropyl ring, were coupled in modest to good yields (4-33 and 4-34).

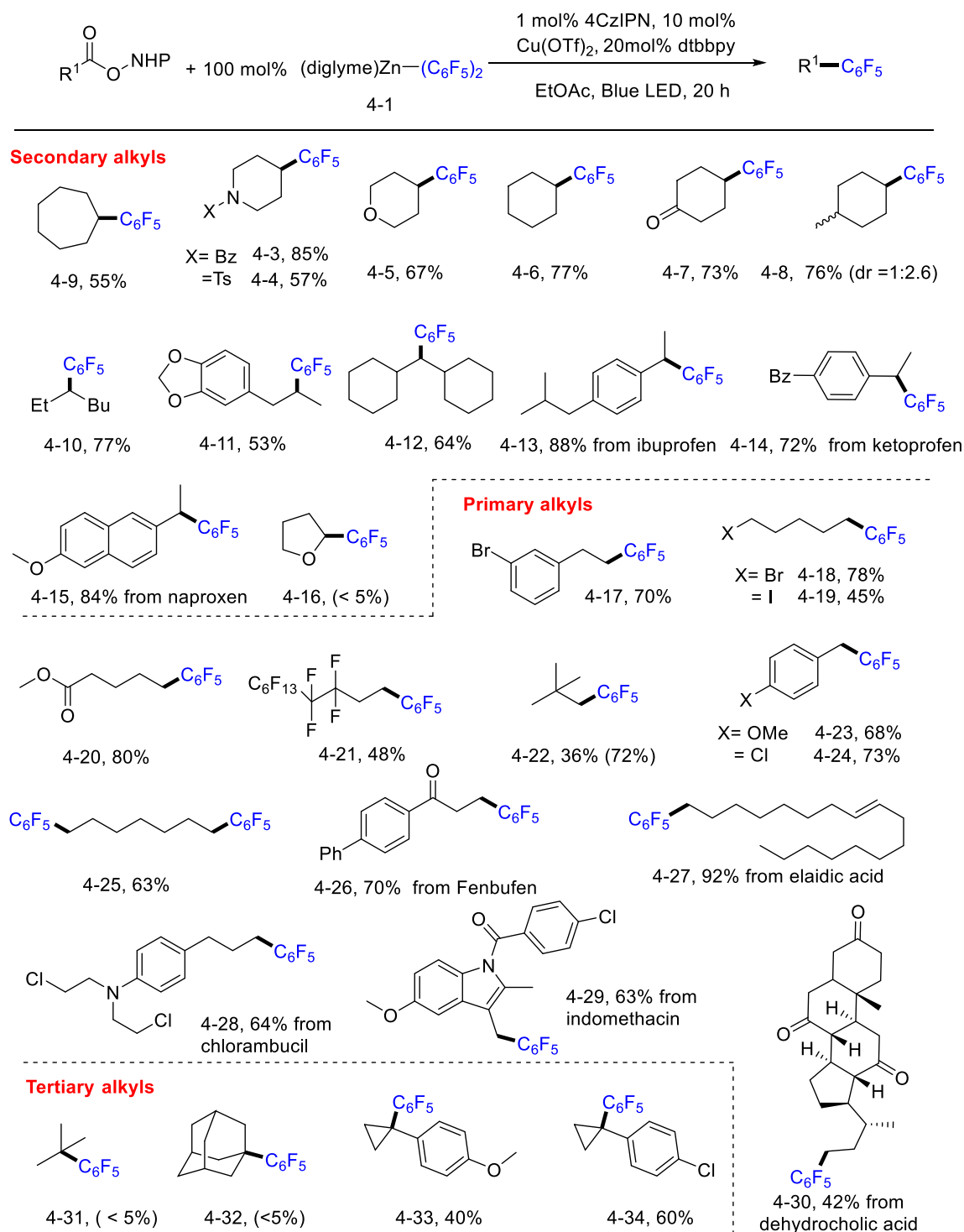


Figure 4.4 Scope investigations on NHPI esters. Reaction conditions: 0.1 mmol NHPI esters, 0.1 mmol 3-1 and other additives in 0.5 mL EtOAc. Reaction under Blue LED for 20 h. Isolated yields and GC yields (in bracket) were shown.

Then, we continued to evaluate the scope on zinc reagents (Figure 4.5). Diaryl zinc reagents with different F-content and F-substitution patterns were prepared via polyfluoroaryl lithium reagents and used as solutions in ethyl acetate. We used two representative alkyl NHPI ester substrates, one with a primary alkyl and one with a secondary alkyl group, the coupling products of which were respectively labeled as a and b. The reactions of the 2,3,5,6-tetrafluoro-4-iodophenyl Zn reagent gave 4-35a and 4-35b in moderate yields. All three isomers of tetrafluorophenyl could be coupled to a primary alkyl (4-36a to 4-38a) or a secondary alkyl (4-36b to 4-38b) in good yields. Trifluorophenyl Zn reagents were successfully reacted as well (4-39a to 4-41a, 4-39b to 4-41b), so were the 2,6-difluorophenyl Zn reagent (4-42a and 4-42b). The coupling of 2,4-difluorophenyl zinc was inefficient (30 % for 4-43b and < 5% for 4-43a). Likewise, the coupling of 4-fluorophenyl zinc reagent was unsuccessful (< 5% yield). In these cases, the relatively electron rich aryl zinc reagents were prone to homocoupling to give biaryls. The electron-deficient tetrafluoropyridyl zinc reagent was not suited to this reaction as well (29% for 4-44b and 0% for 4-44a).

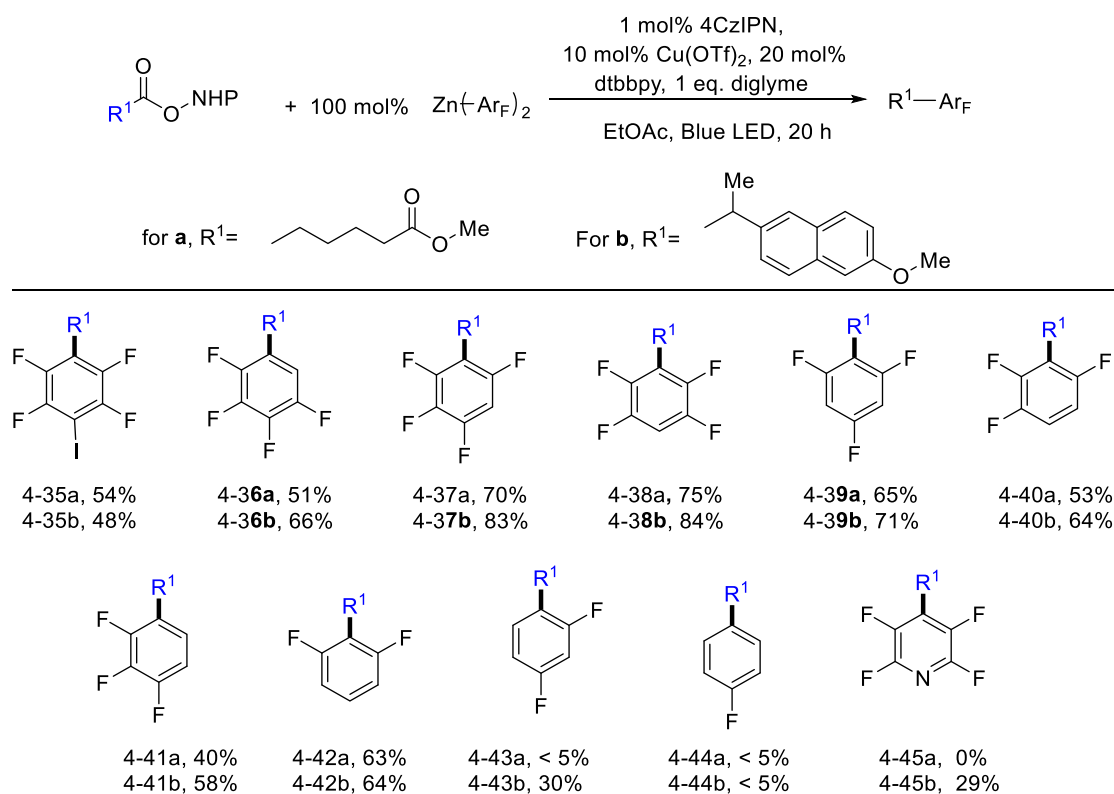


Figure 4.5 Scope investigations on polyfluoroaryl zinc reagents. Reaction conditions: 0.1 mmol NHPI esters, 0.1 mmol zinc reagents and other additives in 0.5 mL EtOAc. Reaction under Blue LED for 20 h. Isolated yields and GC yields (in bracket) were shown.

4.4 Mechanistic investigations

Several experiments were conducted to shed light on the mechanism of this coupling reaction. When the NHPI ester derived from 6-heptenoic acid (4-46) was used as a substrate to couple with 4-1 under the standard conditions (Figure 4.6a), 4-47, a product formed via 5-exo-trig cyclization of 5-hexenyl radical, was obtained as the only cross-coupling product (60% yield). This result is consistent with the intermediacy of an alkyl radical formed from the alkyl NHPI ester. When (dtbbpy)Cu(OTf)₂ was mixed with 1 equivalent of 4-1, the homocoupling product C₆F₅-C₆F₅ was formed in 42% yield (Figure 4.6b). This result is consistent with previous reports that Cu^{II} species could oxidize Zn-Ar_F to Ar_F-Ar_F.^[55] Thus, the resting oxidation state of Cu in the catalytic system is likely Cu^I.

The Cu^I complex [(bpy)Cu(C₆F₅)] 4-4 was then synthesized and was found to be a competent catalyst as well (Figure 4.6c), leading to the target product in 80% yield. However, the stoichiometric reaction of [(bpy)Cu(C₆F₅)] with 4-2 under photochemical conditions didn't give any coupling product (Figure 4.6d). In a crossover experiment, 4-2 was treated with 50 mol% of [(bpy)Cu(C₆F₅)] and 100 mol% of di-(2,3,5,6-tetrafluorophenyl)zinc 4-49 (Figure 4.6e). The coupling with both the -C₆F₅ group and the -C₆F₄H group occurred with a total yield of 52% (-C₆F₄H: -C₆F₅ = 1:0.18 in the products, = 1:0.25 in the starting materials). These results indicate that [(bpy)Cu(C₆F₅)] could enter the catalytic cycle and transfer the -C₆F₅ group on the copper into the product. However, it is not the species that directly transfer the -C₆F₅ group to the alkyl radicals.

When the zinc reagent 4-1 was added to a solution containing [(bpy)Cu(C₆F₅)], an instant color change from orange to light yellow was observed. In the UV-Vis spectra, 4-1 exhibits almost no absorption in the range of 350 -600 nm in dichloromethane. However, increasing the ratio of 4-1 to [(bpy)Cu(C₆F₅)] led to a significant decrease of absorbance of [(bpy)Cu(C₆F₅)] (Figure 4.7), indicating a transmetallation process. Besides, ¹⁹F-NMR was used to characterize 4-1, [(bpy)Cu(C₆F₅)] and their mixture in a ratio of 1:1 (Figure 4.8). The region on the left of the spectrum corresponds to the *ortho*-fluoro of M-C₆F₅. In the spectrum of the mixture (middle, Figure 4.8), a new peak **A** was generated compared to the spectra of 4-1 and [(bpy)Cu(C₆F₅)], suggesting the generation of a new organometallic M-C₆F₅. In the meantime, the peak **B** in the original spectrum of [(bpy)Cu(C₆F₅)] disappeared, which indicates the conversion of [(bpy)Cu(C₆F₅)] with the addition of 4-1. Likewise, in the cyclic voltammograms (Figure 4.9), a new oxidation peak emerged at -0.57 V vs. Fc⁺/Fc (Fc = ferrocene) when the zinc reagent 4-1 was added to [(bpy)Cu(C₆F₅)], which was 0.60 V lower than

the oxidation peak of $[(bpy)Cu(C_6F_5)]$. These results could be attributed to the formation of an anionic $[(bpy)Cu(C_6F_5)_2]^-$ species upon the addition of 4-1 to $[(bpy)Cu(C_6F_5)]$ (Figure 4.6f), which could be the species responsible for transferring the $-C_6F_5$ group to alkyl radicals.

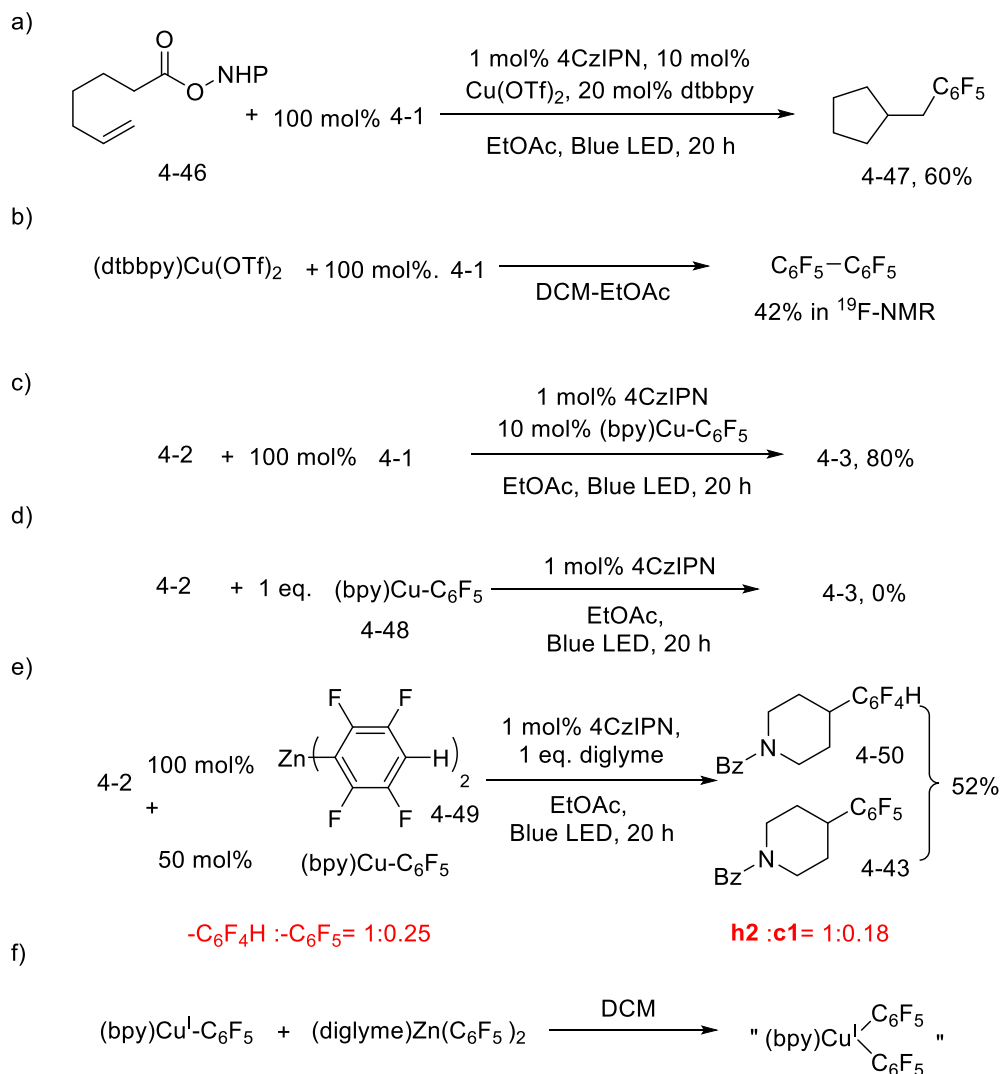


Figure 4.6 Mechanistic investigations.

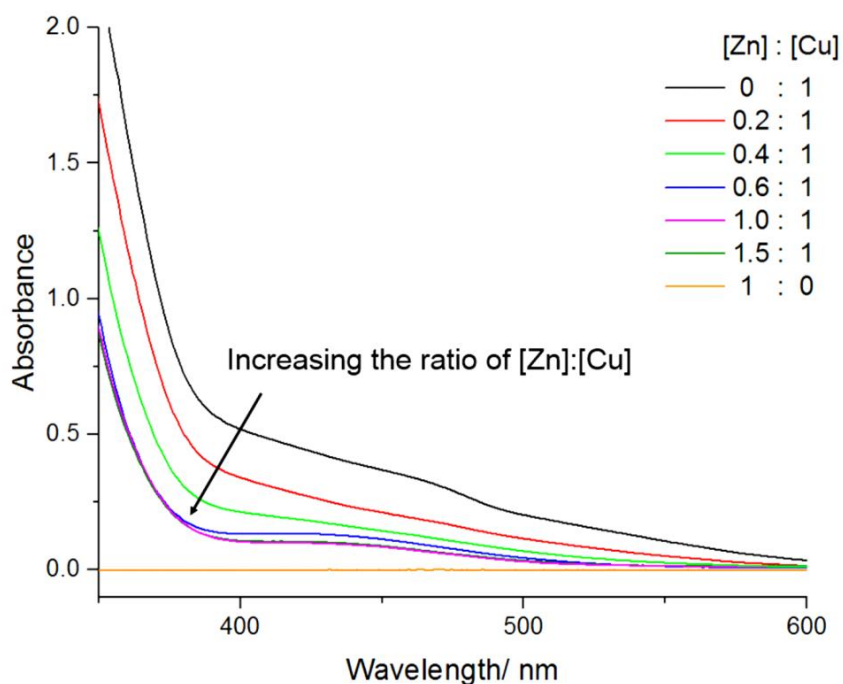


Figure 4.7 UV-Vis spectra of (diglyme)Zn(C₆F₅)₂ (4-1), [(bpy)Cu(C₆F₅)], and their mixtures. C(4-1) was 0.0008 M when alone. In all other samples, c[(bpy)Cu(C₆F₅)] was 0.0008 M and c(4-1) was adjusted according to the given ratios. The solvent was dichloromethane.

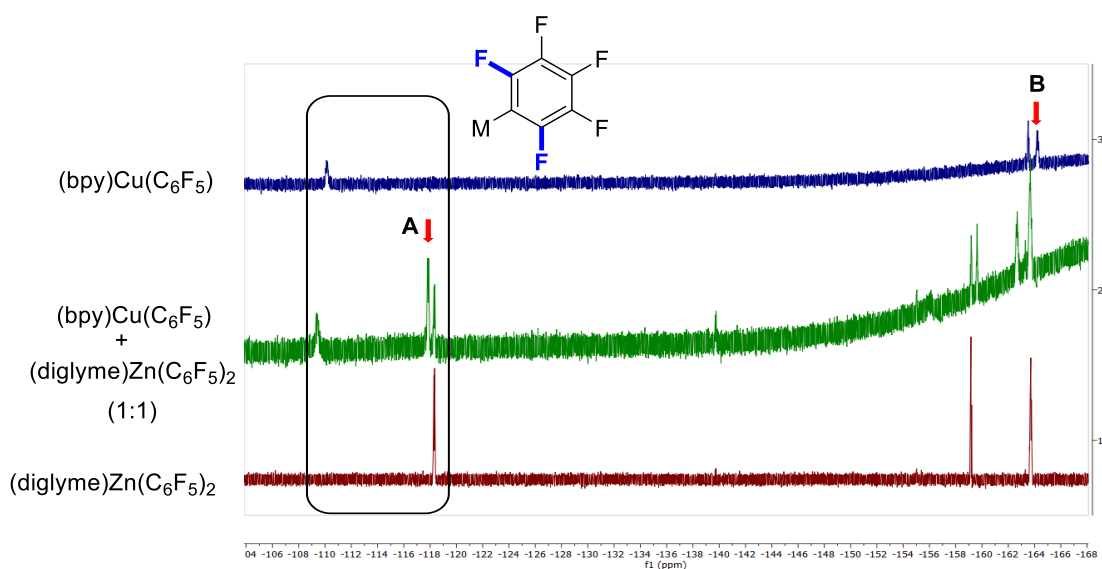


Figure 4.8 ¹⁹F-NMR spectra of 4-1, [(bpy)Cu(C₆F₅)], and their mixtures. C(4-1) = c[(bpy)Cu(C₆F₅)] = 0.002 M in dichloromethane solution.

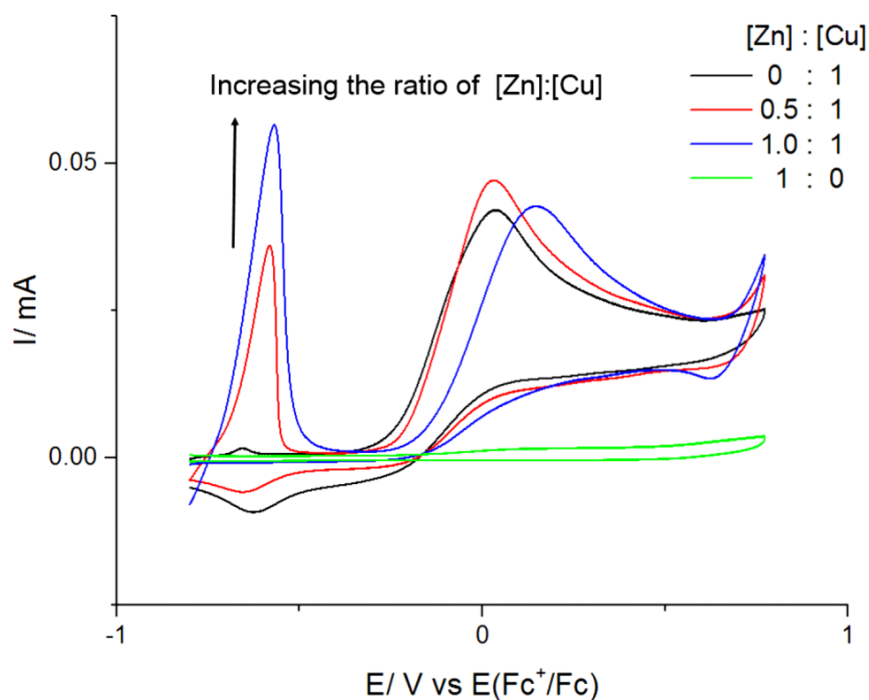


Figure 4.9 Cyclic voltammograms of 4-1, [(bpy)Cu(C₆F₅)], and their mixtures in CH₂Cl₂-CH₃CN (2:1). C(4-1) was 0.0027 M when alone. In all other samples, c[(bpy)Cu(C₆F₅)] was 0.0027 M and c(4-1) was adjusted according to the given ratios. Conditions: Under nitrogen atmosphere, Bu₄NBF₄ (0.03 M), glassy carbon disk as working electrode, Pt wire as counter electrode, Ag|AgCl, KCl(aq) as reference electrode (calibrated with Fc⁺/Fc). The scan rate: 100 mV/s.

Stern-Volmer quenching was used to probe the interaction of the excited photocatalyst with different reagents. NHPI ester 4-2 and the Zn reagent 4-1 could not quench the emission of the excited photocatalyst. When [(bpy)Cu(C₆F₅)] was added to the solution of 4CzIPN, the emission was weakened (Figure 4.10a). The Stern-Volmer quenching plot (Figure 4.10b) revealed a linear correlation between the concentration of [(bpy)Cu(C₆F₅)] and the degree of quenching (I_0/I , I_0 is the emission intensity without quencher, I is the emission intensity without the quencher). The slope was 6226 M⁻¹ for the copper complex. The 1:1 mixture of 4-1 with [(bpy)Cu(C₆F₅)] was also effective quencher for the excited 4CzIPN (Figure 4.11). These data suggest that the reaction possibly starts by a reductive quenching of the excited 4CzIPN by the Cu^I species. Considering the large excess of 4-1 compared to copper catalyst under the coupling conditions, the neutral [LCu(Ar_F)] are expected to have a very low concentration and [LCu(Ar_F)₂]⁻ is more likely to be the quencher of the excited 4CzIPN.

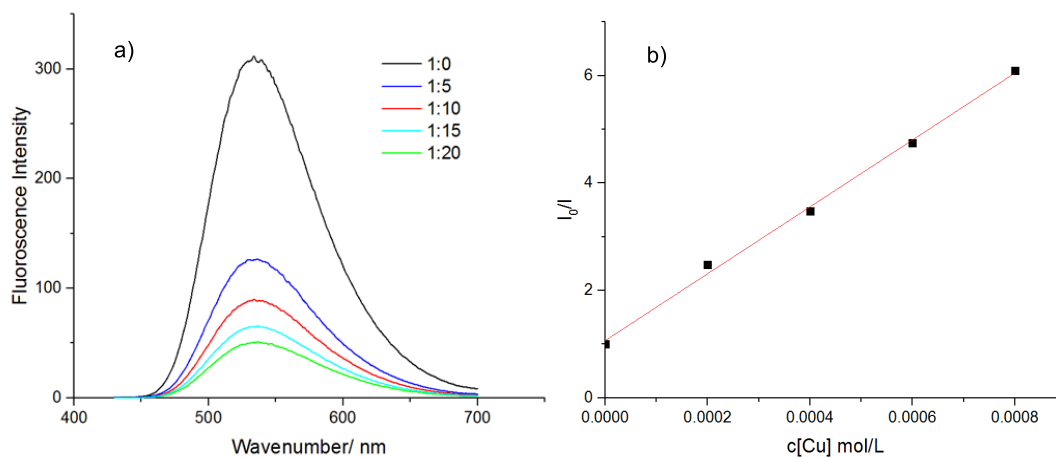


Figure 4.10 a) Emission spectra at different ratios of 4CzIPN to [(bpy)Cu(C₆F₅)]. c[4CzIPN] = 8×10^{-5} M. b) Stern-Volmer quenching plot for [(bpy)Cu(C₆F₅)].

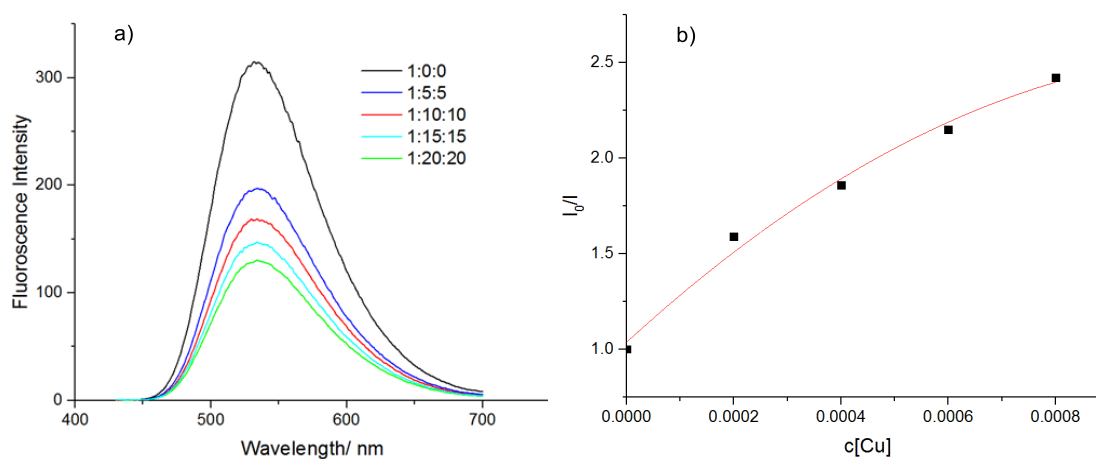
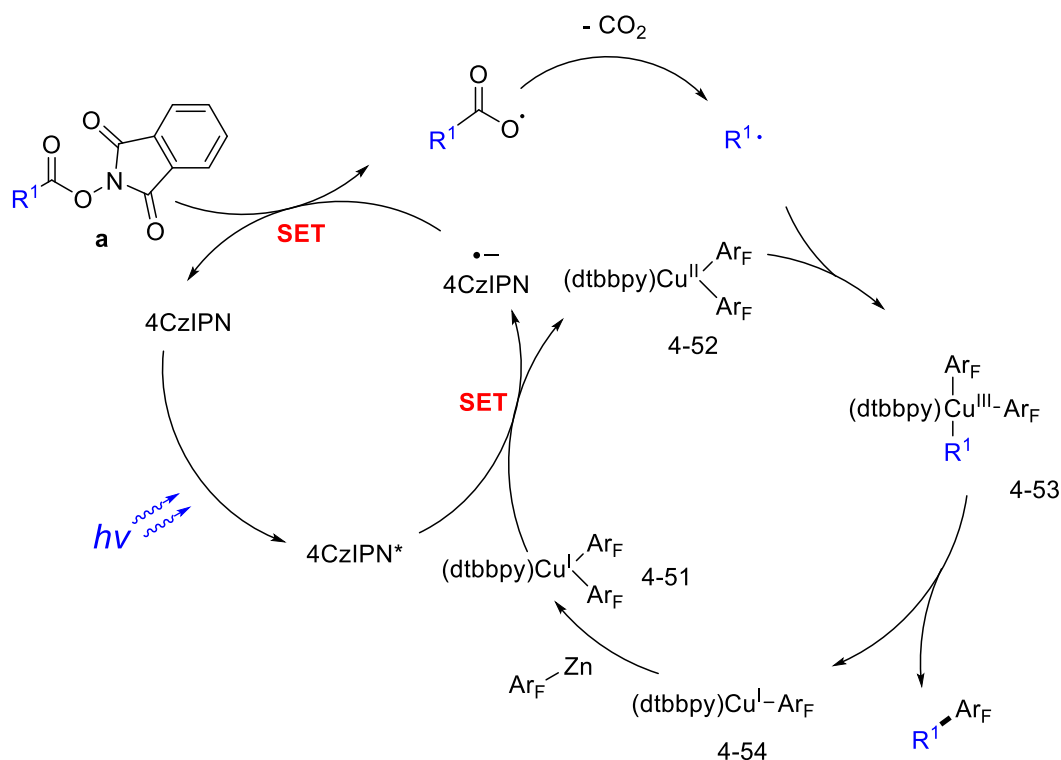


Figure 4.11 a) Emission spectra at different ratios of 4CzIPN to [(bpy)Cu(C₆F₅)] & [(diglyme)Zn(C₆F₅)₂]. c[4CzIPN] = 8×10^{-5} M. b) Stern-Volmer quenching plot in relative to the concentration of [(bpy)Cu(C₆F₅)].

4.5 The proposed reaction mechanism

Based on these results, we propose a plausible mechanism (Scheme 4.2). The reaction starts with the reductive quenching of the excited 4CzIPN by the anionic $[\text{LCu}^{\text{I}}(\text{Ar}_{\text{F}})_2]^-$ species 4-51 to form the reduced 4CzIPN and a $\text{LCu}^{\text{II}}(\text{Ar}_{\text{F}})_2$ species (4-52). The radical anion of 4CzIPN then reduces the NHPI ester to give an alkyl radical after decarboxylation. The alkyl radical is captured by 4-52 to form a formal Cu^{III} intermediate 4-53, which undergoes reductive elimination to give the coupling product and a $\text{LCu}^{\text{I}}(\text{Ar}_{\text{F}})$ species 4-54. Although there is no precedent for the reductive elimination of polyfluoroaryl and alkyl from such a Cu^{III} complex, a facile reductive elimination of $[(\text{bpy})\text{Cu}(\text{CF}_3)_2(\text{CH}_3)]$ was reported to form CF_3CH_3 and $[(\text{bpy})\text{Cu}(\text{CF}_3)]$, which could be analogous.^[56,57] $[\text{LCu}^{\text{I}}(\text{Ar}_{\text{F}})]$ undergoes transmetalation with the $\text{Zn}-\text{Ar}_{\text{F}}$ reagent to regenerate 4-51 and close the catalytic cycle.



Scheme 4.2 the proposed mechanism of the reaction.

4.6 Conclusion

In summary, we have developed a dual photo- and Cu-catalyzed method for the decarboxylative coupling of aliphatic acids with polyfluoroaryl Zn reagents. This method allows the installation of polyfluoroaryls with variable F-content and F-substitution patterns on a primary or secondary alkyl groups, with good compatibility of functional groups. Our strategy might be extended to the coupling of Zn-Ar_F reagents with alkyl radicals generated by other methods, leading to new methods in polyfluoroarylation.

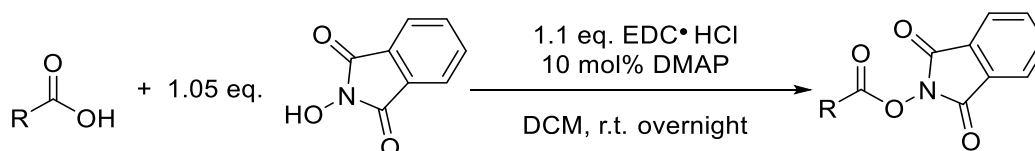
4.7 Experiments

4.7.1 General consideration

Anhydrous dichloromethane (DCM), tetrahydrofuran (THF) and acetonitrile were prepared with solvent drying system. Purchased anhydrous solvents [DMA (N,N-dimethylacetamide) and AcOEt] and commercially available reagents were used without purification. 15 mL Teflon-screw capped vials (d = 2 cm) were used for the photochemical reactions. Blue LEDs (From Kessil Co., Ltd., 40 W max., wavelength centered at 460 nm, product No. A160WE) was used as the radiation source and a cooling fan was used to keep the reaction at around room temperature during photolysis. After the reaction, GC-MS (Agilent Tech. 7890B-5977B) was used to determine the yield of the products for reaction optimization, with 1,3,5-trimethylbenzene as an internal standard. Silica gel columns were used for reaction separation, with hexane-AcOEt as eluent unless otherwise noted. NMR spectra (^1H , ^{19}F , ^{13}C) were recorded on Bruker Avance 400 MHz instrument. Chemical shifts are reported in ppm in reference to the residual signal of CDCl_3 , ^1H (7.26 ppm) and ^{13}C (77.16 ppm). Descriptions of multiplicities are abbreviated as follows: s = singlet, d = doublet, t = triplet, q = quartet, m = multiplet, b = broad. Determinations of high resolution mass spectra (HRMS) of unknown compounds by ESI, APPI or EI ionization technique were performed with a Micro Mass QTOF Ultima spectrometer at the EPFL Mass Spectrometry Center or ETH MoBiAS center. Stern-Volmer quenching experiments were conducted with a Varian Cary Eclipse fluorescence spectrophotometer. UV-Vis spectra were recorded on Cary 60 UV-Vis (Agilent Tech.). Cyclic voltammograms (CV) were recorded on a BIO-LOGIC VSP.

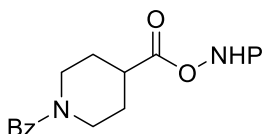
4.7.2 Synthesis of NHPI esters and zinc reagents

Preparation of NHPI esters of carboxylic acids

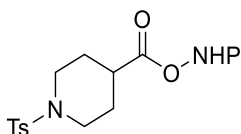


A round-bottom flask was charged with 5 mmol carboxylic acid, 1.05 eq. N-hydroxyphthalimide and 10 mol% of DMAP. 10 mL DCM was added and the stirring was started. Then, 1.1 eq. EDC·HCl (EDC= 1-ethyl-3-(3-dimethylaminopropyl)carbodiimide) dispersed in 5 mL DCM was

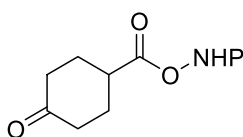
added slowly to the flask. During the addition, the solid N-hydroxyphthalimide was dissolved gradually. The reaction was left overnight. Afterwards, the reaction mixture was diluted with DCM and washed 3 times with H₂O. The organic phase was collected, dried over Na₂SO₄ and concentrated using an evaporator. The residual was separated on a silica gel column with hexane-EtOAc as eluent. The NMR data for the following NHPI esters could be found in the corresponding literature.^[58-60]



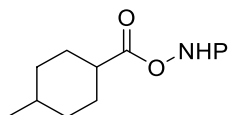
White solid. ¹H NMR (400 MHz, CDCl₃) δ 7.82 (m, 2H), 7.73 (m, 2H), 7.34 (m, 5H), 4.41 (b, 1H), 3.74 (m, 1H), 3.18 (ddd, *J* = 13.7, 10.3, 3.2 Hz, 2H), 2.98 (tt, *J* = 10.0, 4.2 Hz, 1H), 2.29 – 1.74 (m, 4H). ¹³C NMR (101 MHz, CDCl₃) δ 170.7, 170.5, 162.0, 135.8, 135.0, 129.9, 129.0, 128.7, 127.0, 124.2, 38.6, 23.5.



White solid. ¹H NMR (400 MHz, CDCl₃) δ 7.80 (dd, *J* = 5.5, 3.1 Hz, 1H), 7.75 – 7.70 (m, 1H), 7.65 – 7.55 (m, 1H), 7.27 (d, *J* = 8.0 Hz, 1H), 3.57 (dt, *J* = 12.1, 4.4 Hz, 1H), 2.72 – 2.53 (m, 2H), 2.37 (s, 2H), 2.09 (dq, *J* = 12.8, 3.8 Hz, 1H), 2.01 – 1.91 (m, 1H). ¹³C NMR (101 MHz, CDCl₃) δ 170.3, 143.9, 135.0, 133.3, 129.9, 129.0, 127.8, 124.2, 45.0, 37.7, 27.4, 21.7.

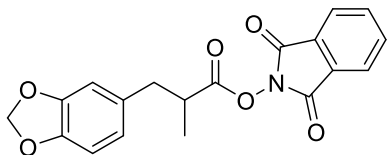


White solid. ¹H NMR (400 MHz, CDCl₃) δ 7.93 – 7.88 (m, 2H), 7.82 (m, 2H), 3.20 (tt, *J* = 8.3, 4.2 Hz, 1H), 2.63 (m, 2H), 2.50 – 2.22 (m, 5H). ¹³C NMR (101 MHz, CDCl₃) δ 209.0, 170.6, 162.1, 135.0, 129.0, 124.2, 39.3, 38.1, 28.4.

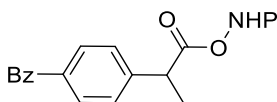


White solid. ¹H NMR (400 MHz, CDCl₃) δ 7.88 (dd, *J* = 5.5, 3.1 Hz, 2H), 7.78 (dd, *J* = 5.5, 3.1 Hz, 2H), 2.62 (tt, *J* = 12.2, 3.6 Hz, 1H), 2.22 – 2.12 (m, 2H), 1.93 – 1.78 (m, 2H), 1.62 (qd, *J* = 13.2, 3.5 Hz, 3H),

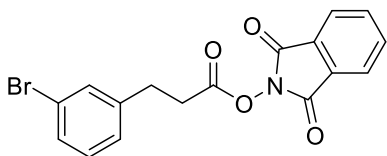
1.47 – 1.35 (m, 1H), 1.11 – 0.95 (m, 2H), 0.92 (d, $J = 6.5$ Hz, 3H). ^{13}C NMR (101 MHz, CDCl_3) δ 172.2, 162.2, 134.8, 129.2, 124.0, 40.7, 34.1, 31.9, 29.0, 22.5.



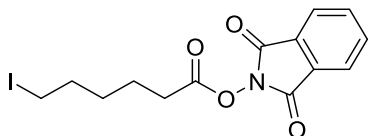
White solid. ^1H NMR (400 MHz, CDCl_3) δ 7.94 – 7.84 (m, 2H), 7.83 – 7.74 (m, 2H), 6.81 – 6.68 (m, 3H), 5.95 (s, 2H), 3.16 (dd, $J = 13.7, 6.4$ Hz, 1H), 3.09 – 3.01 (m, 1H), 2.77 (dd, $J = 13.6, 7.7$ Hz, 1H), 1.33 (d, $J = 6.9$ Hz, 3H). ^{13}C NMR (101 MHz, CDCl_3) δ 172.2, 162.1, 147.9, 146.5, 134.9, 131.7, 129.1, 124.1, 122.4, 109.6, 108.4, 101.1, 39.3, 39.1, 16.5.



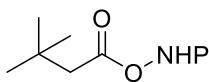
White solid. ^1H NMR (400 MHz, CDCl_3) δ 7.90 – 7.75 (m, 8H), 7.67 (dt, $J = 7.8, 1.5$ Hz, 1H), 7.63 – 7.57 (m, 1H), 7.56 – 7.47 (m, 3H), 4.20 (q, $J = 7.1$ Hz, 1H), 1.71 (d, $J = 7.2$ Hz, 3H). ^{13}C NMR (101 MHz, CDCl_3) δ 196.5, 170.6, 138.7, 138.4, 137.5, 134.9, 132.7, 131.7, 130.3, 129.8, 129.5, 129.1, 129.0, 128.5, 124.1, 43.0, 19.0.



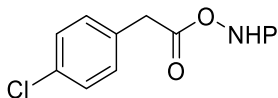
White solid. ^1H NMR (400 MHz, CDCl_3) δ 7.92 – 7.83 (m, 2H), 7.82 – 7.73 (m, 2H), 7.43 – 7.33 (m, 2H), 7.22 – 7.17 (m, 2H), 3.06 (t, $J = 7.0$ Hz, 2H), 2.97 (t, $J = 7.7$ Hz, 2H). ^{13}C NMR (101 MHz, CDCl_3) δ 168.7, 161.9, 141.5, 134.9, 131.5, 130.4, 130.0, 128.9, 127.1, 124.1, 122.8, 32.5, 30.2.



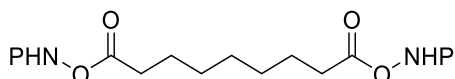
White solid. ^1H NMR (400 MHz, CDCl_3) δ 7.93 – 7.84 (m, 2H), 7.84 – 7.75 (m, 2H), 3.21 (t, $J = 6.9$, 2H), 2.69 (t, $J = 7.4$, 2H), 1.95 – 1.76 (m, 4H), 1.58 (m, 2H). ^{13}C NMR (101 MHz, CDCl_3) δ 169.5, 162.1, 134.9, 129.1, 124.1, 33.1, 30.9, 29.8, 23.8, 6.2.



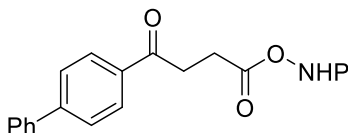
White solid. ^1H NMR (400 MHz, CDCl_3) δ 7.88 (dd, J = 5.5, 3.1 Hz, 2H), 7.83 – 7.74 (m, 2H), 2.53 (s, 2H), 1.16 (s, 9H). ^{13}C NMR (101 MHz, CDCl_3) δ 168.0, 162.2, 134.8, 129.1, 124.1, 44.7, 31.4, 29.6.



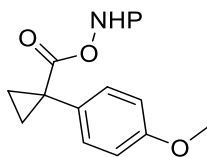
White solid. ^1H NMR (400 MHz, CDCl_3) δ 7.87 (m, 2H), 7.78 (m, 2H), 7.40 – 7.28 (m, 4H), 3.96 (s, 2H). ^{13}C NMR (101 MHz, CDCl_3) δ 167.4, 161.9, 135.0, 134.0, 130.8, 130.1, 129.2, 128.9, 124.1, 37.2.



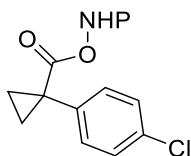
White solid. ^1H NMR (400 MHz, CDCl_3) δ 7.87 (m, 4H), 7.78 (m, 4H), 2.67 (td, J = 7.4 Hz, 4H), 1.80 (p, J = 7.4 Hz, 4H), 1.51 – 1.36 (m, 6H). ^{13}C NMR (101 MHz, CDCl_3) δ 169.7, 162.1, 134.8, 129.1, 124.1, 31.0, 28.7, 28.6, 24.7.



White solid. ^1H NMR (400 MHz, CDCl_3) δ 8.12 – 8.04 (m, 2H), 7.90 (m, 2H), 7.79 (m, 2H), 7.74 – 7.67 (m, 2H), 7.67 – 7.59 (m, 2H), 7.52 – 7.44 (m, 2H), 7.44 – 7.36 (m, 1H), 3.51 (t, J = 6.9 Hz, 2H), 3.18 (t, J = 6.9 Hz, 2H). ^{13}C NMR (101 MHz, CDCl_3) δ 196.2, 169.5, 162.0, 146.3, 139.9, 134.9, 129.1, 129.1, 128.9, 128.5, 127.5, 127.4, 124.1, 33.4, 25.6.

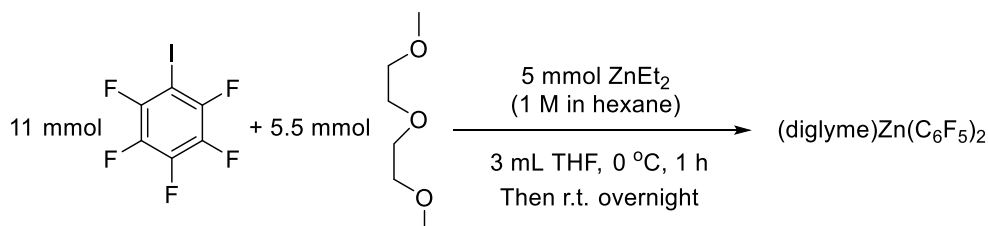


White solid. ^1H NMR (400 MHz, CDCl_3) δ 7.84 (m, 2H), 7.75 (m, 2H), 7.44 (d, J = 8.8 Hz, 2H), 6.89 (d, J = 8.7 Hz, 2H), 3.80 (s, 3H), 1.87 (q, J = 4.3 Hz, 2H), 1.45 (q, J = 4.4 Hz, 2H). ^{13}C NMR (101 MHz, CDCl_3) δ 171.4, 162.0, 159.3, 134.8, 131.8, 129.2, 129.1, 124.0, 114.0, 55.4, 26.7, 19.0.



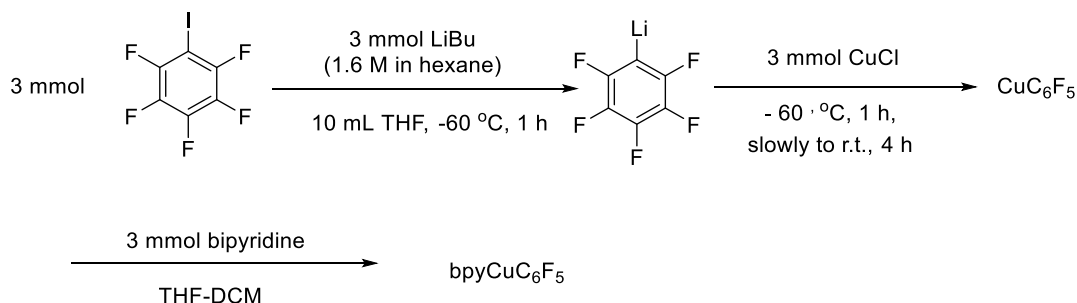
White solid. ^1H NMR (400 MHz, CDCl_3) δ 7.85 (m, 2H), 7.76 (m, 2H), 7.52 – 7.41 (m, 2H), 7.38 – 7.31 (m, 2H), 1.98 – 1.86 (m, 2H), 1.53 – 1.41 (m, 2H). ^{13}C NMR (101 MHz, CDCl_3) δ 170.8, 161.9, 135.6, 134.9, 134.0, 132.1, 129.0, 128.8, 124.0, 26.8, 18.9.

Preparation of (diglyme) $\text{Zn}(\text{C}_6\text{F}_5)_2$ (b1)



A 50-mL Schlenk Tube was charged with 11 mmol pentafluoroiodobenzene, 5.5 mmol diglyme and 3 mL THF under nitrogen. The reaction vessel was cooled to 0 °C, and diethyl zinc (1 M in hexane) was gradually added to the stirred solution. The reaction was maintained at 0 °C for 1 h, and then at room temperature overnight. A white precipitate was observed. The solvent was removed under vacuum, and the residual was washed with hexane and then dried again under vacuum to give fine white powder in 50-60 % yield. In case where there is some impurities observed on NMR spectrum, recrystallization in DCM- Et_2O could give pure crystals. ^1H NMR (400 MHz, CDCl_3) δ 3.94 (t, J = 4.9 Hz, 4H), 3.66 (t, J = 4.9 Hz, 4H), 3.24 (s, 6H). ^{19}F NMR (376 MHz, CDCl_3) δ -117.6 (m), -157.3 (m), -162.13 (dt, J = 18.7, 10.6 Hz). ^{13}C NMR (101 MHz, CDCl_3) δ 149.1 (dd, J = 226.0, 26.9 Hz), 139.8 (d, J = 246.6 Hz), 136.6 (dd, J = 253.1, 31.8 Hz), 119.3, 70.31, 69.6, 58.5.

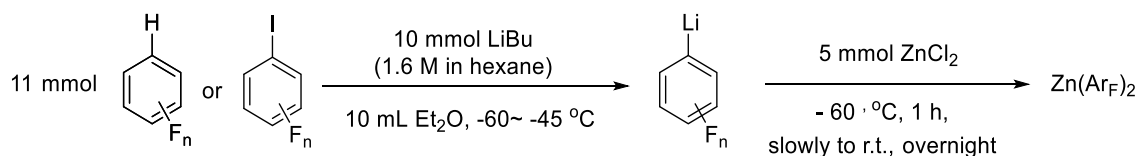
Preparation of [(bpy) $\text{Cu}(\text{C}_6\text{F}_5)$]



A 50-mL Schlenk tube was charged with 3 mmol pentafluoriodobenzene and 10 mL THF under nitrogen. The reaction vessel was cooled to $-78\text{ }^{\circ}\text{C}$, and 1.9 mL Li^nBu (1.6 M in hexane) was gradually added to the stirred solution by a syringe pump in 5 min. The reaction was maintained at $-60\text{ }^{\circ}\text{C}$ for 1 h (using an acetone – dry ice bath). Then, 3 mmol CuCl was added to the solution, which was maintained at $-60\text{ }^{\circ}\text{C}$ for another one hour. The reaction was allowed to slowly warm to room temperature in 4 h (the increase of temperature in acetone – dry ice bath can be pretty slow when the Dewar is covered with cotton layer). Then, the solution was filtered and concentrated under vacuum. The residual was dissolved in 3 mL DCM. 3 mmol bipyridine dissolved in 3 mL THF was added dropwise to the CuC_6F_5 solution, and a dark red solution was obtained. The solution was placed under $-20\text{ }^{\circ}\text{C}$ for 2 h and red crystals formed. By decanting the upper solution, washing the solid with Et_2O and finally drying under vacuum, the product could be obtained. The NMR Data matched with the reported data.^[61]

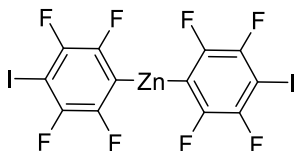
^1H NMR (400 MHz, CD_2Cl_2) δ 9.03 – 8.82 (m, 2H), 8.18 (d, $J = 8.1\text{ Hz}$, 2H), 8.05 (tt, $J = 7.9, 1.6\text{ Hz}$, 2H), 7.68 – 7.50 (m, 2H). ^{19}F NMR (376 MHz, CD_2Cl_2) δ -109.69 (d, $J = 38.0\text{ Hz}$), -162.97 (t, $J = 20.0\text{ Hz}$), -163.69 (m).

Preparation of $\text{Zn}(\text{Ar}_\text{F})_2$ (as solution in EtOAc), method 1 (with Li^nBu)

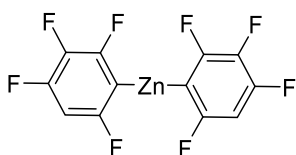


A 50-mL Schlenk tube was charged with 11 mmol polyfluoroarene and 10 mL Et_2O under nitrogen. The reaction vessel was cooled to $-78\text{ }^{\circ}\text{C}$, and 6.25 mL Li^nBu (1.6 M in hexane) was gradually added to the stirred solution by a syringe pump in 10 min. The reaction was maintained at $-60\sim -45\text{ }^{\circ}\text{C}$ for a given period of time. Then, 5 mmol ZnCl_2 was added to the solution, which was maintained at $-60\text{ }^{\circ}\text{C}$ for another one hour. The reaction was allowed to gradually warm to room temperature overnight. A white precipitate was observed. Filtration under nitrogen removed the white solid to give a clear solution. The solvent was removed under vacuum, and then the product was heated under vacuum for 2 h to remove the remaining solvent. A white or yellowish solid was obtained, which was dispersed in 10 mL DCM to give a suspension. Filtration was used to remove the solid and the solvent was again removed under vacuum. The residual was dissolved in 5 mL EtOAc

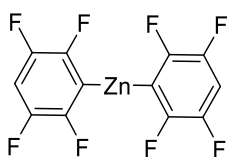
and the concentration of $\text{Zn}(\text{Ar}_\text{F})_2$ was determined using NMR, with pentafluorobenzene or 1,2,3,4-tetrafluorobenzene as internal standard.



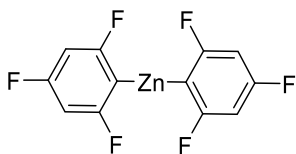
Prepared from 2,3,5,6-tetrafluoro-1,4-diiodobenzene, 1 h for the first step. ^{19}F NMR (376 MHz, EtOAc-CDCl_3) δ -117.10 (m), -122.7 (m). $\text{C}(\text{Ar}_\text{F}) = 1.6$ M.



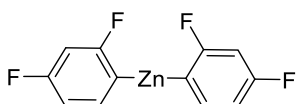
Prepared from 1,2,3,5-tetrafluorobenzene, 2 h for the first step. ^1H NMR (400 MHz, EtOAc-CDCl_3) δ 6.43 – 6.28 (m, 1H). ^{19}F NMR (376 MHz, EtOAc-CDCl_3) δ -93.6 (d, $J = 13.9$ Hz), -113.6 (d, $J = 29.7$ Hz), -137.9 (m), -169.0 (m). $\text{C}(\text{Ar}_\text{F}) = 1.5$ M.



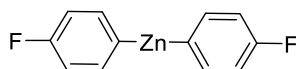
Prepared from 1,2,4,5-tetrafluorobenzene, 2 h for the first step. ^1H NMR (400 MHz, EtOAc-CDCl_3) δ 6.70 (m, 1H). ^{19}F NMR (376 MHz, EtOAc-CDCl_3) δ -120.5 (m), -140.8 (m). $\text{C}(\text{Ar}_\text{F}) = 0.9$ M.



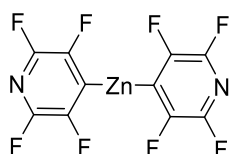
Prepared from 1,3,5-trifluorobenzene, 4 h for the first step. ^1H NMR (400 MHz, EtOAc-CDCl_3) δ 6.39 (dd, $J = 9.5, 5.1$ Hz, 1H). ^{19}F NMR (376 MHz, EtOAc-CDCl_3) δ -87.5 (m), -113.6 (m). $\text{C}(\text{Ar}_\text{F}) = 1.9$ M.



Prepared from 2,4-difluoro-1-iodobenzene, 2 h for the first step. ^1H NMR (400 MHz, EtOAc- CDCl_3) δ 7.33 (m, 1H), 6.68 (m, 1H), 6.55 (m, 1H). ^{19}F NMR (376 MHz, EtOAc- CDCl_3) δ -88.6, -114.7 (m). $\text{C}(\text{Ar}_\text{F}) = 1.2$ M.

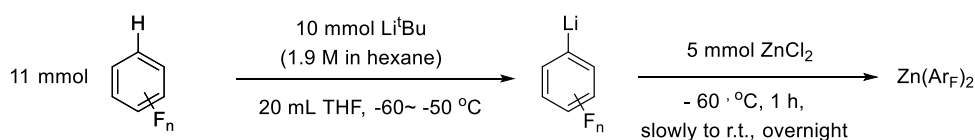


Prepared from 4-fluoro-1-iodobenzene, 2 h for the first step. ^1H NMR (400 MHz, EtOAc- CDCl_3) δ 7.51 (t, $J = 7.5$ Hz, 2H), 6.89 (m, 2H). ^{19}F NMR (376 MHz, EtOAc- CDCl_3) δ -115.38. $\text{C}(\text{Ar}_\text{F}) = 1.2$ M.



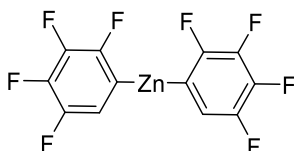
Prepared from 2,3,5,6 -tetrafluoropyridine with a different purification process (the product has poor solubility in DCM): After the reaction, the suspension was filtrated to get the solid. The solid was washed with THF and then DCM, and dried under vacuum. A white powder was obtained. Dissolving part of the powder in EtOAc led to a clear solution. ^{19}F NMR (376 MHz, EtOAc- CDCl_3) δ -98.39, -122.93. $\text{C}(\text{Ar}_\text{F}) = 0.5$ M.

Preparation of $\text{Zn}(\text{Ar}_\text{F})_2$ (as solution in EtOAc), method 2 (with Li^tBu)

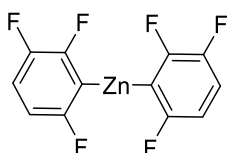


A 100-mL Schlenk tube was charged with 11 mmol polyfluoroarene and 20 mL THF under nitrogen. The reaction vessel was cooled to $-100\text{ }^\circ\text{C}$, and 5.3 mL Li^tBu (1.9 M in hexane) was added to the stirred solution by a syringe pump in 10 min. The reaction was maintained at $-60 \sim -50\text{ }^\circ\text{C}$ for 3 h. Then, 5 mmol ZnCl_2 was added to the solution, which was maintained at $-60\text{ }^\circ\text{C}$ for another one hour. The reaction was allowed to gradually warm to room temperature overnight. A clear solution was obtained. The solvent was removed under vacuum, and then the product was heated under vacuum for 2 h to remove the remaining solvent. A white or yellowish solid was obtained, which was dispersed in 10 mL DCM to give a suspension. Filtration was used to remove the solid and the

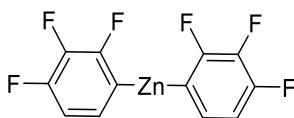
solvent was again removed under vacuum. The residual was dissolved in 5 mL EtOAc and the concentration of $\text{Zn}(\text{Ar}_\text{F})_2$ was determined using NMR, with pentafluorobenzene or 1,2,3,4-tetrafluorobenzene as internal standard.



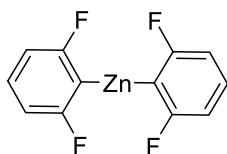
Prepared from 1,2,3,4-tetrafluorobenzene. ^1H NMR (400 MHz, EtOAc- CDCl_3) δ 6.88 (m, 1H). ^{19}F NMR (376 MHz, EtOAc- CDCl_3) δ -118.31 (m), -142.25 (m), -158.5 (m), -160.74 (m). $\text{C}(\text{Ar}_\text{F}) = 1.5$ M.



Prepared from 1,2,4-trifluorobenzene. ^1H NMR (400 MHz, EtOAc- CDCl_3) δ 6.79 – 6.72 (m, 1H), 6.49 (m, 1H). ^{19}F NMR (376 MHz, EtOAc- CDCl_3) δ -95.8, -114.6, -145.9. $\text{C}(\text{Ar}_\text{F}) = 1.6$ M.



Prepared from 1,2,3-trifluorobenzene. ^1H NMR (400 MHz, EtOAc- CDCl_3) δ 7.05 (m, 1H), 6.75 (m, 1H). ^{19}F NMR (376 MHz, EtOAc- CDCl_3) δ -115.00 (dd, $J = 31.1, 7.1$ Hz), -141.02 (dd, $J = 18.4, 7.1$ Hz), -165.08 (dd, $J = 31.1, 18.4$ Hz). $\text{C}(\text{Ar}_\text{F}) = 1.5$ M.

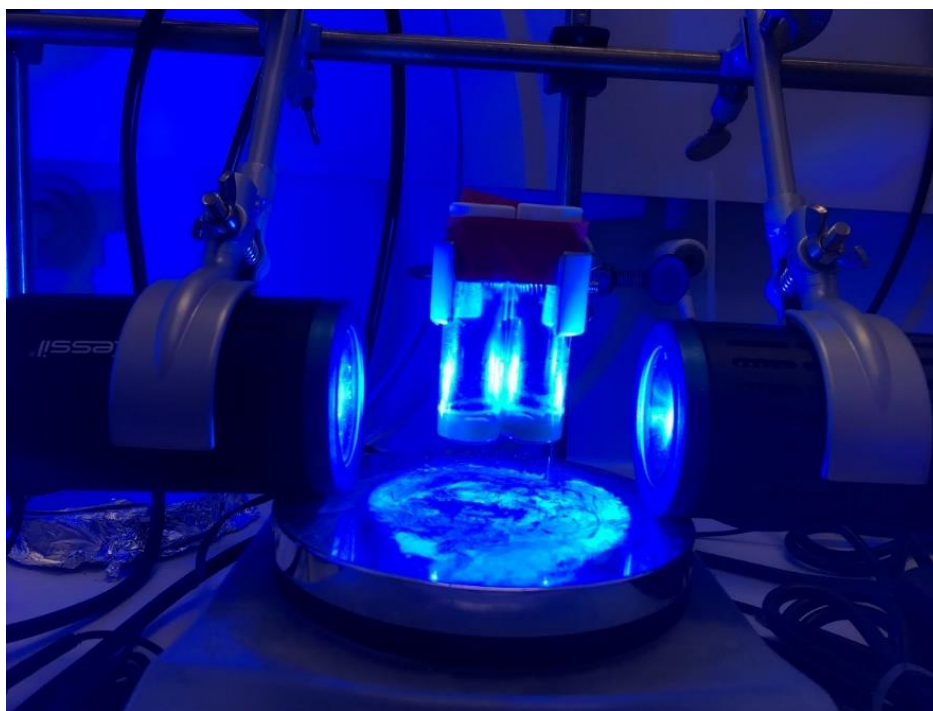


Prepared from 1,3-difluorobenzene. ^1H NMR (400 MHz, EtOAc- CDCl_3) δ 7.04 (tt, $J = 7.7, 6.6$ Hz, 1H), 6.62 (m, 2H). ^{19}F NMR (376 MHz, EtOAc- CDCl_3) δ -89.20. $\text{C}(\text{Ar}_\text{F}) = 1.8$ M.

4.7.3 Procedures for the decarboxylative coupling reaction

General procedure 1 (4-GP1):

0.1 mmol NHPI ester, 0.02 mmol dtbbpy and 0.001 mmol 4CzIPN were added to a glass vial (d=2 cm, 15 mL), which was transferred to the glovebox. 0.01 mmol $\text{Cu}(\text{OTf})_2$ and 0.5 mL EtOAc were added and a green solution was obtained. Then, 0.1 mmol 4-1 was added to the solution, which instantly turned yellow. The vial was properly sealed and placed in the photochemical setup (shown in the picture below). After 20 h, the reaction was stopped. To the reaction solution were added ethyl acetate (4 mL), water (1 mL) and 3 drops of 15% aqueous ammonia for workup. The organic phase obtained by extraction was concentrated. The residue was subsequently analyzed by GC-MS&FID to assess the reaction yield and was separated by chromatography on silica gel to give the final product.



General procedure 2 (4-GP2):

0.1 mmol NHPI ester, 0.02 mmol dtbbpy and 0.001 mmol 4CzIPN were added to a glass vial (d=2 cm, 12 mL), which was transferred to the glovebox. 0.01 mmol $\text{Cu}(\text{OTf})_2$, 0.1 mmol diglyme and (0.5-x) mL EtOAc were added and a green solution was obtained (x is the volume of $\text{Zn}(\text{Ar}_\text{F})_2$ solution

in EtOAc). Then, x mL of $\text{Zn}(\text{Ar}_\text{F})_2$ solution (0.1 mmol) was added to the vial, and the mixture turned yellow. The vial was properly sealed and placed in the photochemical setup. After 20 h, the reaction was stopped. To the reaction solution were added ethyl acetate (4 mL), water (1 mL) and 3 drops of 15% aqueous ammonia for workup. The organic phase obtained by extraction was concentrated. The residue was subsequently analyzed by GC-MS&FID to assess the reaction yield and was separated by chromatography on silica gel to give the final product.

4.7.4 Mechanistic investigations

4.7.4.1 UV-Vis spectroscopic study

All solutions and samples were prepared in the glovebox, including the stock solutions of (diglyme) $\text{Zn}(\text{C}_6\text{F}_5)_2$ (21.3 mg in 10.0 mL DCM, 4.0×10^{-3} M), (bpy) $\text{Cu}(\text{C}_6\text{F}_5)$ (15.4 mg in 10.0 mL DCM, 4.0×10^{-3} M) and (bpy) $\text{Cu}(\text{OTf})_2$ (14.4 mg $\text{Cu}(\text{OTf})_2$, 6.3 mg bipyridine in 10.0 mL DCM, 4.0×10^{-3} M). The sample solutions were prepared by mixing a given volume of stock solutions, and then diluted to 2.0 mL with DCM. The sample solution was placed in a cuvette with screw cap for further measurements on the UV-Vis spectrometer.

4.7.4.2 Cyclic voltammograms of the reagents

The CVs were recorded in DCM- CH_3CN (2:1, 4 mL) in a four-neck flask, with Bu_4NBF_4 (0.03 M) as electrolyte, glassy carbon disk as working electrode (diameter, 3 mm), Pt wire as counter electrode, $\text{Ag}|\text{AgCl}$, $\text{KCl}(\text{aq})$ as reference electrode. The device was assembled in the glovebox to guarantee an inert atmosphere. The scan rate for CV was 100 mV/s.

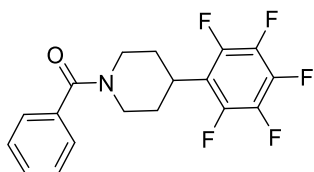
$E(\text{Fc}^+/\text{Fc})$ comparing to the reference electrode was 0.227 V (determined with 0.003 M Fc). All the potential values were converted using $E(\text{Fc}^+/\text{Fc})$ as reference.

4.7.4.3 Stern-Volmer quenching

All solutions and samples were prepared in a glovebox, including the stock solutions of 4CzIPN (3.2 mg in 10.0 mL DCM, 4.0×10^{-4} M), 4-2 (37.8 mg in 10.0 mL DCM, 10^{-2} M), (diglyme) $\text{Zn}(\text{C}_6\text{F}_5)_2$ (21.3 mg in 10.0 mL DCM, 4.0×10^{-3} M), (bpy) $\text{Cu}(\text{C}_6\text{F}_5)$ (15.4 mg in 10.0 mL DCM, 4.0×10^{-3} M). The sample solutions were prepared by mixing given volume of stock solutions, and

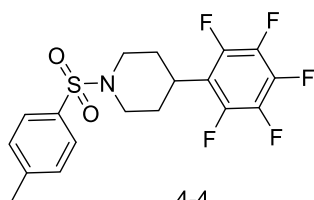
then diluted to 2.0 mL with DCM. The sample solution was placed in a cuvette with screw cap for further measurements on a fluorescence spectrometer. Parameters: exciting wavelength (420 nm, slit 2.5 nm), emission measurement (430 nm-700 nm).

4.7.5 Characterization data of the products



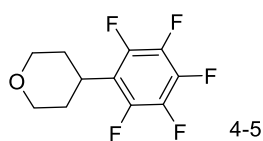
4-3

4-(4-(Perfluorophenyl)piperidin-1-yl)(phenyl)methanone, synthesized via 4-GP1, colorless crystal, 30.1 mg (Yield = 85%). ^1H NMR (400 MHz, CDCl_3) δ 7.42 (m, 5H), 4.91 (b, 1H), 3.90 (b, 1H), 3.26 (tt, J = 12.5, 3.7 Hz, 1H), 3.08 (b, 1H), 2.84 (b, 1H), 2.04 (b, 2H), 1.89 – 1.63 (b, 2H). ^{19}F NMR (376 MHz, CDCl_3) δ -142.7 (m), -156.7 (t, J = 20.7 Hz), -162.0 (td, J = 22.0, 7.8 Hz). ^{13}C NMR (101 MHz, CDCl_3) δ 170.6, 136.0, 129.8, 128.7, 126.9, 48.3, 42.9, 33.6, 30.5. GC-MS: 355. HRMS (ESI/QTOF) m/z : $[\text{M} + \text{H}]^+$ Calcd for $\text{C}_{18}\text{H}_{15}\text{F}_5\text{NO}^+$ 356.1068; Found 356.1065.



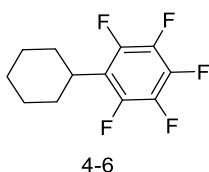
4-4

4-(4-(Perfluorophenyl)-1-tosylpiperidine, synthesized via 4-GP1, colorless crystal, 23.1 mg (Yield = 57%). ^1H NMR (400 MHz, CDCl_3) δ 7.67 (d, J = 8.0 Hz, 2H), 7.35 (d, J = 8.0 Hz, 2H), 3.96 (d, J = 11.6, 2H), 2.88 (tt, J = 12.4, 3.6 Hz, 1H), 2.45 (s, 3H), 2.39 – 2.28 (m, 2H), 2.25 – 2.10 (m, 2H), 1.76 (d, J = 12.2 Hz, 2H). ^{19}F NMR (376 MHz, CDCl_3) δ -142.5 (m), -156.5 (t, J = 20.9 Hz), -161.9 (td, J = 21.6, 7.7 Hz). ^{13}C NMR (101 MHz, CDCl_3) δ 143.9, 133.2, 129.9, 127.9, 46.9, 32.8, 29.5, 21.7. GC-MS: 405. HRMS (ESI/QTOF) m/z : $[\text{M} + \text{H}]^+$ Calcd for $\text{C}_{18}\text{H}_{17}\text{F}_5\text{NO}_2\text{S}^+$ 406.0895; Found 406.0895.

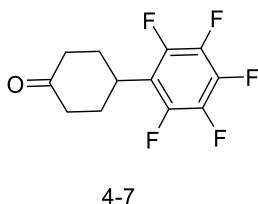


4-5

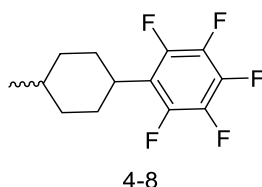
4-(Perfluorophenyl)tetrahydro-2H-pyran, synthesized via 4-GP1, white solid, 18.8 mg (Yield = 67%). ^1H NMR (400 MHz, CDCl_3) δ 4.08 (dd, $J = 11.7, 4.5$ Hz, 2H), 3.50 (td, $J = 11.9, 1.9$ Hz, 2H), 3.24 (tt, $J = 12.5, 3.8$ Hz, 1H), 2.26 – 2.10 (m, 2H), 1.63 (dd, $J = 12.9, 3.7$ Hz, 2H). ^{19}F NMR (376 MHz, CDCl_3) δ -142.9 (m), -157.28 (t, $J = 20.9$ Hz), -162.37 (td, $J = 21.5, 7.3$ Hz). ^{13}C NMR (101 MHz, CDCl_3) δ 68.4, 32.6, 30.8. GC-MS: 252. HRMS (APPI/LTQ-Orbitrap) m/z : $[\text{M} + \text{H}_1]^+$ Calcd for $\text{C}_{11}\text{H}_8\text{F}_5\text{O}^+$ 251.0490; Found 251.0496.



1-Cyclohexyl-2,3,4,5,6-pentafluorobenzene, synthesized via 4-GP1, colorless liquid, 19.3mg (Yield = 77%). ^1H NMR (400 MHz, CDCl_3) δ 2.98 (m, 1H), 1.91 – 1.68 (m, 7H), 1.45 – 1.21 (m, 3H). ^{19}F NMR (376 MHz, CDCl_3) δ -143.0 (m), -158.7 (t, $J = 20.6$ Hz), -163.1 (td, $J = 22.3, 7.4$ Hz, 2F). ^{13}C NMR (101 MHz, CDCl_3) δ 35.4, 31.1, 26.9, 25.8. GC-MS: 250.

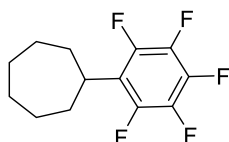


4-(Perfluorophenyl)cyclohexan-1-one, synthesized via 4-GP1, white solid, 19.4 mg (Yield = 73 %). ^1H NMR (400 MHz, CDCl_3) δ 3.48 (tt, $J = 12.4, 3.6$ Hz, 1H), 2.59 – 2.42 (m, 4H), 2.36 – 2.20 (m, 2H), 2.18 – 2.06 (m, 2H). ^{19}F NMR (376 MHz, CDCl_3) δ -142.6 (m), -156.6 (t, $J = 21.2$ Hz), -161.8 (m, 2F). ^{13}C NMR (101 MHz, CDCl_3) δ 209.4, 41.3, 33.6, 30.5. GC-MS: 264. HRMS (APPI/LTQ-Orbitrap) m/z : $[\text{M} + \text{H}]^+$ Calcd for $\text{C}_{12}\text{H}_{10}\text{F}_5\text{O}^+$ 265.0646; Found 265.0651.



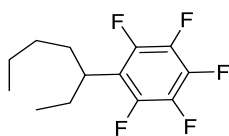
1,2,3,4,5-Pentafluoro-6-(4-methylcyclohexyl)benzene, synthesized via 4-GP1, colorless liquid, 20.1 mg (Yield = 76 %, dr = 1:2.6). ^1H NMR (400 MHz, CDCl_3) δ 2.94 (m, 1H), 2.11 – 1.95 (m, 1H), 1.92 – 1.56 (m, 6H), 1.56 – 1.39 (m, 1H), 1.14 – 0.90 (m, 4H). ^{19}F NMR (376 MHz, CDCl_3) δ -142.9 (major), -

143.2 (minor), -158.6, -163.1. ^{13}C NMR (101 MHz, CDCl_3) δ (major & minor) 35.5, 35.0, 32.1, 32.0, 30.9, 26.5, 25.0, 22.7, 17.3. GC-MS: 264. HRMS (nanochip-ESI/LTQ-Orbitrap) m/z : $[\text{M} + \text{H}_1]^+$ Calcd for $\text{C}_{13}\text{H}_{12}\text{F}_5^+$ 263.0854; Found 263.0853.



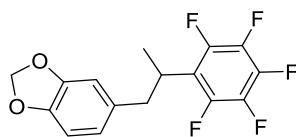
4-9

(Perfluorophenyl)cycloheptane, synthesized via 4-GP1, colorless liquid, 14.6 mg (Yield = 55 %). ^1H NMR (400 MHz, CDCl_3) δ 3.11 (tt, $J = 10.7, 3.3$ Hz, 1H), 1.95 – 1.73 (m, 6H), 1.72 – 1.41 (m, 6H). ^{19}F NMR (376 MHz, CDCl_3) δ -143.0 (dd, $J = 22.7, 7.9$ Hz), -159.1 (t, $J = 20.7$ Hz), -162.9 – -163.4 (m). ^{13}C NMR (101 MHz, CDCl_3) δ 36.9, 33.7, 27.9, 27.7. GC-MS: 264.



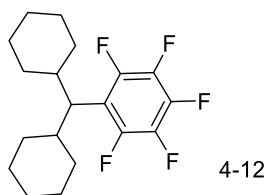
4-10

(1,2,3,4,5-Pentafluoro-6-(heptan-3-yl)benzene, synthesized via 4-GP1, colorless liquid, 20.5 mg (Yield = 77 %). ^1H NMR (400 MHz, CDCl_3) δ 2.97 (tt, $J = 9.2, 6.4$ Hz, 1H), 1.83 – 1.63 (m, 4H), 1.37 – 1.01 (m, 4H), 0.83 (m, 6H). ^{19}F NMR (376 MHz, CDCl_3) δ -142.4 (dd, $J = 22.9, 8.0$ Hz), -158.1 (td, $J = 20.6, 4.0$ Hz), -162.9 (m). ^{13}C NMR (101 MHz, CDCl_3) δ 38.4, 33.5, 30.3, 27.0, 22.7, 14.1, 12.6. GC-MS: 266. HRMS (EI/LTQ-Orbitrap) m/z : $[\text{M}]^+$ Calcd for $\text{C}_{13}\text{H}_{15}\text{F}_5^+$ 266.1088; Found 266.1087.

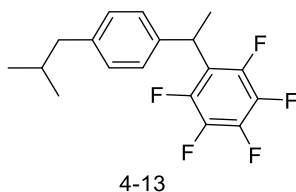


4-11

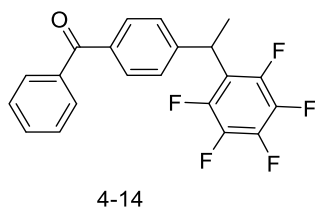
5-(2-(perfluorophenyl)propyl)benzo[d][1,3]dioxole, synthesized via 4-GP1, colorless liquid, 17.6 mg (Yield = 53 %). ^1H NMR (400 MHz, CDCl_3) δ 6.66 (d, $J = 7.8$ Hz, 1H), 6.60 (d, $J = 1.8$ Hz, 1H), 6.53 (dd, $J = 7.9, 1.7$ Hz, 1H), 5.91 (s, 2H), 3.45 (h, $J = 7.4$ Hz, 1H), 2.90 (d, $J = 8.1$ Hz, 2H), 1.37 (d, $J = 7.1$ Hz, 3H). ^{19}F NMR (376 MHz, CDCl_3) δ -142.8 (m), -157.6 (t, $J = 21.1$ Hz), -162.7 (td, $J = 22.3, 7.7$ Hz). ^{13}C NMR (101 MHz, CDCl_3) δ 147.8, 146.2, 133.4, 121.7, 109.0, 108.3, 101.0, 41.2, 32.8, 19.1. GC-MS: 330. HRMS (APPI/LTQ-Orbitrap) m/z : $[\text{M}]^+$ Calcd for $\text{C}_{16}\text{H}_{11}\text{F}_5\text{O}_2^+$ 330.0674; Found 330.0678.



((Perfluorophenyl)methylene)dicyclohexane, synthesized via 4-GP1, colorless liquid, 22.1 mg (Yield = 64 %). ^1H NMR (400 MHz, CDCl_3) δ 2.80 (t, $J = 7.6$ Hz, 1H), 1.99 (qd, $J = 7.8, 4.1$ Hz, 2H), 1.87 – 1.49 (m, 10H), 1.36 – 0.97 (m, 6H), 0.94 – 0.65 (m, 4H). ^{19}F NMR (376 MHz, CDCl_3) δ -135.6 (dd, $J = 22.9, 8.0$ Hz), -139.3 (dd, $J = 24.0, 8.0$ Hz), -157.7 (t, $J = 20.6$ Hz), -162.9 (td, $J = 21.7, 8.0$ Hz), -163.2 (td, $J = 22.9, 8.0$ Hz). ^{13}C NMR (101 MHz, CDCl_3) δ 48.7, 48.6, 37.2, 32.4, 30.5, 30.4, 26.6. GC-MS: 346. HRMS (EI/LTQ-Orbitrap) m/z : $[\text{M}]^+$ Calcd for $\text{C}_{19}\text{H}_{23}\text{F}_5^+$ 346.1714; Found 346.1717.

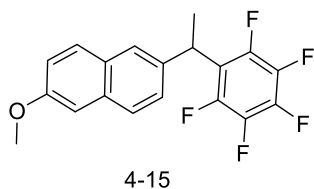


1,2,3,4,5-pentafluoro-6-(1-(4-isobutylphenyl)ethyl)benzene, synthesized via 4-GP1, colorless liquid, 28.9 mg (Yield = 88 %). ^1H NMR (400 MHz, CDCl_3) δ 7.19 (d, $J = 8.2$ Hz, 2H), 7.08 (d, $J = 8.2$ Hz, 2H), 4.55 (q, $J = 7.3$ Hz, 1H), 2.44 (d, $J = 7.2$ Hz, 2H), 1.83 (m, 1H), 1.74 (dt, $J = 7.5, 1.2$ Hz, 3H), 0.89 (d, $J = 6.6$ Hz, 6H). ^{19}F NMR (376 MHz, CDCl_3) δ -142.5 (m), -157.7 (t, $J = 21.2$ Hz), -162.5 (td, $J = 22.3, 8.0$ Hz). ^{13}C NMR (101 MHz, CDCl_3) δ 140.5, 139.5, 129.4, 126.9, 45.1, 34.3, 30.3, 22.5, 18.5. GC-MS: 328. HRMS (APPI/LTQ-Orbitrap) m/z : $[\text{M}]^+$ Calcd for $\text{C}_{18}\text{H}_{17}\text{F}_5^+$ 328.1245; Found 328.1253.

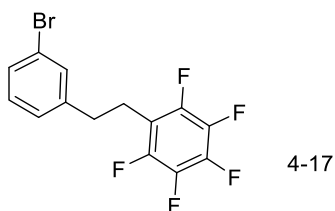


4-(1-(perfluorophenyl)ethyl)phenyl(phenyl)methanone, synthesized via 4-GP1, colorless liquid, 27.1mg (Yield = 72 %). ^1H NMR (400 MHz, CDCl_3) δ 7.83 – 7.74 (m, 3H), 7.68 – 7.55 (m, 2H), 7.54 – 7.46 (m, 3H), 7.42 (t, $J = 7.7$ Hz, 1H), 4.66 (q, $J = 7.4$ Hz, 1H), 1.79 (dt, $J = 7.4, 1.2$ Hz, 3H). ^{19}F NMR (376 MHz, CDCl_3) δ -142.3 (m), -156.6 (t, $J = 20.9$ Hz), -161.9 (td, $J = 21.9, 7.9$ Hz). ^{13}C NMR (101 MHz, CDCl_3) δ 196.6, 142.5, 138.1, 137.6, 132.7, 131.3, 130.2, 128.9, 128.6,

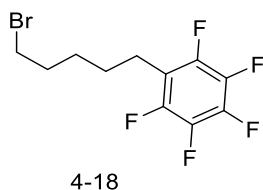
128.4, 34.4, 18.4. GC-MS: 376. HRMS (APPI/LTQ-Orbitrap) m/z : $[M + H]^+$ Calcd for $C_{21}H_{14}F_5O^+$ 377.0959; Found 377.0972.



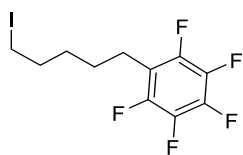
2-methoxy-6-(1-(perfluorophenyl)ethyl)naphthalene, synthesized via 4-GP1, white solid, 29.5 mg (Yield = 84 %). 1H NMR (400 MHz, $CDCl_3$) δ 7.75 – 7.65 (m, 3H), 7.39 – 7.32 (m, 1H), 7.21 – 7.08 (m, 2H), 4.72 (q, $J = 7.4$ Hz, 1H), 3.92 (s, 3H), 1.85 (dt, $J = 7.3, 1.1$ Hz, 3H). ^{19}F NMR (376 MHz, $CDCl_3$) δ -142.5 (m), -157.4 (d, $J = 21.0$ Hz), -162.3 (m). ^{13}C NMR (101 MHz, $CDCl_3$) δ 157.9, 137.3, 133.6, 129.4, 129.0, 127.3, 126.3, 125.3, 119.2, 105.7, 55.4, 34.6, 18.4. GC-MS: 352. HRMS (APPI/LTQ-Orbitrap) m/z : $[M]^+$ Calcd for $C_{19}H_{13}F_5O^+$ 352.0881; Found 352.0893.



1-(3-bromophenethyl)-2,3,4,5,6-pentafluorobenzene, synthesized via 4-GP1, white solid, 24.5 mg (Yield = 70 %). 1H NMR (400 MHz, $CDCl_3$) δ 7.40 – 7.31 (m, 2H), 7.16 (t, $J = 7.8$ Hz, 1H), 7.09 (dt, $J = 7.6, 1.5$ Hz, 1H), 2.98 (m, 2H), 2.84 (m, 2H). ^{19}F NMR (376 MHz, $CDCl_3$) δ -144.2 (m), -157.1 (t, $J = 21.2$ Hz), -162.5 (m). ^{13}C NMR (101 MHz, $CDCl_3$) δ 142.4, 131.6, 130.3, 129.9, 127.1, 122.7, 35.1, 24.3. GC-MS: 350. HRMS (EI/LTQ-Orbitrap) m/z : $[M]^+$ Calcd for $C_{14}H_8BrF_5^+$ 349.9724; Found 349.9729.

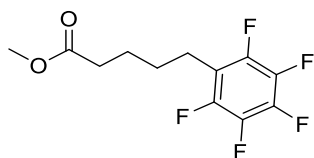


1-(5-bromopentyl)-2,3,4,5,6-pentafluorobenzene, synthesized via 4-GP1, colorless liquid, 24.7 mg (Yield = 78 %). 1H NMR (400 MHz, $CDCl_3$) δ 3.40 (t, $J = 6.7$ Hz, 2H), 2.71 (tt, $J = 7.6, 1.8$ Hz, 2H), 1.89 (p, $J = 6.9$ Hz, 2H), 1.68 – 1.56 (m, 2H), 1.55 – 1.44 (m, 2H). ^{19}F NMR (376 MHz, $CDCl_3$) δ -144.3 (m), -157.95 (t, $J = 21.1$ Hz), -162.91 (td, $J = 22.2, 8.5$ Hz). ^{13}C NMR (101 MHz, $CDCl_3$) δ 33.2, 32.1, 28.2, 27.4, 21.9. GC-MS: 316.



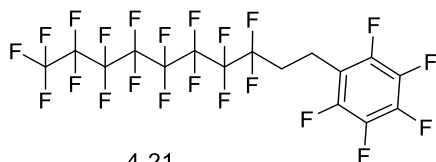
4-19

1-(5-iodopentyl)-2,3,4,5,6-pentafluorobenzene, synthesized via 4-GP1, colorless liquid, 16.2 mg (Yield = 45 %). ^1H NMR (400 MHz, CDCl_3) δ 3.21 (t, J = 7.0, 2H), 2.74 (m, 2H), 1.94 – 1.82 (m, 2H), 1.64 (p, J = 7.6 Hz, 2H), 1.48 (p, J = 7.7 Hz, 2H). ^{19}F NMR (376 MHz, CDCl_3) δ -144.4 (m), -157.9 (t, J = 20.8 Hz), -162.87 (td, J = 22.0, 8.5 Hz). ^{13}C NMR (101 MHz, CDCl_3) δ 33.1, 30.1, 28.3, 22.2, 6.4. GC-MS: 364. HRMS (EI/LTQ-Orbitrap) m/z : $[\text{M}]^+$ Calcd for $\text{C}_{11}\text{H}_{10}\text{F}_5\text{I}^+$ 363.9742; Found 363.9748.



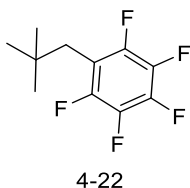
4-20

methyl 5-(perfluorophenyl)pentanoate, synthesized via 4-GP1, colorless liquid, 22.5 mg (Yield = 80 %). ^1H NMR (400 MHz, CDCl_3) δ 3.66 (s, 3H), 2.76 – 2.67 (m, 2H), 2.34 (t, J = 7.0 Hz, 2H), 1.64 (m, 4H). ^{19}F NMR (376 MHz, CDCl_3) δ -144.3 (dd, J = 22.1, 8.4 Hz), -157.9 (t, J = 20.6 Hz), -162.92 (td, J = 22.1, 8.5 Hz). ^{13}C NMR (101 MHz, CDCl_3) δ 173.8, 51.7, 33.7, 28.8, 24.4, 22.1. GC-MS: 282. HRMS (EI/LTQ-Orbitrap) m/z : $[\text{M}]^+$ Calcd for $\text{C}_{12}\text{H}_{11}\text{F}_5\text{O}_2^+$ 282.0674; Found 282.0679.

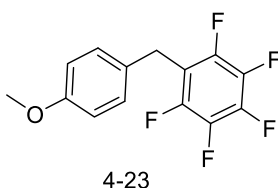


4-21

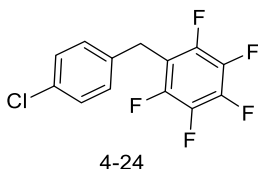
1,2,3,4,5-pentafluoro-6-(3,3,4,4,5,5,6,6,7,7,8,8,9,9,10,10,10-heptafluorodecyl)benzene, synthesized via 4-GP1, colorless liquid, 29.5 mg (Yield = 48 %). ^1H NMR (400 MHz, CDCl_3) δ 3.04 (m, 2H), 2.38 (m, 2H). ^{19}F NMR (376 MHz, CDCl_3) δ -80.8 (m), -115.3 (m), -121.5 – -122.1 (m), -122.7 (m), -123.5 (m), -126.1 (m), -143.9 (dt, J = 20.0, 9.6 Hz), -155.7 (t, J = 20.6 Hz), -161.8 (dt, J = 20.7, 10.7 Hz). ^{13}C NMR (101 MHz, CDCl_3) δ 29.3 (t, J = 22.3 Hz), 13.0. HRMS (EI/LTQ-Orbitrap) m/z : $[\text{M}]^+$ Calcd for $\text{C}_{16}\text{H}_4\text{F}_{22}^+$ 613.9956; Found 613.9965.



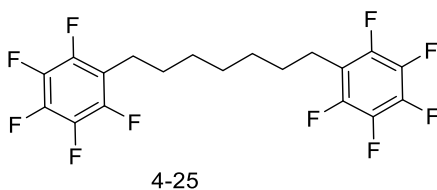
1,2,3,4,5-pentafluoro-6-neopentylbenzene, synthesized via 4-GP1, colorless liquid, 8.5 mg (Yield = 36 %). ^1H NMR (400 MHz, CDCl_3) δ 2.60 (s, 2H), 0.95 (t, $J = 1.3$ Hz, 9H). ^{19}F NMR (376 MHz, CDCl_3) δ -140.1 (m), -157.5 (t, $J = 21.1$ Hz), -163.2 (m). ^{13}C NMR (101 MHz, CDCl_3) δ 35.9, 33.1, 29.3. GC-MS: 238. HRMS (EI/LTQ-Orbitrap) m/z : $[\text{M}]^+$ Calcd for $\text{C}_{11}\text{H}_{11}\text{F}_5^+$ 238.0775; Found 238.0770.



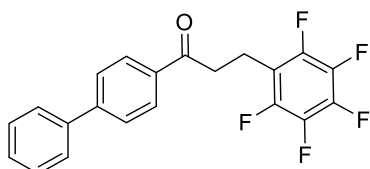
1,2,3,4,5-pentafluoro-6-(4-methoxybenzyl)benzene, synthesized via 4-GP1, colorless liquid, 19.5 mg (Yield = 68 %). ^1H NMR (400 MHz, CDCl_3) δ 7.21 – 7.13 (m, 2H), 6.87 – 6.79 (m, 2H), 3.96 (t, $J = 2.1$ Hz, 2H), 3.78 (s, 3H). ^{19}F NMR (376 MHz, CDCl_3) δ -143.6 (dd, $J = 22.9, 8.0$ Hz), -157.4 (t, $J = 20.6$ Hz), -162.4 (m). ^{13}C NMR (101 MHz, CDCl_3) δ 158.7, 129.7, 129.6, 114.3, 55.4, 27.5. GC-MS: 288. HRMS (APPI/LTQ-Orbitrap) m/z : $[\text{M}]^+$ Calcd for $\text{C}_{14}\text{H}_9\text{F}_5\text{O}^+$ 288.0568; Found 288.0578.



1-(4-chlorobenzyl)-2,3,4,5,6-pentafluorobenzene, synthesized via 4-GP1, colorless liquid, 21.3 mg (Yield = 73 %). ^1H NMR (400 MHz, CDCl_3) δ 7.29 – 7.21 (m, 2H), 7.15 (d, $J = 8.2$ Hz, 2H), 3.98 (s, 2H). ^{19}F NMR (376 MHz, CDCl_3) δ -143.24 – -143.38 (m), -156.47 (t, $J = 21.1$ Hz), -161.99 (td, $J = 22.1, 8.5$ Hz). ^{13}C NMR (101 MHz, CDCl_3) δ 136.0, 133.1, 129.9, 129.1, 27.7. GC-MS: 292. HRMS (APPI/LTQ-Orbitrap) m/z : $[\text{M}-\text{H}]^-$ Calcd for $\text{C}_{13}\text{H}_5\text{F}_5\text{O}^-$ 291.0005; Found 291.0002.

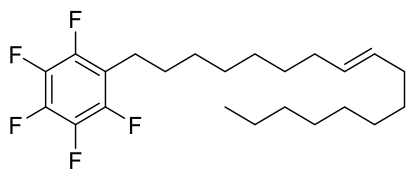


1,7-bis(perfluorophenyl)heptane, synthesized via modified 4-GP1 (with 200 mol% **b1**), colorless liquid, 27.2 mg (Yield = 63 %). ^1H NMR (400 MHz, CDCl_3) δ 2.68 (m, 4H), 1.63 – 1.50 (m, 4H), 1.41 – 1.27 (m, 6H). ^{19}F NMR (376 MHz, CDCl_3) δ -144.5 (m), -158.4 (m), -163.1 (m). ^{13}C NMR (101 MHz, CDCl_3) δ 29.3, 29.0, 28.9, 22.4. GC-MS: 432. HRMS (EI/LTQ-Orbitrap) m/z : $[\text{M}]^+$ Calcd for $\text{C}_{19}\text{H}_{14}\text{F}_{10}^+$ 432.0930; Found 432.0929.



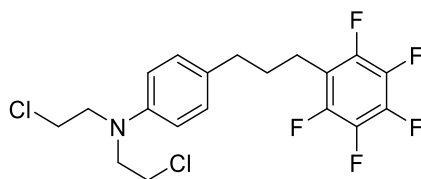
4-26

1-([1,1'-biphenyl]-4-yl)-3-(perfluorophenyl)propan-1-one, synthesized via 4-GP1, white solid, 26.4mg (Yield = 70 %). ^1H NMR (400 MHz, CDCl_3) δ 8.02 (d, J = 8.5 Hz, 2H), 7.69 (d, J = 8.4 Hz, 2H), 7.63 (d, J = 6.9 Hz, 2H), 7.48 (t, J = 7.3 Hz, 2H), 7.41 (t, J = 7.3 Hz, 1H), 3.33 (t, J = 7.4 Hz, 2H), 3.21 – 3.12 (m, 2H). ^{19}F NMR (376 MHz, CDCl_3) δ -143.4 (m), -157.3 (t, J = 20.7 Hz), -162.6 (td, J = 21.8, 8.1 Hz). ^{13}C NMR (101 MHz, CDCl_3) δ 197.4, 146.3, 139.9, 135.1, 129.1, 128.7, 128.5, 127.5, 127.4, 37.6, 17.3. GC-MS: 376. HRMS (ESI/QTOF) m/z : $[\text{M} + \text{H}]^+$ Calcd for $\text{C}_{21}\text{H}_{14}\text{F}_5\text{O}^+$ 377.0959; Found 377.0962.



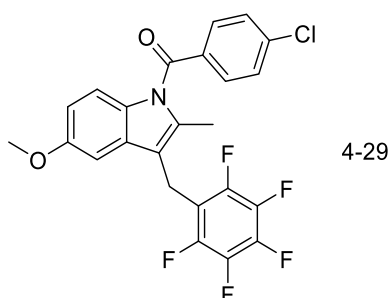
4-27

(E)-1,2,3,4,5-pentafluoro-6-(heptadec-8-en-1-yl)benzene, synthesized via 4-GP1, colorless liquid, 37.3 mg (Yield = 92 %). ^1H NMR (400 MHz, CDCl_3) δ 5.42 – 5.35 (m, 2H), 2.73 – 2.63 (m, 2H), 1.96 (q, J = 6.6 Hz, 4H), 1.56 (dd, J = 14.8, 7.3 Hz, 2H), 1.34 – 1.19 (m, 20H), 0.92 – 0.84 (m, 3H). ^{19}F NMR (376 MHz, CDCl_3) δ -144.5 (m), -158.5 (t, J = 20.8 Hz), -163.3 (m). ^{13}C NMR (101 MHz, CDCl_3) δ 130.7, 130.3, 32.8, 32.7, 32.1, 29.8, 29.7, 29.7, 29.5, 29.4, 29.3, 29.2, 29.2, 29.1, 22.8, 22.5, 14.2. GC-MS: 404.

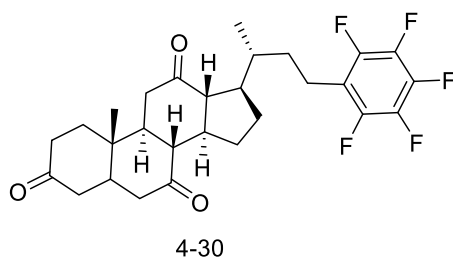


4-28

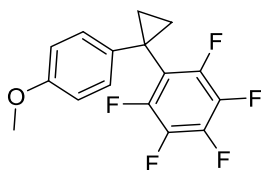
N,N-bis(2-chloroethyl)-4-(3-(perfluorophenyl)propyl)aniline, synthesized via 4-GP1, yellowish liquid, 27.2 mg (Yield = 64 %). ^1H NMR (400 MHz, CDCl_3) δ 7.12 – 7.04 (m, 2H), 6.68 – 6.58 (m, 2H), 3.71 (m, 4H), 3.65 – 3.59 (m, 4H), 2.73 (t, J = 7.6 Hz, 2H), 2.59 (t, J = 7.8 Hz, 2H), 1.94 – 1.81 (m, 2H). ^{19}F NMR (376 MHz, CDCl_3) δ -144.2 (m), -158.1 (t, J = 20.8 Hz), -163.0 (m, 2F). ^{13}C NMR (101 MHz, CDCl_3) δ 144.5, 130.5, 129.6, 112.3, 53.7, 40.6, 34.3, 31.0, 22.2. GC-MS: 425. HRMS (ESI/QTOF) m/z : $[\text{M} + \text{H}]^+$ Calcd for $\text{C}_{19}\text{H}_{19}\text{Cl}_2\text{F}_5\text{N}^+$ 426.0809; Found 426.0813.



(4-chlorophenyl)(5-methoxy-2-methyl-3-((perfluorophenyl)methyl)-1H-indol-1-yl)methanone, synthesized via 4-GP1, white solid, 30.1 mg (Yield = 63 %). ^1H NMR (400 MHz, CDCl_3) δ 7.69 – 7.60 (m, 2H), 7.51 – 7.43 (m, 2H), 6.96 (d, J = 2.5 Hz, 1H), 6.84 (d, J = 9.0 Hz, 1H), 6.65 (dd, J = 9.0, 2.5 Hz, 1H), 4.05 (d, J = 1.7 Hz, 2H), 3.82 (s, 3H), 2.46 (s, 3H). ^{19}F NMR (376 MHz, CDCl_3) δ -142.1 (m), -156.7 (t, J = 20.9 Hz), -162.2 (m). ^{13}C NMR (101 MHz, CDCl_3) δ 168.5, 156.1, 139.6, 135.7, 134.0, 131.3, 130.9, 130.1, 129.3, 115.1, 114.8, 111.7, 100.9, 55.7, 17.6, 13.3. GC-MS: 479. HRMS (ESI/QTOF) m/z : $[\text{M} + \text{H}]^+$ Calcd for $\text{C}_{24}\text{H}_{16}\text{ClF}_5\text{NO}_2^+$ 480.0784; Found 480.0794.

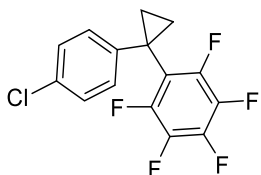


Synthesized via 4-GP1, white solid, 21.4 mg (Yield = 42 %). ^1H NMR (400 MHz, CDCl_3) δ 2.96 – 2.71 (m, 4H), 2.60 (m, 1H), 2.40 – 1.92 (m, 11H), 1.86 (m, 1H), 1.64 (m, 1H), 1.46 – 1.21 (m, 7H), 1.07 (s, 3H), 0.97 (d, J = 6.5 Hz, 3H). ^{19}F NMR (376 MHz, CDCl_3) δ -144.9 (dd, J = 22.5, 8.2 Hz), -158.4 (t, J = 20.9 Hz), -163.0 (td, J = 21.8, 8.2 Hz). ^{13}C NMR (101 MHz, CDCl_3) δ 212.0, 209.1, 208.8, 116.0, 57.0, 51.9, 49.1, 47.0, 45.7, 45.4, 45.1, 42.9, 38.8, 36.6, 36.2, 36.2, 35.4, 35.2, 27.8, 25.3, 22.1, 19.7, 18.8, 12.0. HRMS (ESI/QTOF) m/z : $[\text{M} + \text{Na}]^+$ Calcd for $\text{C}_{29}\text{H}_{33}\text{F}_5\text{NaO}_3^+$ 547.2242; Found 547.2259.



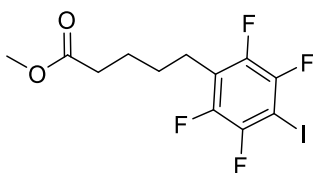
4-33

1,2,3,4,5-pentafluoro-6-(1-(4-methoxyphenyl)cyclopropyl)benzene, synthesized via 4-GP1, colorless liquid, 12.5 mg (Yield = 40 %). ^1H NMR (400 MHz, CDCl_3) δ 7.34 – 7.28 (m, 2H), 6.84 – 6.78 (m, 2H), 3.77 (s, 3H), 1.40 – 1.35 (m, 2H), 1.25 – 1.19 (m, 2H). ^{19}F NMR (376 MHz, CDCl_3) δ -140.7 (m), -156.9 (t, J = 20.8 Hz), -162.6 (m). ^{13}C NMR (101 MHz, CDCl_3) δ 158.7, 135.2, 129.4, 114.1, 55.4, 19.1, 14.4. GC-MS: 314. HRMS (APPI/LTQ-Orbitrap) m/z : $[\text{M}]^+$ Calcd for $\text{C}_{16}\text{H}_{11}\text{F}_5\text{O}^+$ 314.0725; Found 314.0737.



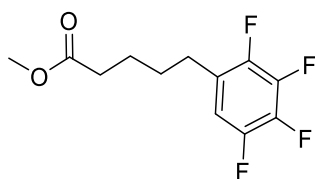
4-34

1,2,3,4,5-pentafluoro-6-(1-(4-chlorophenyl)cyclopropyl)benzene, synthesized via 4-GP1, colorless liquid, 19.1 mg (Yield = 60 %). ^1H NMR (400 MHz, CDCl_3) δ 7.25 (m, 4H), 1.41 (m, 2H), 1.32 – 1.22 (m, 2H). ^{19}F NMR (376 MHz, CDCl_3) δ -140.3 (dd, J = 22.0, 8.1 Hz), -155.9 (t, J = 21.0 Hz), -162.2 (td, J = 21.8, 8.0 Hz). ^{13}C NMR (101 MHz, CDCl_3) δ 141.4, 132.9, 129.3, 128.9, 19.2, 15.0. GC-MS: 318. HRMS (APPI/LTQ-Orbitrap) m/z : $[\text{M}]^+$ Calcd for $\text{C}_{15}\text{H}_8\text{ClF}_5^+$ 318.0229; Found 318.0240.



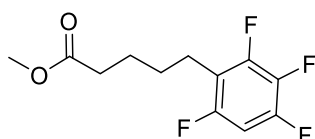
4-35a

methyl 5-(2,3,5,6-tetrafluoro-4-iodophenyl)pentanoate, synthesized via 4-GP2, colorless liquid, 21.0 mg (Yield = 54 %). ^1H NMR (400 MHz, CDCl_3) δ 3.67 (s, 3H), 2.75 (t, J = 7.0 Hz, 2H), 2.35 (t, J = 7.0 Hz, 2H), 1.67 (m, 4H). ^{19}F NMR (376 MHz, CDCl_3) δ -121.5 (m), -142.3 (m). ^{13}C NMR (101 MHz, CDCl_3) δ 173.8, 51.7, 33.7, 28.5, 24.5, 23.0. GC-MS: 390. HRMS (EI/LTQ-Orbitrap) m/z : $[\text{M}]^+$ Calcd for $\text{C}_{12}\text{H}_{11}\text{IF}_4\text{O}_2^+$ 389.9734; Found 389.9724.



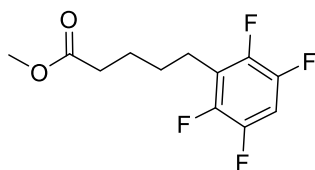
4-36a

methyl 5-(2,3,4,5-tetrafluorophenyl)pentanoate, synthesized via 4-GP2, colorless liquid, 13.4 mg (Yield = 51 %). ^1H NMR (400 MHz, CDCl_3) δ 6.79 (m, 1H), 3.67 (s, 3H), 2.67 – 2.57 (m, 2H), 2.34 (t, J = 7.0 Hz, 2H), 1.73 – 1.55 (m, 4H). ^{19}F NMR (376 MHz, CDCl_3) δ -140.3 (dd, J = 21.1, 12.6 Hz), -144.2 (dd, J = 20.8, 12.4 Hz), -156.3 (t, J = 20.1 Hz), -159.3 (t, J = 20.2 Hz). ^{13}C NMR (101 MHz, CDCl_3) δ 173.9, 111.2, 51.7, 33.8, 29.3, 28.3, 24.4. GC-MS: 264. HRMS (EI/LTQ-Orbitrap) m/z : $[\text{M}]^+$ Calcd for $\text{C}_{12}\text{H}_{12}\text{F}_4\text{O}_2^+$ 264.0768; Found 264.0770.



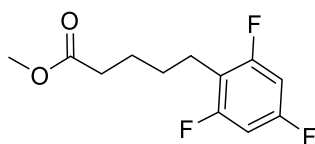
4-37

methyl 5-(2,3,4,6-tetrafluorophenyl)pentanoate, synthesized via 4-GP2, colorless liquid, 18.5mg (Yield = 70 %). ^1H NMR (400 MHz, CDCl_3) δ 6.79 – 6.67 (m, 1H), 3.66 (s, 3H), 2.66 (t, J = 7.1, 2H), 2.34 (t, J = 7.2 Hz, 2H), 1.73 – 1.54 (m, 4H). ^{19}F NMR (376 MHz, CDCl_3) δ -119.6 (d, J = 10.9 Hz), -136.0 (dd, J = 21.0, 4.8 Hz), -136.9 – -137.1 (m), -165.8 (td, J = 21.2, 11.4 Hz). ^{13}C NMR (101 MHz, CDCl_3) δ 173.9, 100.6, 51.7, 33.8, 28.9, 24.5, 22.0. GC-MS: 264. HRMS (EI/LTQ-Orbitrap) m/z : $[\text{M}]^+$ Calcd for $\text{C}_{12}\text{H}_{12}\text{F}_4\text{O}_2^+$ 264.0768; Found 264.0772.



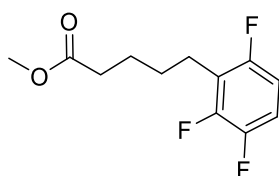
4-38a

methyl 5-(2,3,5,6-tetrafluorophenyl)pentanoate, synthesized via 4-GP2, colorless liquid, 19.7 mg (Yield = 75 %). ^1H NMR (400 MHz, CDCl_3) δ 6.91 (m, 1H), 3.67 (s, 3H), 2.75 (t, J = 7.1, 2H), 2.35 (t, J = 7.1 Hz, 2H), 1.75 – 1.56 (m, 4H). ^{19}F NMR (376 MHz, CDCl_3) δ -140.0 (dd, J = 22.4, 12.9 Hz), -144.9 (dd, J = 22.1, 13.0 Hz). ^{13}C NMR (101 MHz, CDCl_3) δ 173.9, 103.7, 51.7, 33.7, 28.7, 24.5, 22.7. GC-MS: 264. HRMS (EI/LTQ-Orbitrap) m/z : $[\text{M}]^+$ Calcd for $\text{C}_{12}\text{H}_{12}\text{F}_4\text{O}_2^+$ 264.0768; Found 264.0771.



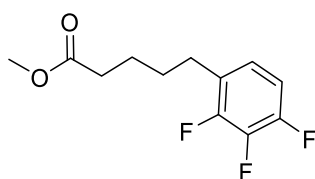
4-39a

methyl 5-(2,4,6-trifluorophenyl)pentanoate, synthesized via 4-GP2, colorless liquid, 16.1 mg (Yield = 65 %). ^1H NMR (400 MHz, CDCl_3) δ 6.67 – 6.54 (m, 2H), 3.66 (s, 3H), 2.71 – 2.57 (m, 2H), 2.33 (t, J = 7.3 Hz, 2H), 1.74 – 1.51 (m, 4H). ^{19}F NMR (376 MHz, CDCl_3) δ -111.8 (m), -113.12 (d, J = 4.6 Hz). ^{13}C NMR (101 MHz, CDCl_3) δ 174.0, 100.0, 51.7, 33.8, 29.0, 24.5, 21.7. GC-MS: 246. HRMS (EI/LTQ-Orbitrap) m/z : $[\text{M}]^+$ Calcd for $\text{C}_{12}\text{H}_{13}\text{F}_3\text{O}_2^+$ 246.0862; Found 246.0865.



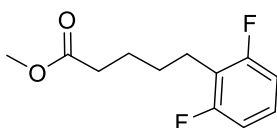
4-40a

methyl 5-(2,3,6-trifluorophenyl)pentanoate, synthesized via 4-GP2, colorless liquid, 13.1 mg (Yield = 53 %). ^1H NMR (400 MHz, CDCl_3) δ 6.96 (m, 1H), 6.76 (m, 1H), 3.66 (s, 3H), 2.75 – 2.67 (m, 2H), 2.35 (t, J = 6.9 Hz, 2H), 1.65 (m, 4H). ^{19}F NMR (376 MHz, CDCl_3) δ -121.2 (dd, J = 15.5, 4.1 Hz), -139.1 (dd, J = 21.1, 3.9 Hz), -143.0 (dd, J = 21.0, 15.3 Hz). ^{13}C NMR (101 MHz, CDCl_3) δ 174.0, 114.4, 110.4, 51.7, 33.8, 28.8, 24.6, 22.5. GC-MS: 246. HRMS (EI/LTQ-Orbitrap) m/z : $[\text{M}]^+$ Calcd for $\text{C}_{12}\text{H}_{13}\text{F}_3\text{O}_2^+$ 246.0862; Found 246.0867.



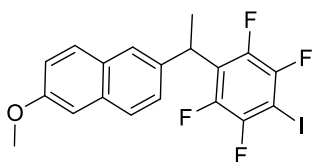
4-41a

methyl 5-(2,3,4-trifluorophenyl)pentanoate, synthesized via 4-GP2, colorless liquid, 9.7 mg (Yield = 40 %). ^1H NMR (400 MHz, CDCl_3) δ 6.95 – 6.80 (m, 2H), 3.66 (s, 3H), 2.64 (t, J = 7.3 Hz, 2H), 2.34 (t, J = 7.1 Hz, 2H), 1.73 – 1.56 (m, 4H). ^{19}F NMR (376 MHz, CDCl_3) δ -138.1 (dd, J = 20.4, 6.1 Hz), -139.5 (dd, J = 20.3, 6.2 Hz), -161.2 (t, J = 20.2 Hz). ^{13}C NMR (101 MHz, CDCl_3) δ 174.0, 123.5, 111.7, 51.7, 33.9, 29.5, 28.4, 24.5. GC-MS: 246. HRMS (EI/LTQ-Orbitrap) m/z : $[\text{M}]^+$ Calcd for $\text{C}_{12}\text{H}_{13}\text{F}_3\text{O}_2^+$ 246.0862; Found 246.0865.



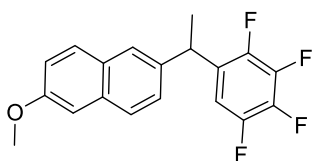
4-42a

methyl 5-(2,6-difluorophenyl)pentanoate, synthesized via 4-GP2, colorless liquid, 14.7 mg (Yield = 64 %). ^1H NMR (400 MHz, CDCl_3) δ 7.12 (m, 1H), 6.83 (m, 2H), 3.66 (s, 3H), 2.74 – 2.62 (m, 2H), 2.34 (t, J = 7.3 Hz, 2H), 1.74 – 1.53 (m, 4H). ^{19}F NMR (376 MHz, CDCl_3) δ -116.1 (s). ^{13}C NMR (101 MHz, CDCl_3) δ 174.1, 127.4, 117.62, 110.5, 51.6, 33.9, 29.0, 24.6, 22.0. GC-MS: 228. HRMS (EI/LTQ-Orbitrap) m/z : $[\text{M}]^+$ Calcd for $\text{C}_{12}\text{H}_{14}\text{O}_2\text{F}_2^+$ 228.0956; Found 228.0953.



4-35b

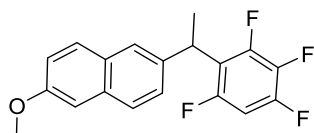
2-methoxy-6-(1-(2,3,5,6-tetrafluoro-4-iodo-phenyl)ethyl)naphthalene, synthesized via 4-GP2, white solid, 22.0 mg (Yield = 48 %). ^1H NMR (400 MHz, CDCl_3) δ 7.73 – 7.65 (m, 3H), 7.36 (dd, J = 8.5, 1.9 Hz, 1H), 7.15 (dd, J = 9.0, 2.5 Hz, 1H), 7.10 (d, J = 2.5 Hz, 1H), 4.75 (q, J = 7.3 Hz, 1H), 3.91 (s, 3H), 1.86 (dt, J = 7.4, 1.1 Hz, 3H). ^{19}F NMR (376 MHz, CDCl_3) δ -120.9 – -121.1 (m), -140.1 – -140.5 (m). ^{13}C NMR (101 MHz, CDCl_3) δ 157.8, 137.1, 133.6, 129.4, 129.0, 127.3, 126.4, 125.4, 119.2, 105.7, 69.8, 55.5, 35.3, 18.2. GC-MS: 460. HRMS (APPI/LTQ-Orbitrap) m/z : $[\text{M}]^+$ Calcd for $\text{C}_{19}\text{H}_{13}\text{F}_4\text{IO}^+$ 459.9942; Found 459.9960.



4-36b

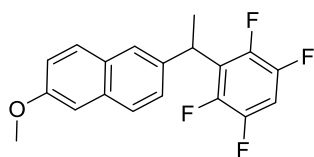
2-methoxy-6-(1-(2,3,4,5-tetrafluorophenyl)ethyl)naphthalene, synthesized via 4-GP2, oil, 22.1 mg (Yield = 66 %). ^1H NMR (400 MHz, CDCl_3) δ 7.70 (m, 2H), 7.63 – 7.60 (m, 1H), 7.27 – 7.23 (m, 1H), 7.16 (dd, J = 8.9, 2.6 Hz, 1H), 7.12 (d, J = 2.6 Hz, 1H), 6.85 – 6.69 (m, 1H), 4.59 (q, J = 7.2 Hz, 1H), 3.92 (s, 3H), 1.69 (d, J = 7.2 Hz, 3H). ^{19}F NMR (376 MHz, CDCl_3) δ -139.6 (dd, J = 21.2, 12.3 Hz), -143.7 (ddd, J = 20.2, 12.2, 2.5 Hz), -156.0 (t, J = 20.0 Hz), -158.9 – -159.1 (m). ^{13}C NMR (101 MHz, CDCl_3) δ

157.9, 138.3, 133.6, 129.4, 129.0, 127.4, 126.7, 125.5, 119.3, 109.7, 105.8, 55.5, 37.3, 20.6. GC-MS: 334. HRMS (APPI/LTQ-Orbitrap) m/z : $[M + H-1]^+$ Calcd for $C_{19}H_{13}F_4O^+$ 333.0897; Found 333.0904.



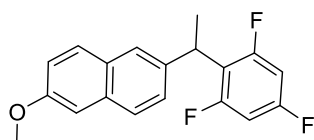
4-37b

2-methoxy-6-(1-(2,3,4,6-tetrafluorophenyl)ethyl)naphthalene, synthesized via 4-GP2, oil, 27.8 mg (Yield = 83 %). 1H NMR (400 MHz, $CDCl_3$) δ 7.74 – 7.64 (m, 3H), 7.40 – 7.33 (m, 1H), 7.15 (dd, J = 8.9, 2.6 Hz, 1H), 7.11 (d, J = 2.5 Hz, 1H), 6.74 (m, 1H), 4.69 (q, J = 7.4 Hz, 1H), 3.92 (s, 3H), 1.84 (d, J = 7.3, 3H). ^{19}F NMR (376 MHz, $CDCl_3$) δ -116.9 (d, J = 10.8 Hz), -134.8 (dd, J = 20.9, 5.3 Hz), -135.4 (dd, J = 21.3, 5.0 Hz), -165.0 (td, J = 21.0, 10.7 Hz). ^{13}C NMR (101 MHz, $CDCl_3$) δ 157.7, 138.0, 133.5, 129.4, 129.0, 127.1, 126.5, 125.2, 119.5, 119.1, 105.7, 101.0, 55.4, 34.4, 18.5. GC-MS: 334. HRMS (APPI/LTQ-Orbitrap) m/z : $[M + H-1]^+$ Calcd for $C_{19}H_{13}F_4O^+$ 333.0897; Found 333.0906.



4-38b

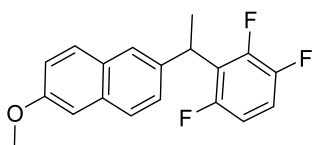
2-methoxy-6-(1-(2,3,5,6-tetrafluorophenyl)ethyl)naphthalene, synthesized via 4-GP2, white solid, 28.0 mg (Yield = 84 %). 1H NMR (400 MHz, $CDCl_3$) δ 7.75 – 7.65 (m, 3H), 7.39 (dd, J = 8.5, 1.9 Hz, 1H), 7.16 (ddd, J = 8.9, 2.6, 0.9 Hz, 1H), 7.11 (d, J = 2.5 Hz, 1H), 6.93 (tt, J = 9.7, 7.3 Hz, 1H), 4.77 (q, J = 7.4 Hz, 1H), 3.91 (s, 3H), 1.87 (d, J = 7.4, 3H). ^{19}F NMR (376 MHz, $CDCl_3$) δ -139.4 (dd, J = 21.8, 12.6 Hz), -143.0 (dd, J = 21.8, 12.7 Hz). ^{13}C NMR (101 MHz, $CDCl_3$) δ 157.8, 137.5, 133.5, 129.5, 129.0, 127.2, 126.5, 125.4, 125.3, 119.1, 105.7, 104.0, 55.4, 35.0, 18.3. GC-MS: 334. HRMS (APPI/LTQ-Orbitrap) m/z : $[M + H-1]^+$ Calcd for $C_{19}H_{13}F_4O^+$ 333.0897; Found 333.0908



4-39b

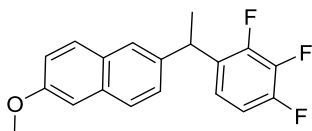
2-methoxy-6-(1-(2,4,6-trifluorophenyl)ethyl)naphthalene, synthesized via 4-GP2, white solid, 22.5 mg (Yield = 71 %). 1H NMR (400 MHz, $CDCl_3$) δ 7.64 – 7.53 (m, 3H), 7.27 (dd, J = 8.5, 1.9 Hz, 1H), 7.09

– 6.98 (m, 2H), 6.53 (t, $J = 8.5$ Hz, 2H), 4.58 (q, $J = 7.3$ Hz, 1H), 3.81 (s, 3H), 1.72 (d, $J = 7.4$ Hz, 3H). ^{19}F NMR (376 MHz, CDCl_3) δ -110.2 (d, $J = 5.7$ Hz), -111.2 (t, $J = 6.0$ Hz). ^{13}C NMR (101 MHz, CDCl_3) δ 157.6, 138.8, 133.3, 129.4, 129.0, 126.9, 126.7, 125.1, 118.9, 118.3, 105.7, 100.6, 55.4, 33.9, 18.7. GC-MS: 316. HRMS (APPI/LTQ-Orbitrap) m/z : $[\text{M}]^+$ Calcd for $\text{C}_{19}\text{H}_{15}\text{F}_3\text{O}^+$ 316.1070; Found 316.1078.



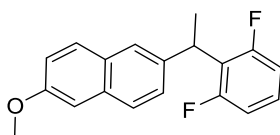
4-40b

2-methoxy-6-(1-(2,3,6-trifluorophenyl)ethyl)naphthalene, synthesized via 4-GP2, white solid, 20.1 mg (Yield = 64 %). ^1H NMR (400 MHz, CDCl_3) δ 7.74 – 7.63 (m, 3H), 7.38 (dd, $J = 8.5, 1.9$ Hz, 1H), 7.17 – 7.07 (m, 2H), 6.98 (qd, $J = 9.2, 4.9$ Hz, 1H), 6.78 (m, 1H), 4.73 (q, $J = 7.3$ Hz, 1H), 3.90 (s, 3H), 1.84 (d, $J = 7.3$, 3H). ^{19}F NMR (376 MHz, CDCl_3) δ -118.5 (dd, $J = 14.9, 3.3$ Hz), -137.0 (d, $J = 21.7$ Hz), -142.3 (dd, $J = 20.6, 14.9$ Hz). ^{13}C NMR (101 MHz, CDCl_3) δ 157.7, 138.3, 133.4, 129.4, 129.0, 127.0, 126.7, 125.2, 124.0, 119.0, 114.8, 111.0, 105.7, 55.4, 34.7, 18.5. GC-MS: 316. HRMS (APPI/LTQ-Orbitrap) m/z : $[\text{M}]^+$ Calcd for $\text{C}_{19}\text{H}_{15}\text{F}_3\text{O}^+$ 316.1070; Found 316.1076.



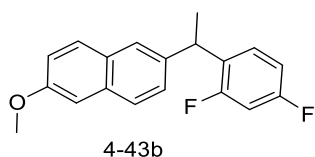
4-41b

2-methoxy-6-(1-(2,3,6-trifluorophenyl)ethyl)naphthalene, synthesized via 4-GP2, white solid, 18.2 mg (Yield = 58 %). ^1H NMR (400 MHz, CDCl_3) δ 7.68 (dd, $J = 11.1, 8.7$ Hz, 2H), 7.63 – 7.60 (m, 1H), 7.30 – 7.25 (m, 1H), 7.15 (dd, $J = 8.8, 2.5$ Hz, 1H), 7.11 (d, $J = 2.6$ Hz, 1H), 6.94 – 6.83 (m, 2H), 4.57 (q, $J = 7.2$ Hz, 1H), 3.91 (s, 3H), 1.70 (d, $J = 7.2$ Hz, 3H). ^{19}F NMR (376 MHz, CDCl_3) δ -137.5 – -137.9 (m), -138.8 (dd, $J = 20.6, 6.8$ Hz), -160.8 (d, $J = 20.6$ Hz). ^{13}C NMR (101 MHz, CDCl_3) δ 157.7, 139.2, 133.5, 131.2, 129.4, 129.0, 127.2, 126.9, 125.4, 122.0, 119.1, 111.9, 105.8, 55.5, 37.4, 20.8. GC-MS: 316. HRMS (APPI/LTQ-Orbitrap) m/z : $[\text{M}]^+$ Calcd for $\text{C}_{19}\text{H}_{15}\text{F}_3\text{O}^+$ 316.1070; Found 316.1072.

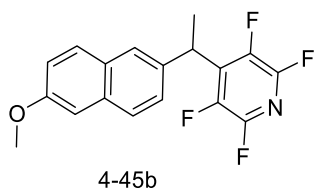


4-42b

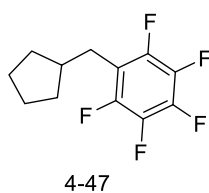
2-methoxy-6-(1-(2,6-difluorophenyl)ethyl)naphthalene, synthesized via 4-GP2, white solid, 18.7 mg (Yield = 63 %). ^1H NMR (400 MHz, CDCl_3) δ 7.71 (m, 2H), 7.66 (d, J = 8.5 Hz, 1H), 7.44 – 7.37 (m, 1H), 7.18 – 7.08 (m, 3H), 6.85 (t, J = 8.3 Hz, 2H), 4.74 (q, J = 7.4 Hz, 1H), 3.90 (s, 3H), 1.84 (d, J = 7.4 Hz, 3H). ^{19}F NMR (376 MHz, CDCl_3) δ -113.2 (s). ^{13}C NMR (101 MHz, CDCl_3) δ 162.5, 157.5, 139.1, 133.3, 129.4, 129.0, 127.9, 126.9, 126.8, 125.1, 122.0, 118.8, 111.8, 105.7, 55.4, 34.1, 18.7. GC-MS: 298. HRMS (APPI/LTQ-Orbitrap) m/z : $[\text{M} + \text{H}]^+$ Calcd for $\text{C}_{19}\text{H}_{17}\text{F}_2\text{O}^+$ 299.1242; Found 299.1243.



2-methoxy-6-(1-(2,4-difluorophenyl)ethyl)naphthalene, synthesized via 4-GP2, liquid, 9.0 mg (Yield = 30 %). ^1H NMR (400 MHz, CDCl_3) δ 7.67 (m, 2H), 7.63 – 7.60 (m, 1H), 7.28 (dd, J = 8.5, 1.9 Hz, 1H), 7.19 – 7.10 (m, 3H), 6.87 – 6.72 (m, 2H), 4.56 (q, J = 7.2 Hz, 1H), 3.91 (s, 3H), 1.69 (d, J = 7.2 Hz, 3H). ^{19}F NMR (376 MHz, CDCl_3) δ -113.6 (d, J = 6.9 Hz), -113.9 (d, J = 7.1 Hz). ^{13}C NMR (101 MHz, CDCl_3) δ 157.6, 140.0, 133.4, 129.5, 129.4, 129.1, 127.1, 127.1, 125.3, 119.0, 111.2, 105.8, 103.9, 55.5, 37.2, 20.9. GC-MS: 298. HRMS (APPI/LTQ-Orbitrap) m/z : $[\text{M} + \text{H}]^+$ Calcd for $\text{C}_{19}\text{H}_{17}\text{F}_2\text{O}^+$ 299.1242; Found 299.1246.

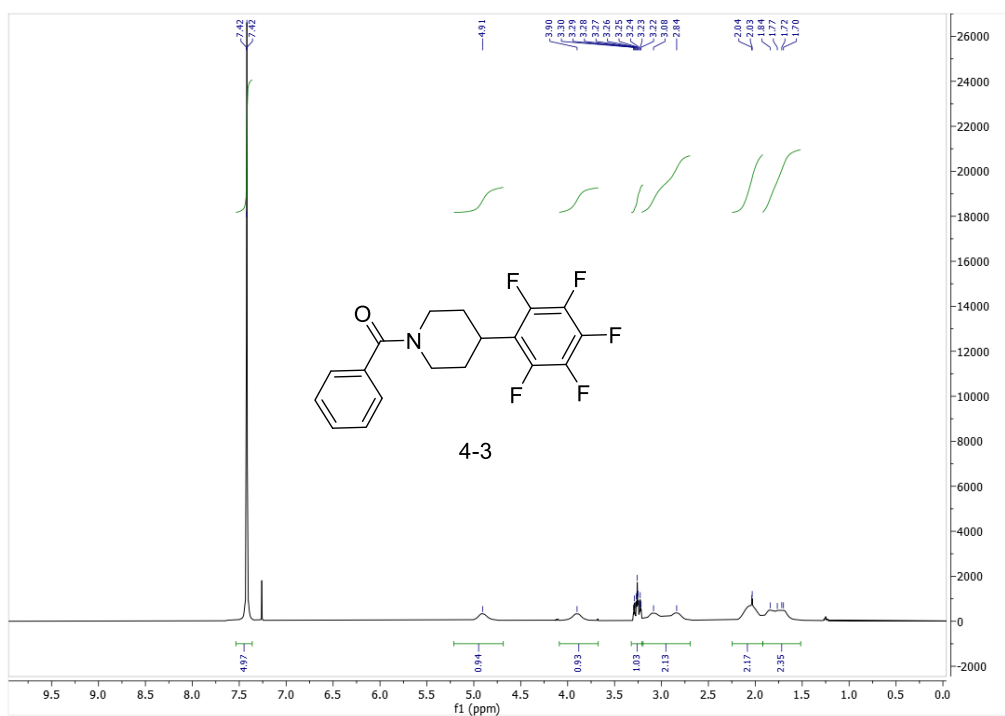
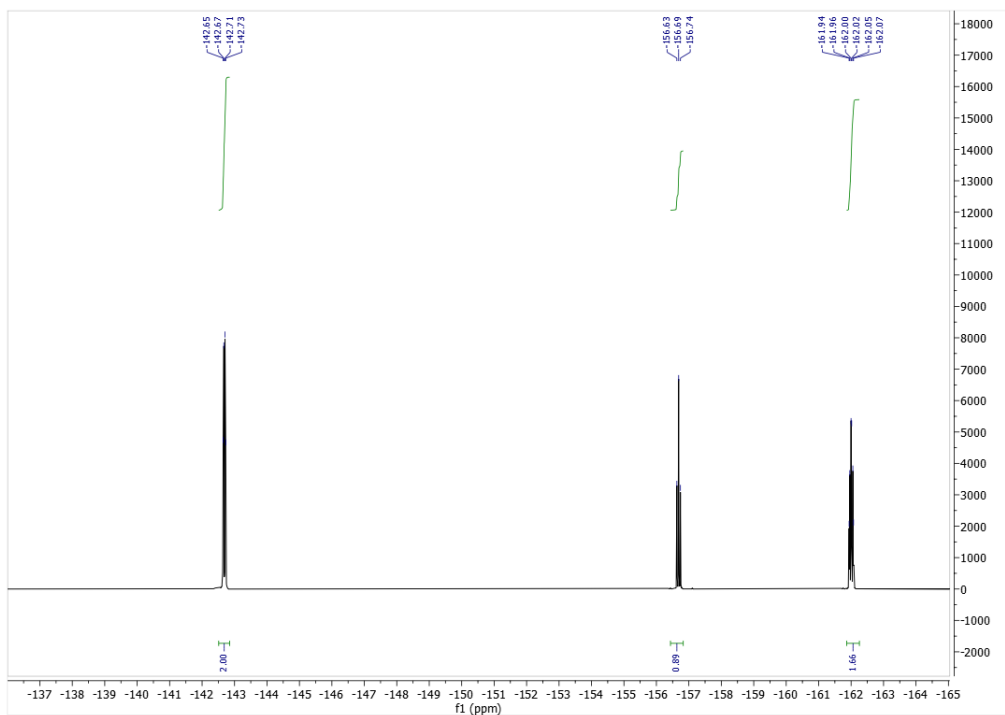


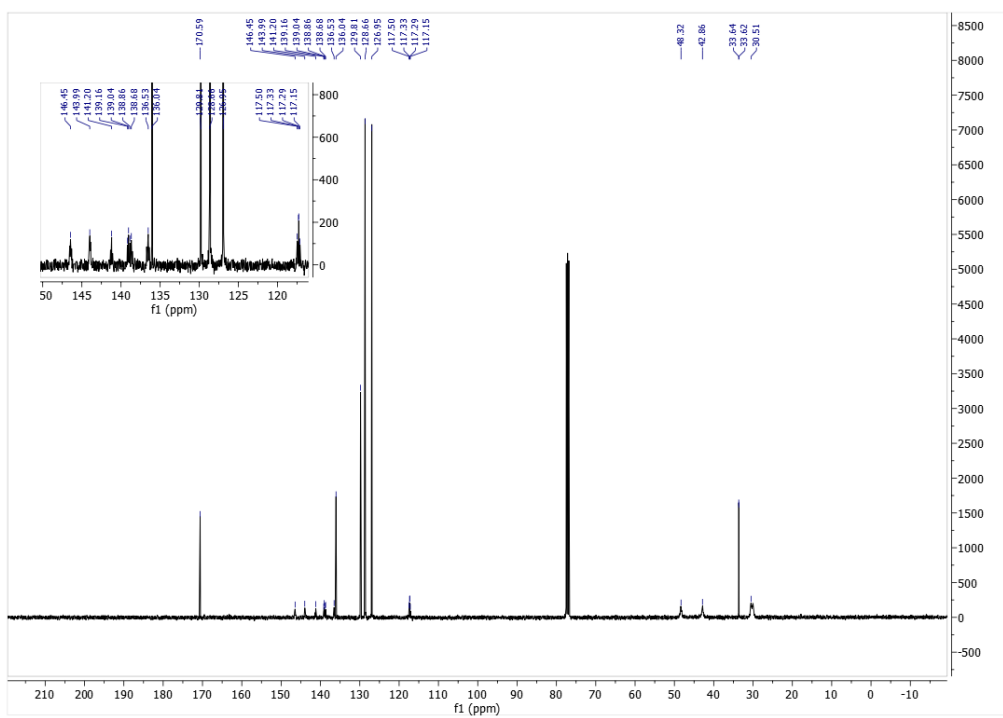
2,3,5,6-tetrafluoro-4-(1-(6-methoxynaphthalen-2-yl)ethyl)pyridine, synthesized via 4-GP2, liquid, 10.1 mg (Yield = 29 %). ^1H NMR (400 MHz, CDCl_3) δ 7.76 – 7.68 (m, 3H), 7.36 (dd, J = 8.4, 1.9 Hz, 1H), 7.16 (dd, J = 9.0, 2.5 Hz, 1H), 7.11 (d, J = 2.5 Hz, 1H), 4.79 (q, J = 7.3 Hz, 1H), 3.91 (s, 3H), 1.89 (d, J = 7.4, 3H). ^{19}F NMR (376 MHz, CDCl_3) δ -91.1 – -91.3 (m), -143.6 – -143.8 (m). ^{13}C NMR (101 MHz, CDCl_3) δ 158.1, 135.7, 133.8, 129.5, 129.0, 127.6, 126.1, 125.7, 119.5, 105.7, 55.5, 35.9, 17.8. GC-MS: 335. HRMS (APPI/LTQ-Orbitrap) m/z : $[\text{M} + \text{H}]^+$ Calcd for $\text{C}_{18}\text{H}_{14}\text{F}_4\text{NO}^+$ 336.1006; Found 336.1008.



1-(cyclopentylmethyl)-2,3,4,5,6-pentafluorobenzene, synthesized via 4-GP1, colorless liquid, 15.0 mg (Yield = 60 %). ^1H NMR (400 MHz, CDCl_3) δ 2.69 (d, J = 7.5 Hz, 1H), 2.08 (h, J = 7.7 Hz, 1H), 1.77 – 1.62 (m, 4H), 1.61 – 1.48 (m, 2H), 1.21 (m, 2H). ^{19}F NMR (376 MHz, CDCl_3) δ -143.5 (m), -158.4 (t, J = 20.9 Hz), -163.2 (m). ^{13}C NMR (101 MHz, CDCl_3) δ 40.3, 32.3, 27.9, 24.9. GC-MS: 250. HRMS (EI/LTQ-Orbitrap) m/z : $[\text{M}]^+$ Calcd for $\text{C}_{12}\text{H}_{11}\text{F}_5^+$ 250.0775; Found 250.0778.

4.7.6 NMR spectra of 4-3 (an example of the products)

 ^1H -NMR spectrum of (4-3) (400 MHz, CDCl_3) ^{19}F -NMR spectrum of (4-3) (400 MHz, CDCl_3)



References :

- [1] Berger, R.; Resnati, G.; Metrangolo, P.; Weber, E.; Hulliger, J. Organic fluorine compounds: a great opportunity for enhanced materials properties. *Chem. Soc. Rev.* **2011**, *40*, 3496-3508.
- [2] Dalton, D. M.; Rappe, A. K.; Ravis, T. Perfluorinated Taddol phosphoramidite as an L,Z-ligand on Rh(I) and Co(-I): evidence for bidentate coordination via metal-C6F5 interaction. *Chem. Sci.* **2013**, *4*, 2062-2070.
- [3] Giese, M.; Albrecht, M.; Valkonen, A.; Rissanen, K. The pentafluorophenyl group as pi-acceptor for anions: a case study. *Chem. Sci.* **2015**, *6*, 354-359.
- [4] Gillis, E. P.; Eastman, K. J.; Hill, M. D.; Donnelly, D. J.; Meanwell, N. A. Applications of Fluorine in Medicinal Chemistry. *J. Med. Chem.* **2015**, *58*, 8315-8359.
- [5] Meanwell, N. A. Fluorine and Fluorinated Motifs in the Design and Application of Bioisosteres for Drug Design. *J. Med. Chem.* **2018**, *61*, 5822-5880.
- [6] Zhou, Y.; Wang, J.; Gu, Z. N.; Wang, S. N.; Zhu, W.; Acena, J. L.; Soloshonok, V. A.; Izawa, K.; Liu, H. Next Generation of Fluorine-Containing Pharmaceuticals, Compounds Currently in Phase II-III Clinical Trials of Major Pharmaceutical Companies: New Structural Trends and Therapeutic Areas. *Chem. Rev.* **2016**, *116*, 422-518.
- [7] Meyer, E. A.; Castellano, R. K.; Diederich, F. Interactions with aromatic rings in chemical and biological recognition. *Angew. Chem. Int. Ed.* **2003**, *42*, 1210-1250.
- [8] Reichenbacher, K.; Suss, H. I.; Hulliger, J. Fluorine in crystal engineering - "the little atom that could". *Chem. Soc. Rev.* **2005**, *34*, 22-30.
- [9] Brooke, G. M. The preparation and properties of polyfluoro aromatic and heteroaromatic compounds. *J. Fluorine Chem.* **1997**, *86*, 1-76.
- [10] Li, X. H.; Fu, B.; Zhang, Q.; Yuan, X. P.; Zhang, Q.; Xiong, T.; Zhang, Q. Copper-Catalyzed Defluorinative Hydroarylation of Alkenes with Polyfluoroarenes. *Angew. Chem. Int. Ed.* **2020**, *59*, 23056-23060.
- [11] Lu, W.; Gao, J.; Yang, J. K.; Liu, L.; Zhao, Y. L.; Wu, H. C. Regioselective alkyl transfer from phosphonium ylides to functionalized polyfluoroarenes. *Chem. Sci.* **2014**, *5*, 1934-1939.
- [12] Sun, Y. Q.; Sun, H. J.; Jia, J.; Du, A. Q.; Li, X. Y. Transition-Metal-Free Synthesis of Fluorinated Arenes from Perfluorinated Arenes Coupled with Grignard Reagents. *Organometallics* **2014**, *33*, 1079-1081.
- [13] Arora, A.; Weaver, J. D. Visible Light Photocatalysis for the Generation and Use of Reactive Azolyl and Polyfluoroaryl Intermediates. *Acc. Chem. Res.* **2016**, *49*, 2273-2283.
- [14] Dewanji, A.; Bulow, R. F.; Rueping, M. Photoredox/Nickel Dual-Catalyzed Reductive Cross Coupling of Aryl Halides Using an Organic Reducing Agent. *Org. Lett.* **2020**, *22*, 1611-1617.
- [15] Singh, A.; Kubik, J. J.; Weaver, J. D. Photocatalytic C-F alkylation; facile access to multifluorinated arenes. *Chem. Sci.* **2015**, *6*, 7206-7212.
- [16] Sun, X.; Ritter, T. Decarboxylative Polyfluoroarylation of Alkylcarboxylic Acids. *Angew. Chem. Int. Ed.* **2021**, *60*, 10557-10562.

- [17] Ahrens, T.; Kohlmann, J.; Ahrens, M.; Braun, T. Functionalization of Fluorinated Molecules by Transition-Metal-Mediated C-F Bond Activation To Access Fluorinated Building Blocks. *Chem. Rev.* **2015**, *115*, 931-972.
- [18] Amii, H.; Uneyama, K. C-F Bond Activation in Organic Synthesis. *Chem. Rev.* **2009**, *109*, 2119-2183.
- [19] Eisenstein, O.; Milani, J.; Perutz, R. N. Selectivity of C-H Activation and Competition between C-H and C-F Bond Activation at Fluorocarbons. *Chem. Rev.* **2017**, *117*, 8710-8753.
- [20] Weaver, J.; Senaweera, S. C-F activation and functionalization of perfluoro- and polyfluoroarenes. *Tetrahedron* **2014**, *70*, 7413-7428.
- [21] Do, H. Q.; Daugulis, O. Copper-catalyzed arylation and alkenylation of polyfluoroarene C-H bonds. *J. Am. Chem. Soc.* **2008**, *130*, 1128.
- [22] Lafrance, M.; Rowley, C. N.; Woo, T. K.; Fagnou, K. Catalytic intermolecular direct arylation of perfluorobenzenes. *J. Am. Chem. Soc.* **2006**, *128*, 8754-8756.
- [23] Nakamura, Y.; Yoshikai, N.; Ilies, L.; Nakamura, E. Nickel-Catalyzed Monosubstitution of Polyfluoroarenes with Organozinc Reagents Using Alkoxydiphosphine Ligand. *Org. Lett.* **2012**, *14*, 3316-3319.
- [24] Kanyiva, K. S.; Kashiwara, N.; Nakao, Y.; Hiyama, T.; Ohashi, M.; Ogoshi, S. Hydrofluoroarylation of alkynes with fluoroarenes. *Dalton Trans.* **2010**, *39*, 10483-10494.
- [25] Sun, Z. M.; Zhang, J.; Manan, R. S.; Zhao, P. J. Rh(I)-Catalyzed Olefin Hydroarylation with Electron-Deficient Perfluoroarenes. *J. Am. Chem. Soc.* **2010**, *132*, 6935.
- [26] Zhang, X. G.; Fan, S. L.; He, C. Y.; Wan, X. L.; Min, Q. Q.; Yang, J.; Jiang, Z. X. Pd(OAc)₂ Catalyzed Olefination of Highly Electron-Deficient Perfluoroarenes. *J. Am. Chem. Soc.* **2010**, *132*, 4506.
- [27] Wei, Y.; Zhao, H. Q.; Kan, J.; Su, W. P.; Hong, M. C. Copper-Catalyzed Direct Alkynylation of Electron-Deficient Polyfluoroarenes with Terminal Alkynes Using O₂ as an Oxidant. *J. Am. Chem. Soc.* **2010**, *132*, 2522-+.
- [28] Fan, S. L.; He, C. Y.; Zhang, X. G. Direct Pd-catalyzed benzylation of highly electron-deficient perfluoroarenes. *Chem. Commun.* **2010**, *46*, 4926-4928.
- [29] Guo, H. Q.; Kong, F. Z.; Kanno, K.; He, J. J.; Nakajima, K.; Takahashi, T. Early transition metal-catalyzed cross-coupling reaction of aryl fluorides with a phenethyl grignard reagent accompanied by rearrangement of the phenethyl group. *Organometallics* **2006**, *25*, 2045-2048.
- [30] Xu, S.; Wu, G. J.; Ye, F.; Wang, X.; Li, H.; Zhao, X.; Zhang, Y.; Wang, J. B. Copper(I)-Catalyzed Alkylation of Polyfluoroarenes through Direct C-H Bond Functionalization. *Angew. Chem. Int. Ed.* **2015**, *54*, 4669-4672.
- [31] Albeniz, A. C.; Espinet, P.; Martin-Ruiz, B. The Pd-catalyzed coupling of allyl halides and tin aryls: Why the catalytic reaction works and the stoichiometric reaction does not. *Chem.-Eur. J.* **2001**, *7*, 2481-2489.
- [32] Fan, S. L.; Chen, F.; Zhang, X. G. Direct Palladium-Catalyzed Intermolecular Allylation of Highly Electron-Deficient Polyfluoroarenes. *Angew. Chem. Int. Ed.* **2011**, *50*, 5918-5923.

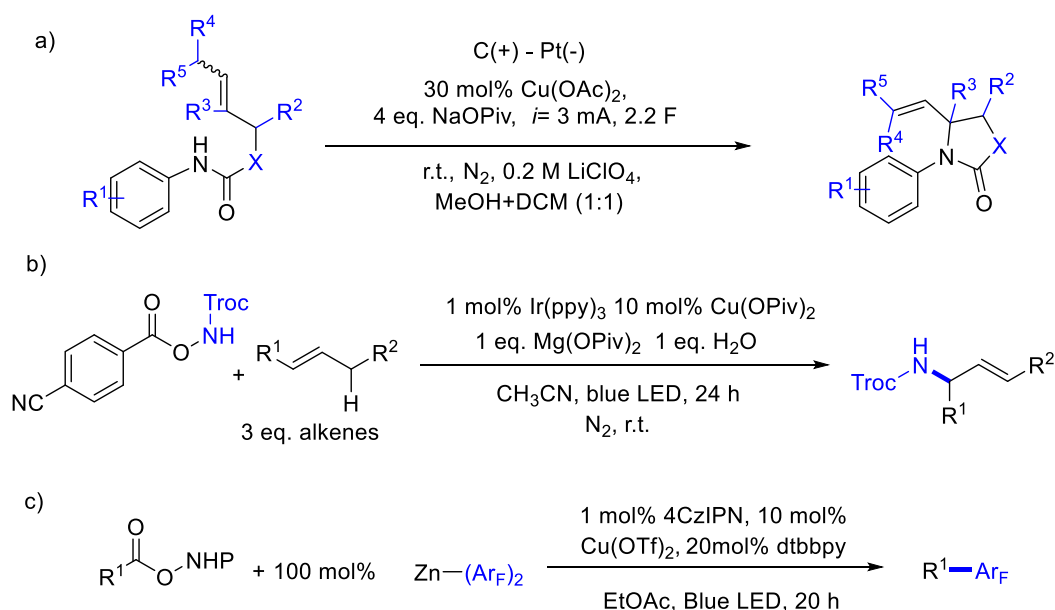
- [33] Yao, T.; Hirano, K.; Satoh, T.; Miura, M. Stereospecific Copper-Catalyzed C-H Allylation of Electron-Deficient Arenes with Allyl Phosphates. *Angew. Chem. Int. Ed.* **2011**, *50*, 2990-2994.
- [34] Xie, W.; Heo, J.; Kim, D.; Chang, S. Copper-Catalyzed Direct C-H Alkylation of Polyfluoroarenes by Using Hydrocarbons as an Alkylating Source. *J. Am. Chem. Soc.* **2020**, *142*, 7487-7496.
- [35] Xie, W. L.; Kim, D.; Chang, S. Copper-Catalyzed Formal Dehydrogenative Coupling of Carbonyls with Polyfluoroarenes Leading to beta-C-H Arylation. *J. Am. Chem. Soc.* **2020**, *142*, 20588-20593.
- [36] Albeniz, A. C.; Espinet, P.; Martin-Ruiz, B.; Milstein, D. Catalytic system for heck reactions involving insertion into Pd-(perfluoro-organyl) bonds. *J. Am. Chem. Soc.* **2001**, *123*, 11504-11505.
- [37] Clot, E.; Megret, C.; Eisenstein, O.; Perutz, R. N. Exceptional Sensitivity of Metal-Aryl Bond Energies to ortho-Fluorine Substituents: Influence of the Metal, the Coordination Sphere, and the Spectator Ligands on M-C/H-C Bond Energy Correlations. *J. Am. Chem. Soc.* **2009**, *131*, 7817-7827.
- [38] McAtee, R. C.; McClain, E. J.; Stephenson, C. R. J. Illuminating Photoredox Catalysis. *Trends Chem.* **2019**, *1*, 111-125.
- [39] Prier, C. K.; Rankic, D. A.; MacMillan, D. W. C. Visible Light Photoredox Catalysis with Transition Metal Complexes: Applications in Organic Synthesis. *Chem. Rev.* **2013**, *113*, 5322-5363.
- [40] Twilton, J.; Le, C.; Zhang, P.; Shaw, M. H.; Evans, R. W.; MacMillan, D. W. C. The merger of transition metal and photocatalysis. *Nat. Rev. Chem.* **2017**, *1*.
- [41] Coe, P. L.; Stephens, R.; Tatlow, J. C. Aromatic Polyfluoro-Compounds .11. Pentafluorophenyl-Lithium and Derived Compounds. *J. Chem. Soc.* **1962**, 3227.
- [42] Harper, R. J.; Tamborski, C.; Soloski, E. J. Reactions of Organometallics with Fluoroaromatic Compounds. *J. Org. Chem.* **1964**, *29*, 2385.
- [43] Vinogradov, A. S.; Krasnov, V. I.; Platonov, V. E. Organozinc reagents from polyfluoroarenes: Preparation and reactions with allyl halides. Synthesis of allylpolyfluoroarenes. *Russ J. Org. Chem.* **2008**, *44*, 95-102.
- [44] Huihui, K. M. M.; Caputo, J. A.; Melchor, Z.; Olivares, A. M.; Spiewak, A. M.; Johnson, K. A.; DiBenedetto, T. A.; Kim, S.; Ackerman, L. K. G.; Weix, D. J. Decarboxylative Cross-Electrophile Coupling of N-Hydroxyphthalimide Esters with Aryl Iodides. *J. Am. Chem. Soc.* **2016**, *138*, 5016-5019.
- [45] Qin, T.; Cornella, J.; Li, C.; Malins, L. R.; Edwards, J. T.; Kawamura, S.; Maxwell, B. D.; Eastgate, M. D.; Baran, P. S. A general alkyl-alkyl cross-coupling enabled by redox-active esters and alkylzinc reagents. *Science* **2016**, *352*, 801-805.
- [46] Toriyama, F.; Cornella, J.; Wimmer, L.; Chen, T. G.; Dixon, D. D.; Creech, G.; Baran, P. S. Redox-Active Esters in Fe-Catalyzed C-C Coupling. *J. Am. Chem. Soc.* **2016**, *138*, 11132-11135.
- [47] Zeng, X. J.; Yan, W. H.; Zacate, S. B.; Chao, T. H.; Sun, X. D.; Cao, Z.; Bradford, K. G. E.; Paeth, M.; Tyndall, S. B.; Yang, K. D.; Kuo, T. C.; Cheng, M. J.; Liu, W. Copper-Catalyzed Decarboxylative Difluoromethylation. *J. Am. Chem. Soc.* **2019**, *141*, 11398-11403.

- [48] Barzano, G.; Mao, R. Z.; Garreau, M.; Waser, J.; Hu, X. L. Tandem Photoredox and Copper-Catalyzed Decarboxylative C(sp³)-N Coupling of Anilines and Imines Using an Organic Photocatalyst. *Org. Lett.* **2020**, *22*, 5412-5416.
- [49] Garreau, M.; Le Vaillant, F.; Waser, J. C-Terminal Bioconjugation of Peptides through Photoredox Catalyzed Decarboxylative Alkynylation. *Angew. Chem. Int. Ed.* **2019**, *58*, 8182-8186.
- [50] Le Vaillant, F.; Garreau, M.; Nicolai, S.; Gryn'ova, G.; Corminboeuf, C.; Waser, J. Fine-tuned organic photoredox catalysts for fragmentation-alkynylation cascades of cyclic oxime ethers. *Chem. Sci.* **2018**, *9*, 5883-5889.
- [51] Shang, T. Y.; Lu, L. H.; Cao, Z.; Liu, Y.; He, W. M.; Yu, B. Recent advances of 1,2,3,5-tetrakis(carbazol-9-yl)-4,6-dicyanobenzene (4CzIPN) in photocatalytic transformations. *Chem. Commun.* **2019**, *55*, 5408-5419.
- [52] Lakshman, M. K.; Vuram, P. K. Cross-dehydrogenative coupling and oxidative-amination reactions of ethers and alcohols with aromatics and heteroaromatics. *Chem. Sci.* **2017**, *8*, 5845-5888.
- [53] Miyaoura, N.; Suzuki, A. Palladium-Catalyzed Cross-Coupling Reactions of Organoboron Compounds. *Chem. Rev.* **1995**, *95*, 2457-2483.
- [54] Shi, R. Y.; Zhang, Z. K.; Hu, X. L. Nickamine and Analogous Nickel Pincer Catalysts for Cross-Coupling of Alkyl Halides and Hydrosilylation of Alkenes. *Acc. Chem. Res.* **2019**, *52*, 1471-1483.
- [55] Miller, A. O.; Krasnov, V. I.; Peters, D.; Platonov, V. E.; Miethchen, R. Perfluorozinc aromatics by direct insertion of zinc into C-F or C-Cl bonds. *Tetrahedron Lett* **2000**, *41*, 3817-3819.
- [56] Liu, S. S.; Liu, H.; Liu, S. H.; Lu, Z. H.; Lu, C. H.; Leng, X. B.; Lan, Y.; Shen, Q. L. C(sp³)-CF₃ Reductive Elimination from a Five -Coordinate Neutral Copper(III) Complex. *J. Am. Chem. Soc.* **2020**, *142*, 9785-9791.
- [57] Tan, X. Q.; Liu, Z. L.; Shen, H. G.; Zhang, P.; Zhang, Z. Z.; Li, C. Z. Silver-Catalyzed Decarboxylative Trifluoromethylation of Aliphatic Carboxylic Acids. *J. Am. Chem. Soc.* **2017**, *139*, 12430-12433.
- [58] Chandrachud, P. P.; Wojtas, L.; Lopchuk, J. M. Decarboxylative Amination: Diazirines as Single and Double Electrophilic Nitrogen Transfer Reagents. *J. Am. Chem. Soc.* **2020**, *142*, 21743-21750.
- [59] Mao, R. Z.; Frey, A.; Balon, J.; Hu, X. L. Decarboxylative C(sp³)-N cross-coupling via synergetic photoredox and copper catalysis. *Nat Catal* **2018**, *1*, 120-126.
- [60] Xu, R. T.; Xu, T. X.; Yang, M. C.; Cao, T. P.; Liao, S. H. A rapid access to aliphatic sulfonyl fluorides. *Nat. Commun.* **2019**, *10*.
- [61] Doshi, A.; Sundararaman, A.; Venkatasubbaiah, K.; Zakharov, L. N.; Rheingold, A. L.; Myahkostupov, M.; Piotrowiak, P.; Jakle, F. Pentafluorophenyl Copper-Pyridine Complexes: Synthesis, Supramolecular Structures via Cuprophilic and pi-Stacking Interactions, and Solid-State Luminescence. *Organometallics* **2012**, *31*, 1546-1558.

Chapter 5 Conclusion

5.1 Achieved results

In this thesis, we present three useful synthetic methods developed based on the combination of electrochemistry or photochemistry with copper catalysis (Scheme 5.1). The radicals generated by electrochemical or photochemical methods were functionalized with copper catalysts for the oxidative amination reactions and polyfluoroarylation reaction. The electrochemical formal aza-Wacker cyclization (Chapter 2) and the photochemical intermolecular oxidative amination of alkenes (Chapter 3) led to a broad scope of N-containing compounds under mild conditions without the use of strong oxidants and with good tolerance of functional groups. The new double bonds formed in the products provide handles for many possible further derivatizations. The photochemical decarboxylative coupling of NHPI esters with polyfluoroaryl nucleophiles offers an easy approach to converting easily available aliphatic acids into alkyl polyfluoroarenes (Chapter 4). Polyfluoroaryls with variable F-content (2F-5F) and F-substitution patterns were installed on a range of primary or secondary alkyls with good tolerance of functional groups. Such a controllable polyfluoroaryl of alkyl groups is challenging for the previous methods.



Scheme 5.1 A summary of achieved results.

5.2 Future development

The basic idea of this thesis is the combination of the radical generation by electrochemical or photochemical methods and radical functionalization by copper catalysis. We believe that there is much more that we can explore beyond the reported three projects.

- 1) The oxidative amination reactions testify that the amidyl radicals, despite being highly reactive, could coexist with the copper catalytic system. The amidyl radical was not quenched by the metal catalyst before adding to the alkenes. This was also observed in Li's work of aminotrifluoromethylation (Scheme 1.17e). In the future, it's possible to develop other copper-catalyzed functionalizations of carboradicals generated from the addition of amidyl radicals to alkenes. In section 1.6, we have described the formation of various chemical bonds from carboradicals by copper catalysis. If all these copper catalytic system are compatible with the amidyl radical process, a range of synthetic methods could be developed for functionalized N-containing compounds.
- 2) The polyfluoroarylation reaction should not be restricted to NHPI esters. The recent development of photochemistry and electrochemistry has revealed diversified methods for the generation of carboradicals from ubiquitous starting materials. The copper catalysts plus polyfluoroaryl zinc reagents could be tried to trap all these radical intermediates to obtain polyfluoroaryl compounds. We believe that this mode of reaction has a great potential in building up the diversity of polyfluoroaryl compounds.
- 3) There are so far many examples for the enantioselective functionalization of alkyl radicals with copper catalysis, including cyanation, arylation, alkynylation and trifluoromethylation. By a careful selection of chiral ligand and method for alkyl radical generation, it is also possible to develop the enantioselective selective polyfluoroarylation process. The capability to construct chiral polyfluoroaryl compounds would further promote the application of this method in the field of medical chemistry and pharmaceuticals.

Curriculum Vitae

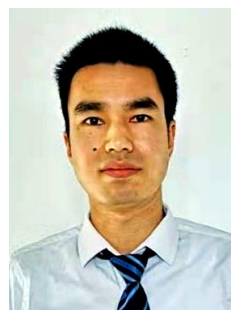
Xiangli Yi

Ave. D'Apples 14, CH-1006, Lausanne, Switzerland

+41-787239776

alanyi1002@gmail.com

[LinkedIn](#) | [Skype](#)



Education:

- | | |
|--------------|---|
| | Ph.D. in Organic Chemistry |
| 2017-present | École Polytechnique Fédérale de Lausanne (EPFL), Lausanne, Switzerland. |
| | M.S. in Chemistry |
| 2014-2017 | Tsinghua University, Beijing, China. |
| | B.S. in Chemistry |
| 2010-2014 | Tsinghua University, Beijing, China. |

Technical skills:

- Organic synthetic skills: Handling sensitive reagents, reproducing various organic reactions, developing new reactions, investigating reaction mechanisms.
- Characterization and analysis of organic compounds: IR, UV-Vis, 1D-NMR, 2D-NMR, GC-MS, HPLC, CV, fluorescence quenching.
- Electrochemical and photochemical technologies
- Primary DFT calculation
- IT skills: Origin (Data processing), MestreNova (NMR data), MS Office.
- Project management: Planning projects, managing risks, learning new techniques for problem solving, handling pressure, scientific communication and presentation.

Publications:

- 1) Yi, X. L.; Hu, X. L. Formal Aza-Wacker Cyclization by Tandem Electrochemical Oxidation and Copper Catalysis *Angew. Chem. Int. Ed.* **2019**, *58*, 4700-4704.
- 2) Yi, X. L.; Hu, X. L. Intermolecular oxidative amination of unactivated alkenes by dual photoredox and copper catalysis *Chem. Sci.* **2021**, *12*, 1901-1906.
- 3) Yi, X. L.; Xi, C. J. Copper-Promoted Tandem Reaction of Azobenzenes with Allyl Bromides via N=N Bond Cleavage for the Regioselective Synthesis of Quinolines *Org. Lett.* **2015**, *17*, 5836-5839.

- 4) Yi, X. L.; Jiao, L.; Xi, C. J. I-2-Mediated 2H-indazole synthesis via halogen-bond-assisted benzyl C-H functionalization *Org. Biomol. Chem.* **2016**, *14*, 9912-9918.
- 5) Yi, X. L.; Xi, C. J. Iodine-catalyzed aerobic oxidation of o-alkylazoarenes to 2H-indazoles *Tetrahedron* **2017**, *73*, 1311-1316.
- 6) Yan, X. Y.; Yi, X. L.; Xi, C. J. Direct cleavage of the N=N bond of azobenzenes by MeOTf leading to N-arylbenzimidazoles *Org. Chem. Front.* **2014**, *1*, 657-660.
- 7) Cai, S. J.; Lin, S. Y.; Yi, X. L.; Xi, C. J. Substrate-Controlled Transformation of Azobenzenes to Indazoles and Indoles via Rh(III)-Catalysis *J. Org. Chem.* **2017**, *82*, 512-520.
- 8) Liu, Y.; Yi, X. L.; Luo, X. W.; Xi, C. J. MeOTf-Mediated Annulation of Alkyl nitriles and Arylalkynes Leading to Polysubstituted NH-Pyrroles *J. Org. Chem.* **2017**, *82*, 11391-11398.

Selected Conferences and Awards:

- 9th CCS National Organic Chemistry Conference, Changchun, China, July 2015, Poster presentation.
- Chemistry Travel Award 2020 in EPFL

Other experiences:

- Teaching assistant for first online course of the chemistry department (Tsinghua University, 2014). Organic Chemistry: https://www.xuetangx.com/course/THU07031000429/5883025?channel=search_result. Coordinating the shooting and uploading of the class videos, compiling exercises and answering questions.
- Main organiser in a committee of 9 people for organizing an organic chemistry seminar for 8 research groups (Tsinghua University, 2016). Making plans, organizing committee reunion, assigning tasks, controlling the progress of the organization.
- In charge of chemical inventory of the lab (EPFL, 2017-2020). Organizing all lab members for resorting, relocating and rescanning of all chemicals. A more ordered inventory was created, saving much time of group members in looking for chemicals.

Personal hobbies:

Badminton (3 years in the Badminton Club for Universities of Lausanne), Table tennis, tennis, swimming, travelling.

Languages

Chinese (Native)	English (Fluent as working Language)
French (Reading B2, Speaking B1)	

Personal details

29, single, Chinese, from Liling, Hunan, China.

